HYDROPHILIC SURFACE MODIFICATION OF POLYMERS FOR IMPROVED BIOMATERIALS

BY

TUNG-LIANG LIN

A DISSERTATION PRESENTED TO THE GRADUATE SCHOOL
OF THE UNIVERSITY OF FLORIDA IN PARTIAL FULFILLMENT
OF THE REQUIREMENTS FOR THE DEGREE OF
DOCTOR OF PHILOSOPHY

UNIVERSITY OF FLORIDA

1995

ACKNOWLEDGEMENTS

I would like to express my deepest gratitude and appreciation to my research advisor and doctoral committee chairman, Dr. Eugene P. Goldberg, for his guidence, encouragement, generous support, and assistance during preparation of this manuscript. My sincere thanks are also extended to Dr. Batich, Dr. Adair, Dr. Whitney, and Dr. Duran for their participation on the doctoral committee.

My sincere thanks must go to Drs. Hiroyuke Hattori, Eric Luo, Ali Yahiaoui, and Jeanne Quigg for their advice and support. Sincere appreciation is also extended to Paul Martin, Emmanuel Biagtan, and Drew Amery for their assistance and friendship.

In addition, I would like to thank all my fellow students, for their friendship and cooperation.

I would also like to thank my parents, my brothers and my sister for their support and encouragement. Most of all I am grateful to my wife and my children for their love, patience, and support during those years.

TABLE OF CONTENTS

Abstract of Dissertation Presented to the Graduate School of the University of Florida in Partial Fulfillment of the Requirements for the Degree of Doctor of Philosophy

HYDROPHILIC SURFACE MODIFICATION OF POLYMERS FOR IMPROVED BIOMATERIALS

By

Tung-Liang Lin

May, 1995

Chairman: Dr. Eugene P. Goldberg
Major Department: Materials Science and Engineering

In the biomaterials industry, polymeric materials are widely used as medical or prosthetic devices. However, most polymers currently used for these applications do not fully satisfy the biocompatibility requirements. Although the interactions between medical implants and living tissues or cells are very complex and are still not fully understood, it is well known that the interfacial properties of implants play an important role in the interactions. Therefore, the synthesis of biocompatible interfaces using surface modification techniques were considered as one of the most

promising solutions in improving the biocompatibility of implants.

This research was devoted to the synthesis and characterization of hydrophilic surface grafts onto several major biomedical polymers. These biomedical polymers include PMMA, PDMS, PC, PP, FEP, and PVDF. Monomers, including N-vinylpyrrolidone (NVP) and dimethylacrylamide (DMA), were utilized in this study. Also, a new PVP/NVP monomer system was employed for the surface modification.

A novel technique termed the "Plasma/Gamma Method" was used to graft hydrophilic vinyl monomers onto polymeric substrates. The "Plasma/Gamma Method" involves two important steps: radio frequency (RF) water plasma treatment and gamma-induced graft polymerization. The purpose of plasma treatment is to revitalize the inert polymer surface, thereby enhancing interfacial interactions and diffusion of monomer to the substrate surface.

Surfaces were characterized using gravimetric analysis, ellipsometry, contact angle measurements, Fourier transform infrared by attenuated total reflectance (FT-IR/ATR), X-ray photoelectron spectroscopy (XPS), and scanning electron microscopy (SEM).

Preliminary in-vitro evaluations carried out with polymer slabs indicated that PVP-grafted polymers by the "Plasma/Gamma Method" significantly reduced the incidence of cell adhesions.

CHAPTER 1
INTRODUCTION

In the biomaterials industry, polymeric materials are widely used as medical or prosthetic devices. These applications include heart valve stents, artificial heart pumps, vascular grafts, sutures, artificial ligaments, syringes, catheters, contact lenses, intraocular lenses, viscoelastic solutions, orthopedics, wound dressings, cosmetic implants, drug delivery systems, parenteral packagings, and prosthetic fixatives, etc. [1]. Unfortunately, most polymers currently used for these applications do not fully satisfy biocompatibility requirements. The interactions between medical implants and living tissues or cells are very complex and are still not fully understood. However, it is well known that the interfacial properties of implants play an important role in the interactions. Consequently, the synthesis of biocompatible interfaces using surface modification techniques is considered to be one of the most promising approaches to the problem of poor biocompatibility of implants. Surface modification is a technique that only changes the surface properties of substrate without altering the bulk properties. The advantages of surface modification

techniques include maintaining bulk properties of implants such as mechanical strength or geometry, combining graft and substrate properties to form a superior composite structure, and meeting the biological compatibility requirements.

Since Wichterle and Lim [2,3] established that poly(2-hydroxyethyl methacrylate) hydrogels are excellent candidates for contact lens applications, hydrogels have received tremendous attention for medical and pharmaceutical applications. Hydrogels are crosslinked networks of hydrophilic homopolymers or copolymers. They are similar to natural tissues and possess the properties of high water content, softness, low interfacial free energy under aqueous environments, and high permeability to oxygen, ions, and small molecules, all of which may contribute to their biocompatibility [4]. The major disadvantage of hydrogels is their relatively low mechanical strength. To combine the advantages of hydrogels with biomedical polymers, hydrophilic surface modifications have been applied to various implants. The hydrophilic surface graft serves as a "slippery" water cushion while the bulk part of implants provides needed strength to maintain mechanical integrity. Therefore, hydrophilic surface modification of polymeric materials has been recognized as one of the most feasible approaches to improve the biocompatibility of medical implants or devices.

Hydrophilic surface modification of intraocular lens (IOL) has been intensely studied in this laboratory for more

than one decade [5,6]. The previous results suggested that the hydrophilic surface modified IOL has the potential advantage of reducing tissue and cell adhesion, thereby improving long-term biocompatibility in the ocular environment [5,7,8].

Surface modifications can be carried out by various techniques. The most popular techniques include conventional chemical reaction, UV induced graft polymerization, gamma induced graft polymerization, and RF-plasma induced graft polymerization [9-11]. Gamma induced graft polymerization of hydrophilic vinyl monomers onto polymeric IOLs has been developed and investigated in this laboratory [5,6]. This is a heterogeneous reaction and is carried out at the solid/aqueous interface by free radical formation. Thermodynamic incompatibility between hydrophilic monomers and hydrophobic substrates usually hinders the heterogeneous grafting reaction. Swelling agents to enhance monomer penetration [12] or use of radical inhibitors to control excess homopolymerization [13] have been employed to improve the grafting reaction. A "Presoak Method," developed by Yahiaoui in this laboratory, was used to control the diffusion of monomers into substrates and resulted in a significant improvement in the grafting yield [6].

This thesis describes a novel technique termed the "Plasma/Gamma Method," also developed by Yahiaoui [6], that was used to graft hydrophilic vinyl monomers onto polymeric

substrates. The "Plasma/Gamma Method" involves two important steps: radio frequency (RF) water plasma treatment and gamma induced graft polymerization. The purpose of the RF water plasma treatment is to activate the inert hydrophobic substrate surface. The non-equilibrium cold plasma oxidizes and may generate peroxides on the surface. After plasma treatment, the substrate surface changes from apolar hydrophobic to polar hydrophilic. This change decreases the thermodynamic incompatibility barrier between the monomer and substrate surfaces. Eventually, these generated weak peroxides could dissociate and form free radicals which would enhance the grafting reaction during gamma induced graft polymerization.

The objective of this research was to investigate the graft process and the properties of grafted surfaces prepared by the "Plasma/Gamma Method." Polymeric substrates selected for this research included poly(methyl methacrylate) (PMMA), poly(dimethyl siloxane) (PDMS), polyproplyene (PP), polycarbonate (PC), poly(vinylidene fluoride) (PVDF), and fluorinated ethylene-propylene copolymer (FEP). The hydrophilic monomers primarily used in this study were N-Vinyl pyrrolidone (NVP) and dimethylacrylamide (DMA). A new monomer system containing poly(vinyl pyrrolidone) (PVP) with NVP monomer was also employed for the surface modification. Poly(vinyl pyrrolidone) is a linear hydrophilic polymer and a good wetting agent. Methods to characterize the grafted surfaces

included gravimetric analysis, contact angle measurement, FTIR/ATR, XPS, SEM, ellipsometry, and optical microscopy. Shear viscosity of polymer solutions was measured with a Brookfield digital viscometer model DV II.

In addition, a two-step gamma method was also used to synthesize PVP-g-PMMA. This method involved two consecutive steps of gamma-induced graft polymerization. The purpose of first gamma-induced graft polymerization is to increase the wettability of PMMA surface and function similar to the RF plasma treatment in the plasma/gamma method. The monomers used were NVP and the PVP/NVP system.

Rabbit lens epithelial cell adhesion and spreading was used to evaluate the biocompatibility of unmodified, plasma treated, and hydrophilic surface modified substrates.

CHAPTER 2
BACKGROUND

2.1 Biomaterials and Related Problems

2.1.1 IOL Implants and Related Problems

Polymethylmethacrylate (PMMA) IOL was introduced into a physiological environment in 1949 by Dr. H. Ridley [14] after his observation that the fragments of Spitfire canopies made of PMMA remained inert within the eyes of pilots during the Second World War. PMMA is an optically clear, rigid, and completely amorphous thermoplastic which has shown relatively good ocular tolerance, biostability and biological inertness [15]. Because of this, most IOL optics today are made of PMMA. Figure 2-1 shows one-piece PMMA lenses and three-piece lenses made of PMMA optics and polypropylene haptic. Some drawbacks do exist with PMMA IOLs, however. The material tends to be rigid and hydrophobic which can lead to ocular tissue trauma, corneal endothelium damage, iris erosion, secondary glaucoma, intermittent hyphema. Residual lens epithelial cell adhesion and associated postoperative inflammation are also possibly related to the hydrophobicity and rigidity of PMMA

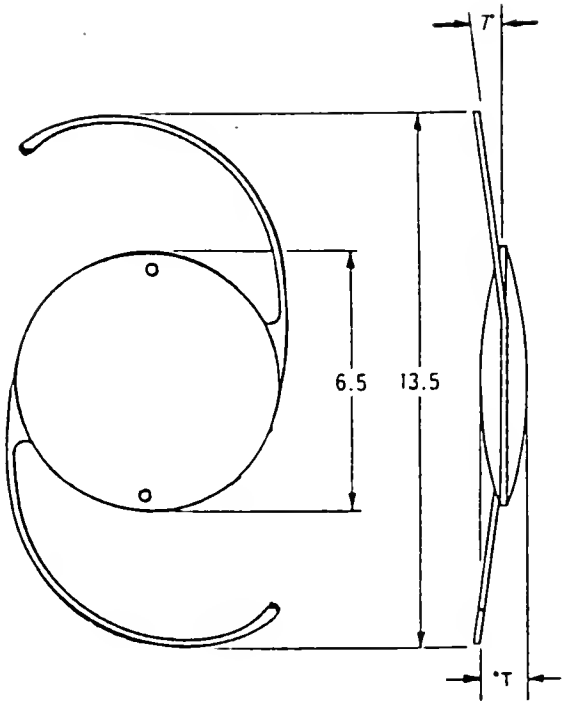

(a)

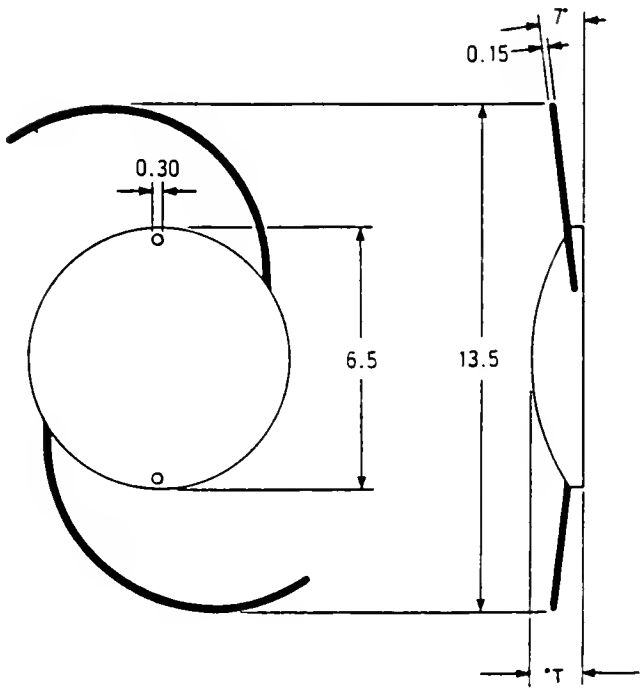

(b)

Figure 2-1. Typical IOL Lenses
(a) one-piece PMMA lens,
(b) three-piece PMMA lens with PP haptic

surfaces [16-18]. Improvements in cataract surgery techniques and PMMA IOL design have not completely eliminated those problems. Also, another disadvantage of PMMA is that it can not be sterilized by autoclaving because of its relatively low glass transition temperature (Tg=105° C). Because of this, other polycarbonate (PC) polymers having higher glass transition temperature (Tg=150° C) have been considered as replacements for PMMA [19].

Presently, in cataract surgery, a new technology called phacoemulsification has been adopted to remove the natural lenses through a small incision ($\leq$4 mm). Phacoemulsification uses high-frequency ultra-sound waves to emulsify the natural cataractous lens [20]. Since this method permits a smaller incision to be made than in the past, it can minimize complications such as wound-induced astigmatism and achieve early rehabilitation. However, the diameter of PMMA IOL optics, usually 5-7 mm, is larger than the size of the incision. This led to the use of foldable IOLs which can be inserted through the small incision in their folded state and then expand to full size. Two foldable materials, polydimethylsiloxane (PDMS) and polyhydroxyethylmethacrylate (PHEMA), have been utilized in intraocular lens and have been evaluated for two decades[21]. Both polymers can be sterilized by autoclaving which is more convenient and is safer than ethylene oxide gas sterilization. The structures of PMMA, PC, PDMS, and PHEMA are shown in Figure 2-2.

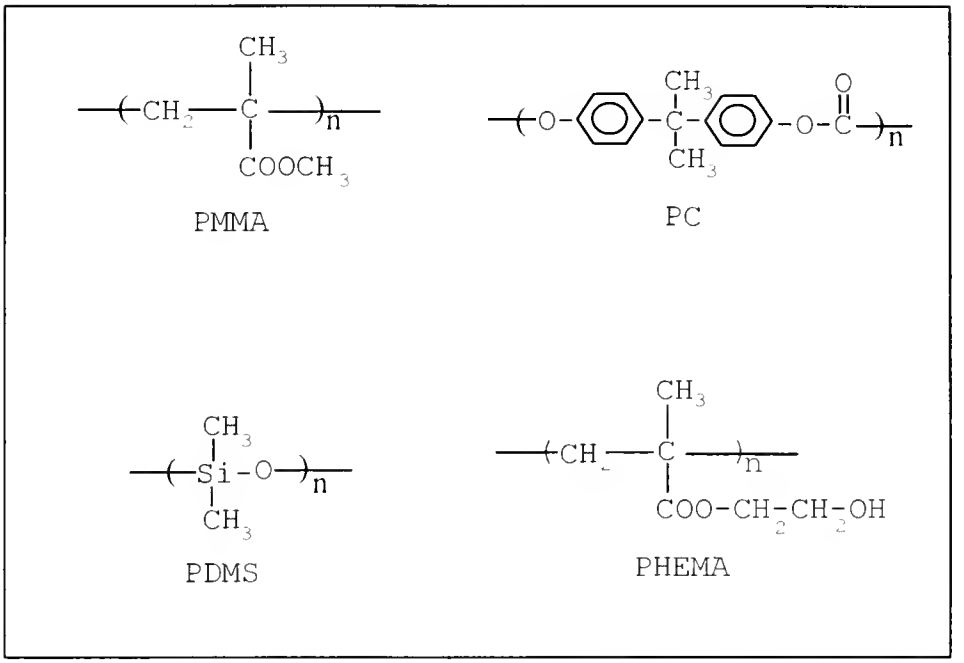

Figure 2-2. Chemical structure of IOL materials.

Silicone (PDMS) IOLs were approved by the Food and Drug Administration (FDA) and are currently commercially available [22]. Silicone is a hydrophobic, soft, and optically clear elastomer with a glass transition temperature of -123° C. It forms a smooth surface without polishing [23]. Silicone is biologically inert and has a long history of implantation into biological tissues [24]. In clinical studies, silicone IOLs showed good stability and tissue tolerance [25,26]. However, several problems have been associated with silicone IOLs. These problems include tissue irritation, adhesion and damage to living tissues due to hydrophobic interactions, and loss of IOL optical properties due to high lipid absorption and impurities [27-29].

Polyhydroxyethylmethacrylate (PHEMA) has also been evaluated as a potential material for flexible IOL design [30,31]. PHEMA is a cross-linked hydrogel polymer which will swell in water but does not dissolve. Hydrated PHEMA is a hydrophilic, soft, and optically clear polymer. PHEMA IOLs showed good tissue tolerance, stability, and visual acuity [31]. In vitro studies indicate that PHEMA has lower lens epithelial cell adhesion than PMMA and PDMS [32]. However, PHEMA lens, like many hydrogels, could result in untimely unfolding and lens tears if it was not properly handled [33].

In contrast, PMMA and PDMS exhibit good mechanical strength, but lack a gentle hydrophilic surface. It is

obvious that a better combination can be created by surface modification of PMMA or PDMS with hydrophilic hydrogel monomers. While the PMMA or PDMS substrates can provide the necessary mechanical strength, the hydrophilic surface layer will supply a gentle interface to the living tissue.

Hydrophilic surface modification of PMMA IOLs has been extensively studied in this research group for the past decade. PMMA IOL surfaces have been covalently grafted with PVP and other hydrogels using the gamma-induced graft polymerization technique. In vitro studies showed that PVP modified PMMA IOLs can significantly reduce lens epithelial cell adhesion, corneal endothelium damage, and iris abrasion [7,8]. Also, in rabbit lens cortex-induced inflammation models, PVP modified PMMA IOLs yielded clean, cell-free lens surfaces 3 weeks after surgery [34,35]. These results indicate that the biocompatibility of PMMA IOLs can be significantly improved by hydrophilic surface modification.

2.1.2 Interfacial Phenomena and Biomaterials

In considering the interfacial phenomena between implant surfaces and biological environment, two major events must be considered: 1) biomolecular interactions such as protein adsorption; and 2) cellular interactions such as platelet adhesion and lens epithelial cell adhesion and spreading [36]. The first event is protein adsorption onto the biomaterial surfaces, which occurs instantaneously when

biomaterials are placed in contact with biological environments and continues until a protein film has covered the biomaterial surface [37,38]. The second event, adhesion of cellular components, may occur during formation of the protein film or after this film has built up to a critical thickness, which varies for different substrates, depending on the surface properties of the materials [38].

Protein adsorption plays an important role in determining the biocompatibility of implants. The amount of protein adsorbed onto a biomaterial surface is strongly dependent upon the implant surface properties such as wettability, critical surface energy, and interfacial free energy. Several studies have demonstrated that the extent of protein adsorption decreases from hydrophobic surfaces to hydrophilic surfaces [38-41]. Absolom et al. [37], comparing several different proteins, also showed that the most hydrophobic protein, fibrinogen, adsorbs to the greatest extent to all surfaces tested, whereas the most hydrophilic protein, bovine serum albumin, adsorbs to the least extent to all the surfaces. Upon adsorption, the first layer of proteins may denature on the solid surface due to surface-induced conformational changes [38]. Therefore, the influence of the substrate is conveyed to the cellular components through the denatured protein film.

Biocompatibility or biotolerability of implants is measured by the degree of their interaction with the biological environment. The biological response of

biomaterials is an extremely complex phenomenon and is influenced by the surface properties of the biomaterials, interfacial properties of the cellular components, biomolecule adsorption, and surface-induced biomolecule conformation changes. Adhesion of cellular components onto biomaterial surfaces may cause inflammation or blood clotting if the biomaterial surface is exposed to the blood. The empirical relation between surface properties with the biological environment have been described in a variety of situations. Several hypotheses, based upon general physicochemical considerations, have been formulated to explain the interfacial properties of these biomaterials. Some of the most interesting of these theories include the moderate surface energy model of Baier [42], the minimum interfacial tension hypothesis originally proposed by Andrade [39], and modifications of these ideas [38]. Unfortunately, none of these theories adequately predict the long-term biological response of biomaterials. It is very difficult to use a single hypothesis to predict these complex interactions between biomaterials and biological environments. Furthermore, various hypotheses based on *in vitro* observations have often conflicted with long term *in vivo* studies.

Despite the contradictions, hydrophilic surfaces are still very promising in terms of biocompatibility. Soft and slippery hydrophilic surfaces are more similar to the natural tissue, and their nonsticking characteristics can

reduce protein and cell adhesion [38-44]. Looking for unique hydrophilic structures to improve biocompatibility or blood compatibility is a challenging task.

2.2 Radio-Frequency (RF) Glow Discharge Plasma

Plasma treatments are widely used to improve the wettability, bonding capability, and biocompatibility of polymers. Three major effects are observed in plasma treatments: ablation, cross-linking, and oxidation to a depth of typically 50-500 Å [45]. Wettability can be improved by introducing polar oxygen and nitrogen groups onto polymer surfaces via nonpolymer-forming plasma (e.g., plasma of water, helium, argon, nitrogen, oxygen). The detailed mechanisms in plasma reactions are complex and are not well understood. Energy can be transferred from a plasma to a polymer surface through optical radiation, through neutral particle fluxes, and through ionic particle fluxes [46]. Yasuda [47] suggested two major energy transferring reactions occur during plasma treatment. These reactions include 1) direct reaction of active species with polymer, and 2) reaction of polymer free radicals with oxygen and nitrogen upon exposure to the air after treatments [47]. Therefore, plasma treatments often introduce polar groups onto the polymer surface even when the plasma is an inert gas. The results of plasma experiments strongly depend on the experimental parameters

such as pressure, field strength, gas velocity, and geometry of reactor [48].

Plasmas can be classified into thermal plasma, cold plasma, and hybrid plasma. Cold plasma (glow discharge in reduced pressure) and hybrid plasma (corona discharge at atmospheric pressure) are mainly used for plasma treatments. Glow discharge plasmas can be generated between point-plate, or wire-plate electrodes, using dc or ac (low frequency; 60 Hz) voltages of 500 to several thousand. On the other hand, electrodeless glow discharges are generated by high frequency oscillations introduced into the gases by means of coils wound around reactors. High frequency oscillations are supplied by a spark-gap generator (10-50 kHz), radio-frequency generator (1.5-50 MHz), or microwave generator (150-10,000 MHz) [49]. Radio-frequency (RF) plasma has received the most attention in biomedical engineering, and is currently used industrially also.

RF plasmas are ionized gases that contain UV radiation ions, electrons, radicals, excited molecules, and atoms [46,49]. Typical examples are

$$He \longrightarrow h\upsilon + He^{*} + He^{+} + e^{-} \qquad (2\text{-}1)$$

$$O_2 \longrightarrow h\upsilon + O_2^{*} + O + O_2^{+} + O^{+} + e^{-} \qquad (2\text{-}2)$$

where an asterisk denotes a metastable neutral species. The gaseous ions and molecules are at ambient temperature, whereas the electrons are at tens of thousands degrees

Kelvin. Chemical reactions are mainly induced by UV radiation, free radicals, and the metastable neutrals [50,51]. In the initiation step, polymer radicals are formed by several different processes [46]:

By UV radiation:

$$RF \xrightarrow{h\nu} R\cdot + F\cdot \qquad (2\text{-}3)$$

By excited noble gas atoms:

$$RF \xrightarrow{He^*} \begin{cases} RF^* + He & (2\text{-}4) \\ R\cdot + F\cdot + He & (2\text{-}5) \\ R_1^{\cdot} + R_2^{\prime} + He & (2\text{-}6) \end{cases}$$

By oxygen radicals:

$$RF \xrightarrow{O\cdot} \begin{cases} R\cdot + F\cdot + O_2 & (2\text{-}8) \\ R_1^{\cdot} + R_2O^{\cdot} & (2\text{-}9) \end{cases}$$

By hydrogen radicals:

$$RF \xrightarrow{H\cdot} R\cdot + HF \qquad (2\text{-}10)$$

The polymer radicals undergo chain scission, radical transfer, oxidation, disproportionation, and recombination. These reactions give rise to a combination of degradation, ablation, oxidation, and cross-linking in the surface layer [45]. Thus, RF plasma is not only able to etch or cross-link the surface of polymers, but also can introduce

functional groups or polar groups in the top surface layer. The introduction of functional groups onto a biomaterial surface will influence protein adsorption and cell adhesion to that surface. In addition, these groups may provide sites for the subsequent covalent coupling of biomolecules or polymers. However, RF plasmas have several disadvantages. These drawbacks include the following: RF plasma has to be carried out under reduced pressure; the life of polar or functional groups on polymer surface is short (from minutes to months) depending on the surface dynamic properties of polymer and the chemical-physical environment; the kinetic mechanisms are very complex and difficult to predict; and the stoichiometry of plasma products is often not related to the chemical structure of starting reactants [47].

2.2.1 The effects of Plasma Treatment on Polymers

RF plasma possesses the following characteristic features: 1) the radiation effect is limited to the surface, so that the depth of penetration is much smaller than with other penetrating radiation and 2) the intensity at the surface is generally stronger than with the more penetrating radiation [47]. Therefore, the plasma discharge process provides a unique and powerful means for altering the surface properties of biomaterials without changing their bulk properties.

2.2.1.1 The Effects of Plasma on PP

Plasma treatment of PP was first studied by Bamford and Ward [52]. The electron spin resonance (ESR) studies on plasma treated PP have shown that the radical formation occurs mainly at the tertiary carbon. Peroxy-radicals (also detected by ESR) were introduced when the plasma treated PP was admitted to air. The peroxy-radicals in PP appear to be stable with little decay in concentration after 17 hrs at room temperature. Hall et al. [53] showed that adhesive-bond strength was dramatically improved when PP was pre-treated with oxygen plasma. Blais and Wiles [54] also showed that the adhesion between nylon and PP was markedly improved by a brief corona discharge treatment of the films in nitrogen prior to coating. Attachment of amino groups to PP surface was investigated by Hollahan et al. [55]. Amino groups were attached to PP surfaces either by NH_3 plasma or by N_2/H_2 mixture plasma. The reaction for amino group attachment is described as in equation (2-11).

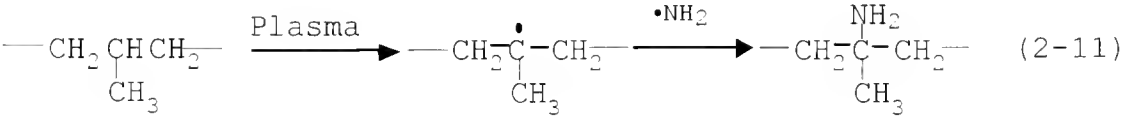

(2-11)

Following the plasma treatment, heparin was attached to PP surface through ionic bonding to the quaternary sites produced from the amino groups.

2.2.1.2 The Effects of Plasma on PMMA

Plasma treatment of PMMA has been extensively studied by Vargo et al.[56]. The surfaces of PMMA films were treated by O_2/H_2O and H_2O radio-frequency glow discharge (RFGD) plasmas and characterized with XPS, ISS (low energy ion scattering), FTIR/ATR, and critical surface energy from contact angle measurements. XPS and ISS show that the depth of treatment for O_2/H_2O and H_2O plasmas is less than 20 Å. Their results for XPS, ISS, and FTIR/ATR also confirm that an O_2/H_2O RFGD is more reactive than the pure H_2O discharge because the C/O ratio on the O_2/H_2O plasma treated surface is less than the ratio on the pure H_2O plasma treated surface. However, the contact angle measurements show that the H_2O plasma treated surfaces have a lower contact angle (a more polar surface) than the O_2/H_2O plasma treated surfaces. Based on the experimental results, Vargo et al. proposed two simple models for the surface modification of PMMA by O_2/H_2O and H_2O plasmas. These models are illustrated in Figures 2-3 and 2-4. Hollahan et al. have also tried to attach heparin to PMMA surfaces by first plasma treating with N_2/H_2 and NH_3 plasmas [55].

2.2.1.3 The Effects of Plasma on PDMS

Hollahan and Carlson [57] have studied the surface oxidation of PDMS using RFGD plasmas. Following the plasma treatments, the PDMS surfaces were examined by FTIR (internal reflection infrared) spectroscopy. The results from IR spectra indicate that RF oxygen plasma and corona

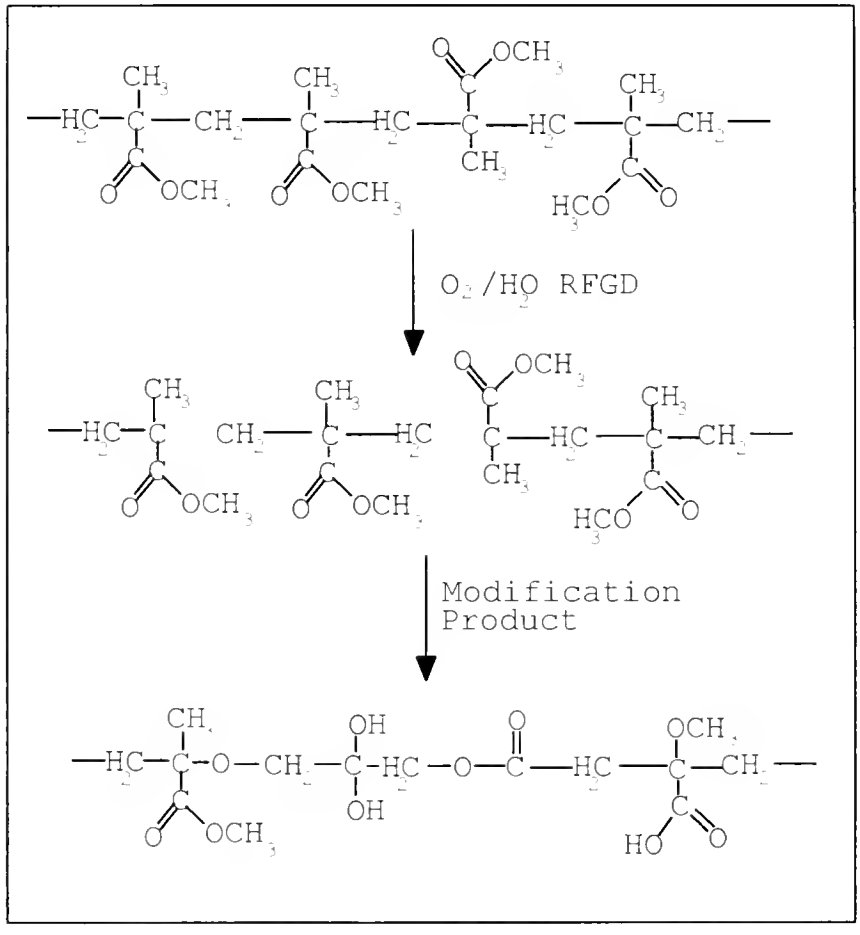

Figure 2-3. O_2/H_2O RFGD modification of PMMA model. [56]

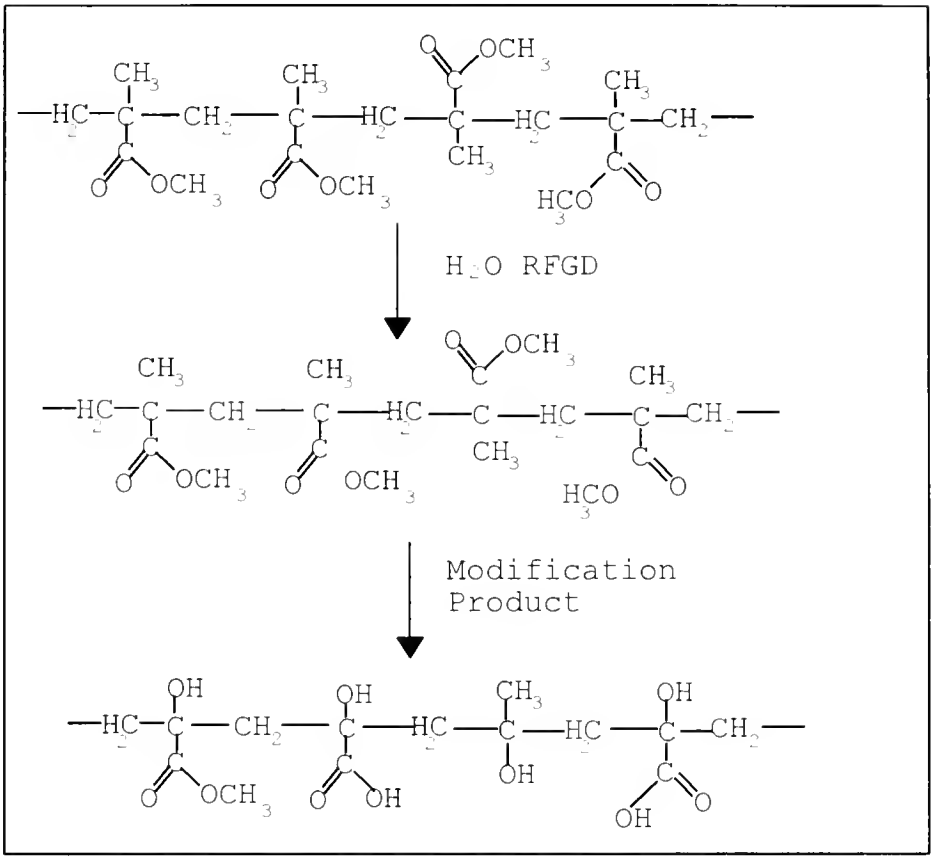

Figure 2-4. H_2O RFGD modification of PMMA model. [56]

treated PDMS exhibit a high density of hydroxyl groups and extensive hydrogen bonding. The IR data also suggested that -OH formation in PDMS by RF oxygen plasma treatment is predominantly of a $-CH_2OH$ structure rather than -SiOH. The development of $-SiCH_2OH$ structure takes place by the sequences in Figure 2-5.

In the case of corona treatment, the localized high temperature at a few plasma surface regions could strip off methyl groups and produce -SiOH groups. Cross-linking processes from radical recombination also possibly occurs via the mechanisms in Figure 2-6.

Similar results were reported by Triolo and Andrade [58] on surface modification of PDMS using RFGD helium plasma. The shift of XPS C1s peak revealed that the carbon became more bound to oxygen rather than to silicon alone as a function of treatment time.

Sowell et al. [59] also studied surface modification of RTV silicone using oxygen and argon RF plasma. The wettability and bond strength were drastically improved by plasma treatments. However, they did not address chemical analysis in their studies.

2.2.1.4 The Effects of Plasma Treatment on PC

Surface modification of PC using RFGD oxygen plasma was first studied by Hansen et al. [60]. Rate of weight loss was monitored during plasma treatment. The oxidized surface layers had remarkably low contact angles with water.

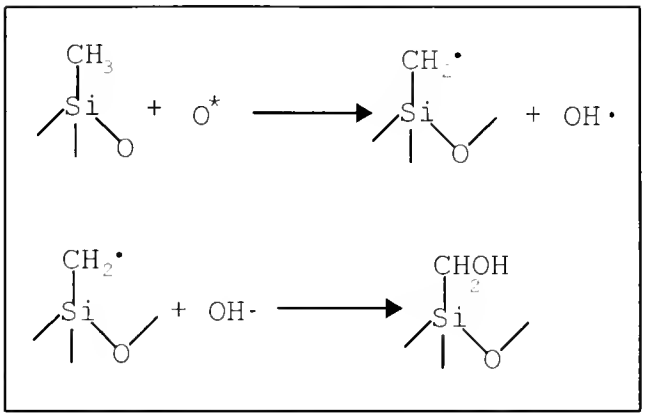

Figure 2-5. Oxygen RFGD modification of PDMS model. [57]

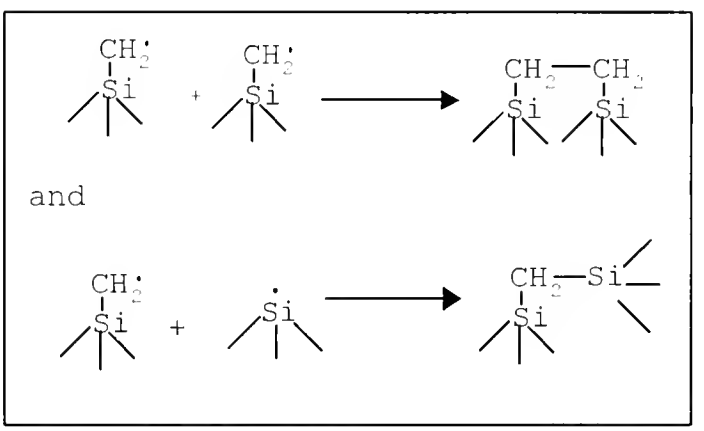

Figure 2-6. Cross-linking model of corona treated PDMS. [57]

The results suggested that the initiation stage during oxidation by atomic oxygen is a direct and rapid attack on the polymer which accounts for a great portion of the overall oxidation of the polymer.

An ESCA (XPS) investigation on surface modification of PC using hydrogen and oxygen RFGD plasmas has been conducted by Clark and Wilson [61]. The data indicate that the effect of hydrogen plasma treatment is to reduce the level of oxygen functionality. On the other hand, oxygen plasma treatment results in the formation of carbonyl and carboxylate structural features. In addition, cross-linking processes might occur during oxygen plasma treatment because there is an increase in the number average of carbon atoms in the oxygen-plasma-treated samples.

2.2.1.5 The Effects of Plasma Treatment on FEP

Fluorinated ethylene-propylene copolymer (FEP, Teflon) is well known for its chemical inertness and thermal stability. Surface treatments of FEP are therefore more difficult than other polymers. Plasma treatments of FEP have been studied by several authors [62-64]. FEP surfaces were treated with helium and oxygen plasmas to improve their wettability and bond strength [62,63]. Oxygen plasma treatment led to noticeably weaker bond strength than helium plasma treatment. The contact angle measurements showed that helium plasma decreased the contact angle of FEP while oxygen plasma had no effect on this property. This could

explain the difference in bond strength between oxygen and helium treatments.

Triolo and Andrade [58] also did extensive work on surface modifications of FEP using RFGD helium plasma treatment. The FEP surfaces were characterized utilizing XPS, SEM, and contact angle measurements before and after plasma treatment. The results showed that the carbon and oxygen contents at the surface increased with increasing RFGD treatment time, and the relative amount of fluorine decreased. The C1s peak located between the C-H and $C-F_2$ peaks in the XPS spectra of RFGD plasma treated FEP indicated the formation of carbon-oxygen and C-FH functionalities.

2.3 Surface Modification of Polymers

Biocompatibility of medical implants or devices is critically dependent upon the interactions between the living tissue and the surface of implants. Surface modification of polymers has therefore become one of the most important approaches for improving the biocompatibility. A variety of techniques for surface modification of polymers has been investigated over the past years. These techniques include gamma or e-beam induced graft polymerization, chemical means, UV coating, and plasma coating. The utilization of gamma induced graft polymerization for biomedical applications has several

advantages over other techniques. These advantages include the following: 1) no chemical initiators or external heat is needed to initiate or assist the reaction; 2) gamma radiation can generate the free radicals in monomers and activate polymeric substrates simultaneously; 3) complex geometries can be uniformly modified; 4) extremely clean processes can minimize the presence of toxic residual materials, and 5) grafting procedures are simple, making production cost very low.

Besides, gamma induced graft copolymerization has been used to increase surface wettability, dyeability, solvent resistance, light resistance, and other properties considered useful for many industrial applications [65]. The two major techniques generally used are indirect or preirradiation methods, and simultaneous or mutual irradiation of substrate and monomer. One-step simultaneous irradiation is probably the simplest technique and was the method of choice in this research.

2.3.1 Gamma Induced Surface Modification of Polymers

2.3.1.1 Radiation Effects in PMMA

The effects of radiation on PMMA have been extensively studied and reported in various publications [9,66,67]. The primary effect of gamma irradiation on PMMA is chain scission degradation with the accompanying formation of free radicals [68,69]. Color changes may be noticeable at

moderate radiation doses ($\leq$ 3 Mrad)[9]. Several mechanisms have been proposed by Kircher et al. and also by Todd [68,69]. These mechanisms are illustrated in Figure 2-7. Each main chain break liberates approximately 0.8 ester side groups [67]. In addition, hydrogen abstraction from polymer chain or formation of $CH_3\cdot$ also initiates the main chain scission [68]. Electron spin resonance (ESR) spectra indicated that the primary free radical (IV) appears mainly in the gamma irradiated PMMA, but the free radical (V) has never been observed [68,70,71]. If the free radical (V) forms, it may decay by a hydrogen atom abstraction from a neighboring chain [67]. The G value (sessions per 100 eV of energy absorbed) for PMMA is about 1.6 [66].

2.3.1.2 Radiation Effects in PP

When the irradiation of PP takes place in the presence of air, it tends to undergo a very marked oxidative degradation, even at fairly low doses [9]. The degradation includes discoloration and oxidative embrittlement [72]. The results of ESR indicate that the predominant type of radical formed at low temperature and low dose ($\leq$ 5 Mrad.) is most likely the free radical (I), or the free radical (II) or both [73-75]. At room temperature, the thermally stable radicals are probably either allylic radicals (III) or (IV), or alkyl radicals (I) [73,76]. The sensitivity of PP to oxidative degradation results from the large number of tertiary hydrogens within the polymers [9].

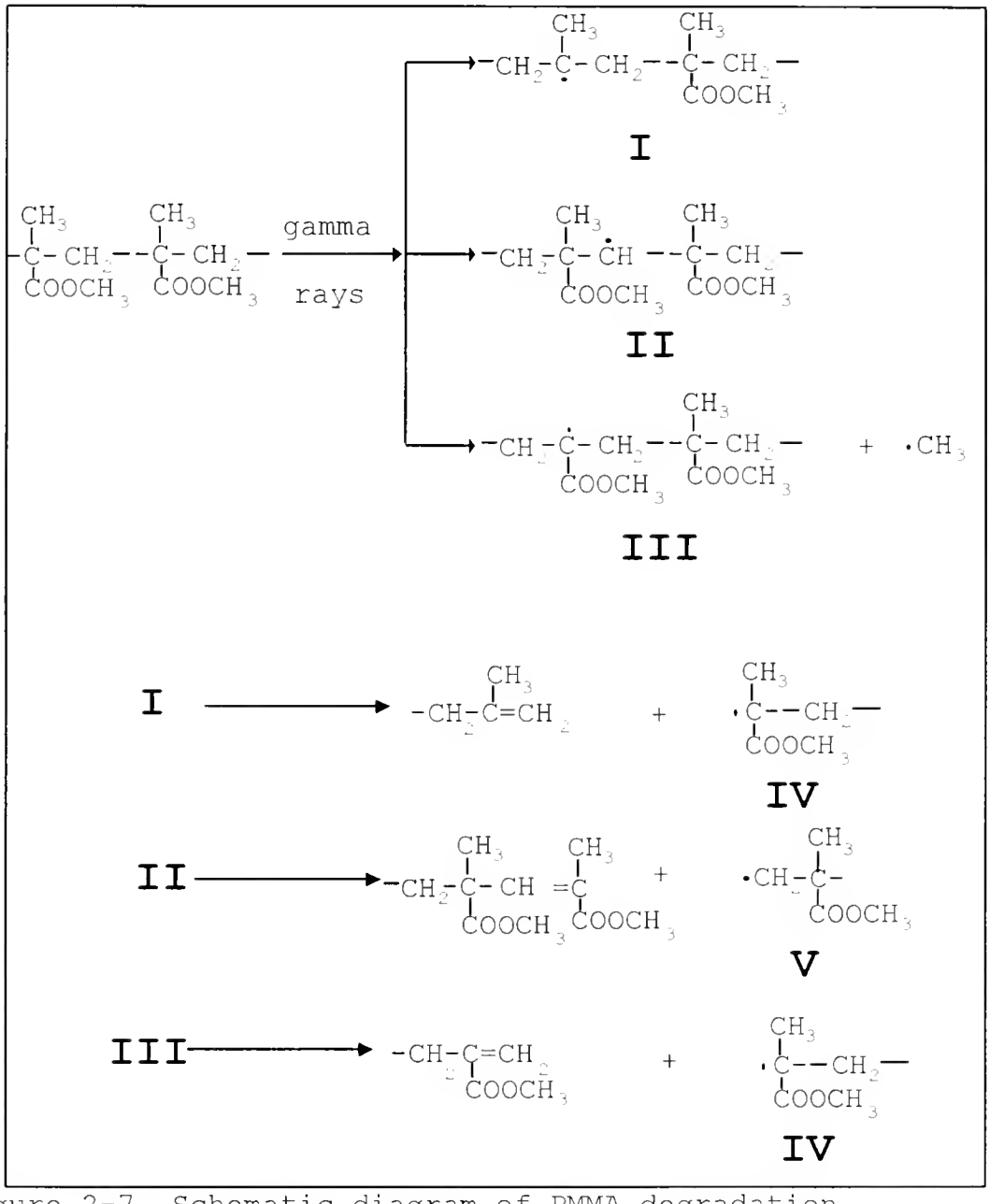

Figure 2-7. Schematic diagram of PMMA degradation mechanisms. [68,69]

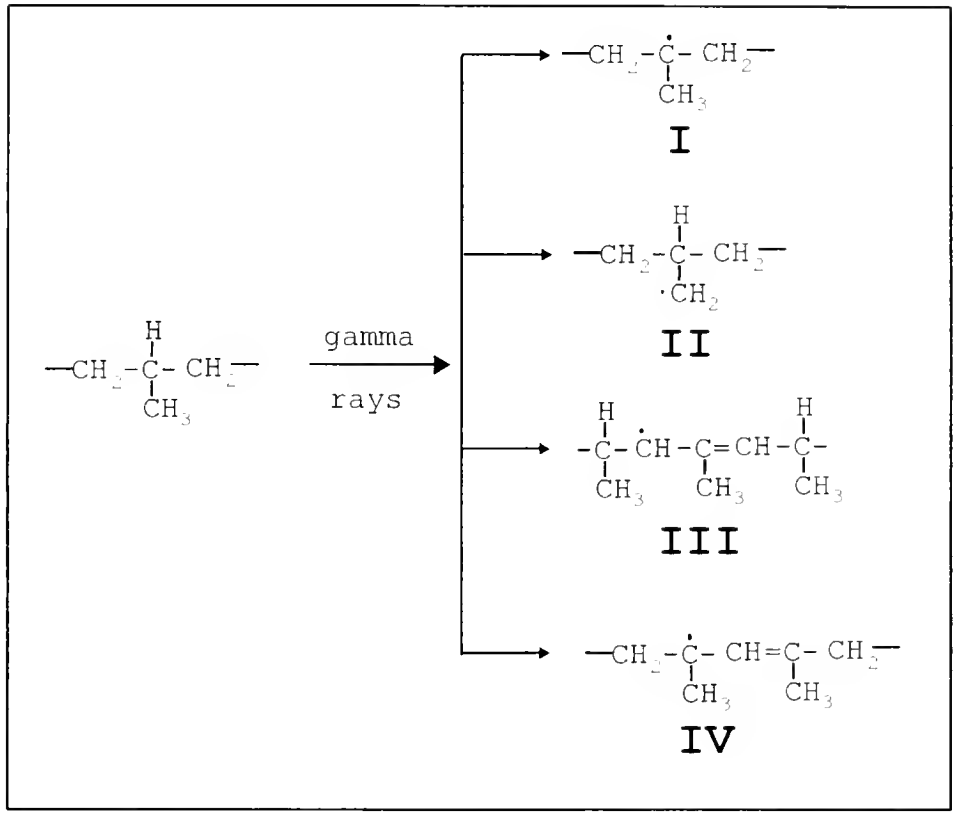

Figure 2-8. Schematic diagram of PP degradation mechanisms. [73-75]

Hydroperoxides may be formed at the tertiary carbon sites, when the PP is irradiated in air or oxygen [9].

2.3.1.3 Radiation Effects in PDMS

Poly(dimethyl siloxane) (PDMS) is relatively radiation stable but tends to cross-link when it is subjected to a high gamma irradiation dose [9]. The yield of cross-links (G) is about 2.5 - 4.5 cross-links per 100 eV absorbed [77,78]. Hydrogen, methane and ethane gases are evolved [9]. Studies using ESR indicate that the C-H and Si-C bonds are easy to fracture, leading to the formation of hydrogen atoms and methyl radicals [79,80]. The schematic diagrams of radical formation are illustrated as follows:

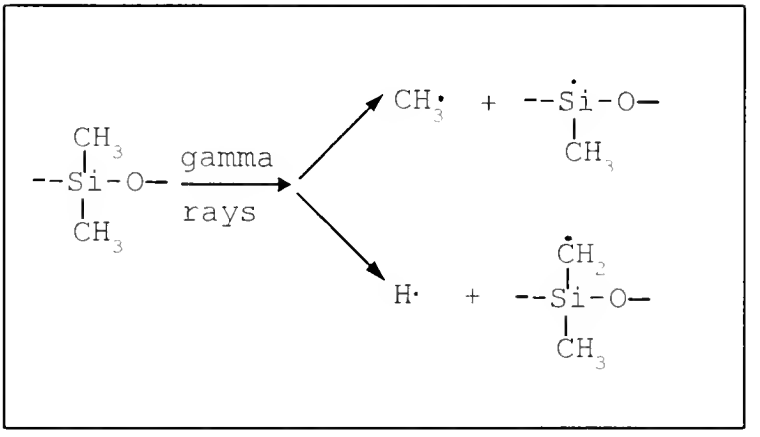

Figure 2-9. Schematic diagram of PDMS degradation mechanisms. [79,80]

2.3.1.4 Radiation Effects in PC

Polycarbonate (PC) contains aromatic rings in the main chain structure and shows good radiation resistance up to high radiation dose (ca. 100 Mrad) [81]. Acierno et al.

[82] have studied the radiation effects on PC and measured the melt flow index and intrinsic viscosity of irradiated PC samples. All the data show that a cross-linking effect predominates at small doses (up to 3 Mrad), while main chain scission occurs at higher doses (> 3 Mrad). The value of G (scissions per 100 eV of energy absorbed) is 0.14 in oxygen and 0.09 in vacuum [83]. The mechanisms of cross-linking and main chain scission in PC are not well established, but may occur as indicated in Figures 2-10 and 2-11.

2.3.1.4 Radiation Effects in Fluoropolymers

Fluorinated polymers can be extremely sensitive to radiation and are among the poorest known polymers in terms of radiation stability [9,81]. For example, PTFE shows significant radiation damage even at a fairly low dose of 0.04 Mrad. [81]. However, FEP polymer is more radiation resistant than PTFE and can be sterilized without extensive damage. Other fluoropolymers, such as poly(vinyl fluoride), and poly(vinylidene fluoride), show much less sensitivity to radiation. Poly(vinylidene fluoride) (PVDF) were found to cross-link at high gamma doses [68].

ESR spectra of PTFE indicate that the free radical (I) and the free radical (II) are yielded from the main chain scission [84,85].

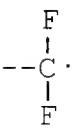

(I)

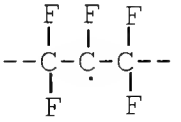

(II)

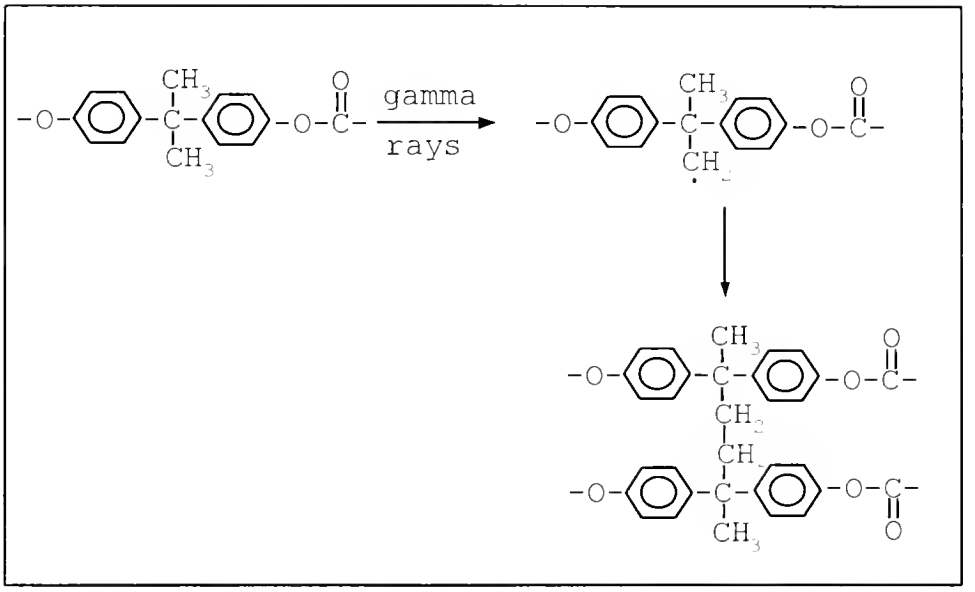

Figure 2-10. Schematic diagram of PC cross-linking mechanisms.

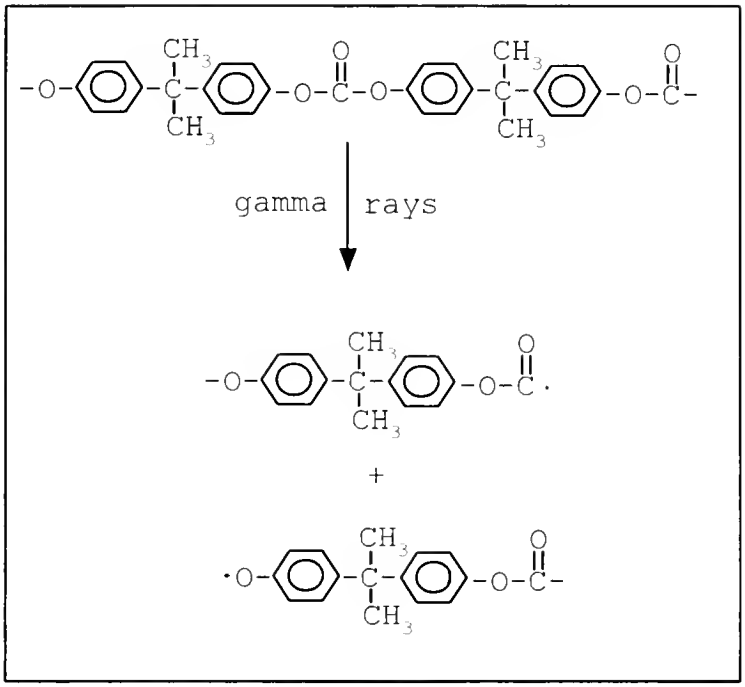

Figure 2-11. Schematic diagram of PC degradation mechanisms.

The presence of double bonds of -CF=CF- and -CF=CF2 in irradiated PTFE was suggested by Ryan [86] on the basis of IR analysis.

2.3.2 Gamma-Induced Graft Copolymerization of Vinyl Monomers onto Polymeric Substrates

Radiation induced grafting is a very efficient method for preparing polymers with specific surface properties. This method has been used in several studies for the synthesis of polymers for biomedical applications. The grafting reaction can either be carried out homogeneously through thick layers of polymer, or limited to a surface zone of any desired thickness. Among the various methods for radiation grafting, four have received special attention. These are 1) the direct radiation grafting of a vinyl monomer onto a polymer; 2) grafting onto radiation-peroxidized polymers; 3) grafting initiated by trapped radicals; and 4) the intercross-linking of two different polymers [9]. It was shown that most radiation induced grafting proceeds by free radical mechanisms [87].

Grafting onto polymers that have been radiation-peroxidized or via trapped radicals usually requires a high radiation dose to generate the radicals or peroxides on the polymer. However, surface uniformity of the graft and reproducibility are often poor with either methods. Furthermore, the high dose of radiation may cause permanent damage to polymers.

Very low dose (< 0.2 Mrad) direct radiation grafting of vinyl monomers onto polymers has been developed in this laboratory. This is particularly beneficial with bioactive molecules involved in medical applications. Grafting is accomplished in only a single step, and the graft surfaces are much more uniform than with the other methods mentioned above. However, one problem with this method can be the gelation or homopolymerization of the monomer solution before grafting is completed [9,88]. Gelation or homopolymerization of monomer limits the grafting by restricting monomer diffusion to the polymer surface. Gelation also makes sample handling and washing difficult. The use of selective inhibitors has been suggested to minimize homopolymerization in this method [89,90]. Swelling agents have been used to assist monomer diffusion to the polymer and open the physical structure of the polymer [91]. Since the residues of chemical inhibitors and swelling agents may cause unnecessary biological responses after implantation, the use of these chemicals may be problematic for biomedical applications.

Yahiaoui [6], in this laboratory, has studied the "presoak method" in order to help monomer diffusion into the polymer and to increase the grafting yield without using chemical inhibitors or swelling agents. In the "presoak method" [6], polymeric substrates are first soaked in aqueous monomer solutions at various concentrations, temperatures, and times. Soon after presoaking, samples are

transferred to fresh monomer solutions and irradiated by Cobalt-60 gamma radiation or electron beam in an argon atmosphere. Results indicate that the presoak method improves grafting yields by creating a monomer-rich interface and allowing the monomer to diffuse into the polymeric substrate. An interpenetrating network (IPN) type of graft is obtained by this method.

The use of polyvinylpyrrolidone (PVP) in graft copolymerization of N-vinylpyrrolidone onto polymeric substrates was investigated in this research. Poly(vinyl pyrrolidone) (PVP) is a linear and water soluble polymer. PVP can wet most hydrophobic polymeric surfaces and serves as an interfacial mediator between a polymeric surface and the monomer solution. Consequently, interfacial thermodynamic compatibility between polymeric surface and the monomer solution may be improved by adding PVP into the monomer solution. In addition, the presence of both PVP and NVP molecules in the same solution may inhibit the solution gelation during gamma-induced graft copolymerization. The large molecules of PVP may also intercross-link onto polymeric surface to make the graft more stable. Mentak [92], in this laboratory, has shown that the PVP/NVP modified PDMS surface is more stable than the NVP modified PDMS surface.

2.3.3 Plasma/Gamma Induced Graft Copolymerization Vinyl Monomers onto Polymeric Substrates

Plasma treatment of polymeric substrates has been extensively reviewed in section 2.2. Depending on the nature of the gas molecules, plasma reactions can be divided into two categories: 1) plasma polymerization in which a cross-linked thin polymeric film is deposited on the substrate surface and 2) plasma treatment in which intensive oxidation or cross-linking is introduced on the substrate surface [11]. In addition, several investigators have utilized the free radicals or peroxides generated by plasma treatment to initiate graft copolymerization of a vinyl monomer onto a polymeric substrate [93-96]. Thus, plasma-induced graft copolymerization was performed by exposing the substrate to a glow discharge plasma of inert gases followed by contact with monomers, with or without allowing the plasma treated polymers to be first exposed to air or oxygen.

In this laboratory, Yahiaoui [6] investigated a novel technique, a "Plasma/Gamma method" for graft copolymerization. This method combines the two most powerful surface modification techniques. At first, polymeric substrates are treated with a glow discharge water plasma. After plasma treatment, substrates are exposed to air and then transferred to an aqueous monomer solution. Finally, the plasma treated substrates in a monomer solution are irradiated in a cobalt-60 gamma source. The purpose of

the water plasma pretreatment is to introduce polar oxygen-containing functional groups on the polymer surface in order to enhance the interfacial thermodynamic compatibility between a hydrophobic surface and a hydrophilic monomer solution. Results using the "Plasma/Gamma method" demonstrated that it can improve graft efficiency and produce a very thin, high quality, and stable graft on a polymer surface. This method was therefore also investigated further in this research.

CHAPTER 3
MATERIALS AND METHODS

3.1 Materials

3.1.1 Substrates

Polymeric substrates used for this study include PMMA (Perspex® acrylic sheet, from ICI), PDMS (KE-1935, from Shin-Etsu Silicones of America), PP (from Himont), PC (Makrofol De, from Bayer), PVDF (Kynar® 730, from Pennwalt), and FEP (Teflon®, from Dupont). Their chemical structure and physical properties are shown in Figure 3-1 and Table 3-1, respectively. Substrates were cut into rectangular strips with an approximate dimension of 1 cm x 2.5 cm. For XPS analysis, substrates were cut into 1 cm x 1 cm square slabs.

3.1.2 Monomers

Hydrophilic vinyl monomers used for graft polymerization included 2-N-vinylpyrrolidone (NVP, from Kodak) and dimethylacrylamide (DMA, from Polyscience). Monomers were purified by distillation under reduced pressure (1-2 mmHg at 55-60 °C) and stored at 4 °C until

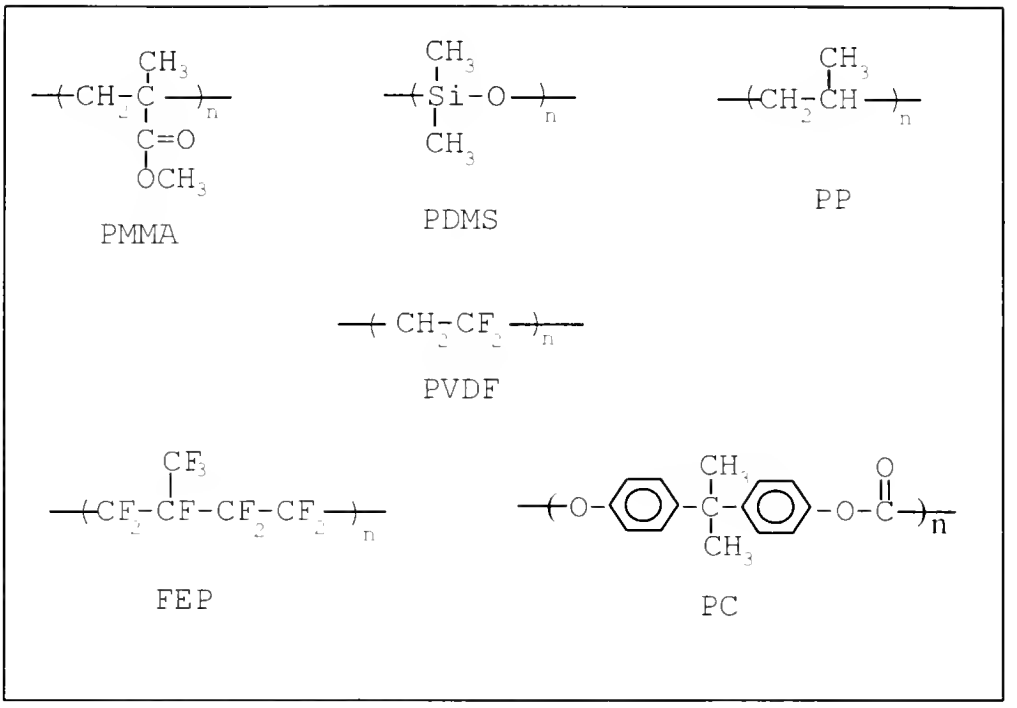

Figure 3-1. Chemical structures of polymeric substrates.

Table 3-1. Physical and mechanical properties of polymeric substrates. [97]

Property	PMMA	PDMS	PP	PC	PVDF	FEP
Density (g/cc)	1.18	1.14	0.91	1.2	1.75	2.12
Tg (^{o}C)	105	-123	-19	145	-39	--
Modulus (Kpsi)	325	1.16	165	345	220	50
Tensile strength (Kpsi)	8	0.85	4	9	5.5	2.7
Contact angle (^{o}) (with water)	70	90	90	83	90	110
Refractive index	1.49	1.43	1.49	1.58	1.42	1.34
Optical transparency	clear	clear	trans-lucent	clear	opaque	trans-lucent

used. The structures of the monomers are shown in Figure 3-2. Poly(vinyl pyrrolidone) (PVP, Plasdone K-90, from GAF chemicals), a part of monomer in the PVP/NVP system, was used without further purification. Plasdone K-90 has a weight average molecular weight of 1.2×10^6 and a number average molecular weight of 3.6×10^5.

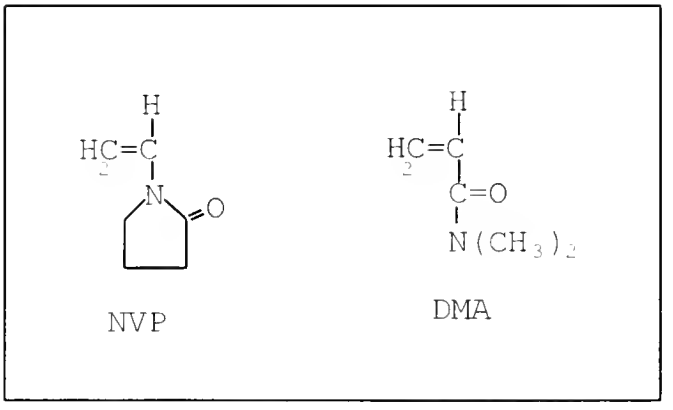

Figure 3-2. Chemical structures of monomers.

3.2 Methods

3.2.1 Substrates Preparation

Substrates of PMMA, PP, PC, PVDF, and FEP were precut into strips, individually sonicated in a 0.1% Triton X-100 (Fisher) aqueous solution for 30 minutes, rinsed in Ultrapure® water, and repeatedly sonicated in Ultrapure® water three times for ten minutes each. PDMS slabs were

sonicated two times for 20 minutes each in a 1:1 acetone/ethanol mixture. After cleaning, all samples were dried under vacuum for 6 hours at 60^{o} C, then stored in a desiccator until further use.

3.2.2 Plasma/Gamma Induced Surface Modification

3.2.2.1 Radio Frequency Water Plasma Treatment

The schematic diagram of the RF plasma system is shown in Figure 3-3. The RF plasma system consists of a vertical "bell-jar" reaction chamber, a monomer/gas inlet system, a vacuum system with nitrogen cold trap, a RF power generator, and a matching network. The reaction chamber was inductively coupled by an eight-turn copper tubing to the RF power generator (RF plasma products, Inc., model HFS 401 S), which operates at a fixed frequency of 13.56 MHz with a maximum output of 500 watts. The matching network was used to match the impedance of plasma discharge to the RF power generator. The flow rate of gas/monomer vapor was controlled by a micro-metering valve (Nupro). The vacuum pressure of the reaction chamber was monitored by a thermocouple vacuum gauge (Adap Torr®, Vacuum General Inc., model ACR-26) located underneath the chamber stage. The reaction chamber was evacuated by a mechanical pump through a liquid nitrogen cold trap.

Before plasma treatment, the reaction chamber was cleaned with 2-propanol/KOH solution, then treated with 50

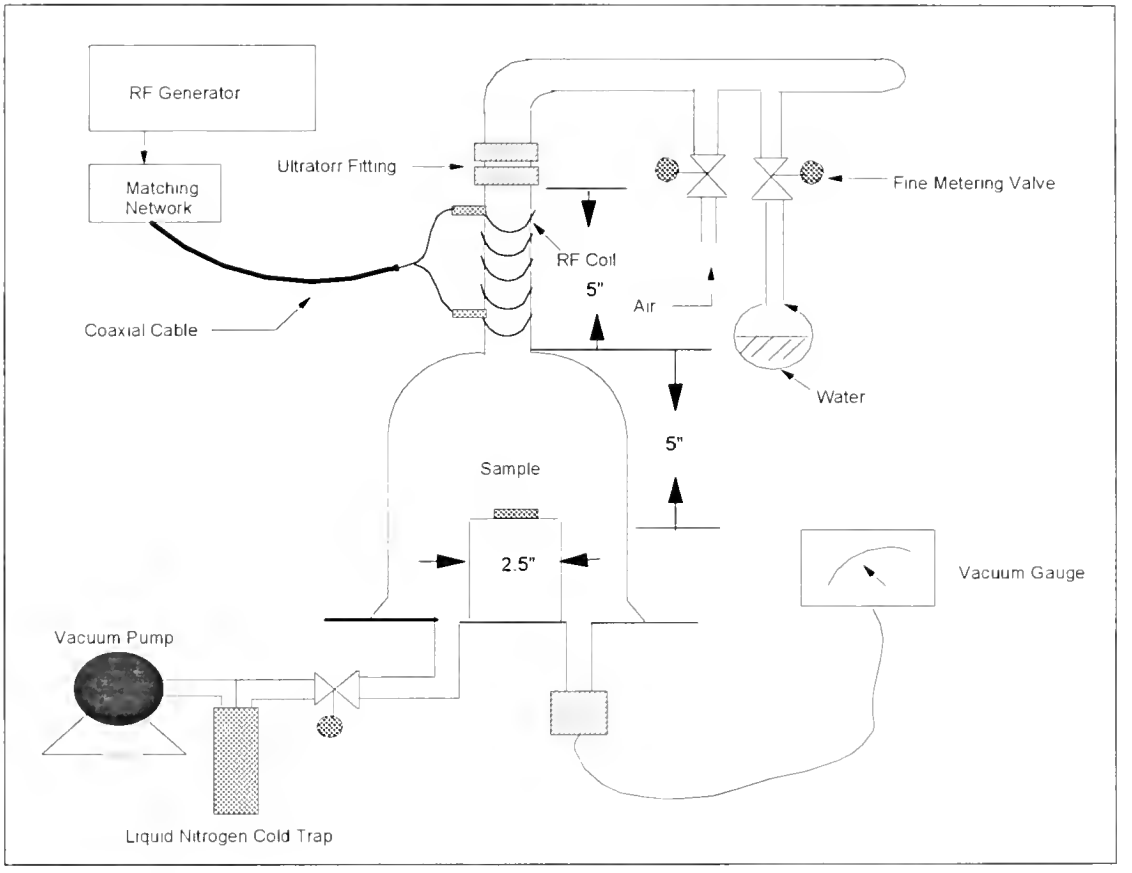

Figure 3-3. Schematic diagram of the RF plasma system.

watts RF water plasma at 100 mTorr for 30 minutes to ensure no contamination. Polymeric substrates to be treated were placed on a 250 ml Pyrex beaker directly under the plasma generation region (plasma was generated inside the portion of the tube that was surrounded by the copper coil). After mounting the samples, the pressure of the reaction chamber was pumped down to 4 mTorr for 10 minutes, then brought up to 100 mTorr by introducing water vapor. When a constant gas flow was reached, plasma power was turned on to generate the gas plasma. Yahiaoui [6] showed that 50 watts of plasma power is the minimum power level needed to oxidize the polymeric surface. In this study, 50 watts of power level was selected for all samples, and plasma treatment time varies from 0 to 25 minutes. The glow discharged throughout the whole reaction chamber. After plasma treatment, samples were retrieved by raising the pressure to one atmosphere with air.

3.2.2.2 Degassing of Monomer Solution

Immediately after plasma treatment, samples were transferred to borosilicate test tubes (Fisher Scientific, size: 16x125 mm) which contained 6 ml aqueous monomer solution. Degassing was done before gamma irradiation. Monomer solutions with substrates were degassed under reduced pressure (100-125 mmHg) in combination with 2 to 3 times sonication (5 seconds each). Usually 5 to 10 minutes were required per sample depending on the type of monomer and the substrate. The pressure was in the test tubes

brought up to one atmosphere by introducing argon gas. The test tubes were then sealed with polyethylene snap caps.

3.2.2.3 Gamma Induced Graft Polymerization

Following the degassing, the samples in monomer solutions were irradiated in a 600 Curie ^{60}Co gamma source at room temperature. The schematic diagram of the gamma source is shown in Figure 3-4. Samples were mounted on polypropylene holders and placed at 4" from the source. The corresponding dose rate was determined by Fricke dosimetry [65,98,99], based on the oxidation of ferrous sulfate in acidic solution. Aerated 10^{-3} *M* solutions of ferrous sulfate (Mohr salt) in 0.8 *N* sulfuric acid are summitted to dose increments of approximately 10^{3} rad. The ferric ion concentration is directly determined with a spectrophotometer at 304 nm.

3.2.2.4 Washing

After gamma irradiation, samples were removed from the polymerized solutions and rinsed with 10 ml Ultrapure® water, then soaked in 10 ml of Ultrapure® water for one week at room temperature with three changes of water per day. After washing, samples were dried under vacuum at 40 °C for 12 hours, then kept in a desiccator until further use.

3.2.3 Two-step Gamma Induced Graft Polymerization

In addition to the plasma/gamma technique, a two-step gamma irradiation method was also developed in which RF

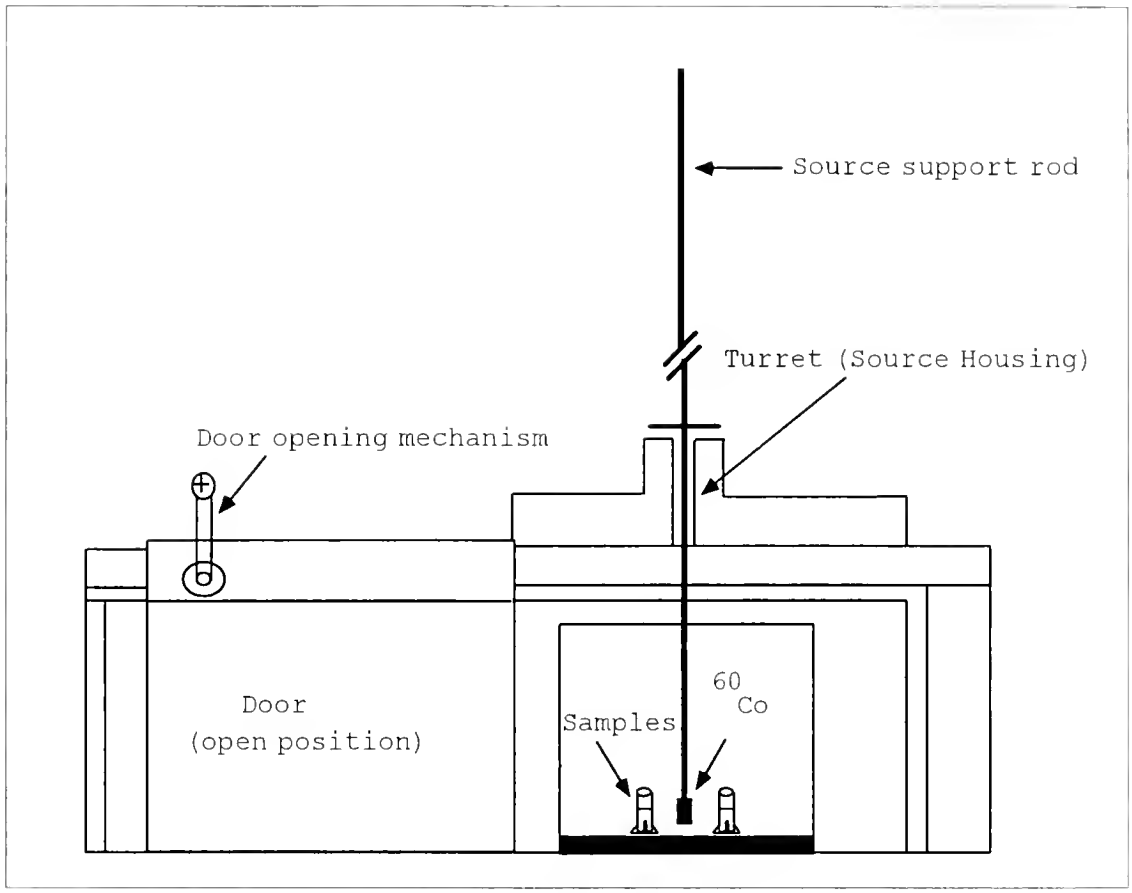

Figure 3-4. Schematic diagram of the gamma source.

plasma was not used. The procedure for two-step irradiation is described as follows:

Step I:

1. Place PMMA slabs into borosilicate test tubes (Fisher Scientific, size: 16x125 mm) which contain 6 ml aqueous monomer solutions.
2. Degas, then irradiate the samples to a desired dose (< 0.15 Mrad) by placing them at 4" from the ^{60}Co gamma source.
3. Retrieve the samples from the test tubes, rinse with 10 ml of Ultrapure® water, then transfer them to clean test tubes for the second step irradiation.

Step II:

1. The procedure for step II is the same as in step I except all samples were irradiated to a dose of 0.15 Mrad.
2. After gamma irradiation, samples were retrieved and rinsed with 10 ml Ultrapure® water, then washed and dried as in the procedures described in section 2.2.4.

3.3 Characterization

3.3.1 Gravimetric analysis

Gravimetric analysis is a simple and convenient technique to monitor the extent of graft yield. In this study, a Sartorius Research electronic balance having a precision of $\leq \pm$ 0.02 mg was used to weigh the samples

before and after grafting. Graft yield was determined as follows:

$$\% \text{ weight gain} = (w_g - w_o / w_o) \times 100 \qquad (3\text{-}1)$$

where w_o and w_g are the dry weight of initial and grafted substrates, respectively. However, depending on the sample's geometry (surface to volume ratio), weight gains of less than 0.1-0.2% were considered insignificant.

3.3.2 Viscosity Measurement

There are several ways to measure the viscosity of polymers. These methods include capillary rheometry, parallel plate viscometry, cone and plate viscometry, and concentric cylinder viscometry. A Wells-Brookfield cone/plate viscometer (model DV-II, Brookfield) was used to measure the viscosity of polymer solutions in this study. A water bath with temperature control was used to maintain the sample temperature during measurements.

The schematic diagram of the cone and plate viscometer is shown in Figure 3-5. The cone is rotated with respect to the plate about the perpendicular axis at an angular velocity of ω. The rate of movement of any point on either surface is proportional to its distance from the axis and the separation of the surface at that point is equivalently proportional to the same radius. The shear rate is defined by the ratio of the rate of movement of the surface (at any point) to the distance of separation.

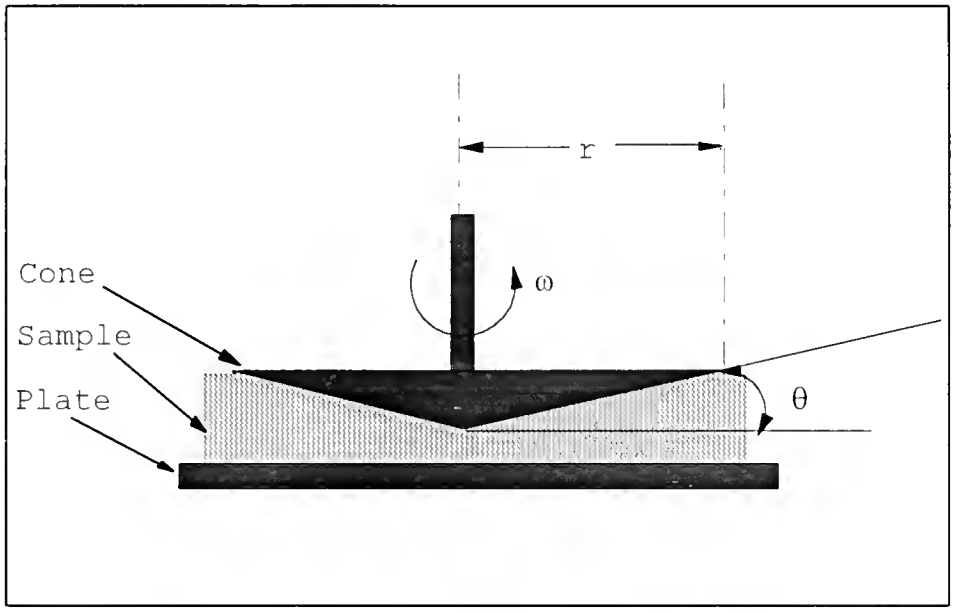

Figure 3-5. Schematic drawing of the cone and plate geometry.

This ratio (shear rate) is fixed for any speed of rotation, and constant over the entire surface. The viscosity η for Newtonian fluid is defined mathematically by the equation [100]:

$$\eta = \tau/S = \text{shear stress/shear rate} \qquad (3\text{-}2)$$

The equations for the Wells-Brookfield cone/plate viscometer are listed as follows [101]:

$$\text{shear rate } (\sec^{-1})\ S = \omega/\sin(\theta) \cong \omega/\theta \qquad (3\text{-}3)$$

$$\text{shear stress } \tau = \frac{M}{2/3\,\pi r^3} \ (\text{dynes/cm}^2) \qquad (3\text{-}4)$$

$$\text{apparent viscosity (poise) } \eta = \tau/S \qquad (3\text{-}5)$$

where θ is the cone angle, r is the cone radius, and M is the torque input by the instrument. Polymer solutions are typically shear thining or pseudoplastic. For pseudoplastic fluids, a logarithmic plot of τ vs. S is found to be linear over a relatively wide shear rate range and hence may be described by a power law expresssion (known as the Ostwald-de Waele model)[102]:

$$\tau = Ks^n \qquad (3\text{-}6)$$

where K and n are constants. For pseudoplastic polymer systems, n is less than unity. By analogy to the Newton's law of equation 3-2, the apparent viscosity of a power law fluid is expressed as

$$\eta = Ks^{n-1} \qquad (3\text{-}7)$$

The limiting apparent viscosity is defined as the intercept of a linearized line which is the tangent of the viscosity vs. shear rate curve at 100 sec^{-1}. Therefore, the slope of this linearized line is expressed as

$$\text{Slope} = K(n-1)100^{n-2} \qquad (3\text{-}8)$$

This linearized line equation can then be derived by the following steps:

$$K(n-1)100^{n-2} = (\eta-\eta_{100})/(S-100) \qquad (3\text{-}9)$$

$$\eta = [\eta_{100}-100K(n-1)100^{n-2}] + K(n-1)100^{n-2}S \qquad (3\text{-}10)$$

where η_{100} is the apparent viscosity at 100 sec^{-1}. The limiting apparent viscosity η_L is expressed as

$$\eta_L = \text{limiting apparent viscosity} = [\eta_{100}-100K(n-1)100^{n-2}] \qquad (3\text{-}11)$$

A typical example of limiting apparent viscosity (LAV) is illustrated in the Figure 3-6.

Also, the viscosity index (VI) is defined as the ratio of apparent viscosity at 3.75 sec^{-1} to apparent viscosity at 100 sec^{-1}.

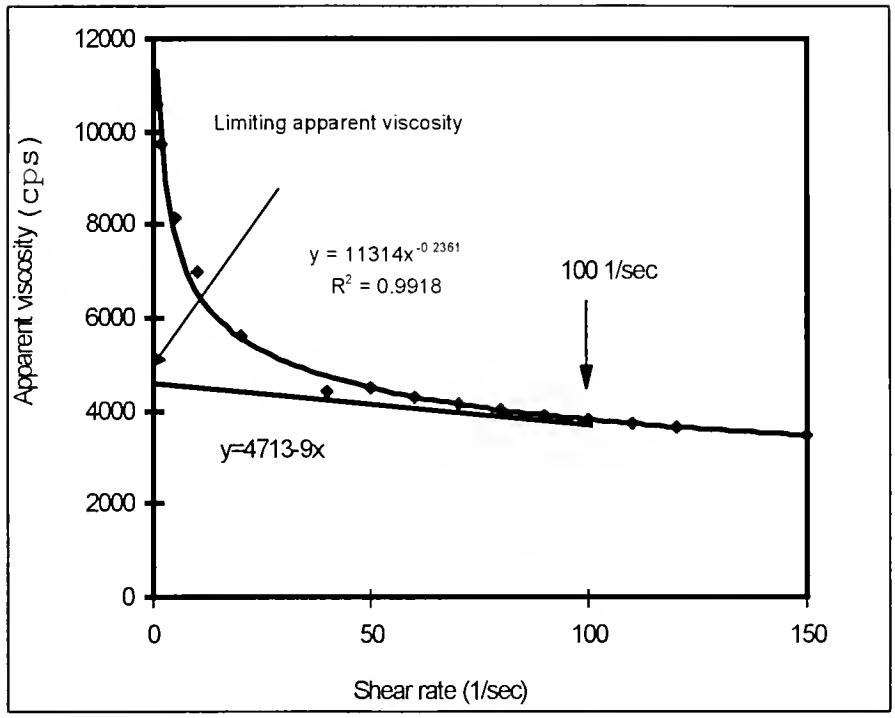

Figure 3-6. Typical example of limiting apparent viscosity (LAV).

VI = viscosity index

$$= \eta_{3.75\ sec^{-1}} / \eta_{100\ sec^{-1}} \qquad (3\text{-}12)$$

A typical procedure for viscosity measurements includes 1) turn on temperature bath and allow sufficient time for sample cup to reach the desired temperature; 2) swing sample cup clip to one side and remove sample cup; 3) using wrench supplied, hold viscometer lower shaft and screw on cone spindle; 4) place sample cup against adjusting ring, being sure to position the notch on the side of cup around the sample clip; 5) run the Viscometer at 10 rpm by setting the speed select knod and turning the motor switch on; 6) turn the adjusting ring to the right in small increments (one or two minor divisions on the ring) while watching the digital display until fluctuation of the display reading indicates that the pins have made contact; 7) once contact has been made, back off the adjusting ring in small increments until stabiliztion of the display reading indicates that the pins are not contacting; 8) turn the adjusting ring to the right in very small increments (about 1/64") until the display reading fluctuates regularly by a small amount; 9) make a pencil mark on the adjusting ring directly under the index mark on the pivot housing and turn the adjusting ring to the left exactly the width of one minor division; 10) remove the sample cup and place 0.5 ml sample in cup, being sure that the sample is bubble-free and spread evenly over the surface of the cup; 11) allow sufficient time for the sample fluid

to reach the desired temperature; 12) press the SPDL key and enter the spindle number; 13) turn the motor switch on and allow time for the display reading to stabilize; 14) record the rpm, viscosity, shear stress, and torque from the display reading; and 15) switch to higher rpm and record the data from the dispay reading if the % mode (torque) is still less than 100%. If the value of torque is over 100%, the viscometer will stop reading automatically.

3.3.3 Contact angle measurement

Contact angle measurement is a simple and convenient technique for surface analysis. In the area of biomaterial research, contact angle measurements are routinely used to measure the hydrophilicity and surface energy of biomaterials. The contact angle (θ) is related to the solid-vapor (γ_{sv}), solid-liquid (γ_{sl}), and liquid-vapor (γ_{lv}) interfacial energies via the Young-Dupree equation [103-105]:

$$\cos \theta = (\gamma_{sv} - \gamma_{sl}) / \gamma_{lv} \qquad (3\text{-}13)$$

If the contact angle is 0 degree, the liquid is completely spreading or completely wets the substrate. An extensive information on contact angles and their variation with liquid and solid constitution has been reported by Zisman's group at the Naval Research Laboratory [106,107].

In this study, a Rame-Hart contact angle goniometer (Mountain Lakes, NJ) with an acrylic water tank (3" X 2" X 2.5" in size) was employed for the contact angle measurements. The samples were allowed to equilibrate in Ultrapure® water for at least 12 hours prior to measuring. The contact angle of polymeric substrates was determined by the underwater captive air bubble technique. The configuration of the captive air bubble is shown in Figure 3-7. Samples were attached to a microscope slide and placed on the top of water tank with the sample face down in the water. Typically, four air bubbles were introduced onto the substrate surface by a microsyringe. The contact angle measurements were taken on both sides of each bubble for all four bubbles. The reported contact angle is an average of all eight measurements.

3.3.4 Fourier transform infrared/attenuated total reflection (FTIR/ATR)

Fourier transform infrared spectra has been recognized as one of the most powerful techniques in chemical analysis. In the area of polymer surface analysis, Fourier transform infrared with attenuated total reflectance (FT-IR/ATR) was used for identifying surface composition and chemical structure. Figure 3-8 shows the optical configuration of attenuated total reflection spectroscopy. The ATR crystals usually have a high refractive index (2.3 to 4.0).

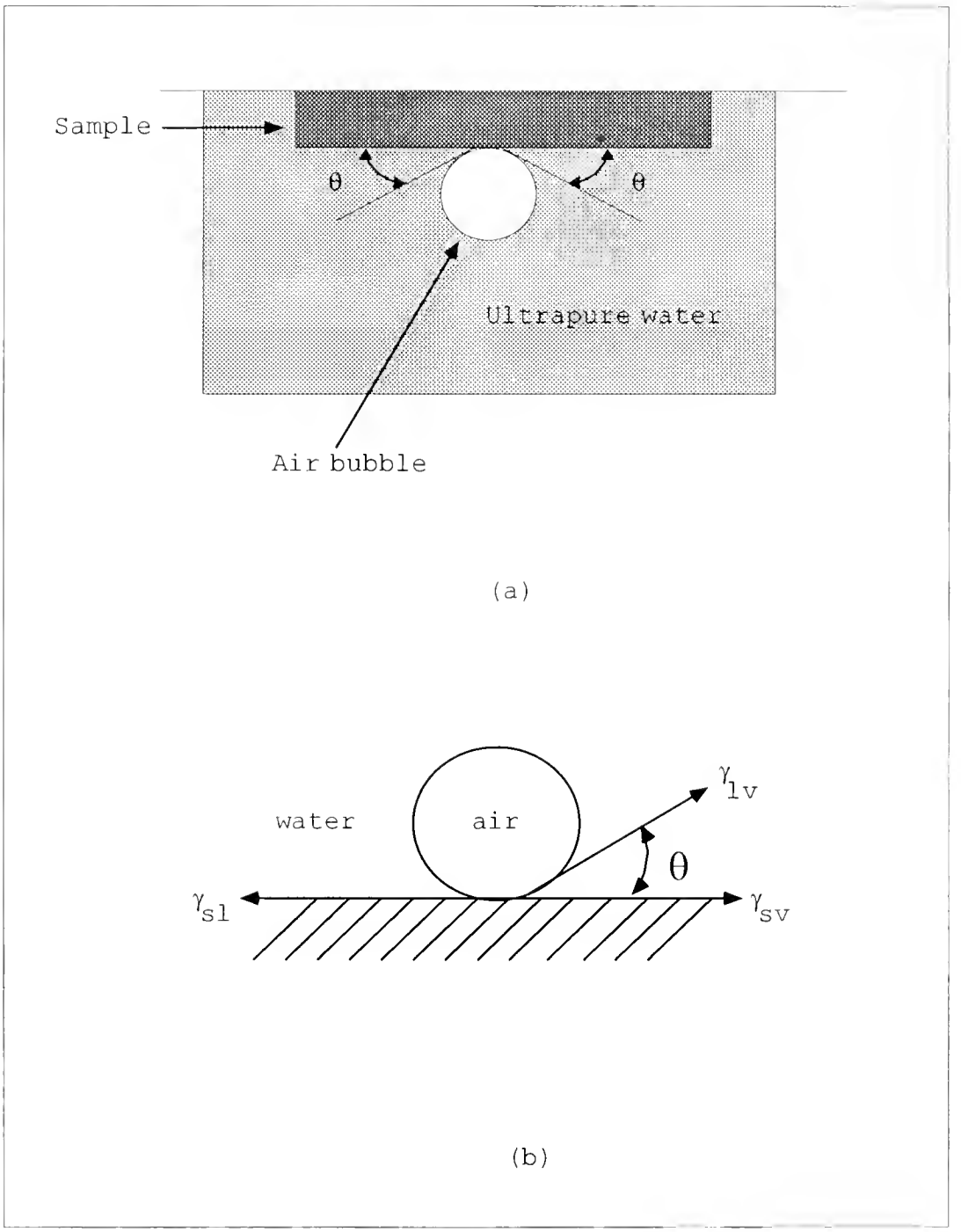

Figure 3-7. Schematic diagram of contact angle measurement.

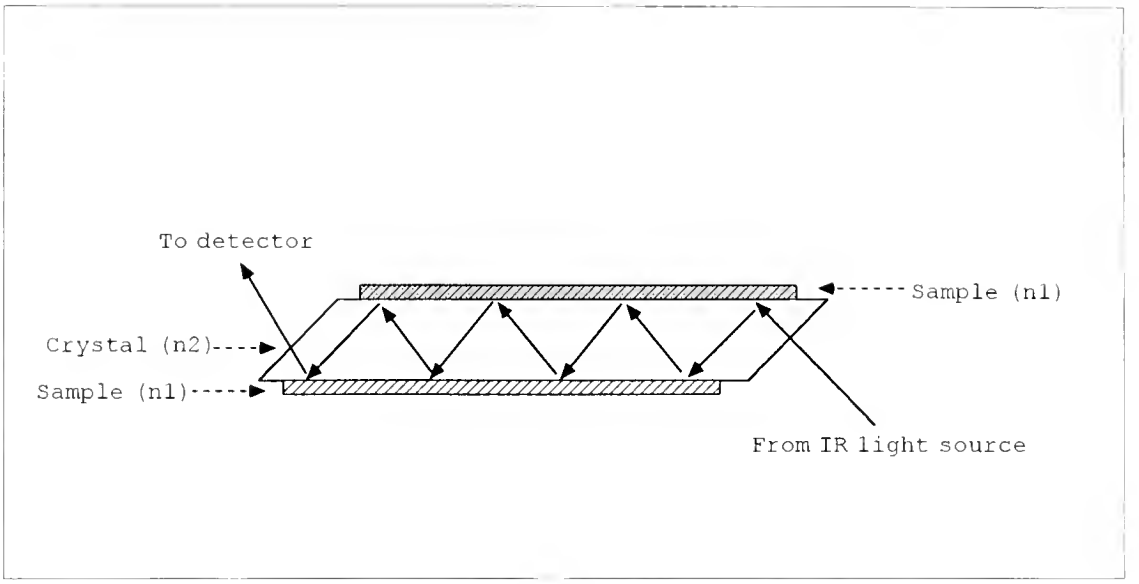

Figure 3-8. Optical configuration of FT-IR/ATR.

When the IR beam passes from a high refractive index medium (crystal) to a lower refractive index medium (polymer), the IR beam can be totally reflected. The depth of penetration (d_p) is a function of IR wavelength (λ), refractive index of crystal (n_1) and sample (n_2), and incident angle (θ). Their relationships are described by the following equation.

$$dp = \frac{\lambda}{2\pi\, n_1\, [\sin^2\theta - n_2/n_1]^{1/2}} \qquad (3\text{-}14)$$

Therefore, the depth of penetration of IR to the polymeric surface is between 0.5 to 3 μm. Penetration depth depends on IR wavelength, the two refractive indices, and the incident angle. A depth profile can be obtained by collecting sample spectra at various angles of incidence of the IR beam.

In this study, a Nicolet 60 SX spectrometer with an MCT (mercury cadmium telluride) detector was used to identify the chemical structure of the polymeric grafts. The MCT detector is cooled with liquid nitrogen. A Wilks model 50 attenuated total reflection (ATR) stage was used with a KRS-5 crystal. Two samples were pressed against the IRE crystal which had an entrance and exit face angle of 45°. Typically, 100 scans at a 4 cm^{-1} resolution were averaged for each measurement. All spectra were processed with standard Nicolet software.

3.3.5 X-ray photoelectron spectroscopy (XPS)

X-ray Photoelectron Spectroscopy (XPS) is another powerful analytical technique for determining the chemical composition of polymer surfaces. It can provide information on the top 5 to 50 A which dominate interface properties of biomaterials. The principle of this technique is based on the photoelectric effect. As the X-ray beams (usually Mg or Al) bombard the surface of a specimen in an ultra-high vacuum environment, the X-ray photons can knock out the inner shell electrons. Only the emitted electrons at or near the surface (≈ 20 Å) can escape the solid to be detected by the hemisphere analyzer. The kinetic energy of the emitted electron is measured by the detector and is related to the binding energy by the following equation:

$$E_b = h\nu - E_k - \varnothing \qquad (3\text{-}15)$$

where E_b is the electron binding energy, $h\nu$ is the photon energy of X-ray, E_k is the electron kinetic energy measured by the instrument, and $\varnothing$ is the work function. The binding energy measured by the instrument is related to the element and its chemical environment (bonding). Figure 3-9 is a typical representation of the photoionization event. The depth of penetration by XPS analysis varies from 10 Å for a take-off angle of 10° to 50 Å for a take-off angle of 90°.

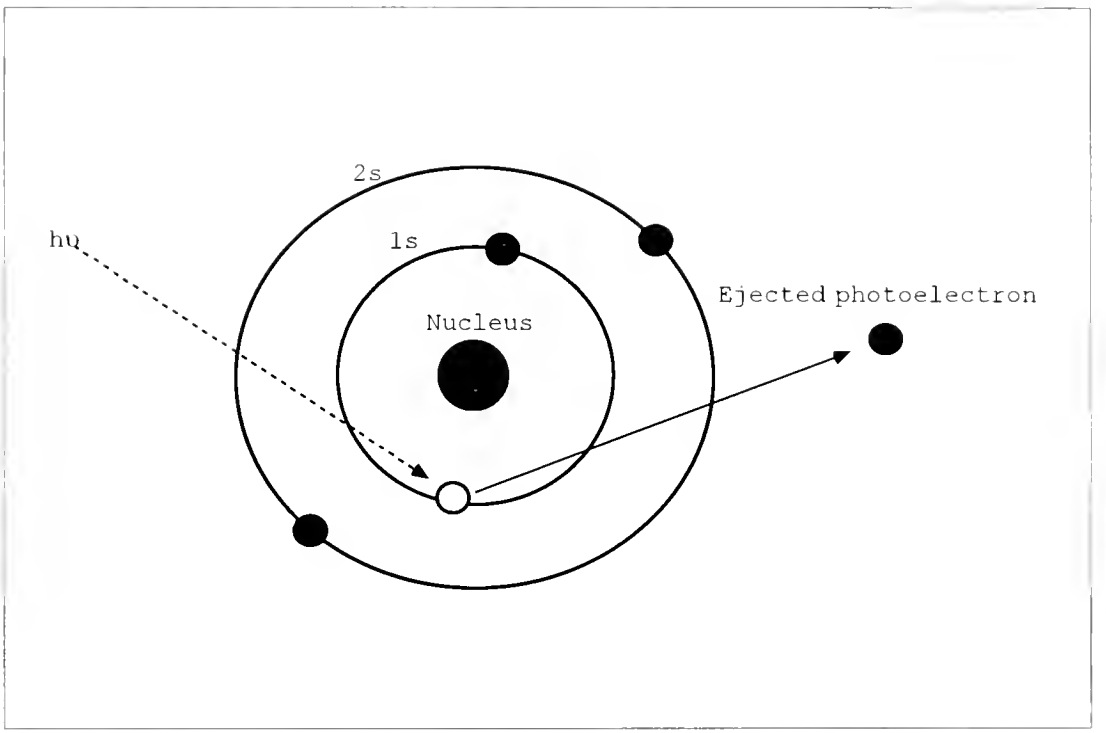

Figure 3-9. A typical representation of photoionization event.

The XPS samples were 1 cm^2 in size for all cases. A Kratos XSAM-800 spectrometer with a Mg Kα X-ray source was used to acquire the spectra. The pressure in the analyzer chamber was 10^{-7} to 10^{-8} Torr and the Mg Kα X-ray gun was operated at 13 kV and 18 mA. All samples were examined with a low resolution survey scan and a high resolution element scan. The spectra were processed and quantified using a Kratos software (DS800) provided with the instrument. The binding energy scale was calibrated to hydrocarbon C1s defined as 285.0 eV.

3.3.6 Ellipsometry

When a light wave is reflected or refracted at the interface between two optically dissimilar media, the state of polarization is changed abruptly. Ellipsometric measurements involve illuminating the surface of a sample with a monochromatic light of known wavelength and polarization and then analyzing the polarization state of the reflected light [108]. Ellipsometry can determine the properties of the surface and the properties of a partly transparent film on a known substrate.

In this research, a Gaertner (Chicago,IL) ellipsometer model L117 was used to measure the refractive index and the thickness of the graft. The assumptions for this technique include 1) the graft surface has parallel-plane boundaries; and 2) the ambient, the graft, and the substrate are all

homogeneous and optically isotropic [108]. Figure 3-10 shows the schematic diagram of an ellipsometer. The angle of reflection is set equal to the angle of incidence. The light source is a helium-neon laser having a wavelength of 632.8 nm. The beam is circularly polarized at the laser output. When the beam passes through the polarizer, it is converted from circular to linear. The linearly polarized beam is then converted to elliptically polarized beam by a quarter-wave compensator. Upon illuminating the surface of the sample, the reflected light passes through the analyzer and an optical interference filter. The amount of light passing by the filter is sensed by a photodetector and is indicated on an extinction meter. Certain azimuth settings (P1,and P2) cause the reflected light to become completely linearly polarized. The analyzer can then be rotated to a corresponding position (A1 and A2) where no light reaches the photodetector. These analyzer and polarizer readings are recorded. The assumption is made that the graft is a thin film, as shown in Figure 3-11, and is sandwiched between semi-infinite ambient and substrate media. The Fresnel equations are shown as follows [108]:

$$r_{01p} = \frac{N_1 \cos\phi_0 - N_0 \cos\phi_1}{N_1 \cos\phi_0 + N_0 \cos\phi_1} \qquad (3\text{-}16)$$

$$r_{12p} = \frac{N_2 \cos\phi_1 - N_1 \cos\phi_2}{N_2 \cos\phi_1 - N_1 \cos\phi_2} \qquad (3\text{-}17)$$

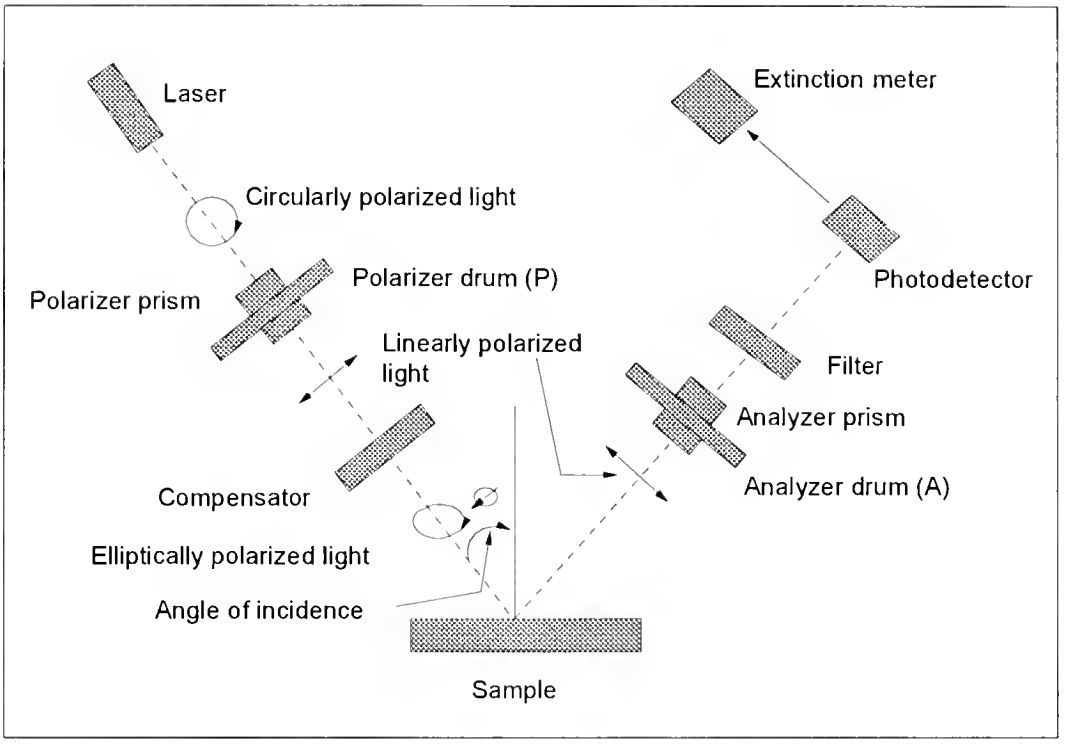

Figure 3-10. Schematic diagram of an ellipsometer.

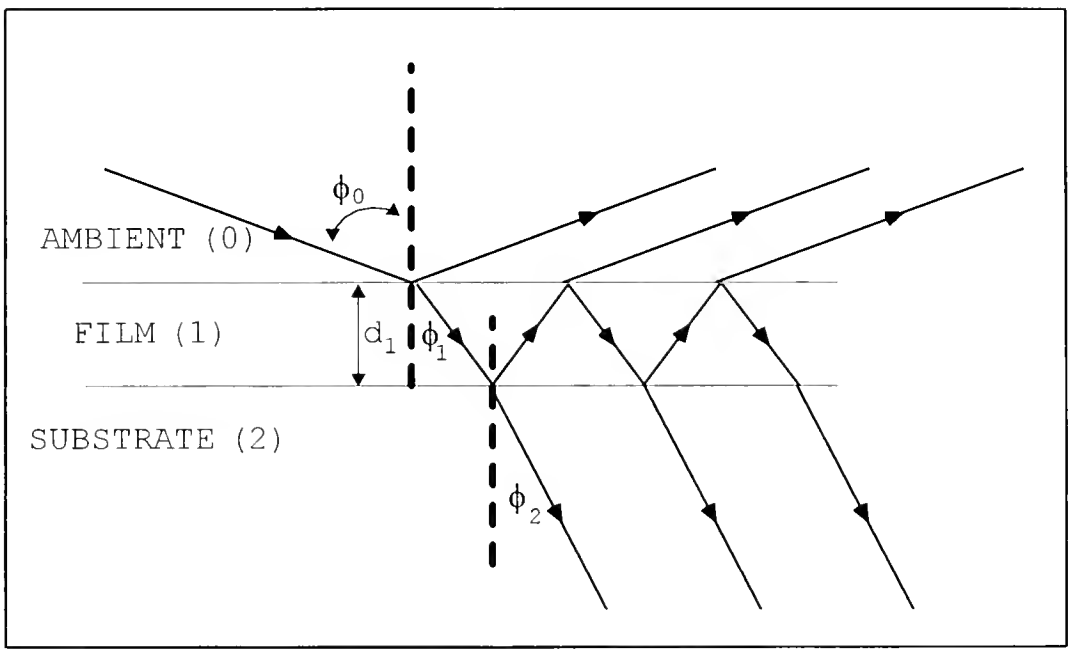

Figure 3-11. Oblique reflection and transmission of a plane wave by an ambient (0)-film (1)-substrate (2) system with parallel-plane bounaries. [108]

$$r_{01s} = \frac{N_0 \cos\phi_0 - N_1 \cos\phi_1}{N_0 \cos\phi_0 + N_1 \cos\phi_1} \qquad (3\text{-}18)$$

$$r_{12s} = \frac{N_1 \cos\phi_1 - N_2 \cos\phi_2}{N_1 \cos\phi_1 + N_2 \cos\phi_2} \qquad (3\text{-}19)$$

where r_{01p}, r_{01s}, r_{12p}, and r_{12s} are the interface Fresnel reflection coefficients. N_0, N_1, and N_2 are the refractive indices of the incident medium (usually air), the unknown film, and the known substrate, respectively. In general, N_i is a complex number; but for a non-absorbing medium it is real number n_i. The three angles ϕ_0, ϕ_1, and ϕ_2 are interrelated by Snell's law.

$$n_0 \sin\phi_0 = n_1 \sin\phi_1 = n_2 \sin\phi_2 \qquad (3\text{-}20)$$

The overall complex-amplitude reflection coefficients (R_p, R_s) for the ambient-film-substrate system in terms of 1) the interface Fresnel reflection coefficients (r_{01}, r_{12}), and 2) the phase change β experienced by the multiply-reflected wave inside the film on a single transversal between its boundaries are given by [108]

$$R_p = \frac{r_{01p} + r_{12p} e^{-i2\beta}}{1 + r_{01p} r_{12p} e^{-i2\beta}} \qquad (3\text{-}21)$$

$$R_s = \frac{r_{01s} + r_{12s} e^{-i2\beta}}{1 + r_{01s} r_{12s} e^{-i2\beta}} \qquad (3\text{-}22)$$

and

$$\beta = 2\pi\left(\frac{d_1}{\lambda}\right) n_1 \cos\phi_1, \qquad (3\text{-}23)$$

where d_1 is the film thickness, and λ is the wavelength of the incident light.

To determine the change in amplitude and phase separately, the overall complex-amplitude reflection (R_p, R_s) coefficients are written in terms of their absolute values and angles:

$$R_p = |R_p| e^{i\Delta_p} \qquad (3\text{-}24)$$

$$R_s = |R_s| e^{i\Delta_s} \qquad (3\text{-}25)$$

From measurements of the incident and reflected polarization, the ratio

$$\rho = \frac{R_p}{R_s} \qquad (3\text{-}26)$$

of overall complex-amplitude reflection coefficients is determined. The ratio ρ can be expressed in terms of the ellipsometric angles Ψ and Δ,

$$\rho = \tan\Psi e^{i\Delta} = \frac{R_p}{R_s} \qquad (3\text{-}27)$$

where Ψ and Δ are ellipsometric angles. The amplitude ratio change can be expressed as

$$\tan\Psi = \frac{|R_p|}{|R_s|} \qquad (3\text{-}28)$$

and the change in phase difference as

$$\Delta = \Delta_p - \Delta_s \qquad (3\text{-}29)$$

From two sets of polarizer and analyzer readings at this condition, ellipsometric parameters PSI (Ψ) and DELTA (Δ) can be derived using the following relations:

$$\Psi = \frac{180 - (A_2 - A_1)}{2} \qquad (3\text{-}30)$$

$$\Delta = 360 - (P_1 + P_2) \qquad (3\text{-}31)$$

Parameter Psi (Ψ) varies from 0 to 90, while Delta (Δ) can assume values from 0 to 360 [109].

Equations (3-16)~(3-31) can not be solved analytically for n_1 and d_1, but numerical methods can be applied. A computer program developed by R. Ochoa of Dr. Simmons' laboratory was available to calculate the graft thickness

(d_1) and refractive index (n_1). The calculated thickness can be determined by the following equation [110,111]:

$$d_1 = d_0 + \left[\frac{1}{2}\left(n_1^2 - n_0^2 \sin^2 \phi_0\right)^{-1/2}\right] m\lambda \quad \text{m} = 0, \pm 1,2,3... \qquad (3\text{-}32)$$

where d_1 is the thickness of graft, and d_0 is the graft's minimum thickness.

A typical procedure for ellipsometric mesurement includes 1) set the polarizer and analyzer angle of incidence; 2) turn on, warm up, and align sample stage; 3) place sample on the sample table; 4) set polarizer drum to read 85° and the analyzer to read 45°; 5) adjust gain control until meter reads midway between 3/4 and full scale (150 to 200); 6) rotate analyzer drum slowly within the red-numbered segment (0° to 90°) and set this drum to yield the lowest reading on the extinction meter; 7) rotate polarizer drum slowly within the red-numbered segment (315° to 135°) and set this drum to yield a new and even lower meter reading; 8) work back and forth between analyzer and polarizer drum setting until the lowest possible meter reading is obtained; 9) record the first analyzer drum reading (A1)' and then the first polarizer drum reading (P1) at extension; 10) add 90° to the first polarizer drum reading (P1) and rotate the polarizer drum to this sum (P1+90°); 11) from 180°, substrate the first analyzer drum reading (A1) and rotate the analyzer drum to this difference

(180°-A1); 12) slowly rotate the polarizer drum to obtain the lowest reading on the meter; 13) slowly rotate the analyzer drum to obtain a still lower meter reading; 14) work back and forth between polarizer and analyzer drum setting to obtain final lowest reading on meter; and 15) record analyzer and polarizer reading (A2 and P2). These polarizer readings (P1, P2) and analyzer readings (A1, A2) were used to determine the minimum graft thickness and refractive index of graft.

3.3.7 Optical microscopy

An optical microscope (Nikon OPTIPHOT, Japan) was used to study rabbit lens epithelial cell adhesion and spreading. The analysis was conducted by Paul Martin in this laboratory.

3.3.8 Scanning electron microscopy (SEM)

A low voltage scanning electron microscope (JEOL JSM-6400 SEM) was used to examine the surface morphology of polymers. Sample preparations are much simpler than with high voltage SEM, since no gold-palladium coating is required. Typically, an accelerating voltage of 0.5 kV was used. SEM operations were performed by Paul Martin. This new low voltage technology is very useful in studying the surface morphology of polymers, biomaterials, biological tissues and coating sensitive surfaces.

3.3.9 Rabbit lens epithelial cell adhesion and spreading

In vitro studies are an important step to understanding the biocompatibility of polymers. During cataract surgery and intraocular lens implantation, the adhesion of lens epithelial cells is deemed to be an important factor in post-surgery inflammation. Therefore, Hofmeister [112] of this laboratory, developed a rabbit lens epithelial cell adhesion and spreading model to investigate the biocompatibility of polymeric materials. The lens epithelial test was done by Paul Martin in this laboratory.

Rabbit lens capsule epithelial cells were cultured from New Zealand rabbits. Cells were trypsinized and suspended in Medium 199, 15% fetal bovine serum at a concentration of 10,000 cells/ml. Samples were placed in the wells of tissue-culture polystyrene plates, and equilibrated with the medium without cells for ten minutes. Two ml of cell suspension were then applied to each well over the samples. The incubation conditions for the samples were 37 °C in a CO_2 atmosphere for 24 hours. After incubation, samples were removed and rinsed with balanced saline solution, and then placed into 10% neutral buffered formalin. Samples were stained with crystal violet solution (2%) after 24 hours fixation. A Nikon optical microscopy was used to determine the number of cell adhesions and spreading. Two photographs were taken from different portions of each sample.

CHAPTER 4
RESULTS AND DISCUSSION

4.1 Initial Studies of the PVP/NVP System

Radiation-induced grafting of N-vinylpyrrolidone (NVP) onto polymeric substrates has been extensively studied in this laboratory [5,6]. Possible gelation of NVP during graft polymerization can be one of the major drawbacks of the grafting process. On the sample handling aspects, gelation makes sample's post-washing very difficult. The "presoak method" [6] enhances the grafting efficiency by soaking the substrate in a highly concentrated monomer solution before performing the radiation induced graft polymerization. This technique provides a monomer-rich environment at the interface between the substrate and monomer solution. However, gelation could still occur at high radiation doses. Presoaking may also affect the dimensional stability of certain polymers. In the present research, a new PVP/NVP monomer system is investigated and evaluated for surface modification of polymers. The incentive for this study is to develop a new monomer system that would exhibit minimal gelation during radiation-induced graft polymerization.

Commercial polyvinylpyrrolidone (PVP), Plasdone K-90 from GAF chemicals, was used in this research without further purification. Plasdone K-90 is currently used as a granulation binder, controlled release matrix, gel former, bioadhesive, and tablet coating [113]. Plasdone K-90 has a weight average molecular weight of 1.2×10^6 and a number average molecular weight of 3.6×10^5 [113]. The glass transition temperature for Plasdone K-90 is 174 °C. Plasdone K-90 can be dissolved in various solvents such as water, alcohol, ketone-alcohol, acids, ether-alcohols, lactone, chlorinated hydrocarbons etc. [113]. PVP also is a good wetting agent for most polymers. Mentak [92], in this research group, has discussed the PVP/NVP system with an emphasis on graft thickness and graft stability of PVP-g-PDMS in his dissertation. This present research focuses on the polymerization solution viscosity, XPS analysis, and contact angle measurements. A PVP/NVP solution producing low solution viscosity, high surface nitrogen concentration, and low contact angle on graft will be selected as a monomer solution for the plasma/gamma surface modification studies.

4.1.1 Solution Viscosity Measurement

4.1.1.1 Viscosity of PVP/NVP system

Since the PVP/NVP system uses a polymer/monomer aqueous solution, the effect of gamma-rays is more complex because of the interaction between PVP and NVP. The interactions

are not easy to study experimentally. On the other hand, the effect of gamma-rays on separate aqueous solutions of NVP or PVP can be experimentally determined.

The results of viscosity measurements for the PVP/NVP, PVP, and NVP solutions are listed in Table 4-1. Viscosity data was expressed in terms of apparent viscosity (AV), limiting apparent viscosity (LAV), and viscosity index (VI). The PVP/NVP solutions were composed of 10 parts of solute with 90 parts of water by weight. The PVP K-90 solutions and NVP solutions were composed of 0 to 10 parts of solute with 90 parts of water by weight. PMMA substrates were placed in the solutions to simulate the real situation of gamma-induced graft polymerization. Before gamma irradiation, all monomer solutions were degassed and filled with argon gas. Samples were then irradiated in a ^{60}Co gamma source with a dose rate of 510 (rad/min.) up to 0.15 Mrad. Viscosities were taken at 25 $^{\circ}C$ soon after gamma irradiation.

For the PVP/NVP solutions, the viscosities increase significantly after gamma irradiation. This implies that the gamma irradiation has promoted monomer polymerization and cross-reaction in the aqueous PVP/NVP solutions. The viscosities of the PVP/NVP solutions after gamma irradiation decrease as the ratio of PVP K-90 to NVP increases. This suggests that PVP-NVP cross-reaction and NVP polymerization is inhibited and that NVP concentration dependence dominates results.

Table 4-1. Apparent viscosity (AV), limiting apparent viscosity (LAV), and viscosity index (VI) of PVP/NVP, PVP, and NVP solutions.

	10N	1P 9N	2P 8N	3P 7N	4P 6N	5P 5N	6P 5N	7P 3N	8P 2N	9P 1N	10P
Av^b (cps)	2	4	10	16	26	33	46	72	92	137	150
Av^a (cps)	8530	1675	1350	1060	810	740	582	674	720	706	720
LAV (cps)	4713	1186	1074	837	668	532	422	494	505	562	566
VI	2.17	1.62	1.38	1.33	1.31	1.39	1.38	1.36	1.43	1.37	1.40

	-	1P	2P	3P	4P	5P	6P	7P	8P	9P	10p
Av^a (cps)	-	firm gel	soft gel	liquid gel	liquid gel	2400	262	190	262	360	720
LAV (cps)						635	197	150	200	281	566
VI						5.7	1.46	1.39	1.44	1.40	1.40

	10N	9N	8N	7N	6N	5N	4N	3N	2N	1N	-
Av^a (cps)	8530	2822	1220	530	210	92	39	13	5	2	-
LAV (cps)	4713	1956	998	466	187	92	39	13	5	2	
VI	2.17	1.66	1.33	1.20	1.16	1	1	1	1	1	

Note: 1. Each solution contains 90 parts of water and 1 to 10 parts of solute, where P=PVP K-90 and N=NVP.
2. The total radiation dose is 0.15 Mrad. Viscosities were measured in a Brookfield c/p #40 rheometer at temperature of 25°C.
3. [a] indicates the apparent viscosity at 3.75 1/sec after gamma irradiation.
4. [b] indicates the apparent viscosity at 3.75 1/sec before gamma irradiation.
5. LAV is the limiting apparent viscosity.
6. VI is the viscosity index for the ratio of $\eta_{3.75}/\eta_{100}$.

For the PVP solutions, the results vary dramatically with the concentration of PVP K-90. The viscosity decreases somewhat at 9% PVP, 8% PVP, 7% PVP, and 6% PVP, probably because radiation chain scission is dominating but then begins to increase at 5% PVP where branching and cross-linking begin to dominate and gelation occurs at 4% PVP, 3% PVP, 2% PVP, and 1% PVP. The degree of gelation, which was determined by visual inspection, increases directly with decreasing PVP concentration. This concentration dependent relationship between radiation induced degradation and gelation for high molecular weight PVP is a very interesting phenomenon.

The effect of gamma radiation on PVP in aqueous solution was first studied by Alexander and Charlesby [114,115]. They also found that PVP, when irradiated at concentrations as low as 1%, were not degraded by irradiation but rather were crosslinked. The critical dose for incipient gel formation in PVP solution increased with the PVP concentration. This is consistent with the gelation of lower concentrations of PVP in this study shown in Table 4-1. However, below 0.3% PVP, degradation was observed. The mechanism for the radiation-induced cross-linking of polymers in solution was discussed by Alexander and Charlesby [114,115] and by Henglein [116]. In an aqueous solution, once a polymeric free radical P• is produced, it can only dimerize by reaction with another P• radical, leading to branching and eventual cross-linking, or combine

with primary H• or OH• radicals formed by the radiolysis of the solvent ("direct action" mechanism). On the other hand, both H• and OH• radicals are very efficient for abstracting hydrogen from the polymer molecule, leading to the formation of polymeric free radicals ("indirect action" mechanism). The radiation-induced cross-linking of PVP in an aqueous environment most likely follows the "indirect action" rather than the "direct action". If the cross-linking of polymers in aqueous solution follows the "direct action" mechanism, the critical dose for incipient gel formation will decrease with the concentration of polymers. This is inconsistent with the experimental results. The "indirect action" mechanism is favored in aqueous solutions. The experimental results obtained by Henglein [116] have supported this hypothesis. When the PVP polymer is dissolved in various solvents, the rate of cross-linking was found to be much higher in water than in methanol. In isobutanol, aniline, and chloroform, no network formation was found [116].

In the case of the very dilute PVP solution (<0.3%), if no adjacent polymer molecule presents itself in a suitable orientation for cross-reaction, the activated polymer molecule would instead suffer main chain cleavage and degradation [114,115]. Both "indirect action" and "direct action" would result in polymer degradation.

For the NVP solutions, the viscosity decreases as the NVP concentration drops. Below 6% NVP, the viscosity becomes very low. At low dose rates, the rate of

polymerization, R_p, is proportional to the square root of the rate of initiation, R_i, and to the first order of monomer concentration if the reaction follows the conventional free radical mechanism [117]. Therefore, as the monomer concentration drops, the degree of polymerization would be reduced as observed.

Obviously, the results in Table 4-1 have shown that the viscosities of the PVP/NVP solutions are much different from the PVP or NVP solutions alone. When the PVP in a PVP/NVP solution is less than 5%, the viscosity of PVP/NVP is lower than PVP alone and higher than NVP alone. On the other hand, when the PVP content in PVP/NVP solution is higher than 5%, the viscosity of PVP/NVP solution is higher than either the PVP or NVP alone. Below 5% PVP, the cross-linking of PVP in aqueous solution was inhibited by the presence of NVP monomer. The activated PVP molecule may not be able to efficiently cross-react with an adjacent PVP molecule due to the competitive reaction with the surrounding NVP monomers. If the PVP content is greater than 5%, the PVP molecule concentration becomes high enough to enable reaction with both surrounding NVP molecules or with an adjacent PVP molecule. Polymerizing NVP may also serve to cross-react two PVP molecules. In general, it appears that the NVP monomer only cross-reacts readily with PVP when the PVP content is greater than the NVP content.

4.1.1.2 The effect oxygen

The presence oxygen during the gamma irradiation has a significant effect on polymer degradation. Figure 4-1 shows the apparent viscosity (at 3.75 1/sec) of the PVP/NVP system irradiated in air and irradiated in argon. The PVP/NVP system irradiated in air exhibited a lower apparent viscosity than the same system irradiated in argon. Most likely, when irradiation is carried out in air, some of the polymeric radicals react with oxygen to form peroxidic structures which eventually decompose and lead to a chain scission [9]. Cross-linking by gamma irradiation in the presence of air produces hydrogels with lower cross-linking density than hydrogels irradiated in vacuum [4]. In the case of a PVP/NVP ratio of 0/10 (NVP only solution), the solution viscosity was dramatically reduced when oxygen was present during gamma irradiation. Also, in the PVP only solution, the cross reaction process between PVP molecules was retarded by the presence oxygen. Usually, at low dose rates, oxygen can diffuse into a solution fast enough to provide sufficient oxygen for peroxide formation. However, at high dose rates (such as e-beam), oxygen is rapidly used up and cannot be replenished in a very short time period thereby leading to less apparent oxygen sensitivity. Therefore, e-beam source is another useful source for radiation-induced graft polymerization.

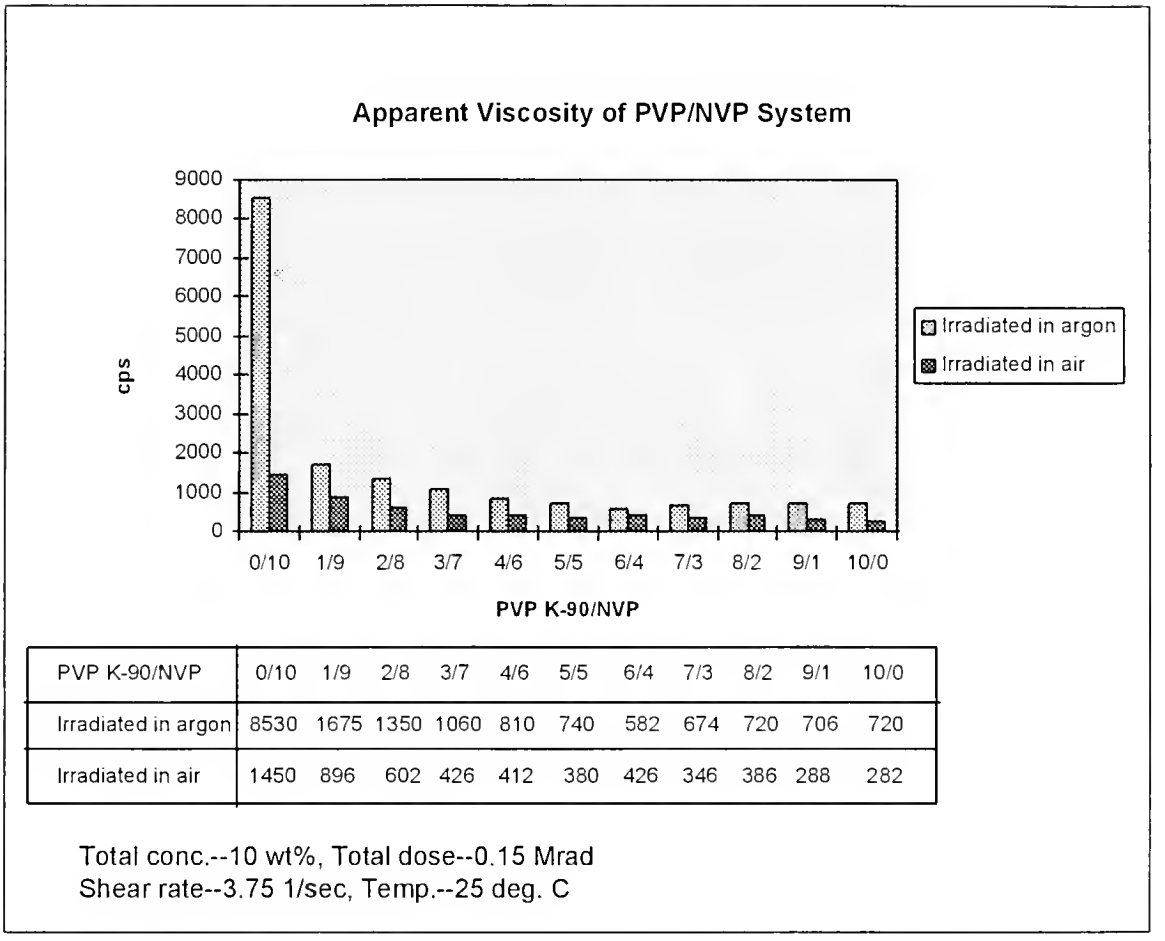

PVP K-90/NVP	0/10	1/9	2/8	3/7	4/6	5/5	6/4	7/3	8/2	9/1	10/0
Irradiated in argon	8530	1675	1350	1060	810	740	582	674	720	706	720
Irradiated in air	1450	896	602	426	412	380	426	346	386	288	282

Total conc.--10 wt%, Total dose--0.15 Mrad
Shear rate--3.75 1/sec, Temp.--25 deg. C

Figure 4-1. Apparent viscosity of PVP/NVP system irradiated in argon and irradiated in air.

4.1.2 XPS Analysis of the Grafting of PVP/NVP noto PMMA

In addition to the viscosity measurements, the grafting of PVP/NVP system onto PMMA by the gamma method (gamma-induced graft polymerization) was examined using XPS analysis. The results are presented in Figure 4-2. XPS analysis provides much information about the top surface layer (ca. 20-50 Å), such as atomic concentrations and interpolated chemical structures. The theoretical atomic composition for PVP is 75% carbon, 12.5% oxygen, and 12.5% nitrogen. The surface nitrogen concentration of PVP/NVP-g-PMMA prepared from the PVP/NVP ratio of 2/8, 4/6, 5/5, 6/4, and 8/2 is 4.92%, 4.08%, 4.24%, 4.85%, and 4.91% respectively. These values are close to or even higher than 4.28% for the 10% NVP solution. Radiation-induced graft polymerization using simultaneous irradiation method involves a hetergeneous polymer-monomer reaction system where the rate of polymerization is usually diffusion-controlled [6]. These grafting reactions are mainly controlled by the rate of production of free radicals on the substrate surface and their accessibility to the monomer [92]. In the PVP/NVP system, large PVP molecules might physically adsorb on the substrate surface before the grafting. Some of the PVP molecules might be grafted through the recombination of the PVP polymeric radicals with substrate surface radicals therefore enhancing the grafting reaction. In the case of 10% PVP only solution, a

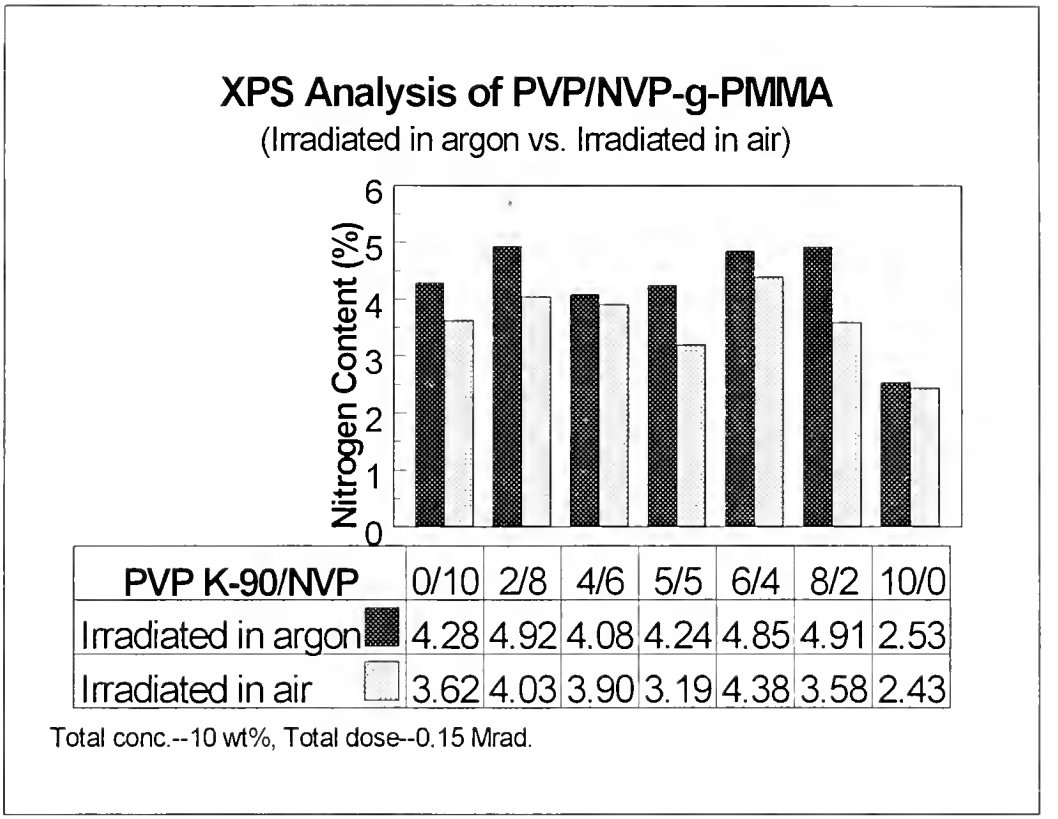

Figure 4-2. XPS analysis of gamma induced graft of PVP/NVP system onto PMMA.

significant amount of nitrogen (ca. 2.53%) was found on the PMMA surface. This indicates that the PVP may be chemically grafted or strongly physically adsorbed on the PMMA surface. Chemical grafting might also occur if PVP polymer radicals can recombine with radicals on the PMMA surface.

The possible strong physisorption of Plasdone K-90 onto PMMA was examined by XPS analysis. Table 4-2 shows the results of physical adsorption of Plasdone K-90 onto PMMA. The polymer solutions for samples #1 to #4 were 10 wt% aqueous Plasdone K-90, but #5 was a gamma irradiated Plasdone K-90 (0.15 Mrad). PMMA samples were soaked in the solutions for various times. The results indicate that one million MW PVP is adsorbed on PMMA surfaces and yields hydrophilic surfaces, but the extent of adsorption was less (ca. 50%) than when the solution is irradiated with the substrate. This implies that some chemical grafting of Plasdone K-90 onto PMMA does occur. For physisorption, the nitrogen content did not increase with increasing soaking time beyond 2 hours.

The results summarized in Figure 4-2 also indicate that the extent of grafting for the PVP/NVP system irradiated in argon are higher than when irradiated in air. These results are consistent with viscosity measurements.

The PVP/NVP system was also examined by the "plasma/gamma" method. PMMA substrates were exposed to a H_2O RF-plasma at 100 mTorr and 50 Watts for 15 minutes before gamma radiation grafting.

Table 4-2. XPS analysis of physical adsorption of Plasdone K-90 onto PMMA surface.

Sample #	Type of Solution	Soaking Time (hours)	Yield (gravimetric) (%)	Contact Angle (°)	Nitrogen Content (%)
PMMA #1	10 wt% pure PVP K-90	2	0.1	30	1.21
PMMA #2	10 wt% pure PVP K-90	3	0.1	24	1.08
PMMA #3	10 wt% pure PVP K-90	4	0.1	24	1.19
PMMA #4	10 wt% pure PVP K-90	5	0.2	25	1.23
PMMA #5	10 wt% gamma irradiated PVP K-90 (0.15 Mrad)	5	0.4	24	1.40

Note: The nitrogen content is 2.53% and the yield of graft is 1.1% for PVP-g-PMMA prepared by gamma-induced graft polymerization.

The results are given in Figure 4-3. Again, the PVP/NVP ratio of 2/8 solution shows the highest nitrogen content in the system. Measurements presented in Figure 4-1 also indicate that at the PVP/NVP ratio of 2/8, the solution viscosity is six times lower than for NVP monomer alone. Mentak's studies [92] in this research group have further shown that for PVP/NVP surface modification of PDMS, less gelation occurs during gamma graft polymerization which benefits sample handling and washing.

4.1.3 Contact Angle Measurements

Contact angle is a simple technique for surface analysis. Since all contact angles for the PVP/NVP system grafted onto PMMA substrates were highly hydrophilic, ca. 20°, PDMS substrates were used to investigate changes in contact angle. PDMS surfaces are more hydrophobic than PMMA surfaces and are difficult to wet with Plasdone K-90, thus avoiding the physical adsorption of Plasdone K-90 or gamma-polymerized PVP. The same preparation conditions as for the PMMA substrates were used for the PVP/NVP-g-PDMS. The contact angles for the PVP/NVP system grafted onto PDMS surfaces are listed in Table 4-3. The contact angle for the PDMS control is about 90 degrees. The results in Table 4-3 indicate that the PVP/NVP ratio of 2/8 solution is the only one that could lower the contact angle of PDMS surface to near 20 degrees.

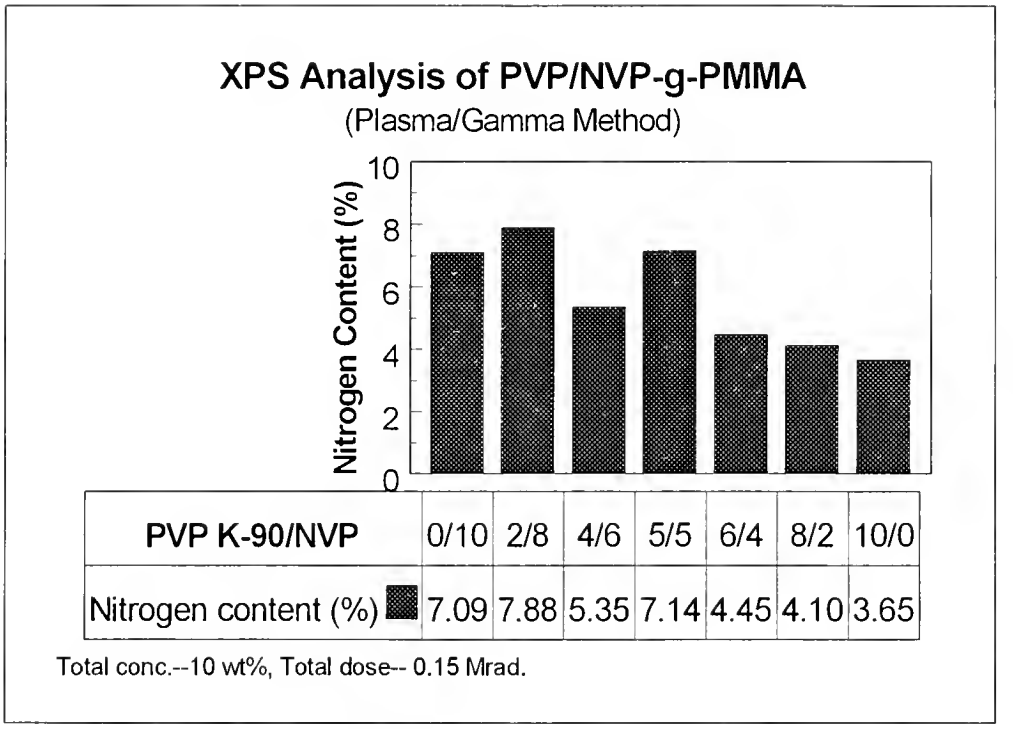

Figure 4-3. XPS analysis of PVP/NVP-g-PMMA using "plasma/gamma" method

Table 4-3. Contact angle measurements of PVP/NVP-g-PDMS

PVP K-90/NVP	Contact Angle (±5°)
Control PDMS	90
0/10	50
1/9	38
2/8	20
5/5	42
8/2	35
9/1	42
10/0	44

(Total conc.-- 10 wt%, Total dose--0.15 Mrad)

This result has further confirmed that the PVP/NVP ratio of 2/8 solution is the best composition for gamma-induced graft polymerization in terms of viscosity, contact angle and the extent of graft.

4.1.3 Summary of Initial Studies of the PVP/NVP System

A polymer/monomer mixture solution, PVP/NVP ratio of 2/8, not only gives a lower viscosity than NVP alone, but also demonstrates a comparable result as NVP alone for the PVP-g-PMMA. Thus, the formation of PVP graft on PMMA surface is attributed to the recombination of surface free radicals with PVP polymer radicals or polymerizing NVP radicals. Since the solution viscosity of PVP/NVP is much

lower than the NVP alone, the PVP graft on PMMA surface must be mainly dominated by the high MW PVP instead of polymerizing NVP.

The PVP/NVP solution is the first system in the current research that combines high MW PVP with unsaturated NVP for the grafting of PVP onto polymeric substrates. A very encouraging aspect from this study is that high MW polymers or biomolecules such as proteins or polysaccharides can be immobilized onto a polymeric substrate through gamma irradiation.

The mechanism due to the effect of gamma radiation on PVP/NVP in aqueous solution are very complex. The presence of NVP monomers or polymerizing NVP may affect the cross-reaction between two PVP polymers which then inhibits the gelation during gamma irradiation. The primary H• or OH• radicals formed by the radiolysis of the solvent also plays an important role in the "indirect action" mechanisms. The present research does not intend to reveal the detail of the mechanism.

However, the results in this study indicate that the PVP/NVP solution has considerably lower solution viscosity than NVP alone, which then can shorten the sample's post-washing cycle during surface treatment. Also, the use of PVP/NVP solution for gamma-induced graft polymerization is an alternate way to reduce the gelation during gamma irradiation without adding unwanted chemicals.

4.2 RF Plasma Treatment of PMMA, PDMS, PP, PC, PVDF, and FEP

Radio frequency glow discharge (RFGD) plasma can activate or oxidize the polymer surface to a depth of 50-500 Å without altering the bulk polymer properties [45]. After plasma treatment, most polymer surfaces are reactive and polar. In this study, PMMA, PDMS, PP, PC, PVDF, and FEP substrates were treated with water vapor RFGD plasma. The vacuum and the power for the RFGD plasma were 100±5 mTorr and 50 watts respectively. The plasma treatment times were varied form 1 to 25 minutes for each substrate. After plasma treatment, samples were characterized by contact angle measurements, FT-IR/ATR, and XPS analysis.

4.2.1 Contact Angle Measurements

The contact angle of each sample was taken right after plasma treatment by the captive bubble method. The contact angle results are summarized in Table 4-4. The PMMA substrate has a contact angle of 70° before treatment, but is reduced to 50° after one minute treatment, and finally decreases to 34° at 15 minutes treatment. The contact angle for the PDMS substrate dramatically decreases from 90° to 23° after a 1 minute treatment and then reaches 19° after 5 minutes of treatment. The PP control has a contact angle of 90°, but changes to 33° after a 1 minute treatment, and finally to 18° after 10 minutes of treatment. The PC

Table 4-4. Contact angle measurements for water RFGD plasma treated PMMA, PDMS, PP, PC, FEP, and PVDF

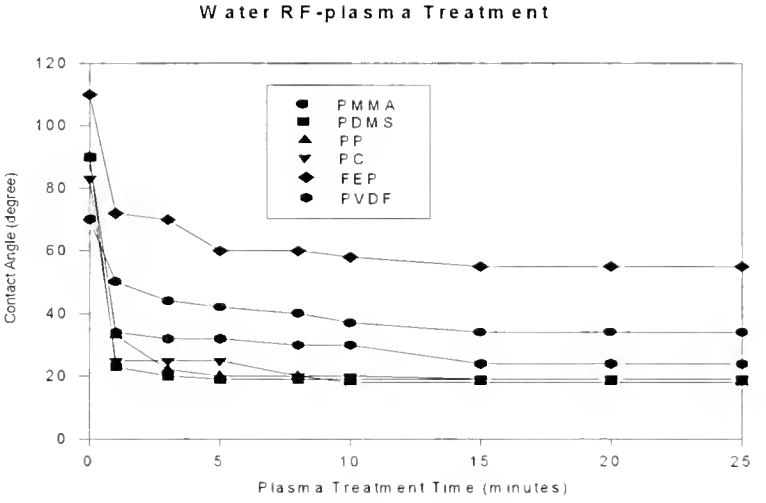

	Plasma Treatment Time (minutes)								
C.A. (±5°)	0	1	3	5	8	10	15	20	25
PMMA	70	50	44	42	40	37	34	34	34
PDMS	90	23	20	19	19	19	19	19	19
PP	90	33	22	20	20	18	18	18	18
PC	83	25	25	25	20	20	19	19	19
FEP	110	72	70	60	60	58	55	55	55
PVDF	90	34	32	32	30	30	24	24	24

(power--50 watts, pressure--100 mTorr)

substrate follows a similar trend as PDMS, but reaches 19° after 15 minutes. FEP also changes contact angle with the plasma treatment, and reaches 55° after 15 minutes. In the case of PVDF, the contact angle changes from 90° to 24° after 15 minutes.

The effect of RFGD plasma treatment on wettability of polymeric substrates is easily noticed using contact angle measurements. Contact angle reveals the interfacial characteristics of polymer surface. A low contact angle indicates that the major functional groups on the polymer surfaces are polar groups, such as hydroxyl (-OH) or carboxyl (-COOH), which can be introduced by RFGD plasma treatment.

The results also indicate that the substrate's surface contact angle is decreasing with increasing the plasma treatment time, and then exhibits a constant value for prolonged treatment after reaching a minimum. Yahiaoui [6] and Iwata et al. [118] reported that the O1s/C1s ratio, which expresses the extent of oxidation, increases with the plasma treatment time, but exhibits a tendency to decline to lower value after reaching a maximum value. This finding suggests that polymer segments in the surface region are highly oxidized at the time of reaching its minimum contact angle. After reaching the minimum, the polymer segments in the surface region might be broken into fragments during the prolonged treatment. These weak oxidized fragments may be ablated from the surface. This leads to a small decrease in

O1s/C1s value which can be observed by XPS analysis, but is not detected by the contact angle measurement.

4.2.2 XPS Analysis

XPS analysis of unmodified substrates and plasma treated substrates are listed in Table 4-5. The results in Table 4-5 after 15 min RF plasma indicate that the oxygen atomic concentration increases in all cases but is rather small for some substrates. The result implies that water RFGD plasma oxidizes the polymer surface and introduces polar functional groups to the polymer chains. The increase in oxygen concentration can be accounted for by the formation of hydroxyl, carboxyl, or hydroperoxide groups.

Figure 4-4 shows the XPS of unmodified PMMA. The elements presented on the PMMA survey scan are carbon and oxygen. Figure 4-5 presents the overlapped C1s peaks for unmodified and plasma modified PMMA. The major peak at 285 eV indicates the $-CH_X$ group. The secondary peak at 288.5 eV indicating the chemical shift for the -CO-O- group, increases slightly after plasma treatment.

The XPS of an unmodified PDMS and the overlapped C1s peaks of a control PDMS and a plasma treated PDMS are shown in Figure 4-6 and 4-7 respectively. The elements presented for unmodified PDMS are carbon, oxygen, and silicon. In Figure 4-7, the difference seen between two overlapped C1s peaks is insignificant, but the right hand side of C1s peak

Table 4-5. XPS data for untreated substrates and after 15 minutes RFGD plasma treatment

	Atomic Concentration (%)				
	C1s	O1s	F1s	Si2p	O1s/C1s
Unmodified PMMA	79.90	20.10			0.25
Plasma treated PMMA	75.55	24.45			0.32
Unmodified PDMS	48.91	22.59		28.49	0.46
Plasma Treated PDMS	31.75	34.99		33.26	1.10
Unmodified PP	100.0	0.0			0.00
Plasma Treated PP	92.66	7.34			0.08
Unmodified PC	86.11	13.89			0.16
Plasma Treated PC	80.81	19.19			0.23
Unmodified FEP	41.58	0.50	57.92		0.01
Plasma Treated FEP	39.10	0.98	59.92		0.02
Unmodified PVDF	55.67	1.29	43.05		0.02
Plasma Treated PVDF	60.24	4.13	35.63		0.07

(power--50 watts, pressure--100 mTorr, plasma time--15 min.)

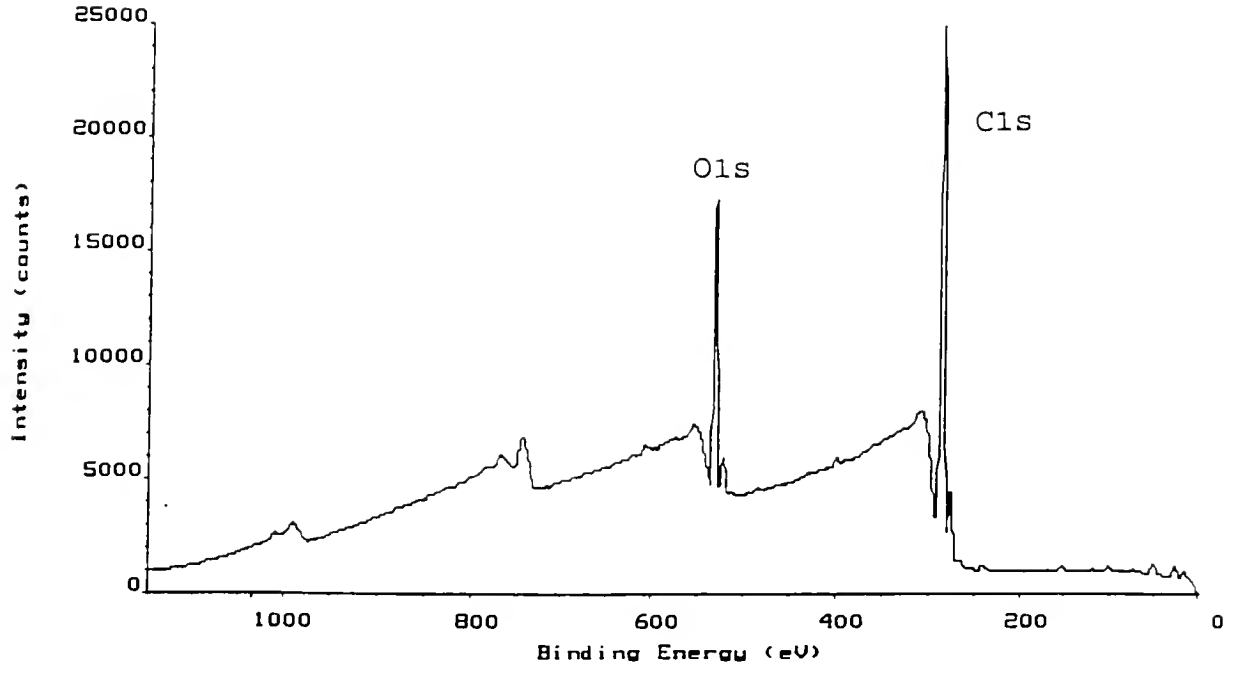

Figure 4-4. XPS spectrum of an unmodified PMMA

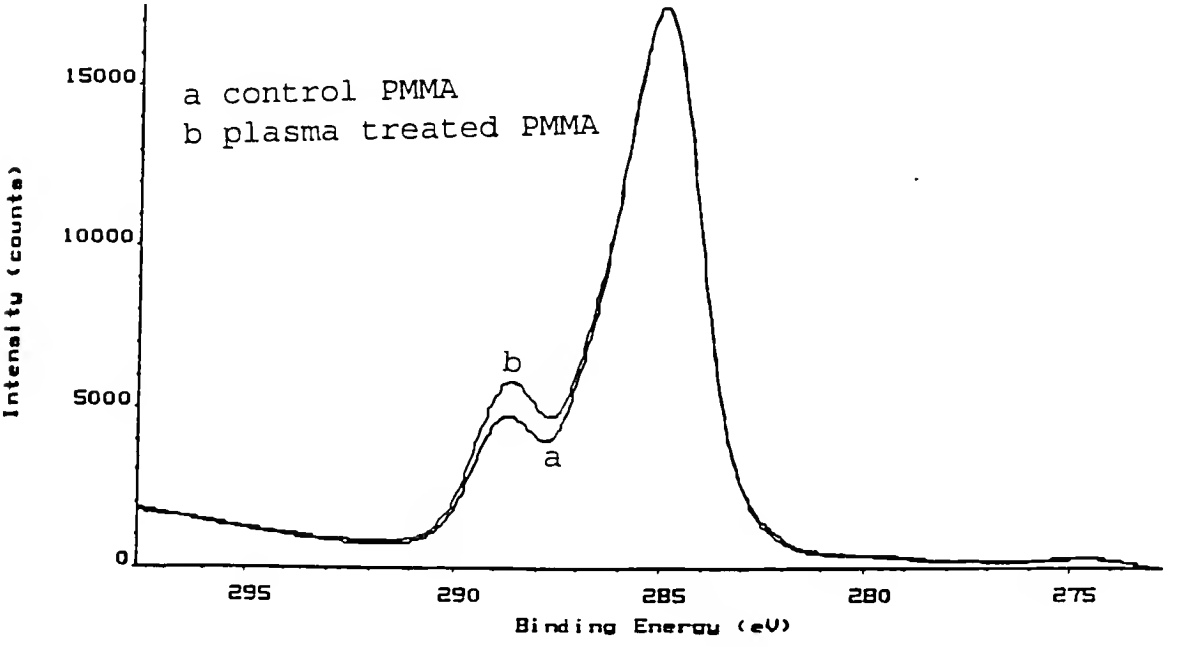

Figure 4-5. Overlapped C1s peaks for a control PMMA and a plasma treated PMMA

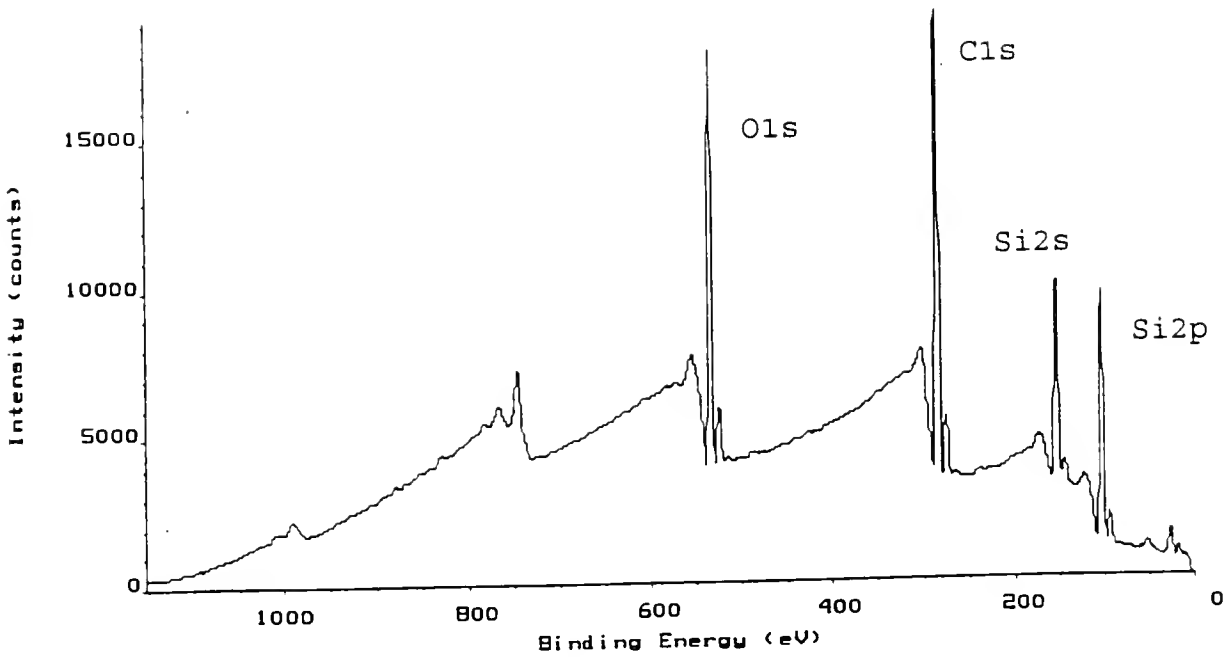

Figure 4-6. XPS spectrum of an unmodified PDMS

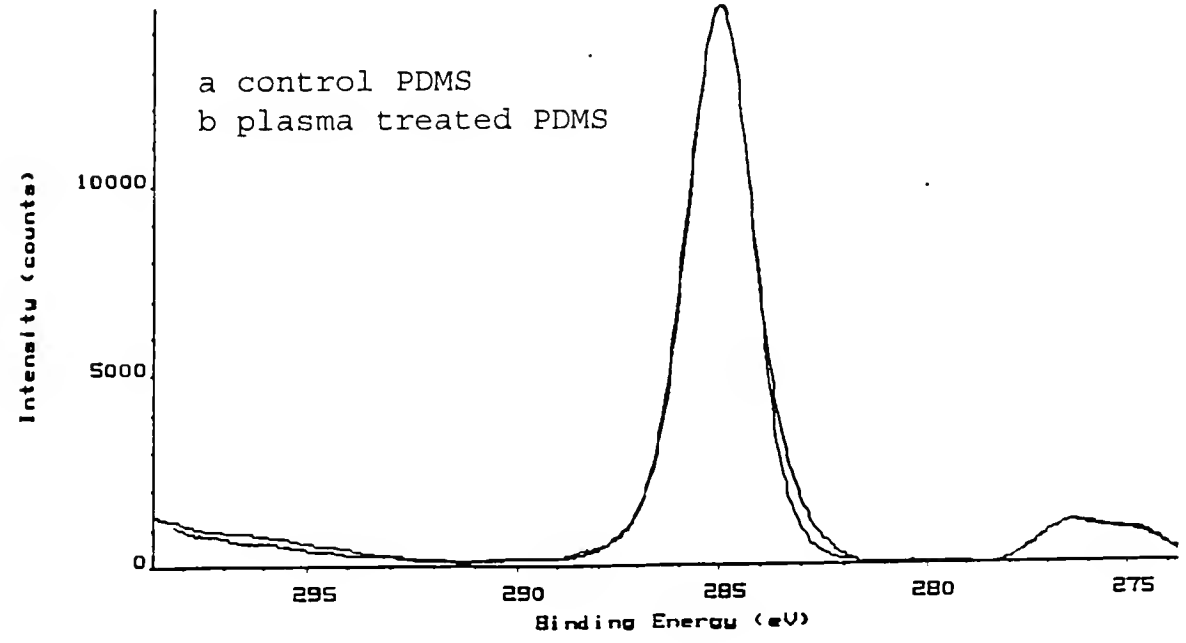

Figure 4-7. Overlapped C1s peaks for a control PDMS and a plasma treated PDMS

for plasma treated PDMS is slightly narrower than the untreated PDMS.

The differences between the control and plasma treated PDMS are the oxygen content and O1s/C1s ratio which have been shown in Table 4-5. The oxygen content increases, as does the O1s/C1s ratio after plasma treatment. This suggests that ablation of methyl groups from the PDMS is the most probable mechanism which is consistent with the decrease in C1s concentration [6].

The XPS of unmodified PP is shown in Figure 4-8. The only element present is carbon. The overlapped C1s peaks for a control PP and a plasma treated PP are present in Figure 4-9. The plasma treated PP C1s peak displays a minor peak adjacent to the major CH_X peak. Also, the oxygen content for plasma treated PP is 7.34% as shown in Table 4-5. Therefore, this suggest that the PP surface is highly oxidized by the plasma treatment. This may occur mainly at the tertitary carbon of PP molecules.

Figure 4-10 is the XPS for unmodified PC. The oxygen content and O1s/C1s ratio for PC in Table 4-5 increase somewhat after plasma treatment and the overlapped C1s peaks for control PC and plasma treated PC are also presented in Figure 4-11. Plasma treated PC has a different minor peak other than the ester peak in the control PC. This minor peak may indicate the presence of hydroxyl or carboxyl groups.

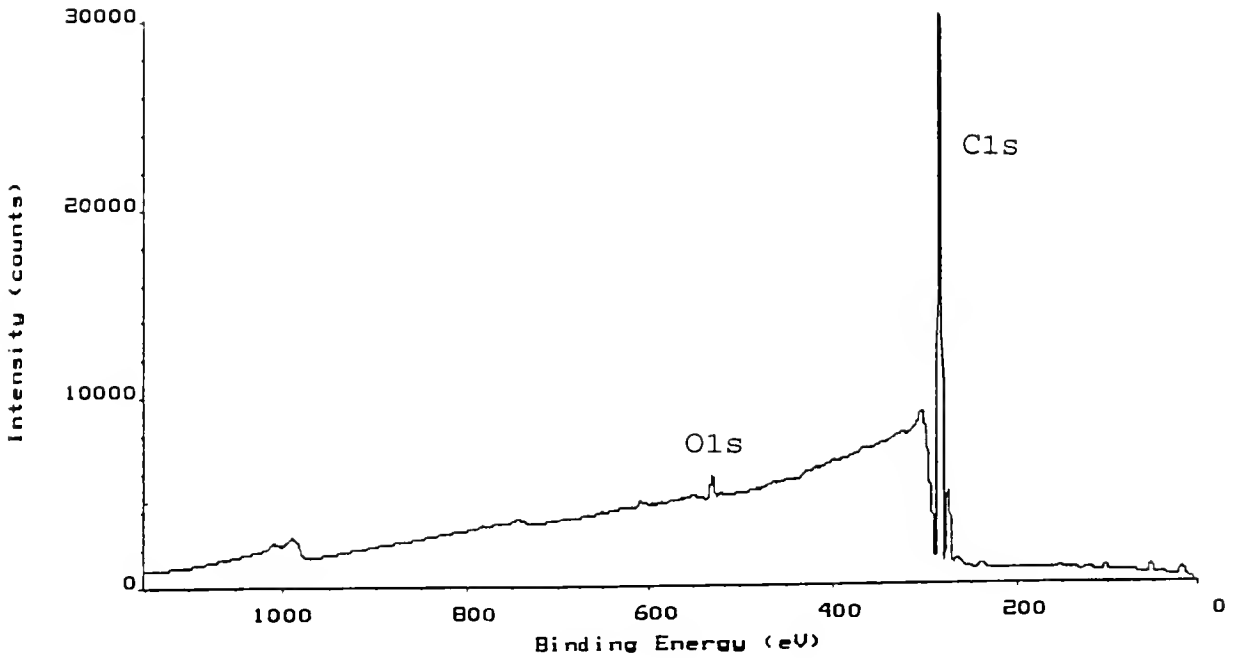

Figure 4-8. XPS spectrum of an unmodified PP

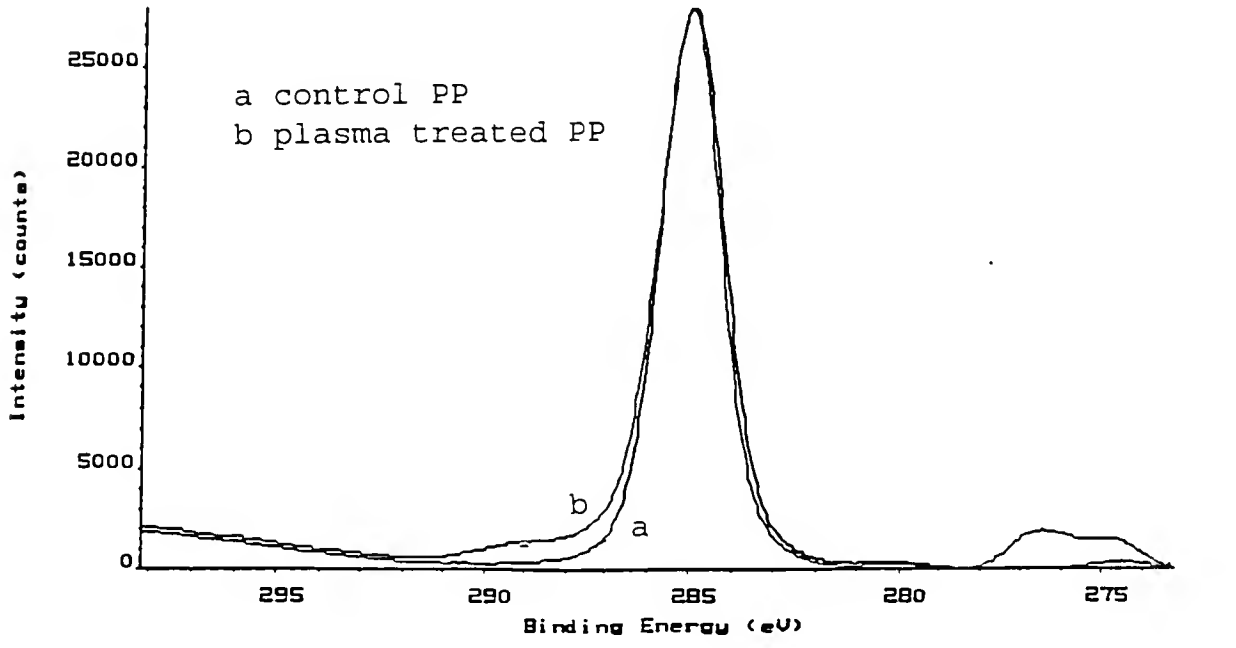

Figure 4-9. Overlapped C1s peaks for a control PP and a plasma treated PP

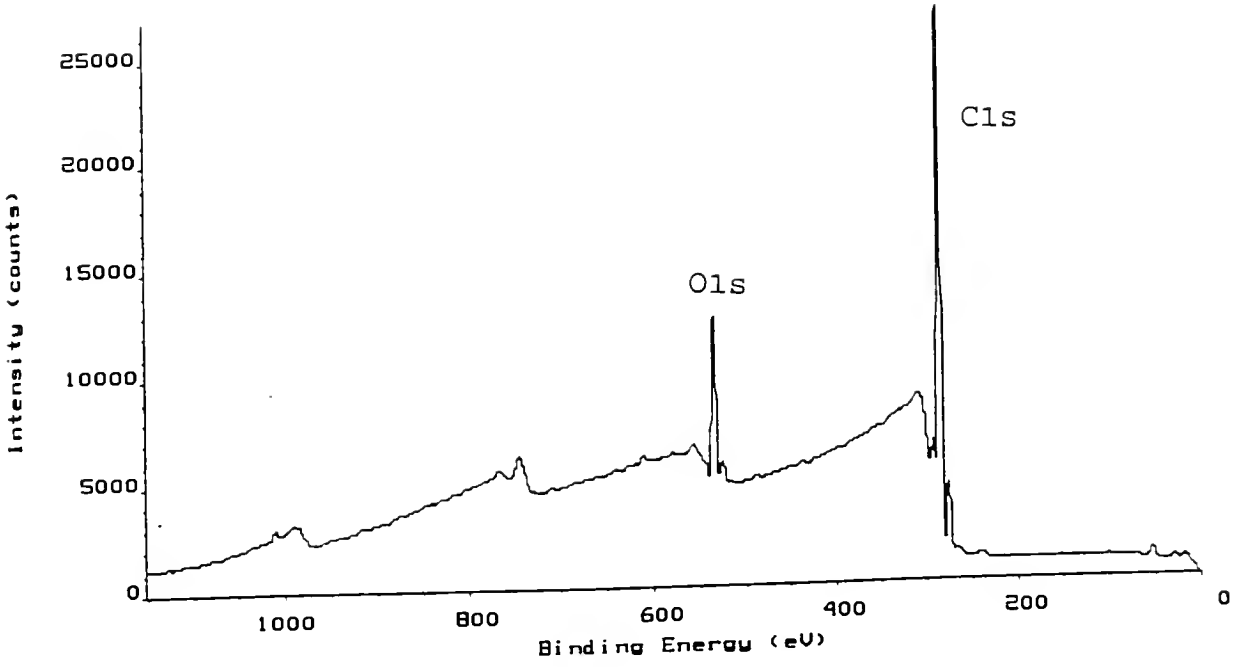

Figure 4-10. XPS spectrum of an unmodified PC

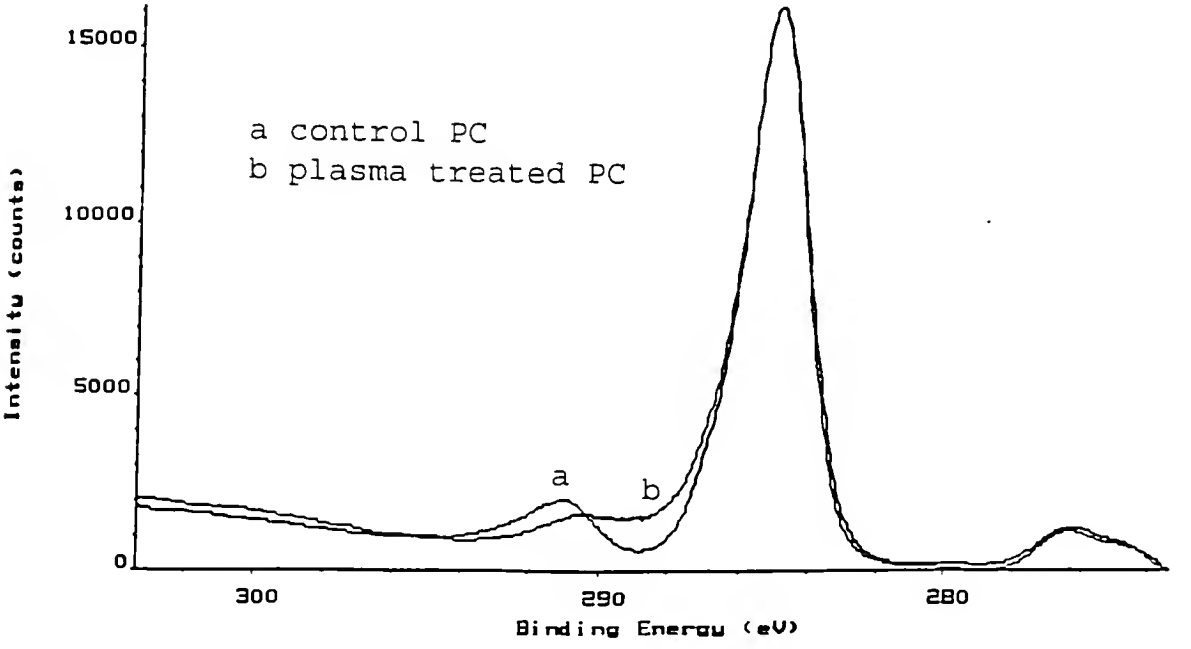

Figure 4-11. Overlapped C1s peaks for a control PC and a plasma treated PC

The XPS for unmodified FEP is shown in Figure 4-12. The overlapped C1s peaks for an unmodified FEP and a plasma treated FEP are presented in Figure 4-13. While the major C1s peak indicates the CF_X group, the minor peak which can be seen in the plasma treated FEP may imply formation of hydroxyl or carboxyl groups. A slight increase in oxygen content can be seen in the Table 4-5 for plasma treated FEP, but defluorination is not observed.

The XPS for unmodified PVDF is shown in Figure 4-14 (a). The overlapped C1s peaks for unmodified PVDF and plasma treated PVDF are presented in Figure 4-14 (b). Two major peaks for C1s are both in the control PVDF and in the plasma treated PVDF. The first major peak at 285 eV indicates the presence of the CH_X group and the second major peak at 290 eV represents the chemical shift of the CF_X group. The minor peak for the CO_X group is in between. Looking at Figure 4-14 (b), it is easy to see that the plasma treatment produces CO_X groups on the PVDF surface. In addition, the defluorination observed is shown on Table 4-5 for plasma treated PVDF since the surface fluorine concentration decreases after plasma treatment.

4.2.3 Summary of RF Plasma Treatment of PMMA, PDMS, PP, PC, PVDF, and FEP

The RF H_2O plasma effectively enhances the wettability of polymer surface without altering the bulk properties of substrate and produces oxygen-rich functional groups on the

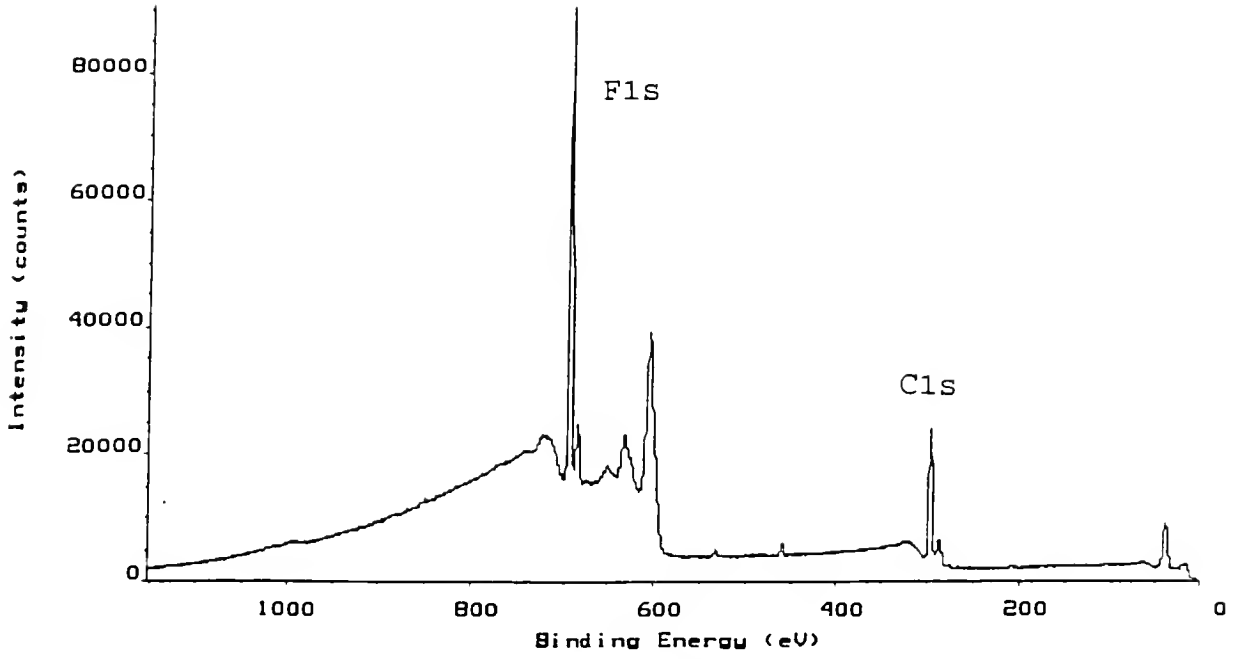

Figure 4-12. XPS spectrum of an unmodified FEP

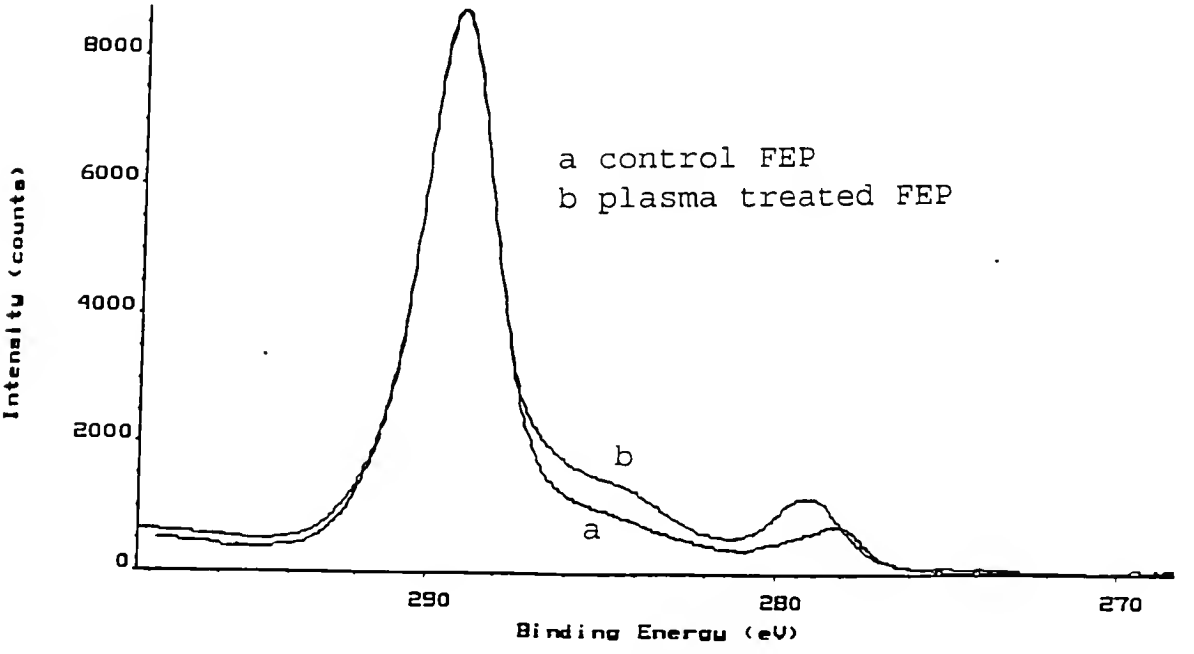

Figure 4-13. Overlapped C1s peaks for a control FEP and a plasma treated FEP

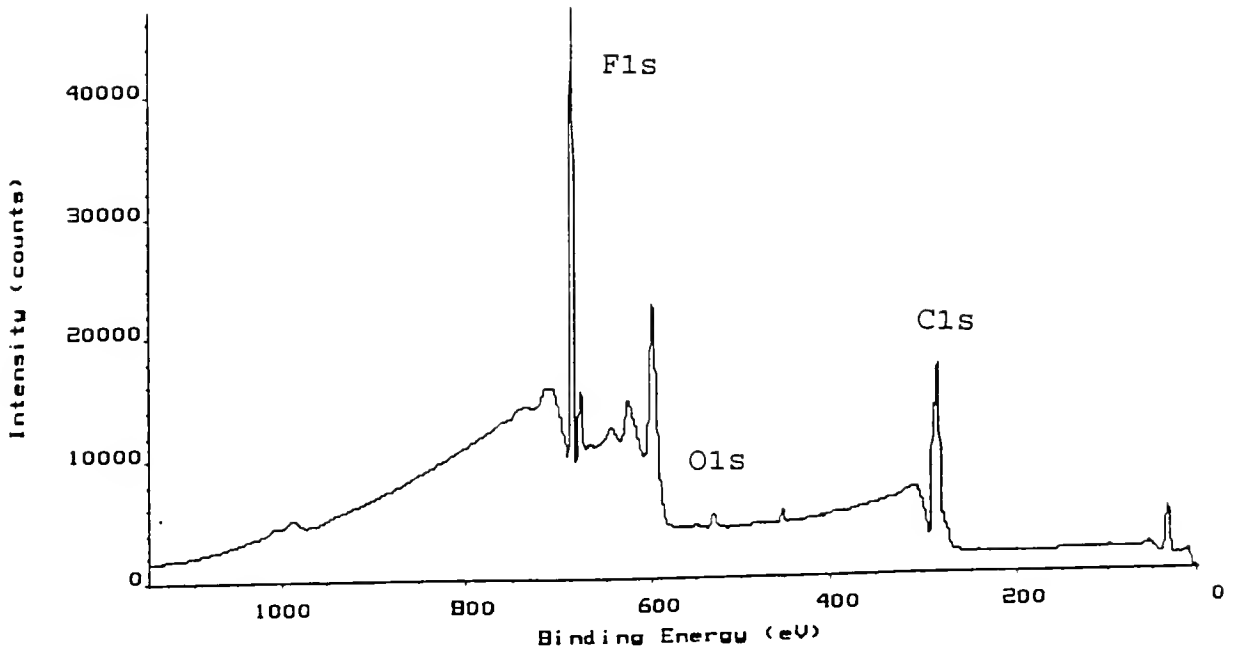

Figure 4-14 (a). XPS spectrum for unmodified PVDF

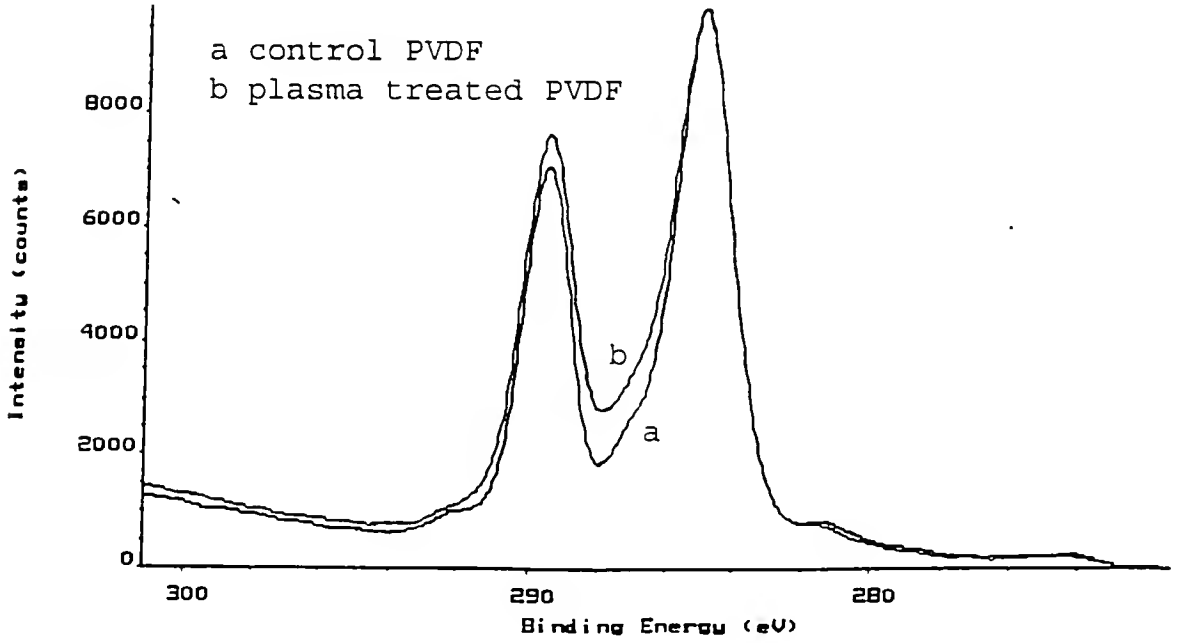

Figure 4-14 (b). Overlapped C1s peaks for control PVDF and plasma treated PVDF

upper surface layer (ca. 50-500 Å). These oxygen-rich functional groups possibly include hydroxyl, carboxyl, and hydroperoxide groups. The detailed mechanisms by which plasmas interact with polymer surface are very complex and can be explained in terms of two major mechanisms: 1) direct energy transfer resulting from the plasma active species such as ions, radicals, excited atoms and molecules interacting with the substrate surface; and 2) radiative (or nondirect) energy transfer from the UV radiation emitted from the plasma [46] as shown in Figure 4-15. Several types of excited species may be present in glow discharge of water vapor. These excited species include H•, OH• [49], H_2, O_2, [119], H_2O_2 [120,121], HO_2 [122,123], H^+, OH^-, H_2O^+, and H_3O^+. Clark and Dilks [124] reported that the direct energy mechanisms might affect only the topmost surface layers (2-3 monolayers) due to the relatively short mean-free path of the plasma species involved. At high power input, such as 50 Watts, the UV radiation emitted from the plasma has a relatively long mean-free path and may produce radicals both on the surface and in the subsurface of the polymer [124]. The prolonged plasma treatment time may further increase the depth of plasma penetration. In addition to the oxidation effect, RF plasma may have ablation effect on the substrate surface which may clean the substrate surface and cause a slight weight loss, or cross-linking effect on the polymer segments in the surface regions and lead to surface cracking (for example PDMS surface).

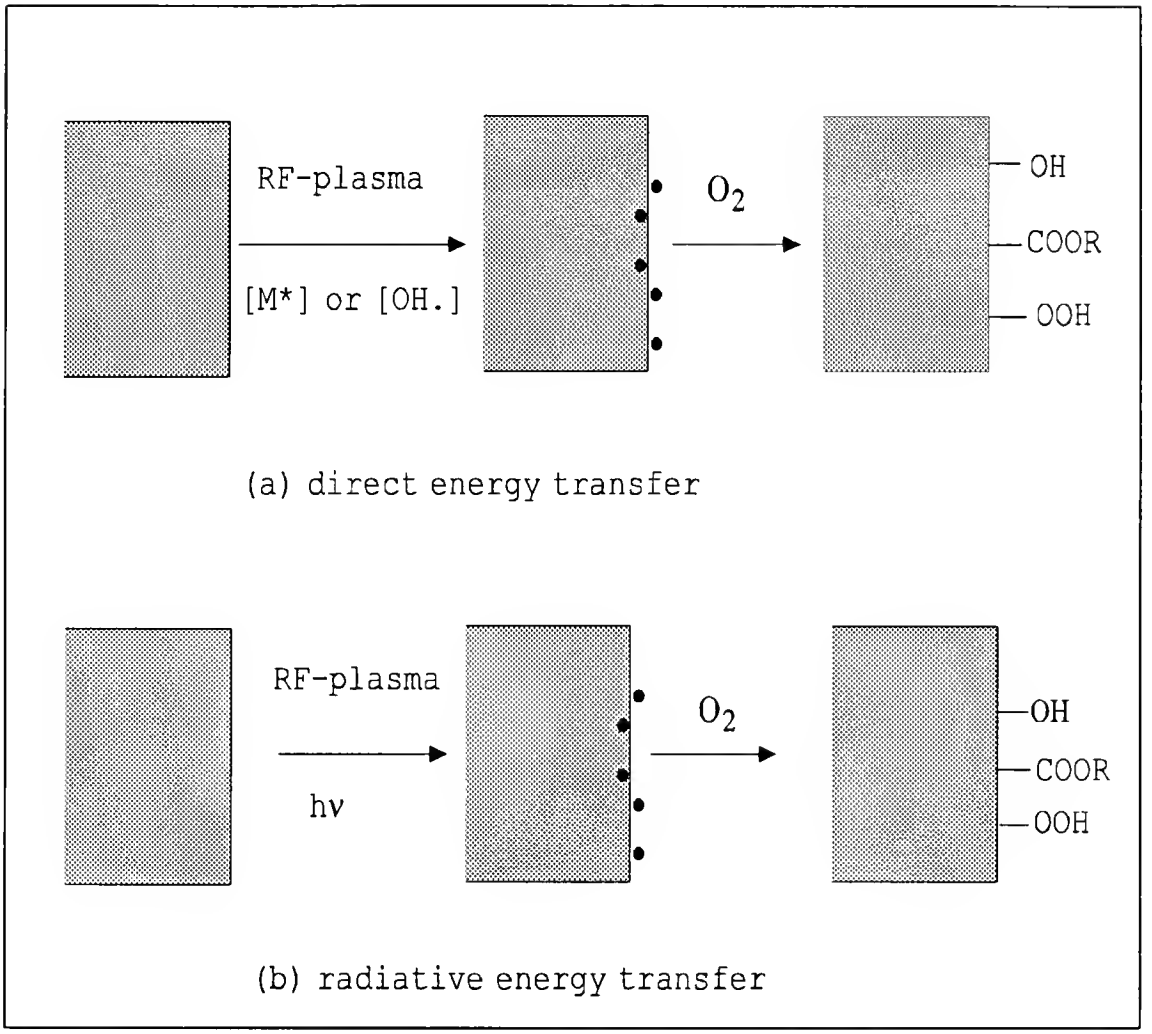

Figure 4-15. Schematic representation of RF plasma treatment.

Since the plasma treatment is the first step of "plasma/gamma" method, the extent of treatment may affect the following gamma-induced graft polymerization. Surface wettability and the reactive sites produced during plasma treatment are expected to enhance the result of gamma-induced graft polymerization.

4.3 Surface Graft Polymerization of PVP/NVP System onto PMMA, PDMS, PP, PC, FEP, and PVDF Using "Plasma/Gamma" Method

The "Plasma/Gamma" method was first studied by Yahiaoui [6] in this research group. This novel method combines two advanced techniques for surface modification. RFGD plasma treatment has been widely investigated as a tool for surface modification. The results in Section 4.2 indicate that the water RFGD plasma oxidizes the polymer surface and increases its wettability. In the case of the "Plasma/Gamma" method, the purpose of the plasma treatment is to provide active sites and a hydrophilic surface to facilitate the second step of gamma-induced graft polymerization using aqueous monomer solutions.

The monomer solution used in the gamma-induced graft polymerization was a 10 wt% PVP/NVP solution composed of two parts PVP and eight parts NVP. The purposes of using the PVP/NVP solution as a monomer solution is to reduce the solution viscosity, improve the grafting reaction, and make

the sample's post-washing easier. The polymeric substrates were pretreated with water RFGD plasma using plasma power of 50 watts and pressure of 100±10 mTorr. Plasma treatment time was varied from one to twenty five minutes. Methods to characterize the treated and untreated surfaces included contact angle measurements, gravimetric analysis, ellipsometry, FTIR/ATR, XPS, and SEM.

4.3.1 Surface Graft Coploymerization of PVP/NVP onto PMMA Using "Plasma/Gamma" Method

4.3.1.1 XPS analysis and contact angle measurements

The results of the XPS analysis and contact angle measurements for PVP/NVP-g-PMMA samples are listed in the Table 4-6. In the XPS analysis, the nitrogen content and N1s/O1s ratio was used to estimate the extent and quality of PVP graft. Results of the XPS analysis indicate that the nitrogen content of PVP/NVP-g-PMMA prepared by the plasma/gamma method was significantly higher than that prepared by the gamma method alone. All substrates exhibited a low contact angle indicating that the very hydrophilic surfaces were produced under all conditions. As indicated by % nitrogen, the water RFGD plasma treatment enhanced the grafting efficiency during the subsequent gamma-induced graft polymerization.

However, the surface nitrogen concentration did not increase significantly as the plasma treatment time increased. A very short treatment time such as one minute

Table 4-6. XPS analysis and contact angle measurements for PVP/NVP grafting onto PMMA using plasma/gamma method. (50 watts, 100 mTorr, 10 wt% PVP/NVP; 2/8, 0.15 Mrad)

Plasma Treatment Time (minutes)	Atomic Concentration (%)				Contact Angle (±5°)
	C1s	O1s	N1s	N1s/O1s	
unmodified PMMA	79.90	20.10			65
0	78.53	16.55	4.92	0.29	20
1	76.96	15.19	7.85	0.52	20
5	76.95	15.63	7.42	0.47	20
15	80.29	11.83	7.88	0.67	19
20	77.39	13.42	9.19	0.68	19

Note: 1. The PVP polymer theoretically contains 75% carbon, 12.5% oxygen and 12.5% nitrogen without counting the hydrogen atoms.

2. The gravimetric yield for the PVP/NVP-g-PMMA prepared by gamma method and 15 minutes plasma/gamma method is 1.16% and 1.23% respectively.

makes a noticeable difference although Yahiaoui [6] has shown that the plasma condition at 50 watts, 100 mTorr, and 15 minutes is the best condition for maximizing the CO_x content on the PMMA surface. Iwata et al. [118] also reported that the dependence of the peroxide formation on the treatment time is not linear in the study of corona surface treatment of the polyethylene. A longer exposure does not help formation of a larger amount of peroxide. The number of active sites may not increase with increasing the plasma treatment time. Therefore, a prolonged exposure in the plasma treatment does not enhance the gamma-induced graft polymerization.

Figure 4-16 (a) gives the XPS spectrum for PVP/NVP-g-PMMA without plasma pretreatment and Figure 4-16 (b) shows the spectrum for a PVP/NVP-g-PMMA sample with a 15 minute water RFGD pretreatment. The nitrogen peak in Figure 4-16 (b) is significantly higher than that in Figure 4-16 (a) indicating the increase in PVP graft. Figure 4-17 shows the overlapped C1s peaks for a control PMMA sample and a PVP/NVP surface modified PMMA sample using the plasma/gamma method. The extra minor peak in the control C1s is attributed to the ester group of PMMA. After the grafting of PVP/NVP onto the PMMA surface, this extra minor peak in PMMA appears covered by the presence of PVP graft. This suggests that the plasma/gamma surface modified PMMA is covered by a uniform layer of the PVP graft.

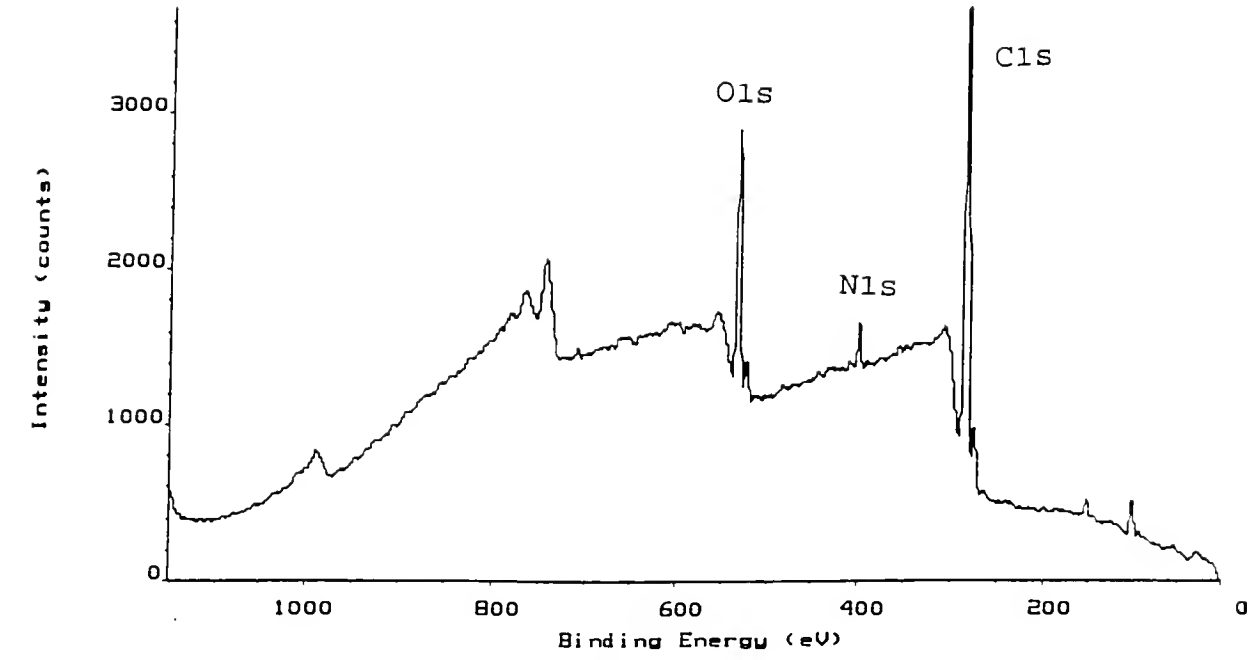

(a)

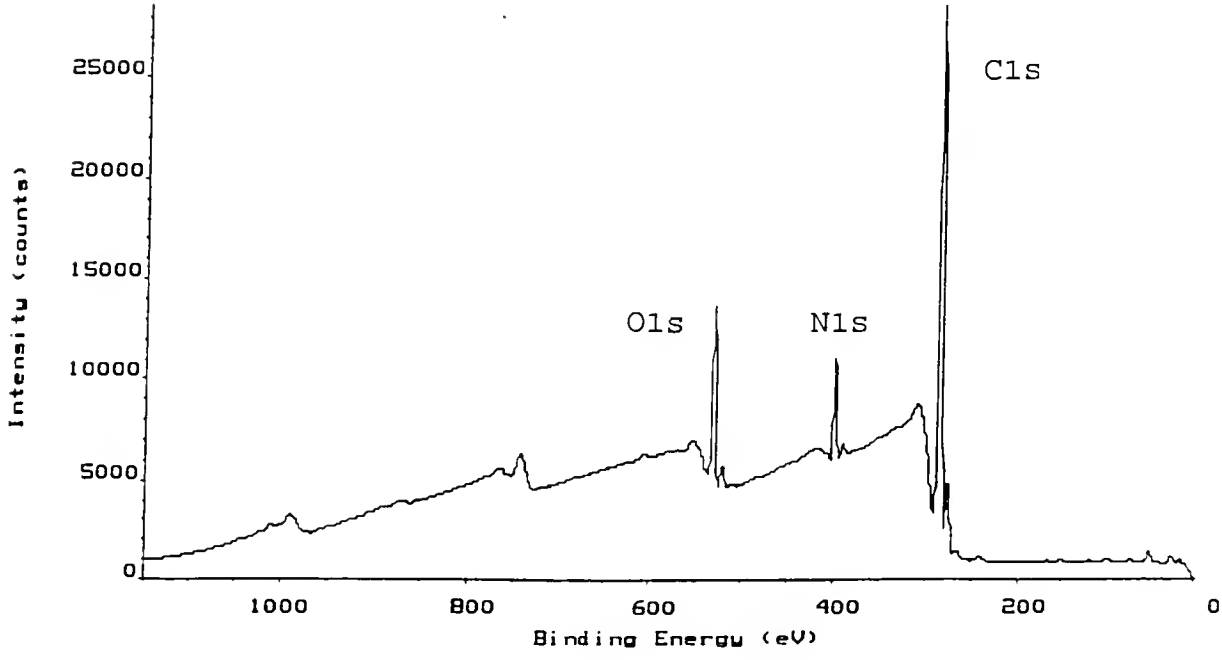

(b)

Figure 4-16. The XPS spectra for PMMA
(a) PVP/NVP-g-PMMA prepared by gamma method. (10 wt% PVP/NVP; 2/8, 0.15 Mrad)
(b) PVP/NVP-g-PMMA prepared by plasma/gamma method. (15 minutes water RFGD, 10 wt% PVP/NVP; 2/8, 0.15 Mrad)

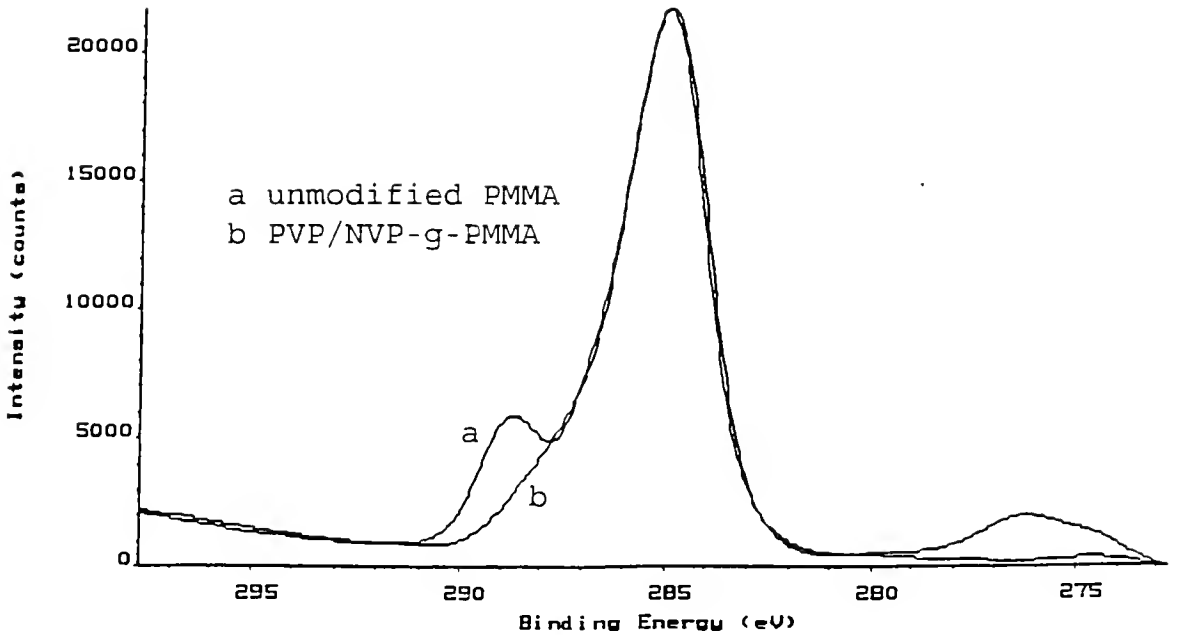

Figure 4-17. Overlapped C1s peaks for an unmodified PMMA and a PVP/NVP modified PMMA made by plasma/gamma method. (15 minutes water RFGD, 10 wt% PVP/NVP; 2/8, 0.15 Mrad)

4.3.1.2 FT-IR/ATR

Figure 4-18 is the FT-IR/ATR spectrum for unmodified PMMA. The vibrational assignment for the pertinent peaks for PMMA are listed in Table 4-7. Figure 4-19 is the FT-IR/ATR spectrum of PVP/NVP-g-PMMA made by the plasma/gamma method. The most distinguishing peak for the PVP polymer is the amide carbonyl peak at 1650 cm^{-1}. Comparison of Figures 4-18 and 4-19 shows no difference between them, except that the intensity of the ester carbonyl group decreased for the plasma/gamma treated sample. The amide carbonyl peak at 1650 cm^{-1} for the plasma/gamma treated sample is too weak to be observed. FT-IR/ATR analysis does not clearly afford the evidence of a PVP graft, probably due to a very thin PVP graft.

4.3.1.3 Graft thickness measurement

The thickness of graft for PVP/NVP-g-PMMA made by the plasma/gamma method is not detectable by optical microscopy. Several biological stains such as eosin Y or crystal violet can stain the PVP graft if the graft thickness is larger than 5 μm, but in the present case the graft thickness for PVP/NVP-g-PMMA appears to be less than 5 μm consistent with the observations of Mentak [92] for PVP/NVP graft polymerization. Also, FT-IR/ATR result in section 4.3.1.2 implies that the graft thickness is less than 3 μm, which is the detection limit of FT-IR/ATR.

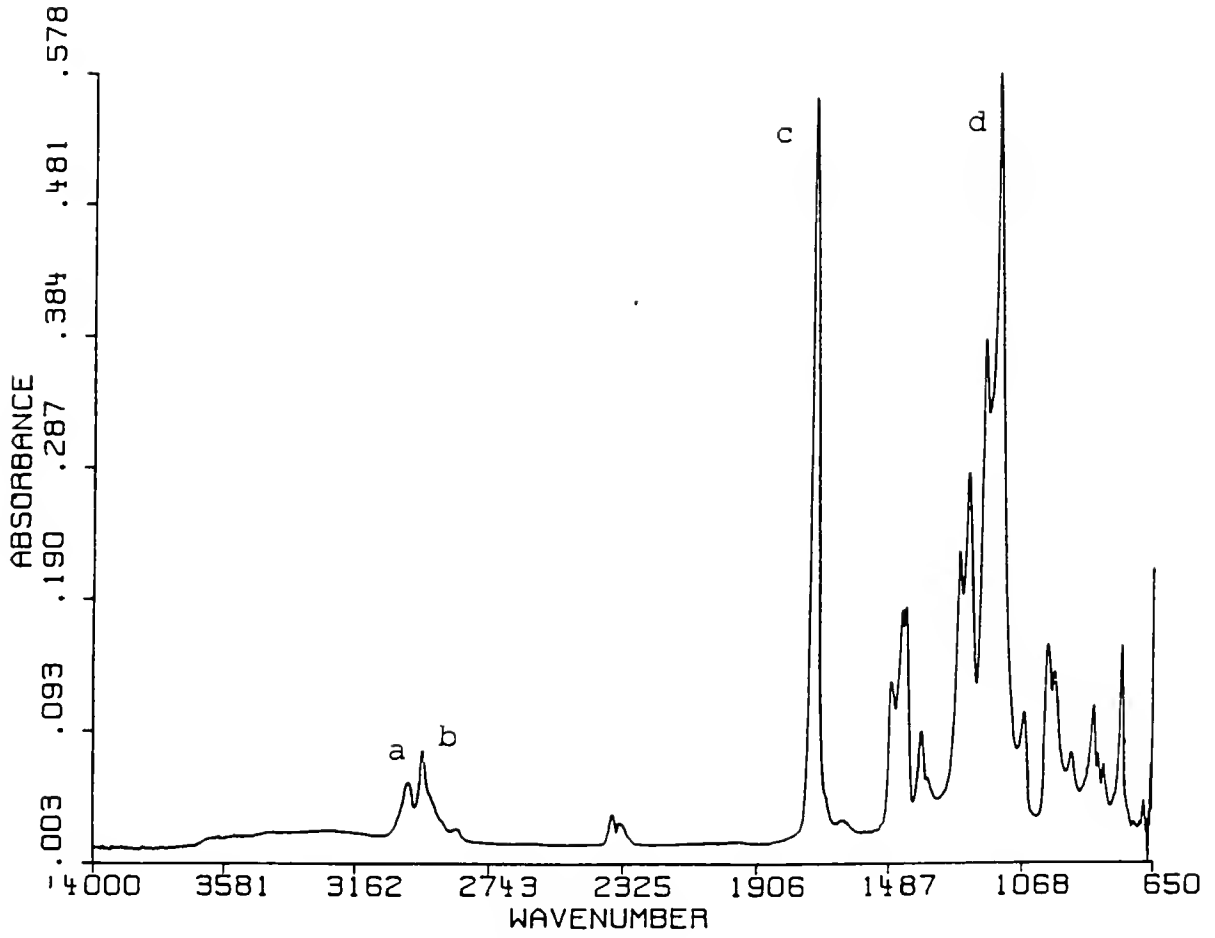

Figure 4-18. FT-IR/ATR spectrum of unmodified PMMA.

Table 4-7. The peak assignments for the unmodified PMMA IR spectrum in Figure 4-18.

Peak	ν (cm^{-1})	assignment
a	2950	$-CH_2-$ assym. stretch
b	2844	$-CH_2-$ sym. stretch
c	1725	-COO- stretch
d	1110-1082	-C-O-C- stretch

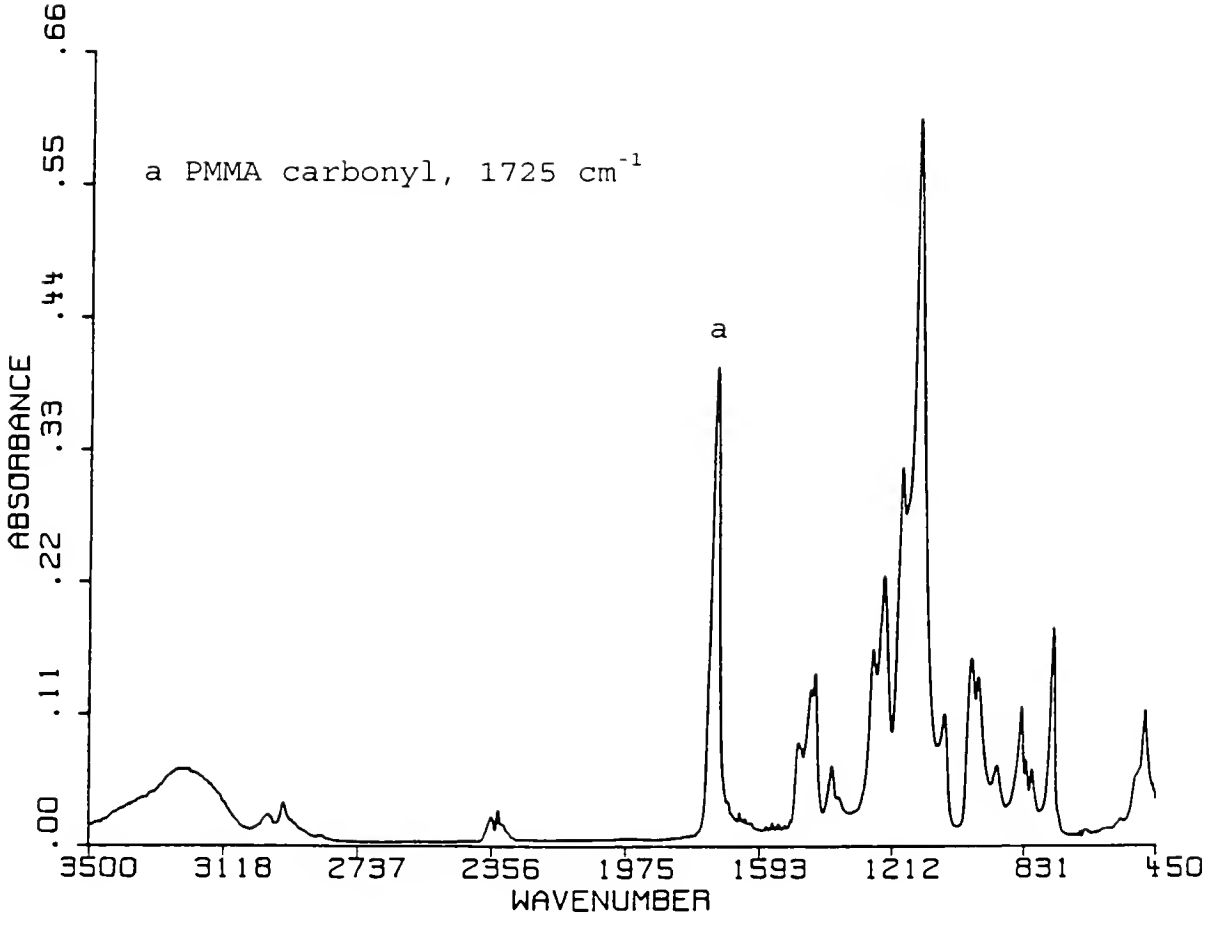

Figure 4-19. FT-IR/ATR spectrum for the PVP/NVP modified PMMA made by the plasma/gamma method. (15 minutes water RFGD, 10 wt% PVP/NVP; 2/8, 0.15 Mrad)

An ellipsometer (L117 ellipsometer, Gaertner Scientific Corp., Chicago, IL) was used to determine graft thickness. Ellipsometry does not give a unique value and has to be confirmed by the other techniques. The minimum thickness and the refractive index of the graft were determined by a computer program and are listed in Table 4-8. The results suggest that the unmodified PMMA is covered by a thin layer of skin which might be oxidized PMMA. The minimum graft thickness is about 2,300 to 2,500 Å for all the samples regardless of the method and monomers used to treat the samples.

4.3.1.4 SEM

Unmodified PMMA, plasma treated PMMA, and PVP/NVP modified PMMA were examined by low voltage SEM. Figure 4-20 shows the SEM micrograph for the three samples at 1000x. All the surfaces look extremely smooth. The plasma treatment and PVP/NVP grafting did not appear to alter the smoothness of the PMMA surface.

4.3.2 Surface Graft Polymerization of PVP/NVP onto PDMS Using "Plasma/Gamma" Method

4.3.2.1 XPS analysis and contact angle measurements

Table 4-9 summarizes the results of the XPS analysis and contact angle measurements for the PVP/NVP-g-PDMS prepared by the plasma/gamma method. The contact angle for the PDMS surface decreased from 90° for the unmodified to

Table 4-8. Thickness measurement for NVP-g-PMMA and PVP/NVP-g-PMMA by ellipsometry

Sample	Angle (°)				n	Graft thickness (Å) $d_0 \pm [1/2(n_1^2 - n_0^2\sin^2\phi_0)^{-1/2}]m\lambda$
	P1	A1	P2	A2		
Unmodified PMMA	48.4	6.5	142.5	173.9	1.485	266±2517*m
NVP-g-PMMA[1]	45.5	10.5	135.8	170.2	1.530	2311±2383*m
NVP-g-PMMA[1]	45.1	9.1	134.8	171.2	1.530	2400±2394*m
NVP-g-PMMA[2]	45	9.5	134.3	169.6	1.530	2428±2386*m
NVP-g-PMMA[2]	41.9	10.7	132.4	170.4	1.531	2571±2382*m
PVP/NVP-g-PMMA[3]	41.4	8.5	134	170	1.530	2549±2391*m
PVP/NVP-g-PMMA[3]	45.5	9.1	136	170.5	1.530	2315±2390*m
PVP/NVP-g-PMMA[4]	45.8	9.5	135	171	1.530	2359±2389*m
PVP/NVP-g-PMMA[4]	45.3	10	135	170	1.528	2370±2390*m

1 gamma method (10% NVP, 0.15 Mrad)
2 plasma/gamma method (15 minutes water RFGD, 10% NVP, 0.15 Mrad)
3 gamma method (10% PVP/NVP; 2/8, 0.15 Mrad)
4 plasma/gamma method (15 minutes water RFGD, 10% PVP/NVP; 2/8, 0.15 Mrad)

(a)

(b)

Figure 4-20. SEM photographs (1000x) for
(a) unmodified PMMA
(b) plasma treated PMMA (15 min. water RFGD)

(c)

Figure 4-20--continued
(c) plasma/gamma surface modified PMMA (15 min. water RFGD, 10 wt% PVP/NVP; 2/8, 0.15 Mrad)

Table 4-9. XPS analysis and contact angle measurements for PVP/NVP grafting onto PDMS using plasma/gamma method. (50 watts, 100 mTorr, 10 wt% PVP/NVP; 2/8, 0.15 Mrad)

	Atomic Concentration (%)					
Plasma Treatment Time (minutes)	C1s	O1s	Si2p	N1s	N1s/Si2p	Contact Angle (±5°)
unmodified PDMS	48.91	22.59	28.49			90
0	49.62	22.24	27.85	0.65	0.023	28
1	51.56	23.21	23.24	2.00	0.086	21
5	52.42	23.44	19.50	4.65	0.238	20
15	54.69	19.98	22.88	2.46	0.107	20
20	48.04	24.54	26.51	0.91	0.034	20

Note: 1. The PVP polymer theoretically contains 75% carbon, 12.5% oxygen, and 12.5% nitrogen without counting the hydrogen atoms.
2. The yield of graft (gravimetric) for the gamma treated and 15 plasma/gamma treated is 0.77% and 0.73%, respectively.

28° for the gamma treated, and then to 21° for the one minute plasma/gamma treated.

The surface nitrogen concentration of the PVP/NVP-g-PDMS samples increased somewhat from 0.65% for the gamma treated to 2% for the one minute plasma/gamma treated. This suggested that the plasma pretreatment enhanced the grafting of PVP/NVP onto PDMS.

The surface of unmodified PDMS is composed of densely packed methyl groups, which exhibit a highly hydrophobic character. Water RF-plasma treatment may cause the ablation of methyl groups ($-CH_3$), since the surface carbon concentration decreased from 48.9% to 31.7% for the fifteeen minute treatment with no decreasing in the surface silicon concentration as shown in the Table 4-5. A slight weight loss (c.a. 0.41% for 15 minute plasma treatment) was also observed during plasma treatment. Therefore, the first step of RF-plasma treatment might mainly cross-link the PDMS surface and introduce the polar groups to the surface. After plasma/gamma treatment, the surface carbon concentration for the fifteen minute plasma pretreated returned to 54.6%. This suggested that the plasma/gamma treated PDMS surface was dominated by PVP/NVP graft. Also, the yield of graft (gravimetric) for the gamma treated and 15 minute plasma/gamma treated is 0.77% and 0.73%, respectively. If the weight loss during plasma treatment is included, the yield of graft for the plasma/gamma treated will be slightly higher than the gamma treated.

However, as the plasma treatment time changed, the surface nitrogen concentration reached a maximum value at 5 minute treatment, and then decreased with increasing plasma treatment time. The glass transition of PDMS is around -130 °C. Thus at room temperature, the polymer segments are highly flexible and in motion [125]. When the plasma treatment time was prolonged for more than 5 minutes, the treatment depth may have increased. And moreover, the grafted PVP may more readily migrate into the bulk of PDMS. Surface ablation in the plasma may also explain somewhat less efficient grafting with prolonged plasma treatment. When the depth of penetration of PVP is beyond the sensitivity for XPS, the atomic concentration nitrogen should decrease. The depth of penetration of FT-IR/ATR is much larger than XPS. This hypothesis for PVP migration was therefore also examined by FT-IR/ATR and discussed in Section 4.3.2.2.

The XPS spectra for PVP/NVP-g-PDMS made by the gamma method and by the plasma/gamma method are shown in Figure 4-21 (a) and (b), respectively. An insignificant nitrogen peak appears in the spectrum when there is no plasma pretreatment. On the other hand, a very visible nitrogen peak appears in the spectrum for PDMS when there is a plasma pretreatment. This indicates that the surface nitrogen concentration for the plasma/gamma treated is significantly higher than that for the gamma treated. Mentak [92] also

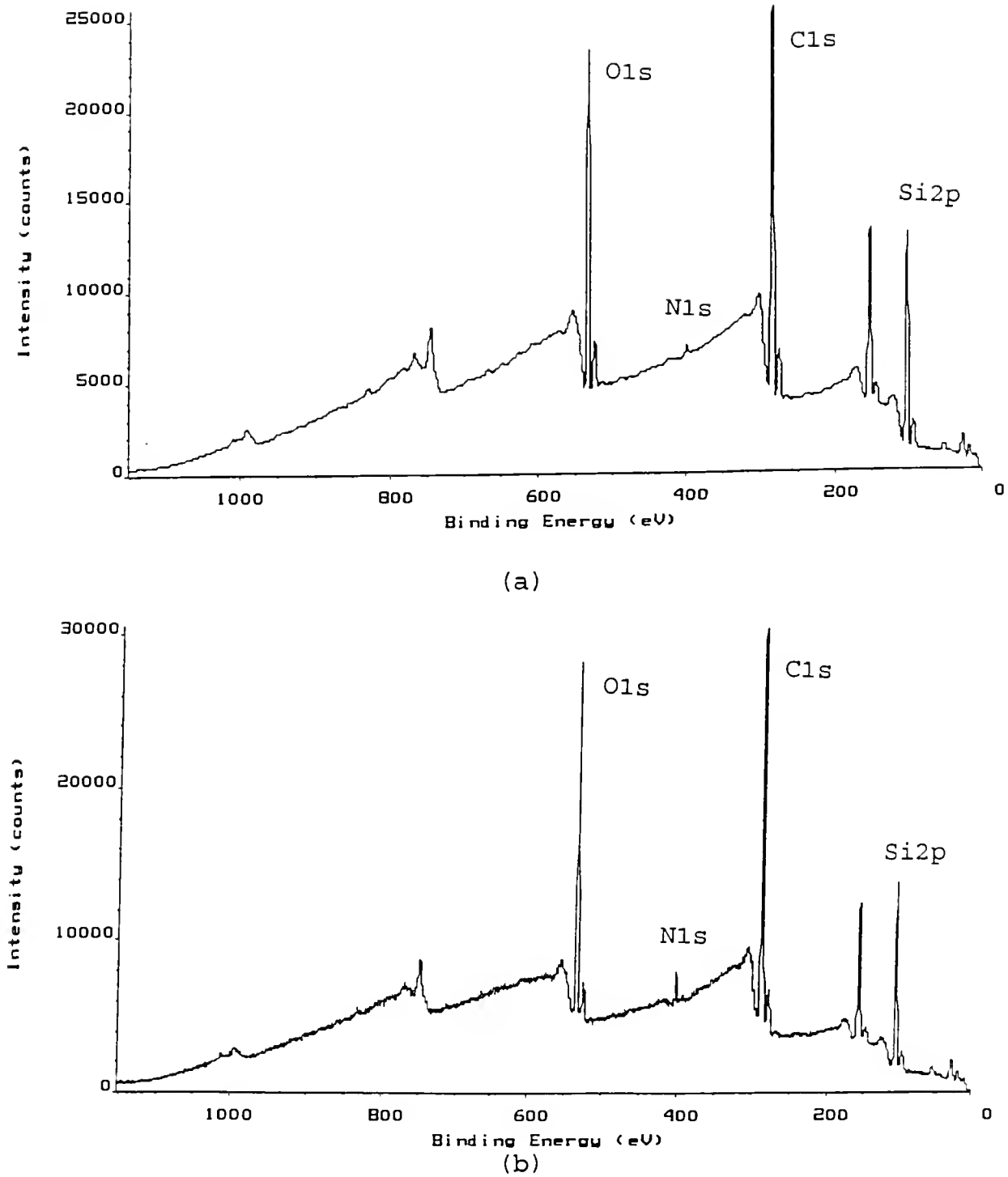

Figure 4-21. The XPS spectra for PDMS
(a) PVP/NVP-g-PDMS prepared by gamma method. (10 wt% PVP/NVP; 2/8, 0.15 Mrad)
(b) PVP/NVP-g-PDMS prepared by plasma/gamma method. (15 minutes water RFGD, 10 wt% PVP/NVP; 2/8, 0.15 Mrad)

showed that the PVP graft on PDMS surface by PVP/NVP solution is more stable than that by the NVP alone. Yahiaoui [6] suggested that most of the PVP graft onto PDMS is not on the surface, but gets buried in the bulk of the substrate. As indicated by the nitrogen peak, the quality of PVP graft on the PDMS surface made by the plasma/gamma method proved to be better than that by the gamma method alone. The evidence for the PVP graft on PDMS is also identifiable by the overlapping C1s peaks in Figure 4-22. The C1s peak for PVP/NVP surface modified PDMS displays an minor peak on the left side. This minor peak is due to the chemical shift of amide carbonyl groups in PVP.

4.3.2.2 FT-IR/ATR

The PVP graft can also be identified by its amide carbonyl group. Figure 4-23 shows the FT-IR/ATR spectrum of unmodified PDMS. The major absorption peaks for unmodified PDMS are listed in Table 4-10. Also, the FT-IR/ATR spectra for PVP/NVP-g-PDMS made by the gamma method and by the plasma/gamma method are given in Figure 4-24 (a) and (b), respectively. The amide carbonyl peak at 1660 cm^{-1} which is not present in Figure 4-23 is clearly present in the Figure 4-24 (a) and (b). However, the amide carbonyl peak in Figure 4-24 (b) is more intense than that in Figure 4-24 (a). This suggests that the PVP graft by the plasma/gamma method is more uniform and thicker than that by the gamma method alone.

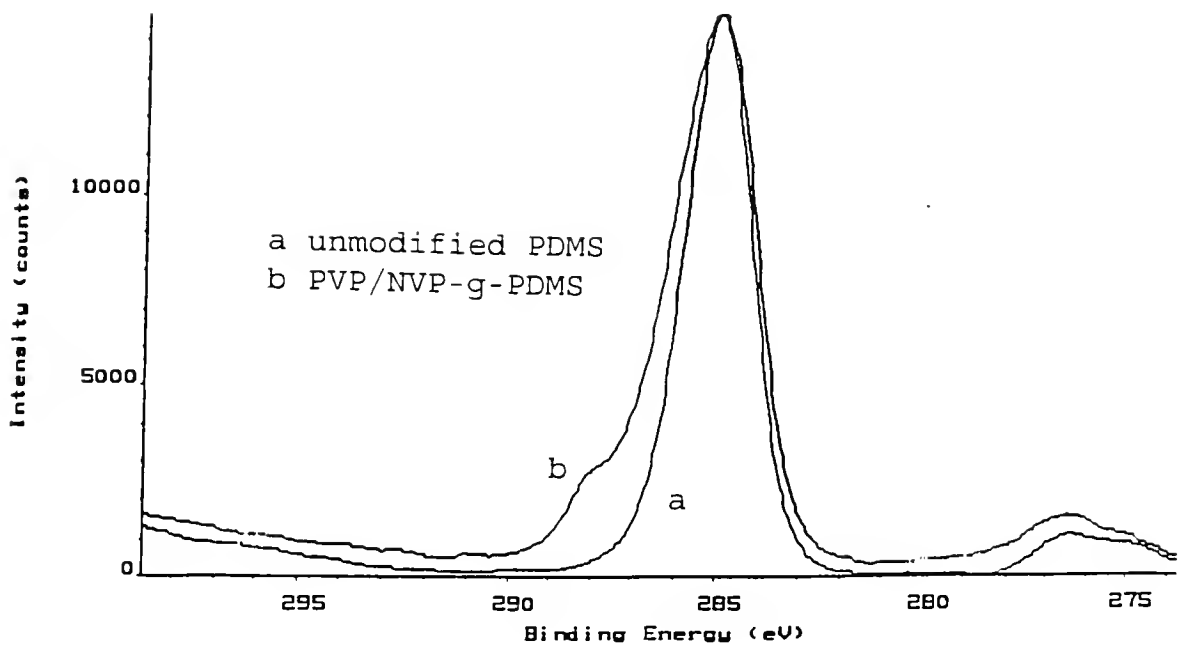

Figure 4-22. Overlapped C1s peaks for an unmodified PDMS and a PVP/NVP modified PDMS made by plasma/gamma method. (5 minutes water RFGD, 10 wt% PVP/NVP; 2/8, 0.15 Mrad)

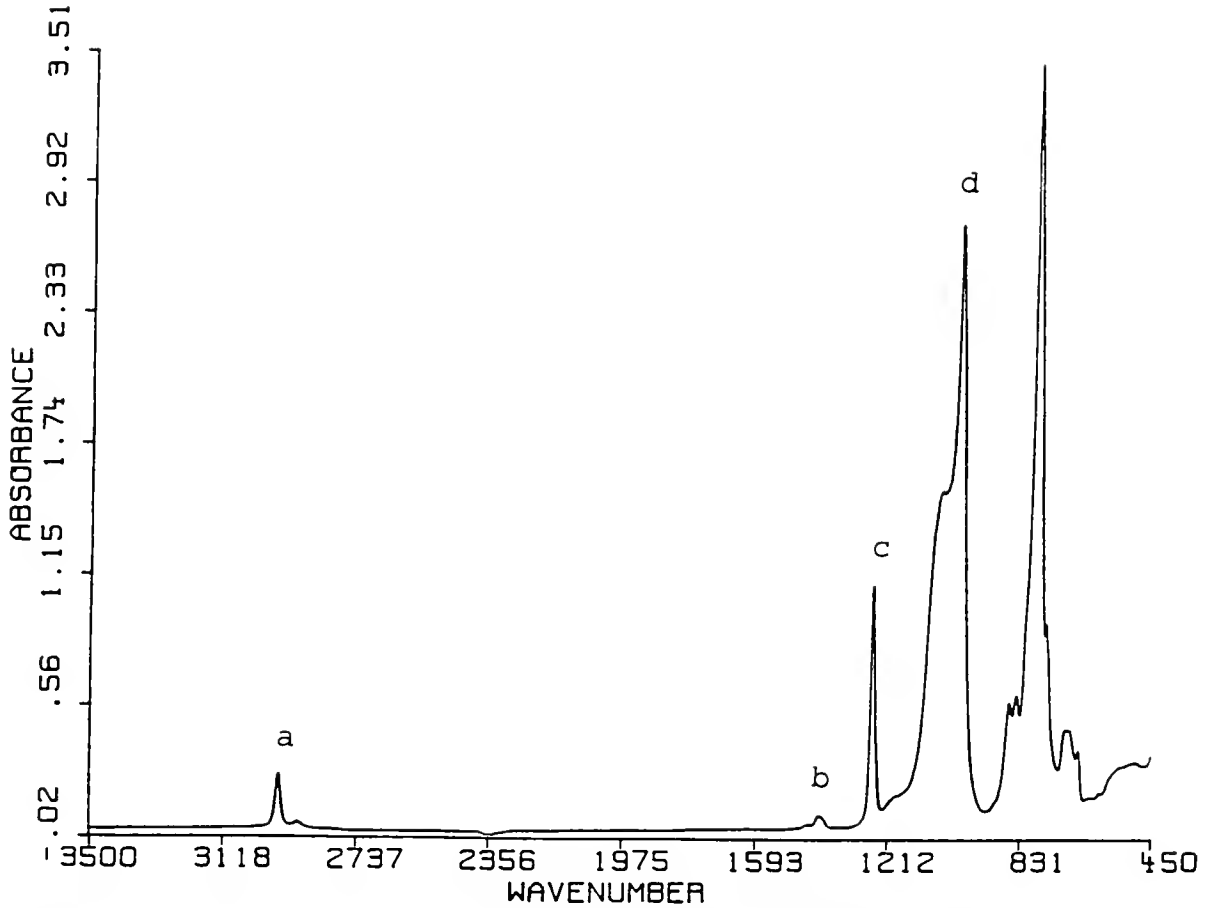

Figure 2-23. FT-IR/ATR spectrum of unmodified PDMS.

Table 4-10. The peak assignments for the unmodified PDMS IR spectrum in Figure 2-23.

peak	ν (cm^{-1})	assignment
a	2961	$-CH_3$ stretch
b	1412	$-CH_3$ bend
c	1256	$-Si-CH_3$ stretch
d	1006	-Si-O-Si- stretch

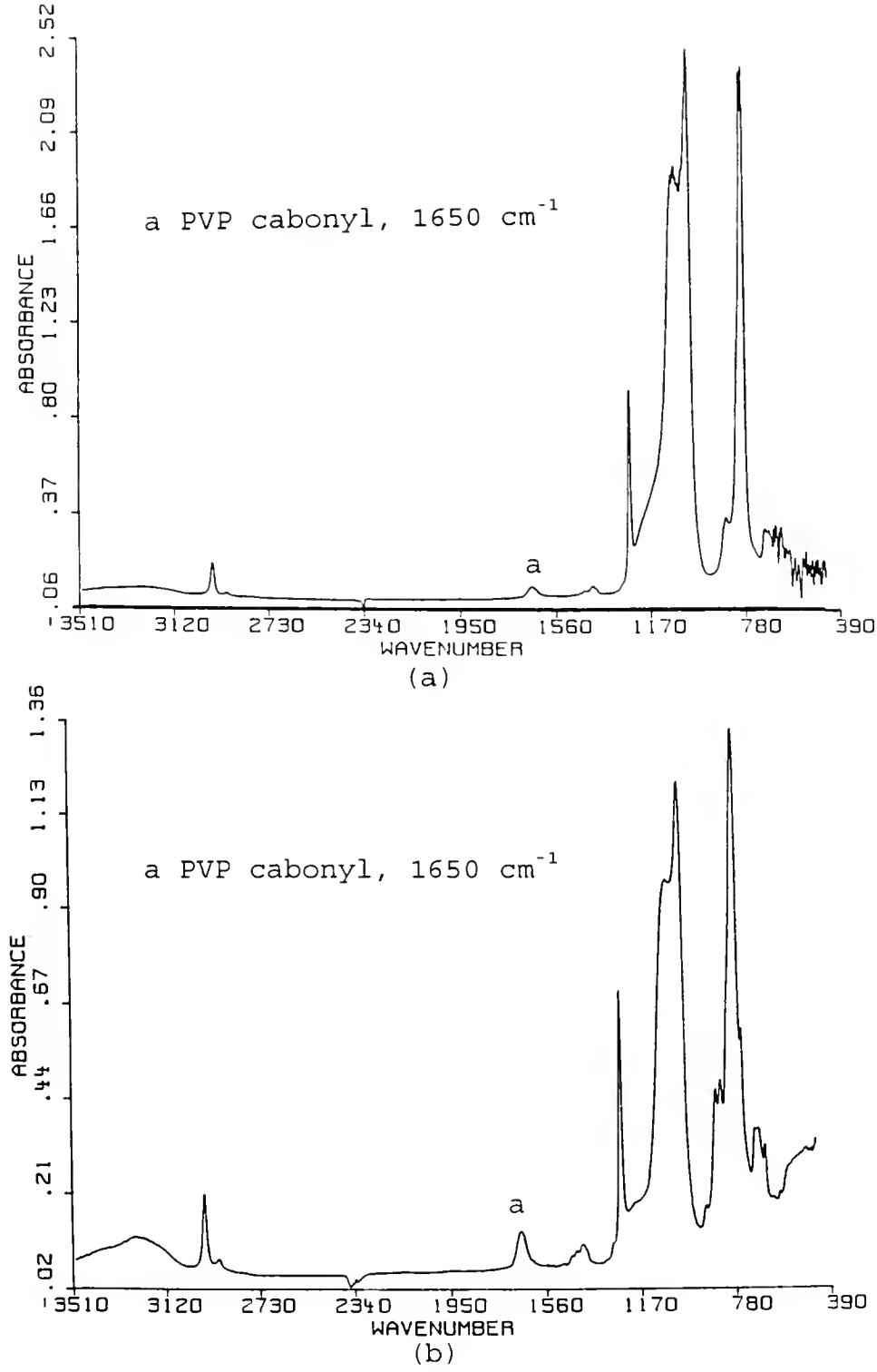

Figure 4-24. FT-IR/ATR spectra for PVP/NVP-g-PDMS
(a) made by the gamma method
(b) made by the plasma/gamma method. (20 minutes water RFGD, 10 wt% PVP/NVP; 2/8, 0.15 Mrad)

The hypothesis of PVP migration in PDMS was investigated using FT-IR/ATR analysis. Four FT-IR/ATR spectra including an unmodified sample and samples plasma pretreated for 5 minutes, 15 minutes, or 20 minutes are shown in the Figure 4-25. The intensity for the amide carbonyl peak at 1660 cm^{-1} increases with increasing plasma treatment time. The peak ratio for the amide carbonyl at 1660 cm^{-1} versus Si-CH_3 stretching at 1256 cm^{-1} indicates the extent of PVP graft. These IR peak ratio and the XPS nitrogen concentrations were plotted against the plasma treatment time and are presented in Figure 4-26. With increasing plasma treatment time, the IR peak ratio increased, but the XPS surface nitrogen content decreased. The IR analysis depth (ca. 0.6-3 μm) is much deeper than the XPS analysis depth (ca. 30-50 Å). The schematic diagram of PVP migration in PDMS is illustrated in Figure 4-27. When the plasma treatment time exceeded 5 minutes, the PVP polymer appears to more readily migrate deeper into the PDMS so that the surface nitrogen concentration decreases by XPS, but increases by FT-IR/ATR analysis. Ratner et al. [126] has also reported the migration of a hydrogel to and from the surface of a graft copolymer exposed alternately to water and drying.

4.3.2.3 SEM

Figure 4-28 (a), (b), and (c) are SEM photographs for the unmodified PDMS, plasma treated PDMS, and PVP/NVP modified PDMS, respectively. The plasma treated PDMS has

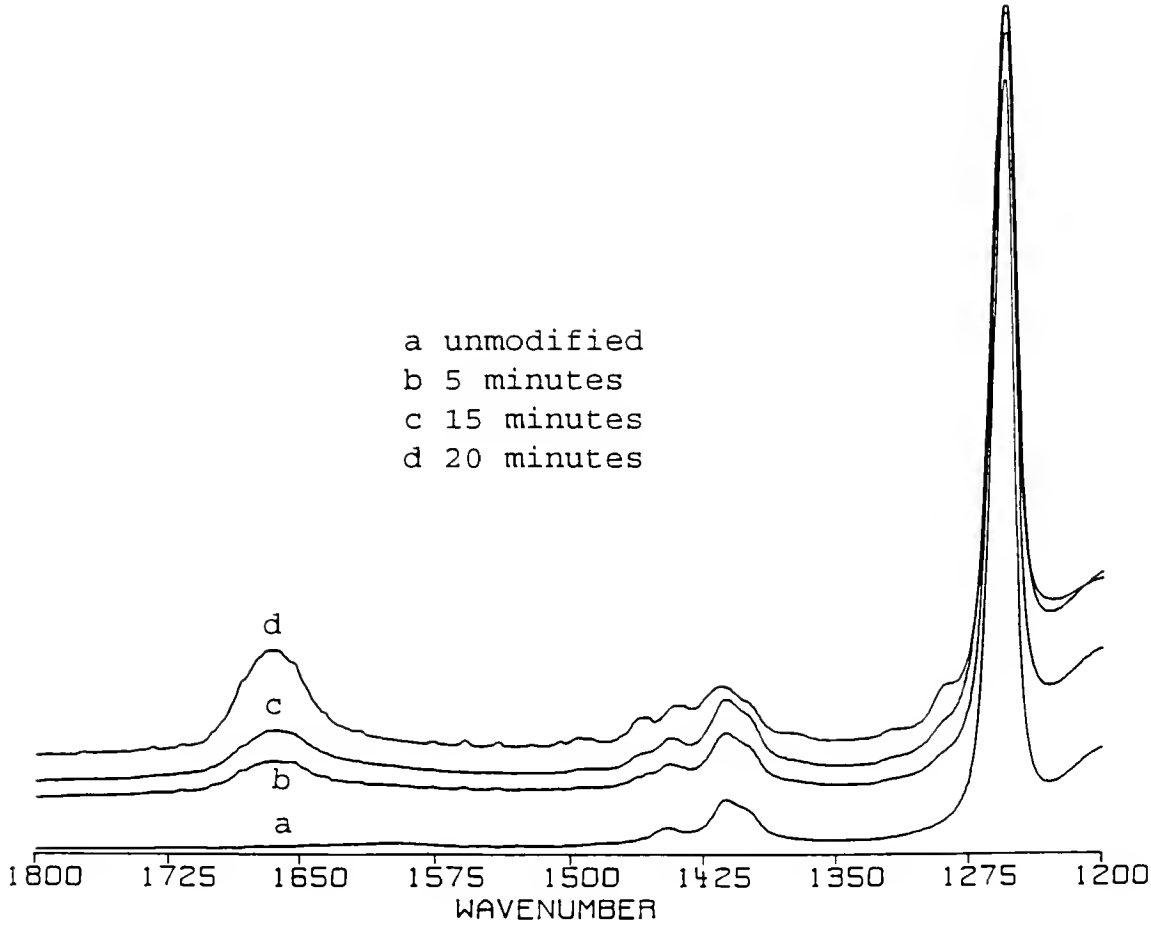

Figure 4-25. Overlapped FT-IR/ATR spectra for the unmodified, 5 minutes, 15 minutes, and 20 minutes plasma pretreated PVP/NVP-g-PDMS.

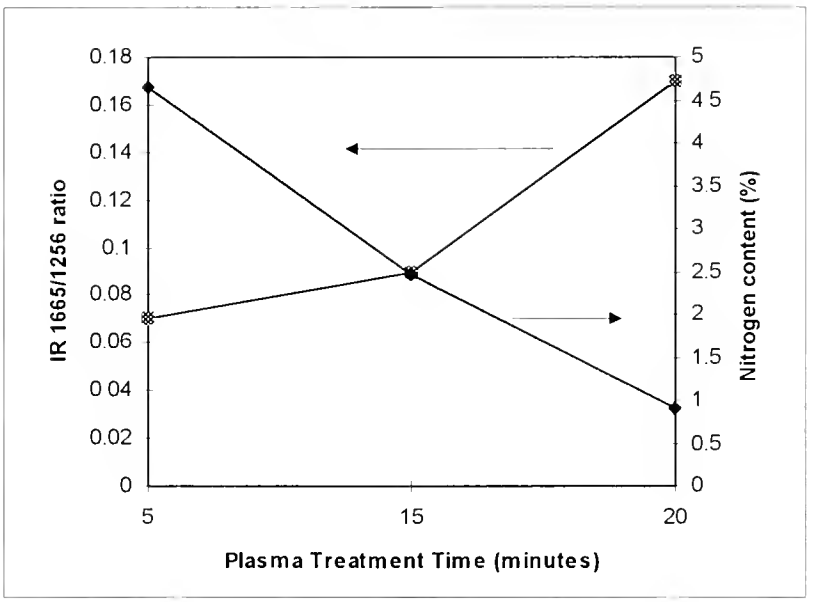

Figure 4-26. Plot of the IR peak ratio (1665 cm-1/1256 cm-1) and the nitrogen content versus the plasma treatment time for the PVP/NVP modified PDMS made by the plasma/gamma method.

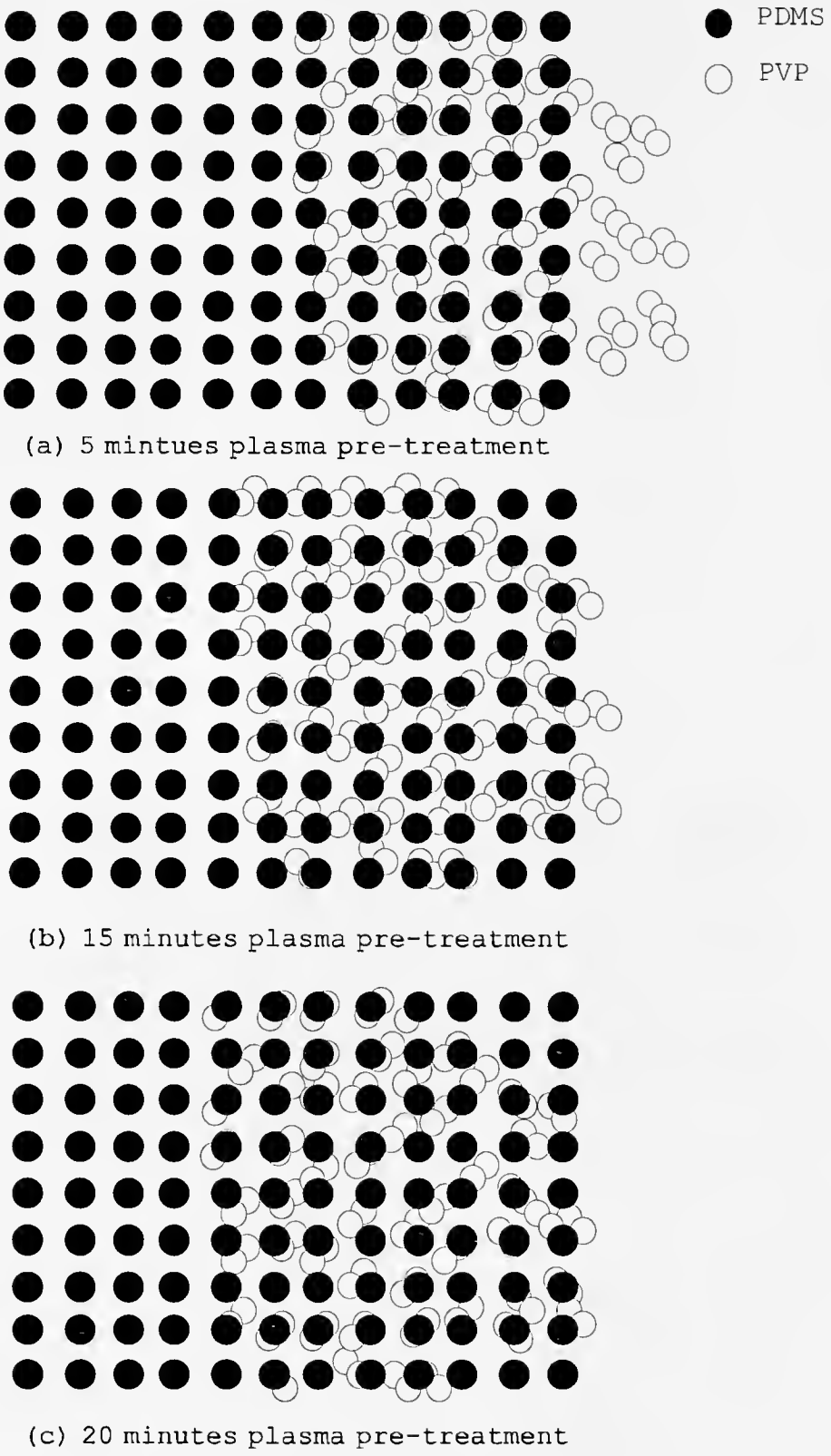

Figure 4-27 Schematic diagram of PVP migration in PDMS.

(a)

(b)

Figure 4-28. SEM photographs (1000 X) for
(a) unmodified PDMS
(b) plasma treated PDMS (15 min. water RFGD)

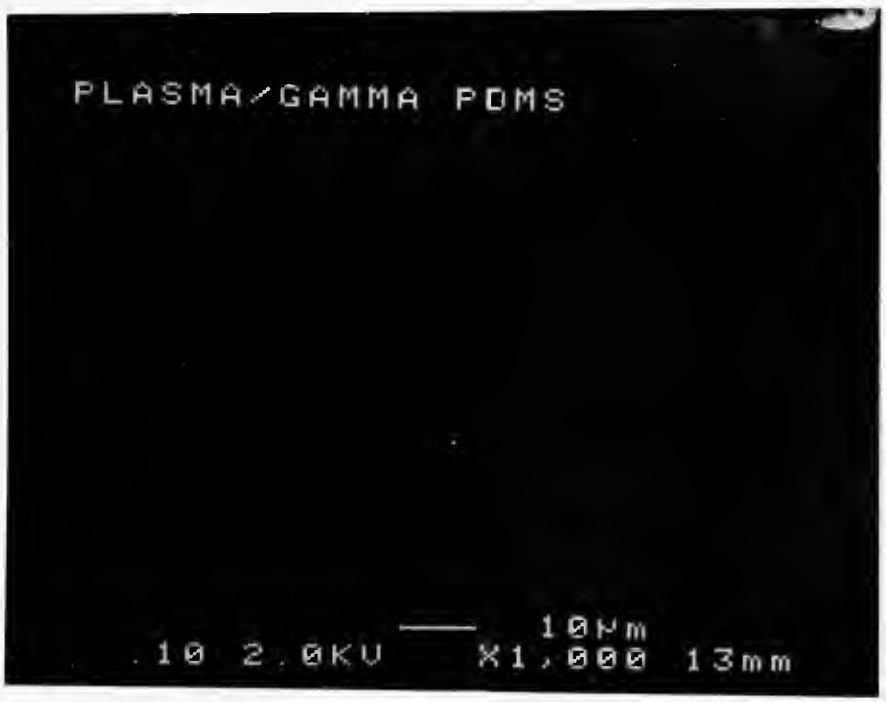

(c)

Figure 4-28--continued
(c) plasma/gamma surface modified PDMS (15 min. water RFGD, 10 wt% PVP/NVP; 2/8, 0.15 Mrad)

some regular scratch lines on surface, which disappear after PVP grafting. The formation of these scratch lines on the plasma treated PDMS surface may be due to the residual stress cracking induced by the cross-linking of PDMS in the surface region during plasma treatment. This also suggests that the PVP graft has a smoothing effect on these scratch lines.

4.3.3 Surface Graft Polymerization of PVP/NVP onto PP Using "Plasma/Gamma" Method

4.3.3.1 XPS analysis and contact angle measurements

The results of the XPS analysis and contact angle measurements for PVP/NVP-g-PP samples are presented in Table 4-11. The surface nitrogen concentration for the PVP/NVP-g-PP significantly increased from 0.98% for the gamma treated to 3.98% for the one minute plasma/gamma treated. The contact angle for unmodified PP is near 90°. The contact angle for the plasma/gamma treated PP is around 20°, compared to 55° for the gamma treatment only. Obviously, PVP K-90 molecules can not effectively wet the untreated PP surface.

Previous results in Table 4-5 showed that the surface carbon concentration for unmodified PP and fifteen minute plasma treated PP was 100% and 92.66%, respectively. The ablation of hydrogen at tertiary carbon and the introduction of hydroxyl or peroxide groups to the PP surface might be

Table 4-11. XPS analysis and contact angle measurements for PVP/NVP grafting onto PP using plasma/gamma method. (50 watts, 100 mTorr, 10% PVP/NVP; 2/8, 0.15 Mrad)

Plasma Treatment Time (minutes)	Atomic Concentration (%)				Contact Angle (±5°)
	C1s	O1s	N1s	N1s/O1s	
unmodified PP	100.00	0.00			90
0	96.51	2.53	0.96	0.38	55
1	91.74	4.33	3.92	0.90	20
5	90.40	5.19	4.41	0.85	20
15	92.76	3.84	3.40	0.88	18
20	90.77	4.94	4.41	0.89	18

Note: 1. The PVP polymer theoretically contains 75% carbon, 12.5% oxygen and 12.5% nitrogen without counting the hydrogen atoms.

predominating during the RF-plasma treatment. These reactive sites produced by the RF-plasma treatment are effectively enhancing the grafting of PVP/NVP onto PP during gamma-induced graft polymerization since the N1s/O1s ratio for the one minute plasma/gamma treated PP as shown in Table 4-11 is very close to the theoretical ratio of PVP. Therefore, the effectiveness of the RF-plasma treatment on the PP is very obvious in terms of surface nitrogen concentration and contact angle.

The results also indicate that a short treatment time of one minute was enough to make a distinct improvement. A longer plasma treatment time for PP did not significantly improve the nitrogen concentration or N1s/O1s ratio. PP behaved similarly to PMMA with the plasma/gamma treatment. Figure 4-29(a) shows the XPS spectrum for PVP/NVP-g-PP treated by the gamma method. The nitrogen peak in the spectrum is negligible. On the other hand, the nitrogen peak is clearly seen in Figure 4-29(b) which is the spectrum for PVP/NVP-g-PP treated by the plasma/gamma method. In addition, Figure 4-30 shows overlapped C1s peaks for an unmodified PP and a PVP/NVP-g-PP made by plasma/gamma method. The C1s peak for PVP/NVP-g-PP made by plasma/gamma method displayed a minor peak on the left shoulder which is due to the chemical shift of the amide carbonyl group of PVP.

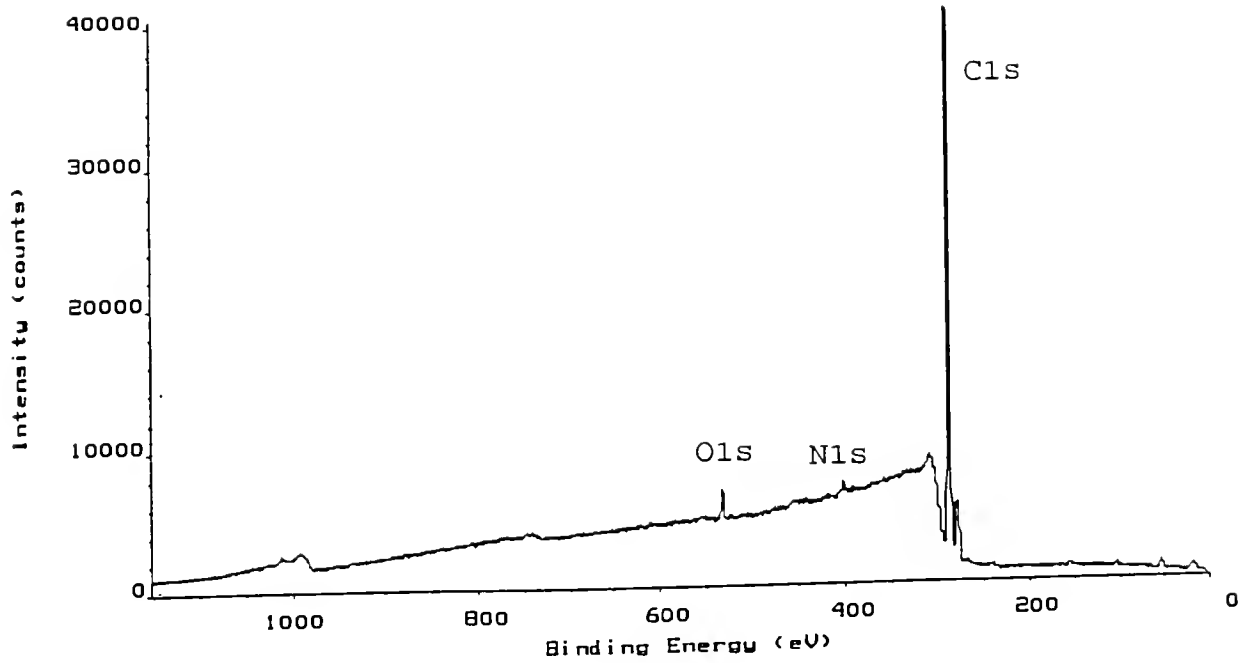

(a)

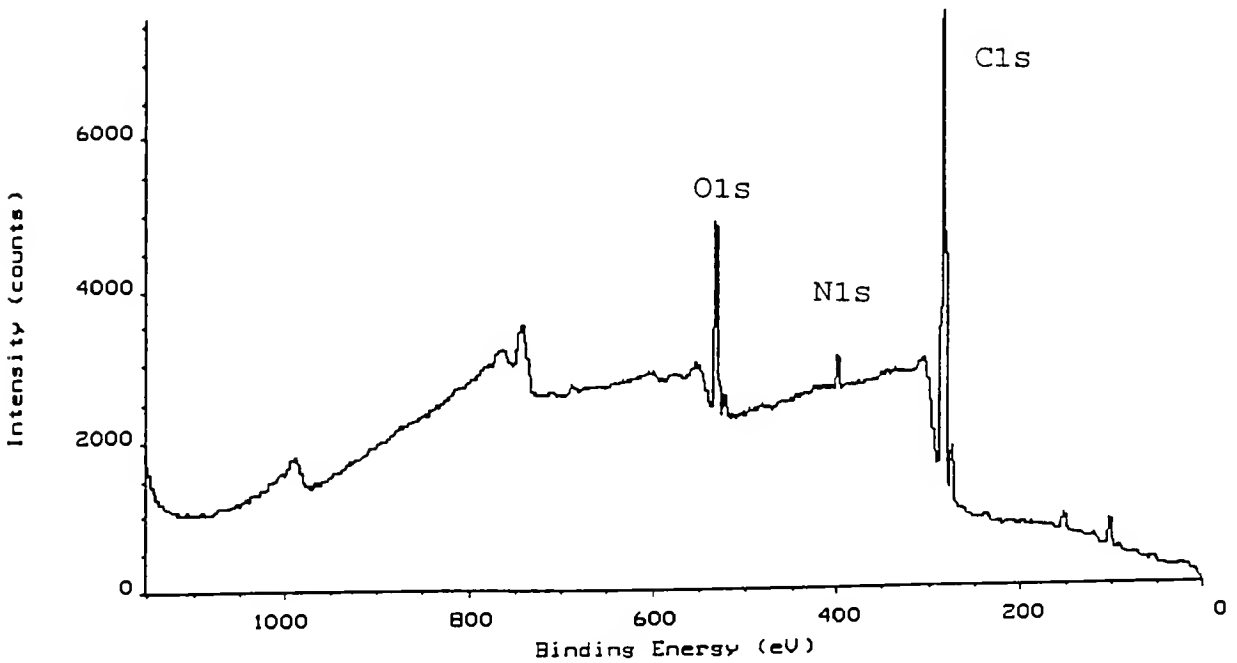

(b)

Figure 4-29. The XPS spectra for PP
(a) PVP/NVP-g-PP prepared by gamma method. (10 wt% PVP/NVP; 2/8, 0.15 Mrad)
(b) PVP/NVP-g-PP prepared by plasma/gamma method. (5 minutes water RFGD, 10 wt% PVP/NVP; 2/8, 0.15 Mrad)

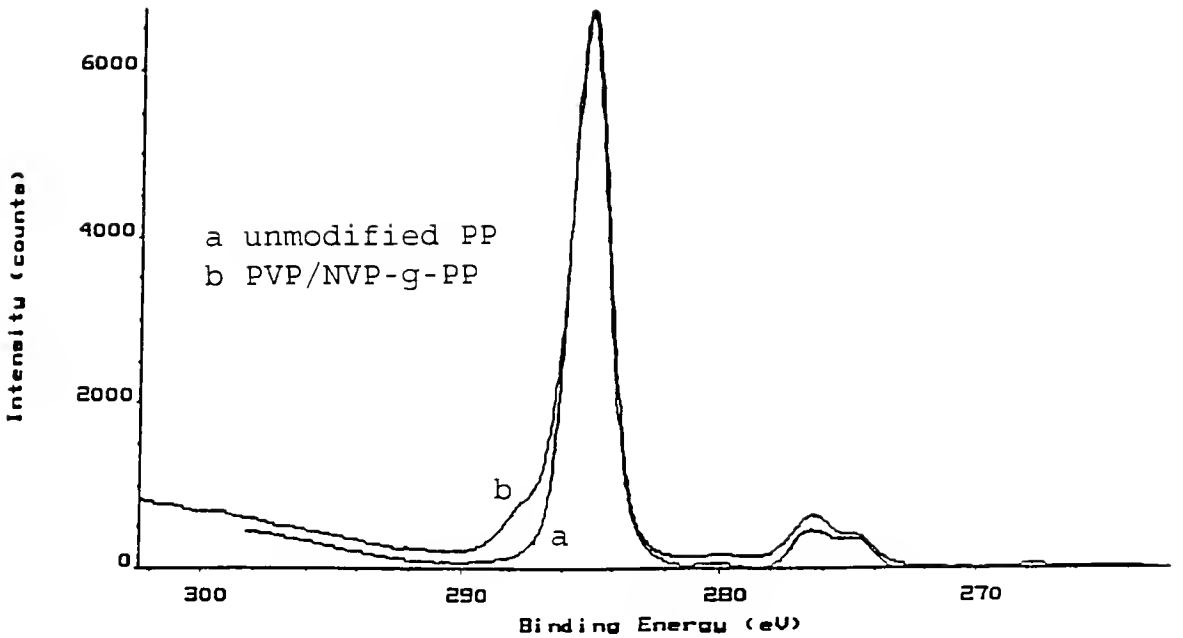

Figure 4-30. Overlapped C1s peaks for an unmodified PP and a PVP/NVP modified PP made by plasma/gamma method (5 minutes water RFGD, 10 wt% PVP/NVP; 2/8, 0.15 Mrad)

4.3.3.2 FT-IR/ATR

Figure 4-31 is the FT-IR/ATR spectrum for unmodified PP. The pertinent peaks of PP IR spectrum are listed in Table 4-12. The major difference between PP and PVP in the IR spectrum is the amide carbonyl group at 1650 cm^{-1} for the PVP. Figure 4-32 is the FT-IR/ATR spectrum for PVP/NVP-g-PP made by the plasma/gamma method. The amide carbonyl peak at 1650 cm^{-1} is present in Figure 4-32, but is not present in Figure 4-31.

4.3.4 Surface Graft Polymerization of PVP/NVP onto PC Using "Plasma/Gamma" Method

4.3.4.1 XPS analysis and contact angle measurements

Table 4-13 summarizes the XPS and contact angle results for the PVP/NVP-g-PC samples. The contact angle for unmodified PC is 83°. The surface becomes very hydrophilic after surface modifications: 22° for the gamma treated and less than 20° for the plasma/gamma treated. Surface nitrogen concentration increased from 4.37 % to 8.17% when the PC surface was pretreated with a one minute water RFGD plasma. As the plasma treatment time increased, the surface nitrogen concentration reached a maximum value of 9.73% and the N1s/O1s ratio exhibited a highest value of 0.94 at 15 minutes plasma treatment.

The results of PVP/NVP surface modification of PC are similar to the grafting of PVP/NVP onto PMMA. Without plasma pre-treatment, the PVP-g-PC exhibits low surface

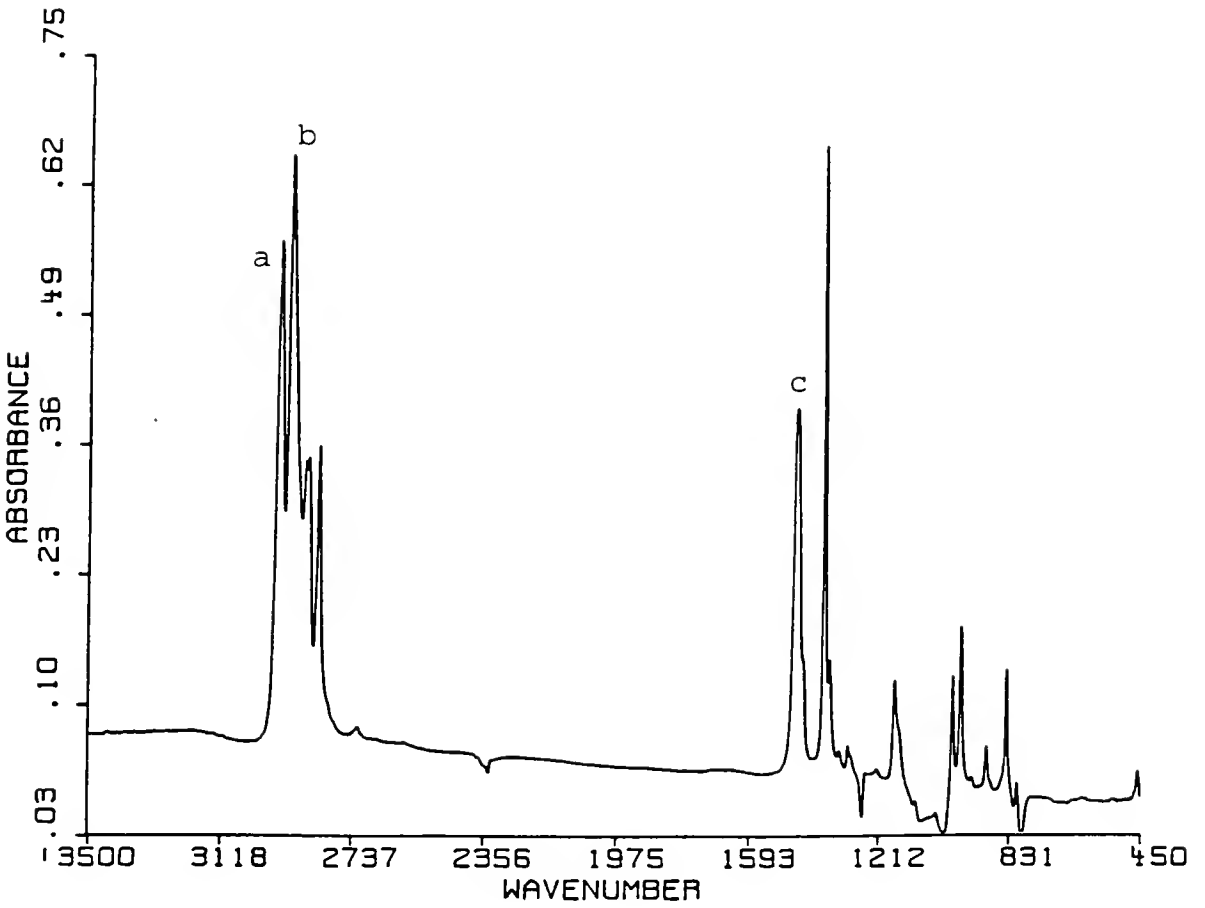

Figure 4-31. FT-IR/ATR spectrum of unmodified PP.

Table 4-12. The peak assignments for the unmodified PP IR spectrum in Figure 4-28.

peak	ν (cm^{-1})	assignment
a	2930	$-CH_3$ stretch
b	2864	-C-H stretch
c	1460	$-CH_3$ deformation

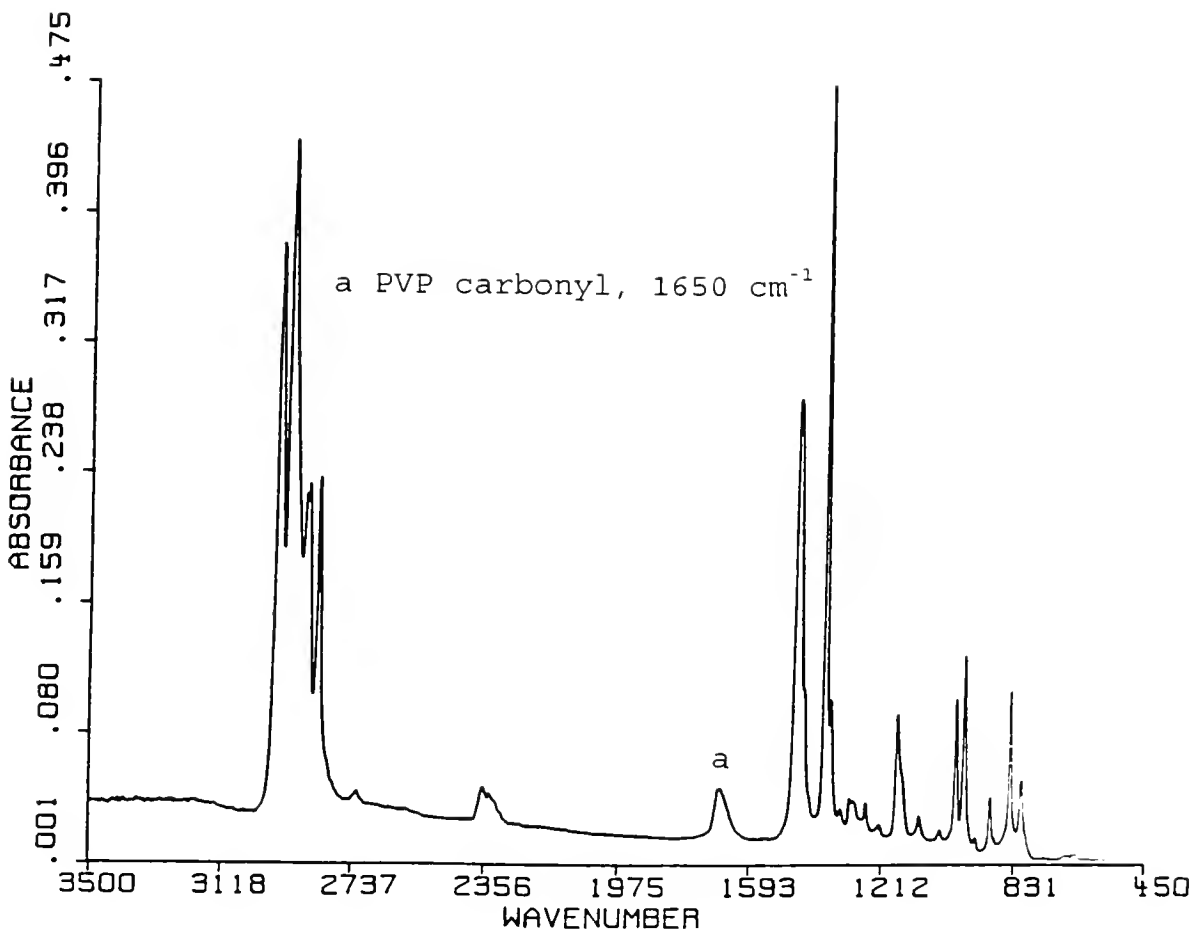

Figure 4-32. FT-IR/ATR spectrum for the PVP/NVP modified PP made by the plasma/gamma method. (20 minutes water RFGD, 10 wt% PVP/NVP; 2/8, 0.15 Mrad)

Table 4-13. XPS analysis and contact angle measurements for PVP/NVP grafting onto PC using plasma/gamma method. (50 watts, 100 mTorr, 10 wt% PVP/NVP; 2/8, 0.15 Mrad)

Plasma Treatment Time (minutes)	Atomic Concentration (%)				Contact Angle (±5°)
	C1s	O1s	N1s	N1s/O1s	
unmodified PC	86.11	13.89			83
0	81.59	14.05	4.37	0.31	22
1	79.52	12.30	8.17	0.66	20
5	79.05	12.76	8.20	0.64	20
15	80.33	9.93	9.73	0.94	19
20	79.24	12.20	8.57	0.70	18

Note: 1. The PVP polymer theoretically contains 75% carbon, 12.5% oxygen and 12.5% nitrogen without counting the hydrogen atoms.

contact angle and moderate surface nitrogen concentration. This might suggest that PC and PMMA surfaces are more compatible to PVP/NVP solution than PP and PDMS surfaces as discussed before.

The effects of RF-plasma treatment on the PVP/NVP-g-PC can be observed in the case of 15 min plasma pretreatment. Previous data in the Table 4-5 indicated that the surface region of PC has been oxidized by the RF-plasma treatment because the surface oxygen concentration increased from 13.89% to 19.19%. These surface hydroxyl or peroxide groups provide a more compatible surface to the PVP/NVP monomers, thereby enhancing the grafting efficiency.

The XPS spectra for PVP/NVP-g-PC made by the gamma method and by the plasma/gamma method are presented in Figures 4-33 (a) and (b), respectively. Comparison of these Figures indicates that the nitrogen peak in the Figure 4-33 (b) was significantly higher than in the Figure 4-33 (a). Figure 4-34 is an overlapping C1s peak for unmodified PC and PVP/NVP-g-PC made by plasma/gamma method. The minor peak present in the spectrum of PVP/NVP-g-PC is due to the chemical shift of amide carbonyl group of PVP. This indicates that PVP was uniformly grafted onto PC surface.

4.3.4.2 FT-IR/ATR

The FT-IR/ATR spectrum of unmodified PC is shown in Figure 4-35. The major peaks for unmodified PC are listed in Table 4-14. Figure 4-36 is the FT-IR/ATR spectrum of

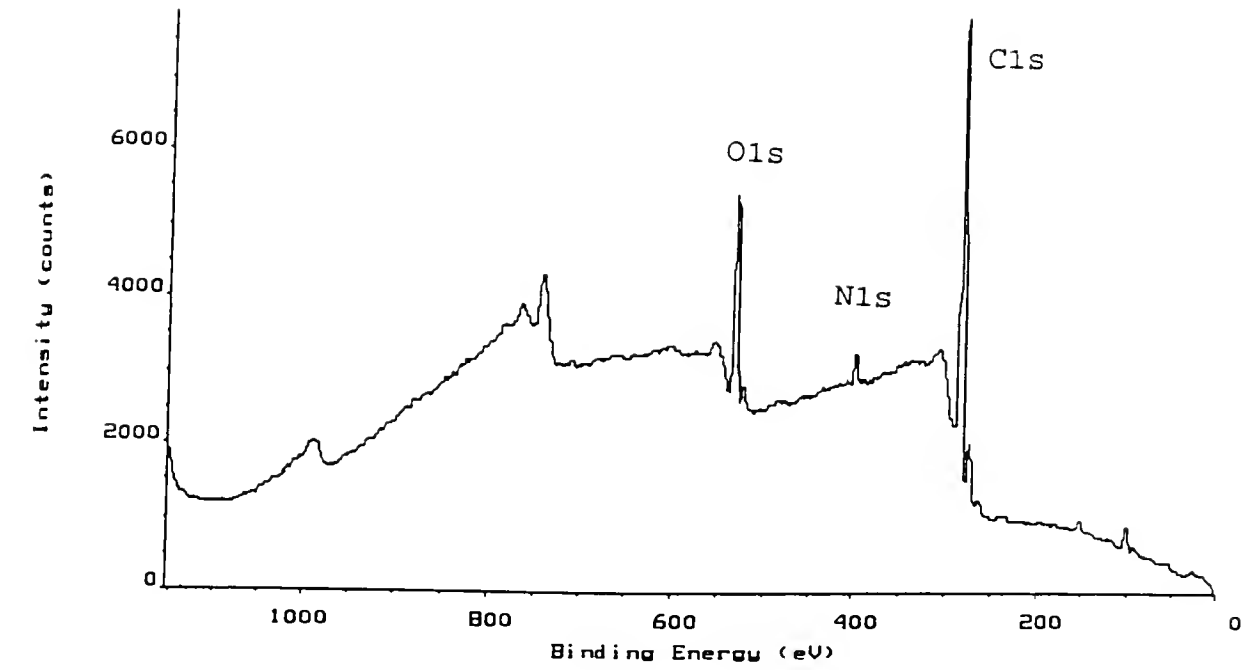

(a)

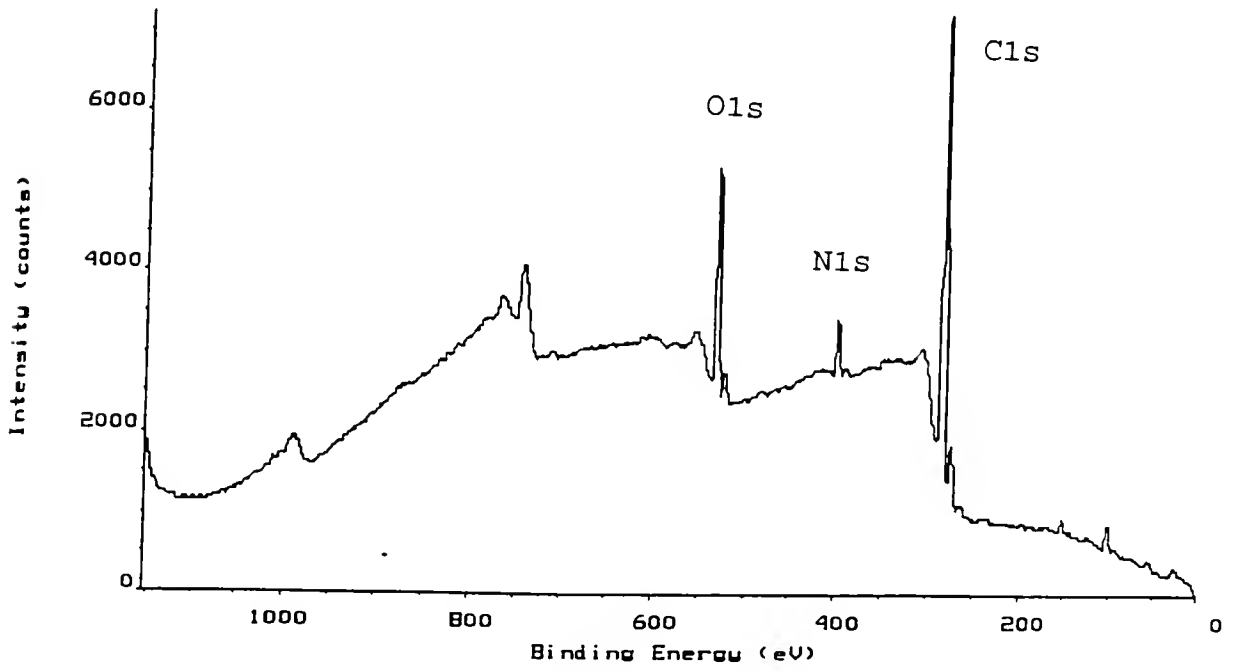

(b)

Figure 4-33. The XPS spectra for PC
(a) PVP/NVP-g-PC prepared by gamma method. (10 wt% PVP/NVP; 2/8, 0.15 Mrad)
(b) PVP/NVP-g-PC prepared by plasma/gamma method. (20 minutes water RFGD, 10 wt% PVP/NVP; 2/8, 0.15 Mrad)

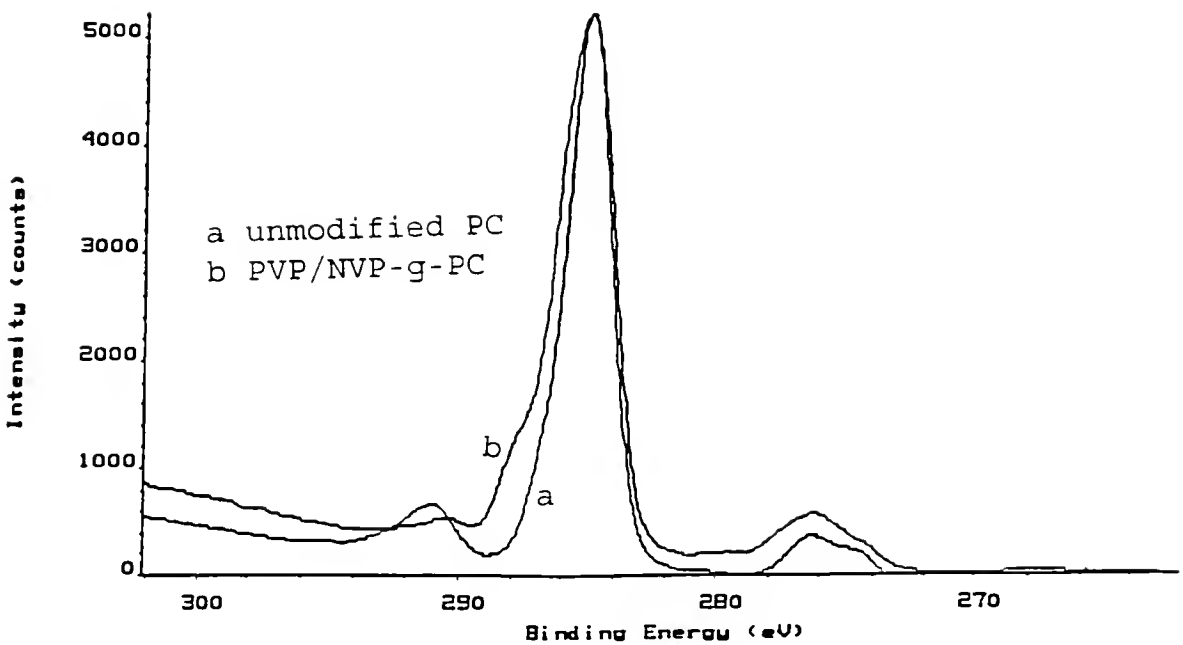

Figure 4-34. Overlapped C1s peaks for an unmodified PC and a PVP/NVP modified PC made by plasma/gamma method. (20 minutes water RFGD, 10 wt% PVP/NVP; 2/8, 0.15 Mrad)

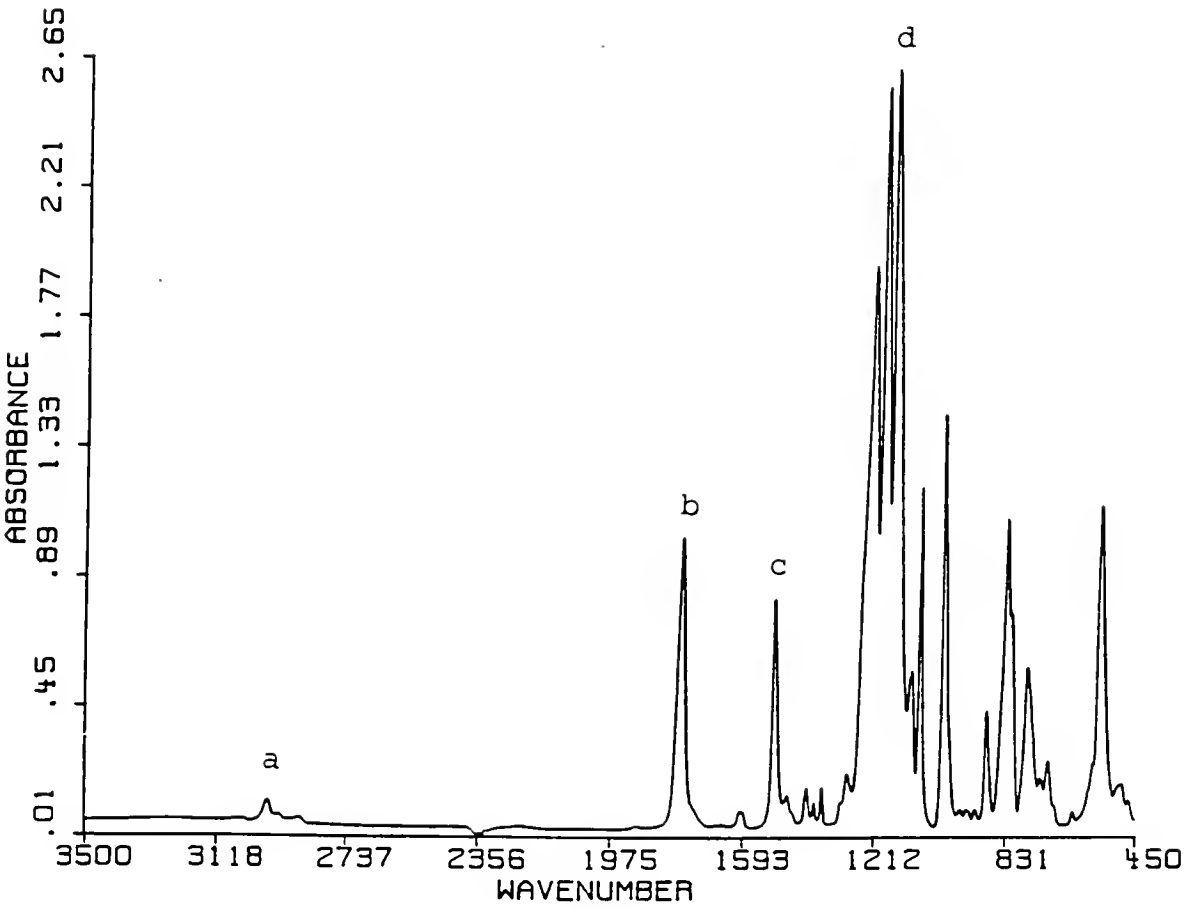

Figure 4-35. FT-IR/ATR spectrum of unmodified PC.

Table 4-14. The peak assignments for the unmodified PC IR spectrum in Figure 4-34.

peak	ν (cm^{-1})	assignment
a	2974	-C-H stretch
b	1768	-COO- stretch
c	1505	aromatic ring
d	1160	-C-O stretch

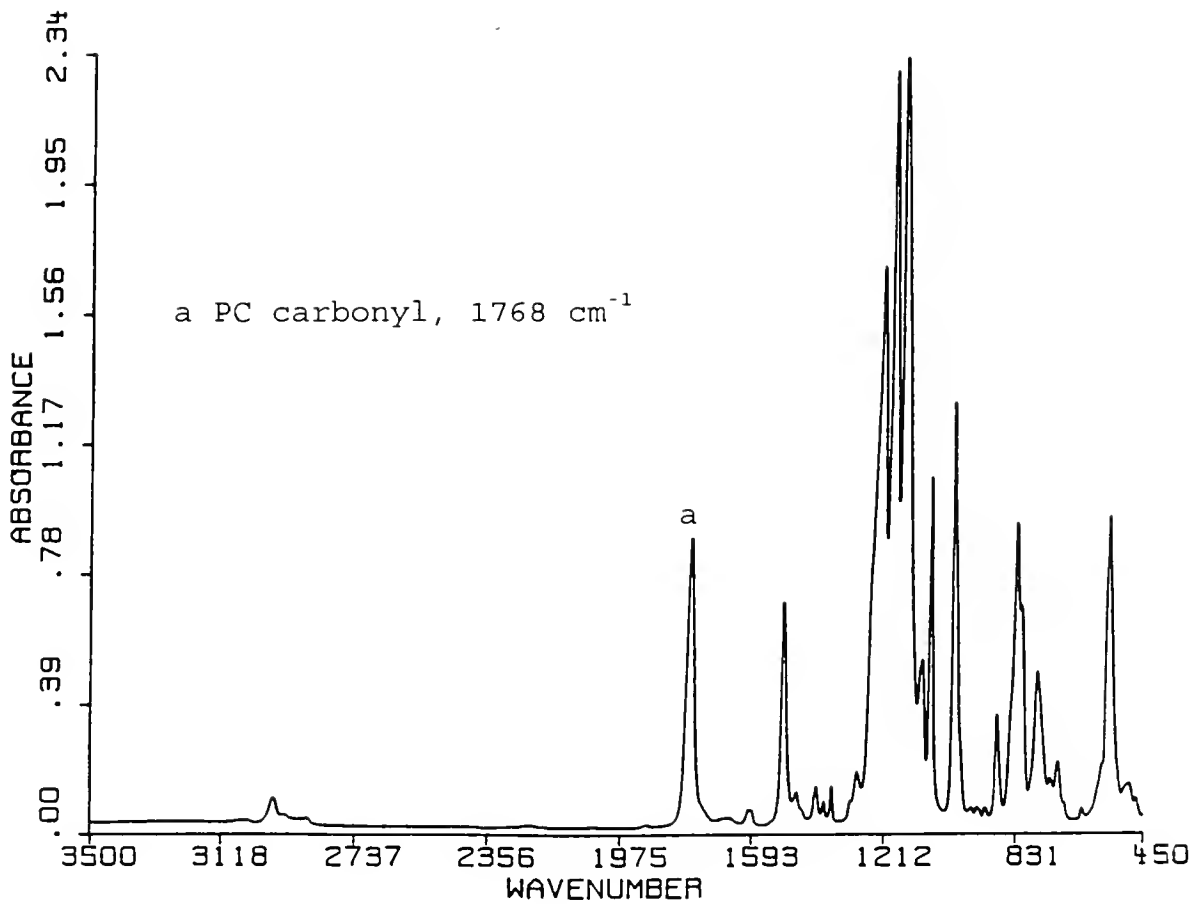

Figure 4-36. FT-IR/ATR spectrum for the PVP/NVP modified PC made by the plasma/gamma method. (20 minutes water RFGD, 10 wt% PVP/NVP; 2/8, 0.15 Mrad)

PVP/NVP-g-PC made by the plasma/gamma method. Comparison of two spectra does not reveal any significant difference. The amide carbonyl peak of PVP polymer at 1650 cm-1 is too weak to be observed in Figure 4-36. This could be due to a very thin PVP graft.

4.3.5 Surface Graft polymerization of PVP/NVP onto FEP Using "Plasma/Gamma" Method

4.3.5.1 XPS analysis and contact angle measurements

Teflon® FEP is a completely fluorinated ethylene-propylene copolymer and its surface is very hydrophobic and inert. Previous data in Table 4-5 indicates that the surface oxygen concentration of FEP exhibits only a slight increase after 15 min. RF-plasma treatment. Therefore, the degree of surface oxidation for the plasma treated FEP is obviously less than other polymers under the same conditions. Also, surface graft polymerization onto an FEP substrate is almost impossible without surface pretreatment. Two of the most widely used methods for PTFE pre-treatment are the sodium-liquid ammonia treatment and the sodium-naphthalene-THF treatment [127,128].

The XPS and contact angle results for the PVP/NVP-g-FEP samples are presented in Table 4-15. The contact angle of unmodified FEP is 110°. On the other hand, the contact angle of PVP/NVP modified FEP is 69° by the gamma method, but reduces to 20° by the plasma/gamma method.

Table 4-15. XPS analysis and contact angle measurements for PVP/NVP grafting onto FEP using plasma/gamma method. (50 watts, 100 mTorr, 10 wt% PVP/NVP; 2/8, 0.15 Mrad)

	Atomic Concentration (%)					
Plasma Treatment Time (minutes)	C1s	O1s	F1s	N1s	N1s/F1s	Contact Angle (±5°)
unmodified FEP	41.58	0.50	57.92	-	-	110
0	41.91	1.26	56.71	0.13	0.002	69
1	49.30	3.86	42.56	4.28	0.100	20
5	58.55	6.57	28.06	6.82	0.243	20
15	61.15	5.26	28.73	4.86	0.169	19
20	54.38	4.19	36.57	4.87	0.133	20

Note: 1. The PVP polymer theoretically contains 75% carbon, 12.5% oxygen, and 12.5% nitrogen without counting the hydrogen atoms.

XPS results indicate the surface nitrogen concentration has dramatically increased when the FEP surface was pretreated with the water RFGD plasma. For example, the surface nitrogen concentration for the gamma treated FEP is 0.13%, but for the one minute plasma/gamma treated FEP is 4.28%. Evidently these RF-plasma produced hydroxyl or peroxide groups which have effectively improved the grafting of PVP/NVP onto FEP surface. Also, both the nitrogen and N1s/F1s ratio reach a maximum at a 5 minutes plasma pretreatment. The results suggest that PVP may be uniformly grafted onto FEP surfaces using this plasma/gamma condition. This can not be done by the gamma only method.

Evidence of PVP/NVP grafting also was observed in the XPS spectra. The spectrum of unmodified FEP and PVP/NVP-g-FEP made by the plasma/gamma method are presented in Figures 4-37 (a) and (b), respectively. A very strong O1s peak and a very distinctive N1s peak are only present in Figure 4-37 (b). Both O1s and N1s peaks are attributed to PVP graft on the FEP surface.

Overlapped C1s peaks for unmodified FEP and PVP/NVP modified FEP made by the plasma/gamma method are presented in Figure 4-38. The unmodified FEP contains only one major C1s peak which indicates the chemical shift of CF_X group, but the PVP/NVP-g-FEP made by the plasma/gamma method contains two major peaks which are the CH_X group at 285 eV and the CF_X group at 292 eV. Because fluorine is the most electronegative element, it induces the largest chemical

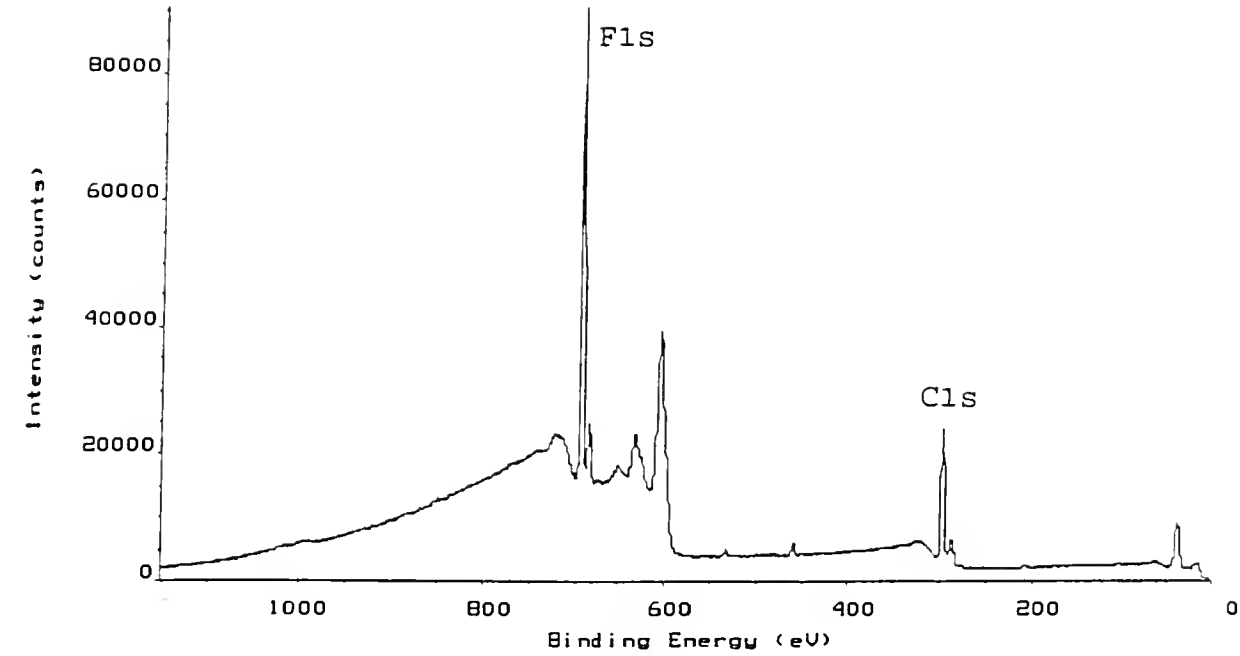

(a)

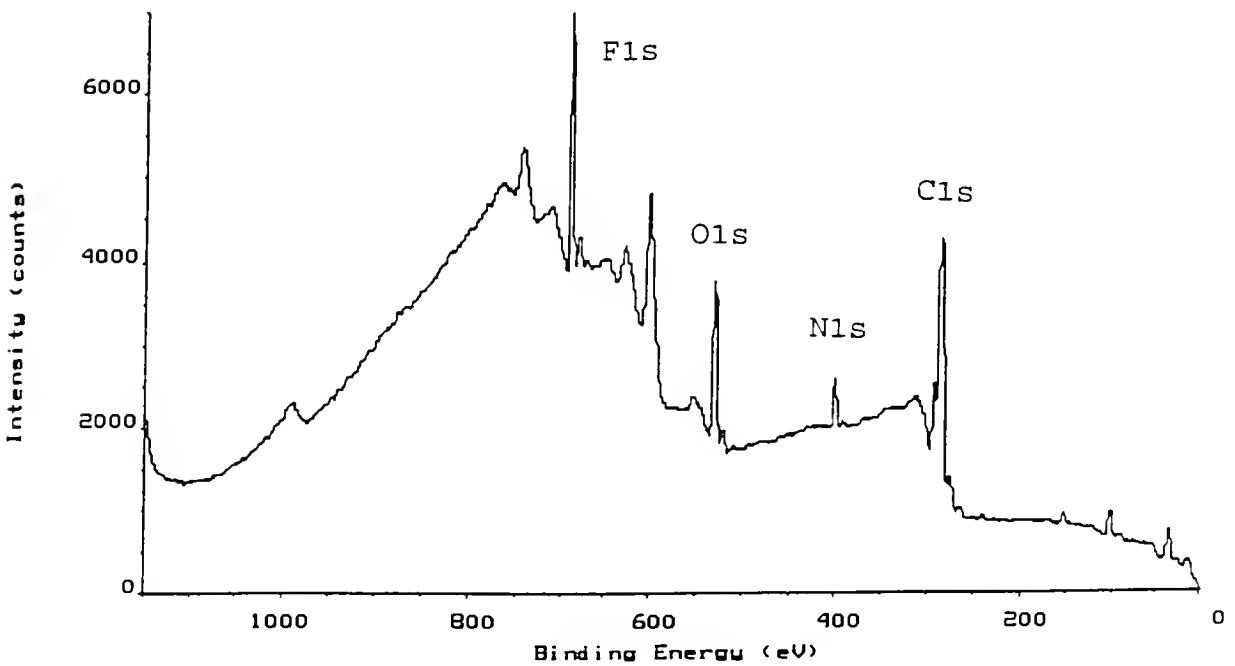

(b)

Figure 4-37. The XPS spectra for FEP
(a) unmodified FEP.
(b) PVP/NVP-g-FEP prepared by plasma/gamma method. (5 minutes water RFGD, 10 wt% PVP/NVP; 2/8, 0.15 Mrad)

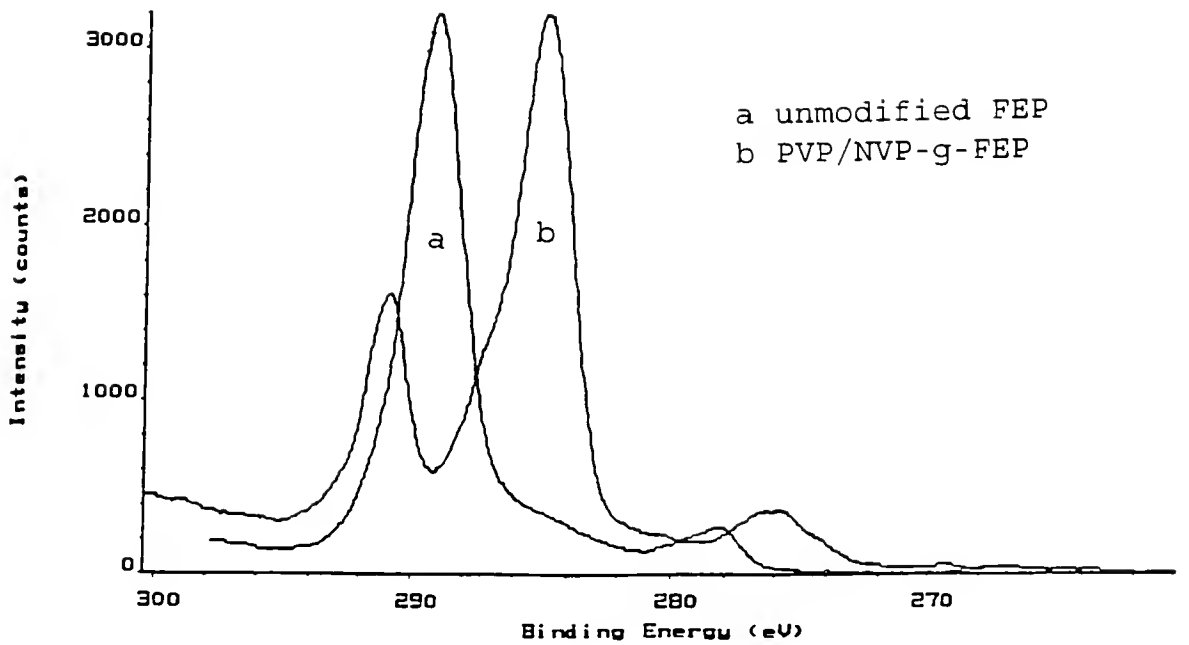

Figure 4-38. Overlapped C1s peaks for unmodified FEP and PVP/NVP modified FEP made by plasma/gamma method. (5 minutes water RFGD, 10 wt% PVP/NVP; 2/8, 0.15 Mrad)

shift in C1s binding energy. The minor peak for amide carbonyl group appears under the major peak of CH_x group.

4.3.5.2 FT-IR/ATR

The FT-IR/ATR spectra for unmodified FEP and PVP/NVP-g-FEP made by the plasma/gamma method are presented in Figures 4-39 (a) and (b), respectively. The major difference between these two spectra is that a distinguishable peak at 1660 cm^{-1} is present in only Figure 4-39 (b). This suggests that the FEP surface was covered with a thin layer of PVP graft.

4.3.6 Surface Graft Polymerization of PVP/NVP onto PVDF Using "Plasma/Gamma" Method

4.3.6.1 XPS analysis and contact angle measurements

Table 4-17 summarizes the XPS and contact angle results for PVP/NVP-g-PVDF samples. PVDF (polyvinylidene fluoride) is a melt processable fluoroplastic. The contact angle of unmodified PVDF is around 90°. After surface modifications, either by the gamma method or by the plasma/gamma method, the contact angle of PVP/NVP modified PVDF is about 20° or below. XPS results indicate that the improvement by the RF-plasma pre-treatment is very significant. For example, the surface nitrogen concentration for the gamma treated PVDF is 2.61%, but the one minute plasma/gamma treated PVDF is 8.77%. Previous data in Table 4-5 indicated that PVDF

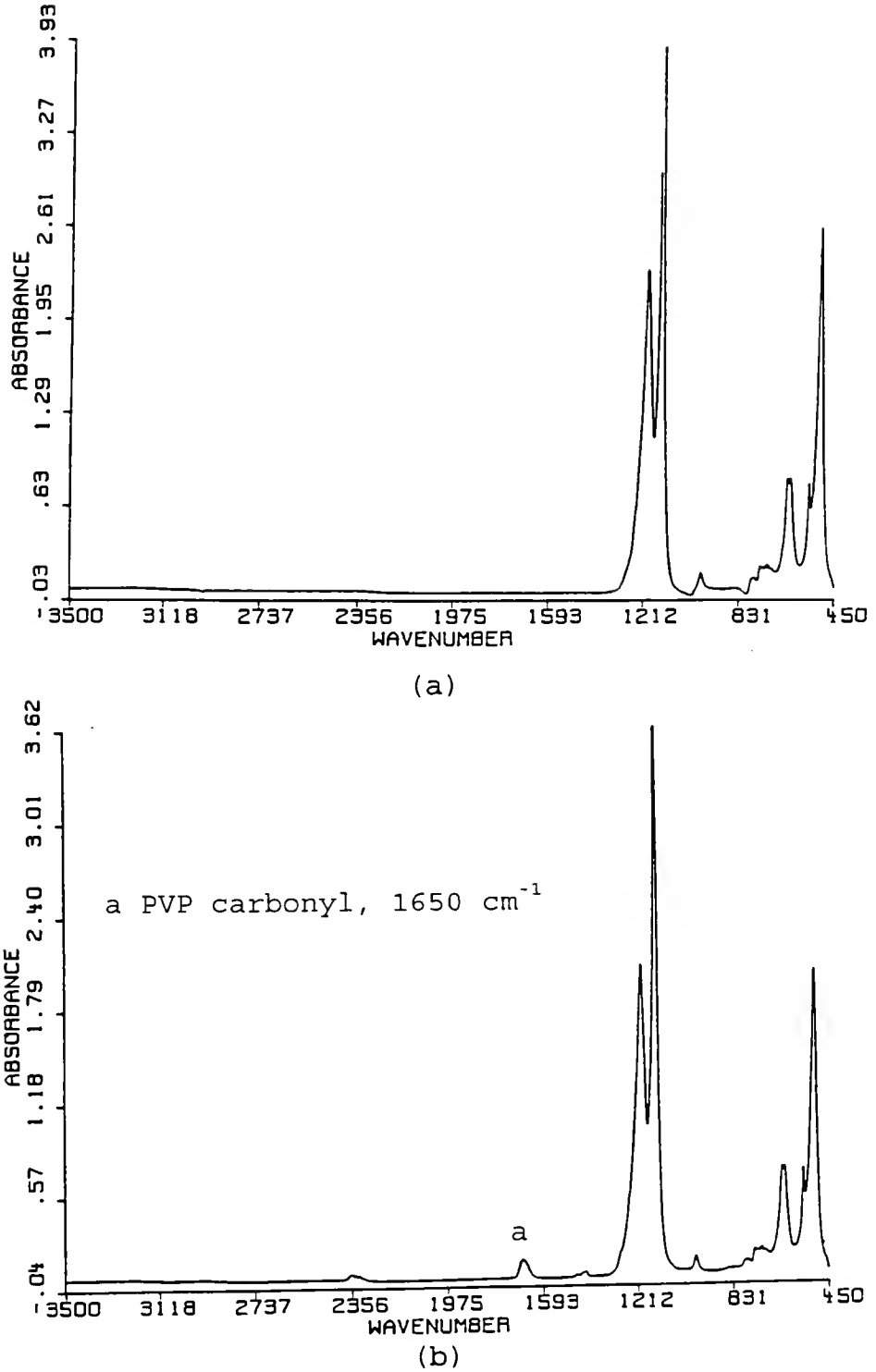

Figure 4-39. FT-IR/ATR spectra for
(a) unmodified FEP
(b) PVP/NVP modified FEP made by the plasma/gamma method. (20 minutes water RFGD, 10 wt% PVP/NVP; 2/8, 0.15 Mrad)

Table 4-17. XPS analysis and contact angle measurements for PVP/NVP grafting onto PVDF using plasma/gamma method. (50 watts, 100 mTorr, 10 wt% PVP/NVP; 2/8, 0.15 Mrad)

	Atomic Concentration (%)					
Plasma Treatment Time (minutes)	C1s	O1s	F1s	N1s	N1s/F1s	Contact Angle (±5°)
unmodified PVDF	55.67	1.29	43.05	-	-	90
0	67.07	4.28	26.04	2.61	0.100	20
1	72.00	8.74	10.49	8.77	0.836	19
5	71.97	8.90	10.55	8.58	0.813	18
15	77.34	9.11	4.06	9.50	2.339	19
20	71.80	10.26	9.35	8.58	0.917	18

Note: 1. The PVP polymer theoretically contains 75% carbon, 12.5% oxygen, and 12.5% nitrogen without counting the hydrogen atoms.

surface has been oxidized and defluorinated by the RF-plasma treatment. These surface hydroxyl or peroxide groups increase the accessibility of PVDF surface to PVP/NVP monomers. Also, the reduction of the surface fluorine concentration on PVDF suggests that PVDF surface is uniformly covered by PVP graft and defluorinating degradation may occur during gamma irradiation since fluoropolymers are sensitive to radiation.

The effect of plasma treatment time on the results was not very significant for PVDF. As the plasma treatment time increased, the surface nitrogen concentration remained in the range of 8.5 to 9.5 %. Therefore, a short plasma treatment time, such as 1 minute, would be enough to produce a significant change for PVDF.

The XPS spectra for unmodified PVDF and PVP/NVP modified PVDF prepared by the plasma/gamma method are presented in Figures 4-40 (a) and (b), respectively. In addition to a new N1s peak, a smaller F1s peak and a much more intense C1s peak are seen in Figure 4-40 (b). Figure 4-41 is the overlapped C1s peak for unmodified PVDF and PVP/NVP-g-PVDF made by the plasma/gamma method. In the PVP/NVP-g-PVDF C1s peak, the second major peak at 290 eV becomes smaller and the first major peak at 285 eV becomes broader than unmodified C1s peak. Also, the left shoulder of the first major peak reveals a minor peak which is attributed to the amide carbonyl group of PVP graft.

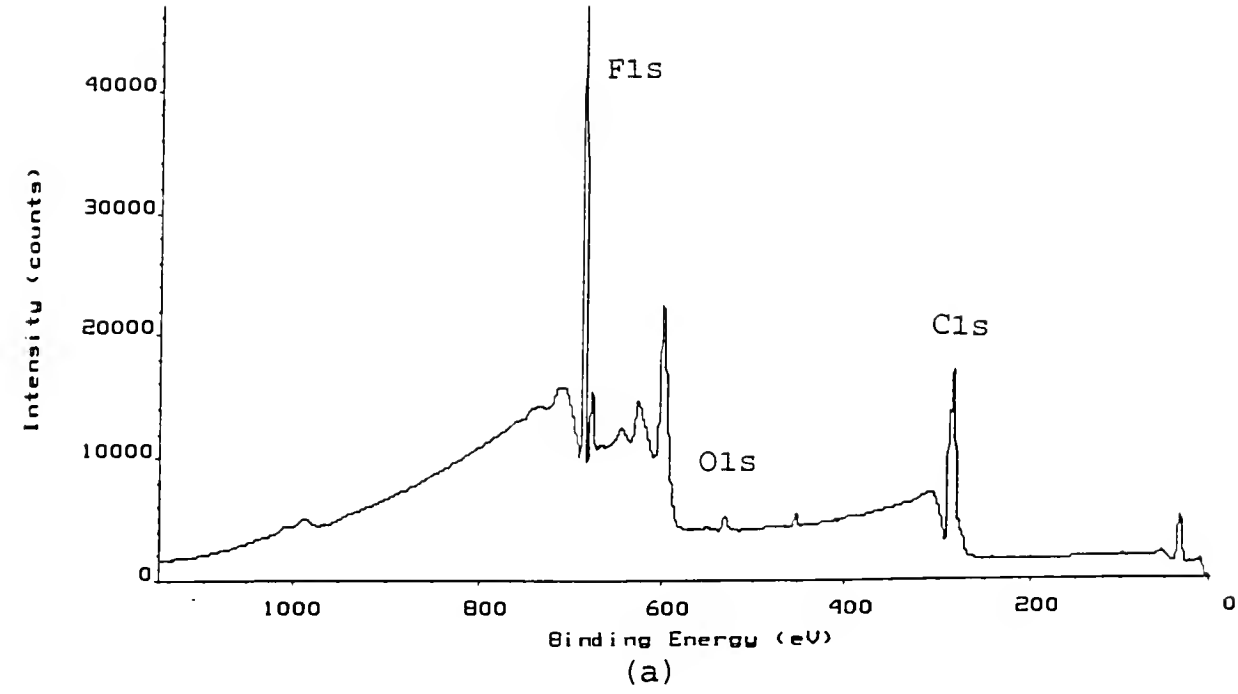

(a)

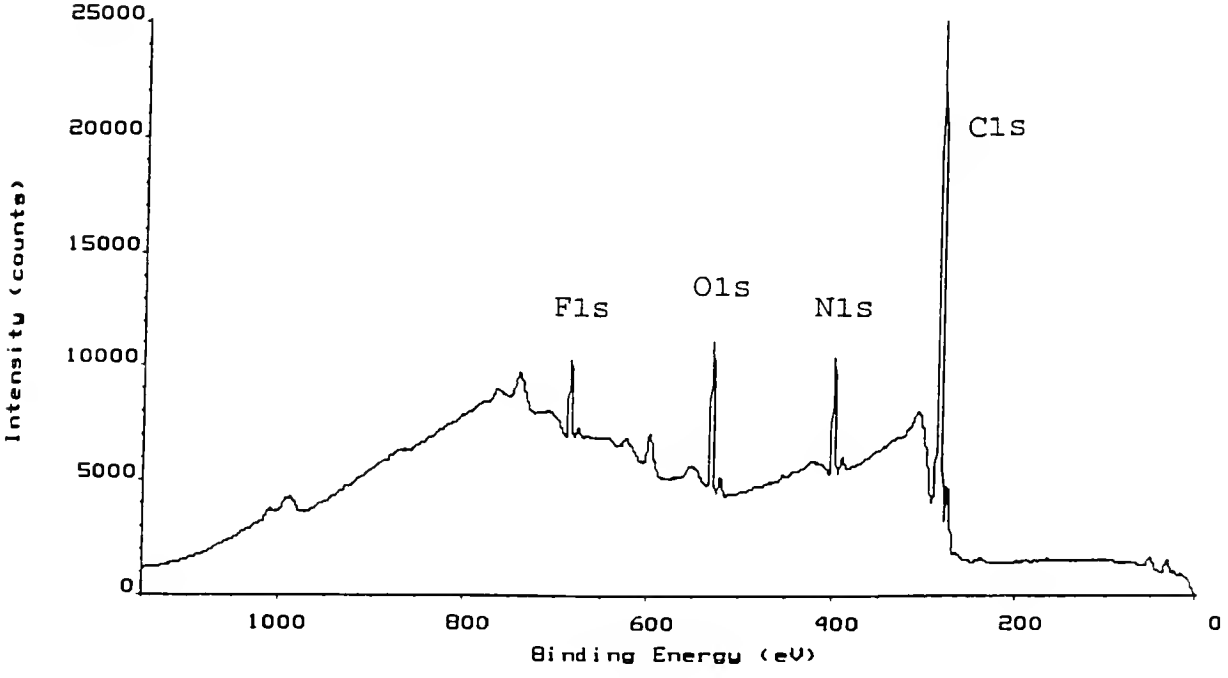

(b)

Figure 4-40. The XPS spectra for PVDF
(a) unmodified PVDF
(b) PVP/NVP-g-PVDF prepared by plasma/gamma method. (15 minutes water RFGD, 10 wt% PVP/NVP; 2/8, 0.15 Mrad)

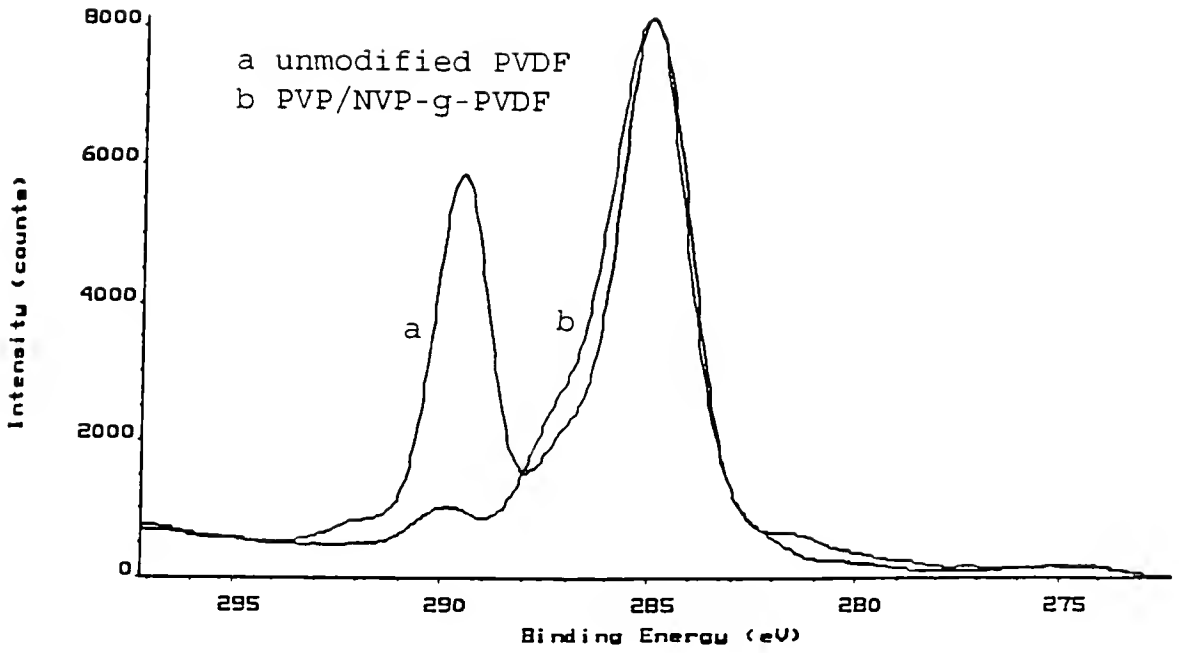

Figure 4-41. Overlapped C1s peaks for unmodified PVDF and PVP/NVP-g-PVDF made by plasma/gamma method. (15 minutes water RFGD, 10 wt% PVP/NVP; 2/8, 0.15 Mrad) (a) unmodified PVDF (b) PVP/NVP-g-PVDF

4.3.6.2 FT-IR/ATR

Figures 4-42 (a) and (b) give the spectra of unmodified PVDF and PVP/NVP modified PVDF prepared by the plasma/gamma method. The difference between two spectra was the appearance of a new absorption peak at 1660 cm^{-1} which was only seen in Figure 4-42 (b).

4.3.7 Summary of Grafting of PVP/NVP onto PMMA, PDMS, PP, PC, FEP, and PVDF Using "Plasma/Gamma" Method

The plasma/gamma method was very successful in improving the grafting of PVP/NVP onto PMMA, PDMS, PP, PC, FEP, and PVDF surfaces. The PVP/NVP modified surface prepared by the plasma/gamma method were somewhat more hydrophilic than those prepared by the gamma method alone. High surface nitrogen concentration shown in XPS analysis suggested that these plasma/gamma treated substrates were covered with a uniform layer of PVP graft.

PVP grafts prepared by the plasma/gamma method could not be visualized using optical microscopy with biological stain and hence were less than 5μm in thickness for most substrates. Even though the XPS revealed high surface nitrogen concentrations on PMMA and PC surfaces, FT-IR/ATR was not able to detect the PVP grafts. This suggested that the thickness of PVP graft on PMMA and PC is less than 3 μm.

The plasma pre-treatment, a critical step before the grafting, effectively transformed the substrate surface from

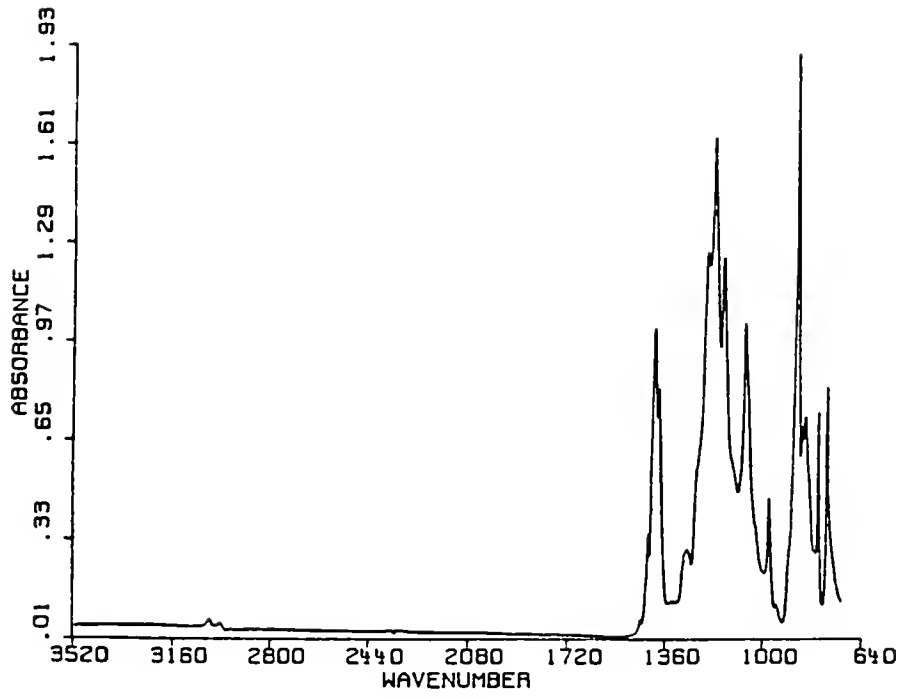

(a)

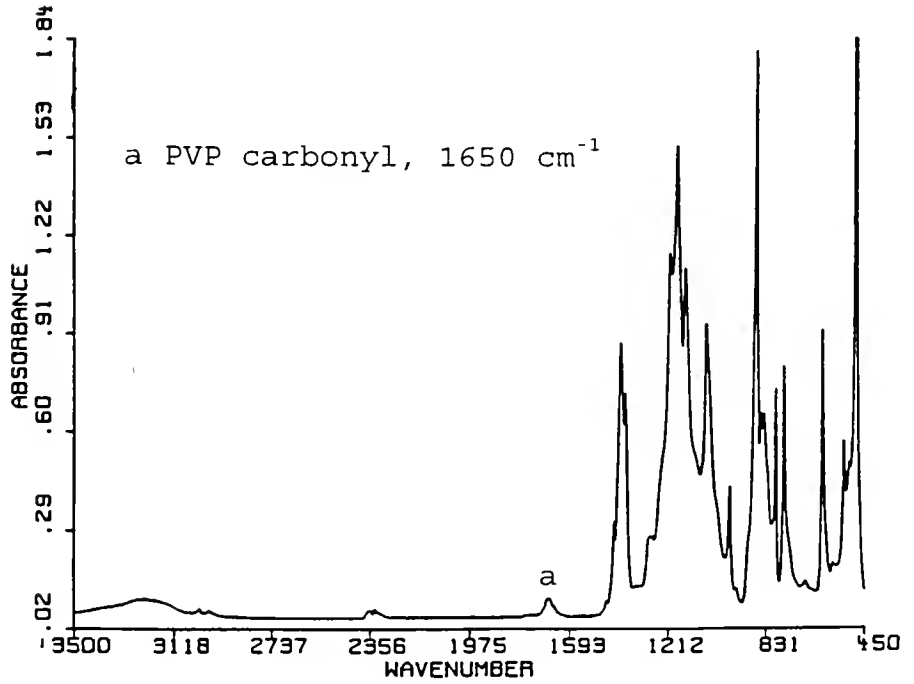

(b)

Figure 4-42. The FT-IR/ATR spectra for PVDF
(a) unmodified PVDF
(b) PVP/NVP-g-PVDF prepared by the plasma/gamma method. (15 minutes water RFGD, 10 wt% PVP/NVP; 2/8, 0.15 Mrad)

hydrophobic to hydrophilic and provided reactive sites, such as peroxide groups, for grafting.

The grafting of PVP/NVP onto polymeric substrates is believed to be mainly through the recombination of substrate surface radicals with PVP polymeric radicals and partially through the addition polymerization of NVP monomer initiated by the substrate surface radicals as shown in Figure 4-43. The grafts prepared by the plasma/gamma method did not diffuse into the bulk of substrates as observed for the "presoak method" in Yahiaoui's [6] study. This occurs because the long chain PVP molecules can not penetrate into the bulk of the substrate as easily as the short chain NVP moelcules. Thus the location of grafting is definitely limited to the surface region of the polymer substrate. The surface nitrogen concentration for both grafts are comparable. Therefore, the structure of PVP/NVP graft may be a thin and dense graft with less penetration.

4.4 Surface Graft Polymerization of DMA onto PMMA, PDMS, PP, PC, FEP, and PVDF Using "Plasma/Gamma" Method

Dimethylacrylamide (DMA) is the second monomer used in this study. Since DMA in solution is very easy to cross-link at low radiation dose, a concentration of 3 wt% and a radiation dose of 0.064 Mrad are used for all cases. The grafting of DMA onto polymeric substrate is expected to be different from the grafting of PVP/NVP discussed above

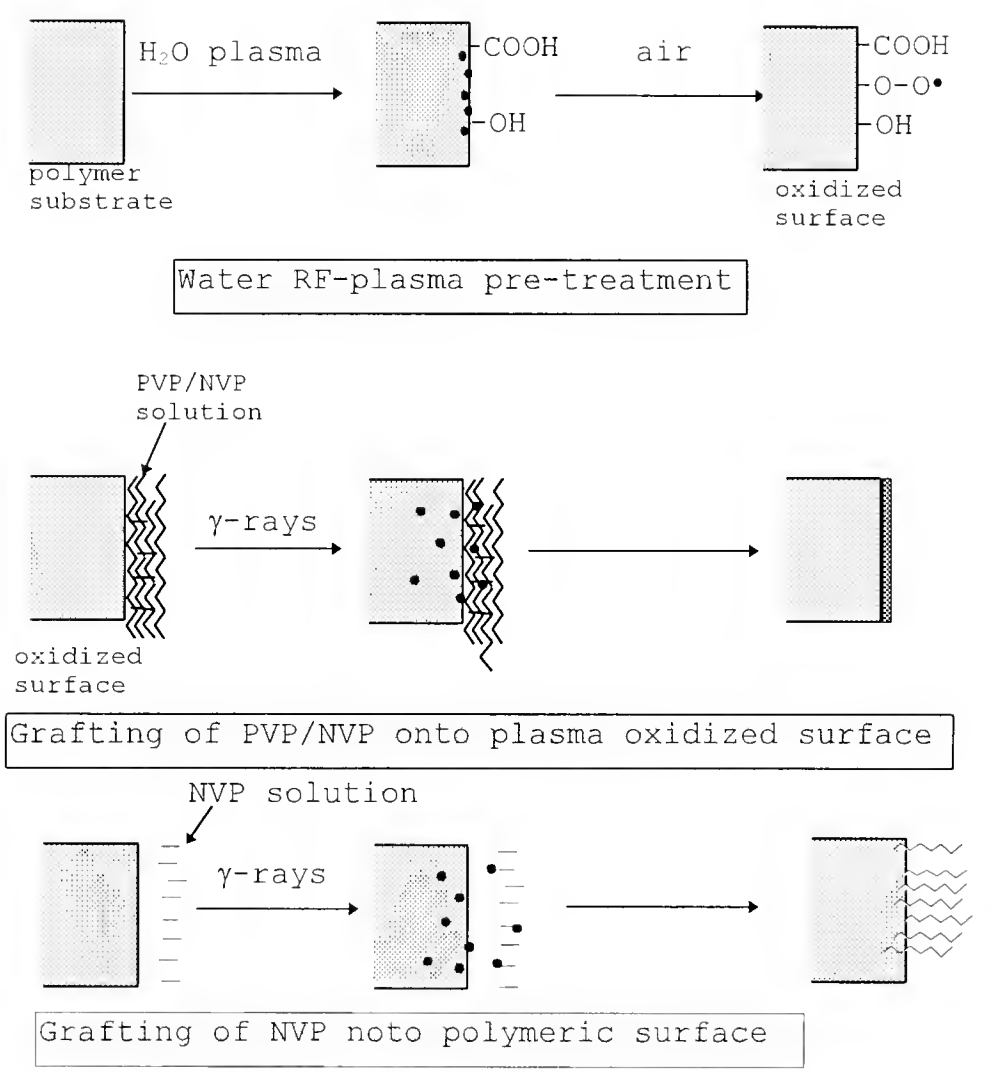

Figure 4-43. Schematic diagram of grafting of PVP/NVP and NVP onto polymeric substrate.

because there is no linearly long chain molecules such as PDMA involving in the grafting. PMMA, PDMS, PP, PC, FEP and PVDF were pretreated with a water RF-plasma at 50 watts and 100±10 mTorr. Plasma treatment time was also varied from one to twenty five minutes. Gamma-induced graft polymerization was conducted in a ^{60}Co source at room temperature.

Characterization included contact angle measurements, XPS, and FT-IR/ATR analysis.

4.4.1 Surface Graft Polymerization of DMA onto PMMA Using "Plasma/Gamma" Method

4.4.1.1 XPS analysis and contact angle measurements

Table 4-18 summarizes the XPS and contact angle results for PDMA-g-PMMA samples. Generally, the PMMA surface becomes very hydrophilic after surface modification with PDMA regardless of the method of treatment since the contact angle for all surface modified samples is around 20° or below. The XPS results indicate that the surface nitrogen concentration for the PDMA-g-PMMA samples prepared by the plasma/gamma method is greatly increased. However, as the plasma treatment time increases, the surface nitrogen concentration for 5, 15, and 20 minutes plasma pre-treated samples is 7.83%, 4.89% and 6.90%, respectively. This suggests that the 5 minutes plasma pre-treatment for the PMMA gives the best PDMA grafting in this group.

Table 4-18. XPS analysis and contact angle measurements for PDMA grafting onto PMMA using plasma/gamma method. (50 watts, 100 mTorr, 3 wt% DMA, 0.064 Mrad)

Plasma Treatment Time (minutes)	Atomic Concentration (%)				Contact Angle (±5°)
	C1s	O1s	N1s	N1s/O1s	
unmodified PMMA	79.90	20.10			65
0	77.45	20.83	1.71	0.08	20
1	75.89	20.22	3.88	0.19	19
5	75.78	16.39	7.83	0.48	19
15	77.10	18.03	4.87	0.27	20
20	75.74	18.07	6.90	0.38	19

Note: 1. The PDMA polymer theoretically contains 71.4% carbon, 14.3% oxygen and 14.3% nitrogen without counting the hydrogen atoms.

Iwata et al. [118] showed that the number of surface peroxide groups on polyethylene (PE) decreased as the corona treatment time exceed a specific time. For PMMA substrate, as the plasma treatment time exceeds 5 minutes, the number of reactive sites produced by plasma treatment may also decrease. Therefore the improvement brought about by the plasma pre-treatment may decrease as the plasma treatment time exceeds 5 minutes. Unlike the PVP/NVP monomer system, which was not affected much by the prolonged plasma treatment, DMA monomer does not have linearly long chain molecules such as PDMA which can physically adsorb and inter-cross-react with PMMA surface. As compared to NVP alone monomer solution, DMA is much more reactive than NVP under the same radiation dose. High gelation rate can limit the diffusion of DMA monomers to a polymer surface during radiation-induced graft polymerization. The grafting of DMA on a polymeric surface is expected to be less effective than the NVP alone. This may be true for most polymeric substrates included in this study.

One typical XPS spectrum for PDMA-g-PMMA made by the plasma/gamma method and its expanded C1s peak are given in Figure 4-44. The evidence of PDMA graft is demonstrated by the presence of a strong nitrogen (N1s) peak at 400 eV in Figure 4-44. In addition, the expanded C1s peak for PDMA-g-PMMA reveals an amide carbonyl peak (-CO-N-) on the left shoulder of C1s peak and covers the ester carbonyl peak of

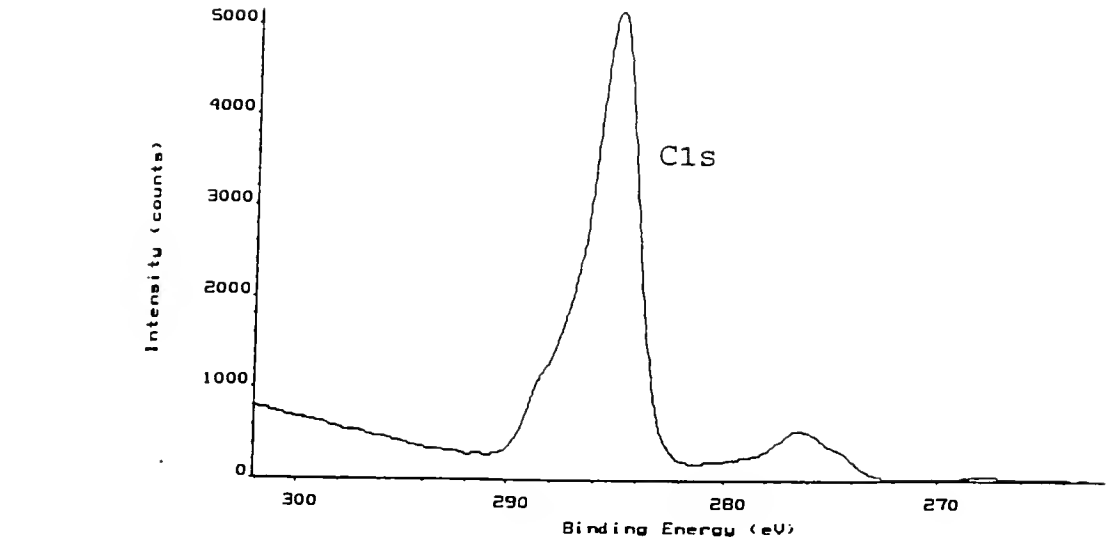

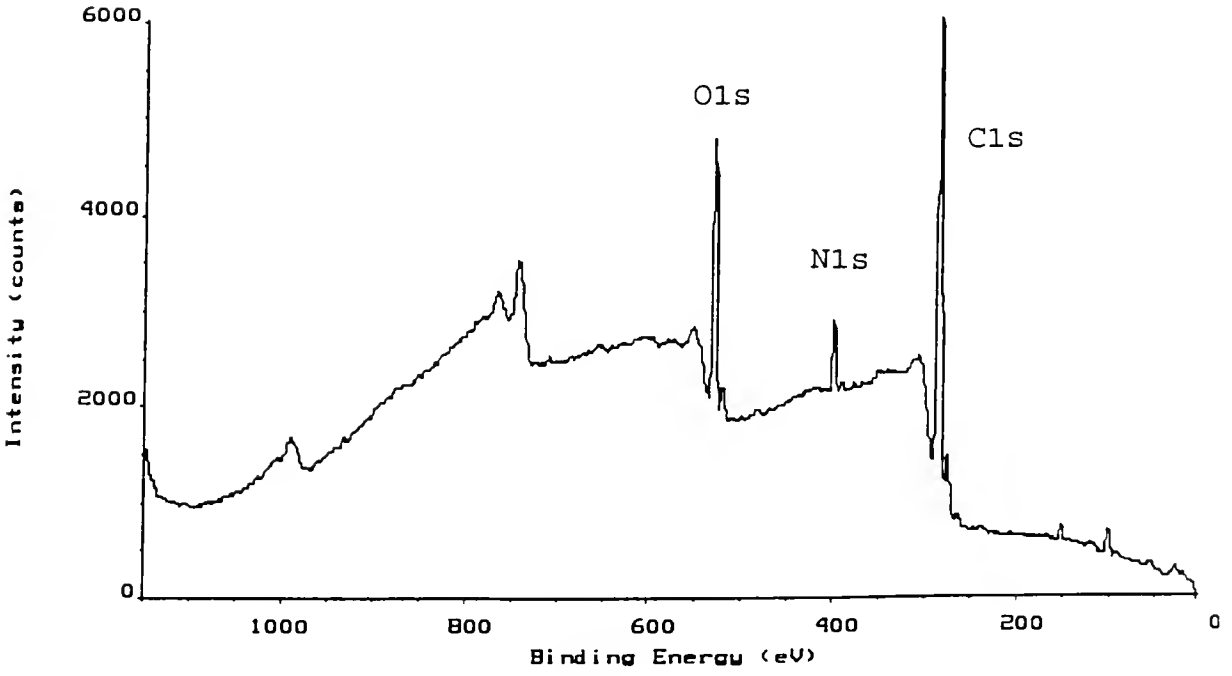

Figure 4-44. Typical XPS spectrum for PDMA-g-PMMA prepared by plasma/gamma method and an expanded C1s peak. (5 minutes water RFGD, 3 wt% DMA, 0.064 Mrad)

unmodified PMMA. This suggests that a thin layer of PDMA was uniformly grafted on PMMA surface.

4.4.1.2 FT-IR/ATR

FT-IR/ATR analysis for PDMA-g-PMMA samples is based on the amide carbonyl group absorption at 1640 cm^{-1} in PDMA. A typical FT-IR/ATR spectrum of PDMA-g-PMMA prepared by the plasma/gamma method is shown in Figure 4-45. The positions of major IR absorption peaks are similar to those of unmodified PMMA (Figure 4-18). The amide carbonyl absorption peak at 1640 cm^{-1} is too weak to be observed in the spectrum. This situation is similar to the PVP/NVP-g-PMMA prepared by the plasma/gamma method. This could be due to a very thin PDMA graft. Thus the location of grafting is also limited to the surface region of the PMMA.

4.4.2 Surface Graft Polymerization of DMA onto PDMS Using "Plasma/Gamma" Method

4.4.2.1 XPS analysis and contact angle measurements

Table 4-19 summarizes the results of XPS analysis and contact angle measurements for PDMA-g-PDMS samples. The contact angle is around 20° for most PDMA-g-PDMS samples regardless of the method of treatment. The XPS results indicate that the plasma/gamma method enhances the grafting of PDMA on PDMS surface. For example, the surface nitrogen concentration for the gamma treated and one minute plasma/gamma treated is 0.66% and 2.4%, respectively. Also,

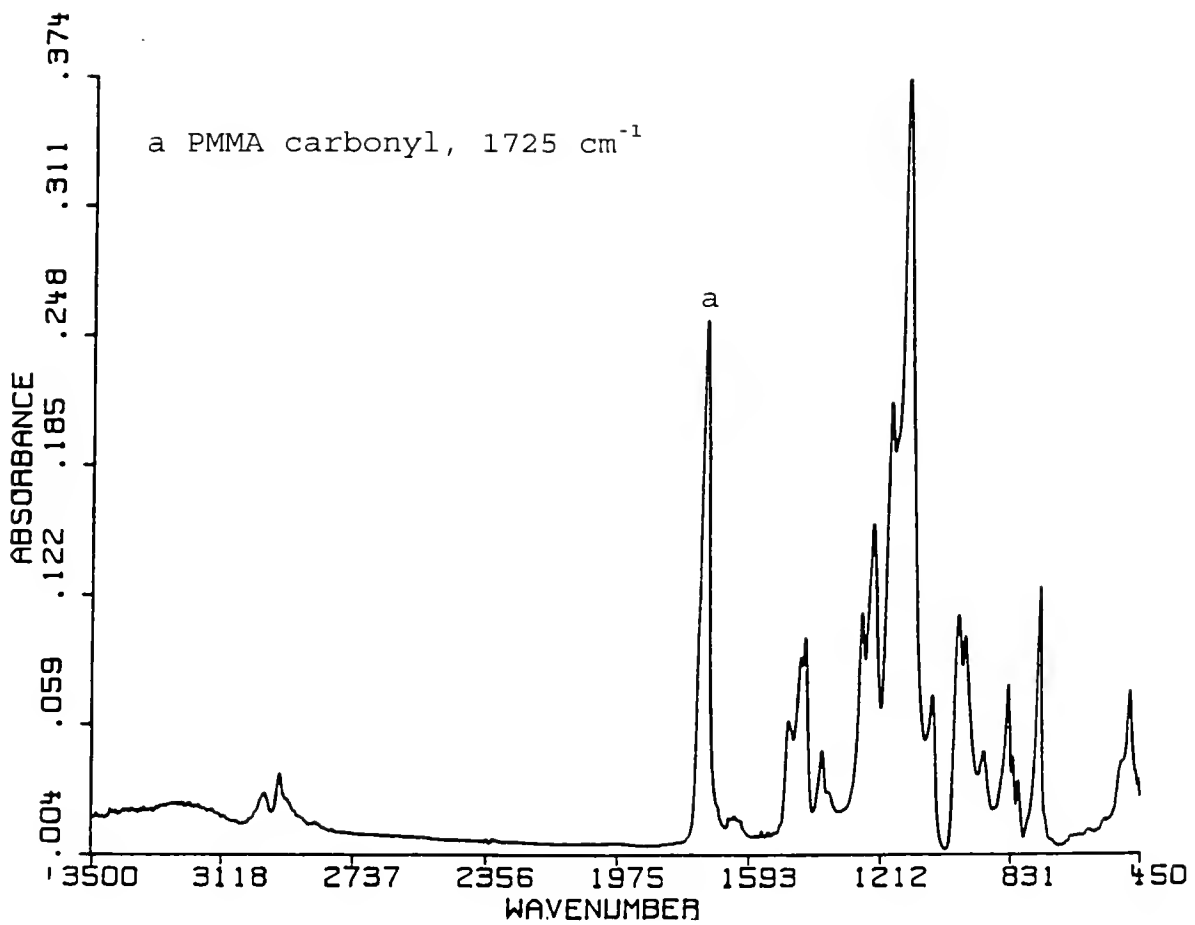

Figure 4-45. Typical FT-IR/ATR spectrum for PDMA-g-PMMA prepared by the plasma/gamma method. (5 minutes water RFGD, 3 wt% DMA, 0.064 Mrad)

Table 4-19. XPS analysis and contact angle measurements for PDMA grafting onto PDMS using plasma/gamma method. (50 watts, 100 mTorr, 3 wt% DMA, 0.064 Mrad)

	Atomic Concentration (%)					
Plasma Treatment Time (minutes)	C1s	O1s	Si2p	N1s	N1s/Si2p	Contact Angle (±5°)
unmodified PDMS	48.91	22.59	28.49			90
0	45.64	25.54	28.17	0.66	0.02	20
1	46.59	26.60	24.41	2.40	0.10	24
5	43.80	28.40	23.22	3.57	0.15	19
15	46.20	29.21	21.96	2.63	0.12	19
20	29.40	38.24	30.76	1.60	0.05	19

Note: 1. The PDMA polymer theoretically contains 71.4% carbon, 14.3% oxygen, and 14.3% nitrogen without counting the hydrogen atoms.

the surface nitrogen concentration reaches a maximum value at 5 minutes of plasma pre-treatment. However, as the plasma pre-treatment time exceeds 5 minutes, the surface nitrogen concentration begins decreasing with increasing treatment time. This results follows the same trend as the results for PVP/NVP-g-PDMS discussed in Section 4.3.2. Since PDMS molecular chains are so flexible, the migration of PDMA graft may account for such phenomena. Also, the longer plasma treatment time may produce the less reactive sites available for grafting. Both mechanisms have significant effects on the PDMA grafting. However, the grafting of DMA on PDMS is expected to be different from the PVP/NVP system. The grafting of DMA onto PDMS is highly dependent upon the number of reactive sites produced on the PDMS surface and the number of monomer molecules availabe to the PMDS surface. Therefore, the diffusion of DMA monomer to the PDMS surface can be a critical step during the grafting.

A typical XPS spectrum of PDMA-g-PDMS prepared by the plasma/gamma method and its expanded C1s peak is shown in Figure 4-46. One can see a distinguishable nitrogen peak which is not present in the spectrum of unmodified PDMS. Also, a minor peak is present on the left shoulder of the expanded C1s peak and is attributed to the chemical shift of amide carbonyl group of PDMA.

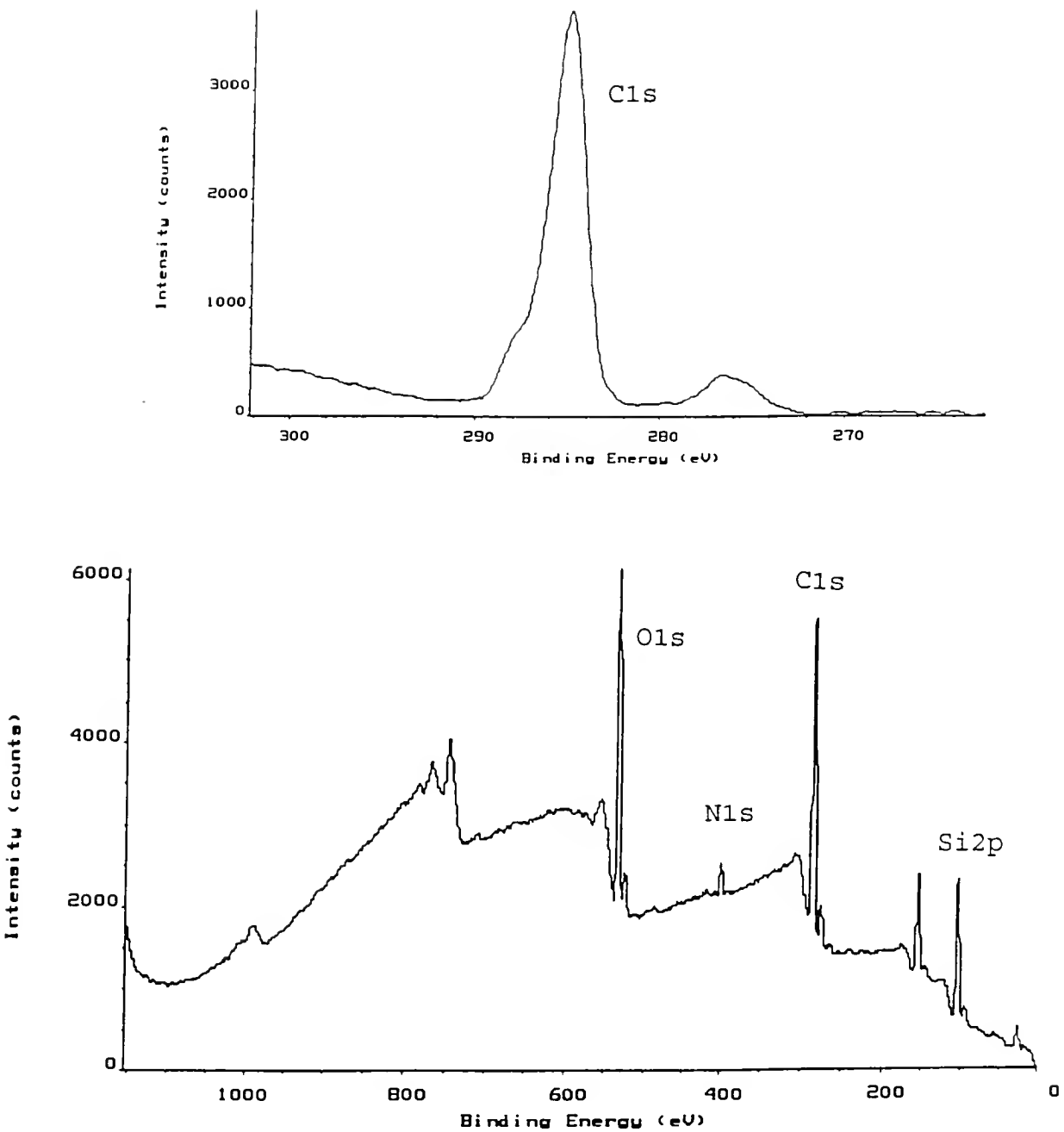

Figure 4-46. Typical XPS spectrum for PDMA-g-PDMS prepared by plasma/gamma method and an expanded C1s peak. (5 minutes water RFGD, 3 wt% DMA, 0.064 Mrad)

4.4.2.2 FT-IR/ATR

A typical FT-IR/ATR spectrum of PDMA-g-PDMS prepared by the plasma/gamma method is present in Figure 4-47. FT-IR/ATR analysis for PDMA-g-PDMS is also based on the amide carbonyl absorption at 1640 cm^{-1} in PDMA. One can find a very weak but observable hump at 1640 cm^{-1} in the spectrum. PDMA may not be detected very well by FT-IR/ATR analysis due to following: 1) a very thin graft, or 2) PDMA migratied into the bulk of PDMS.

4.4.3 Surface Graft Polymerization of DMA onto PP Using "Plasma/Gamma" Method

4.4.3.1 XPS analysis and contact angle measurements

Table 4-20 shows the results of XPS analysis and contact angle measurements for the PDMA-g-PP samples. Obviously, the surfaces of PDMA-g-PP are extremely hydrophilic for those samples prepared using plasma/gamma conditions. The sample prepared by the gamma method alone is also less hydrophilic than that by the plasma/gamma method. Yahiaoui [6] showed that using of NVP monomer solutions for the grafting of NVP on PP did not produce a hydrophilic surface when presoak method was not applied. Although NVP monomer solution has a slower gelation rate than DMA solution, NVP is not successfully grafted on PP by the gamma method alone. The result of the PVP/NVP-g-PP present in Table 4-11 also shows that the gamma method alone does not produce a hydrophilic surface either.

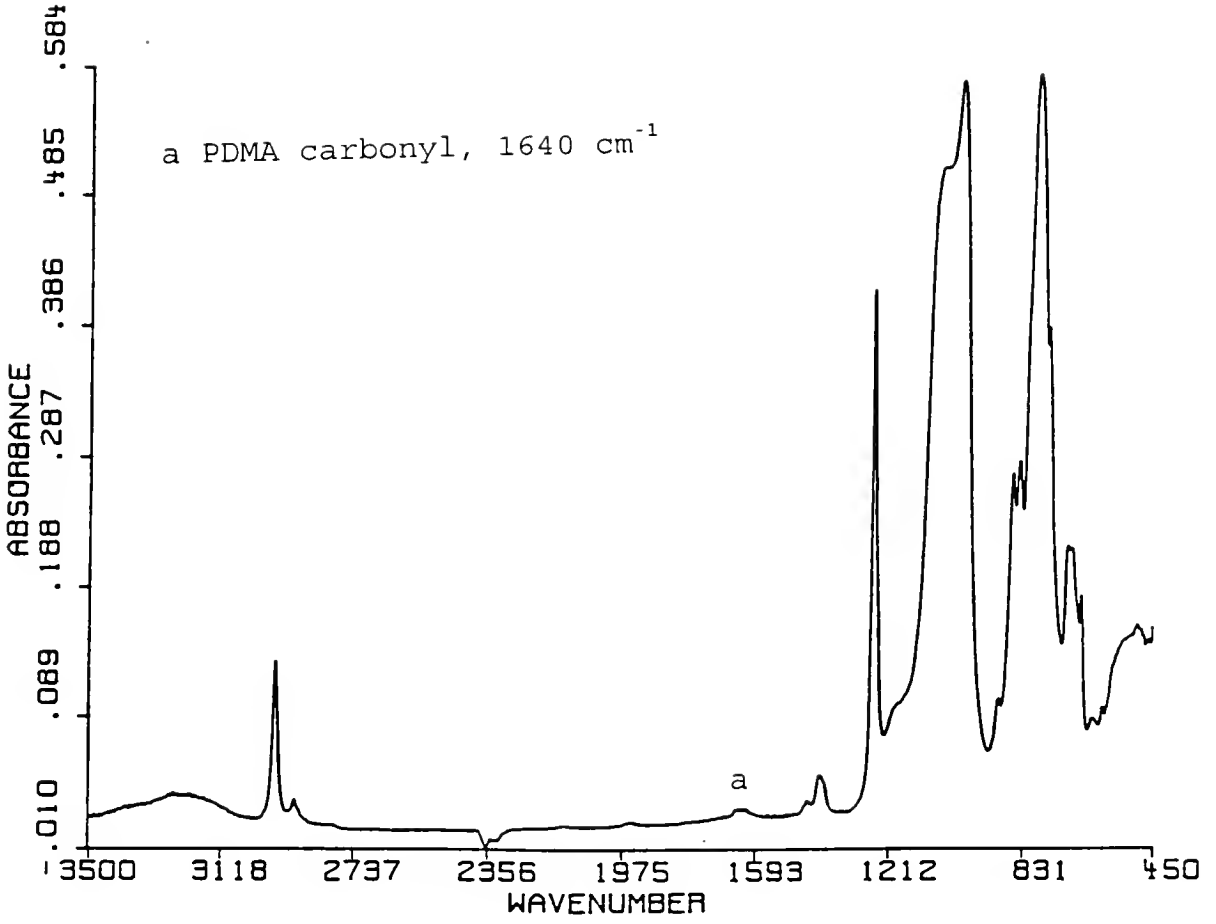

Figure 4-47. Typical FT-IR/ATR spectrum for the PDMA-g-PDMS prepared by the plasma/gamma method. (5 minutes water RFGD, 3 wt% DMA, 0.064 Mrad)

Table 4-20. XPS analysis and contact angle measurements for PDMA grafting onto PP using plasma/gamma method. (50 watts, 100 mTorr, 3 wt% DMA, 0.064 Mrad)

Plasma Treatment Time (minutes)	Atomic Concentration (%)				Contact Angle (±5°)
	C1s	O1s	N1s	N1s/O1s	
unmodified PP	100.00	0.00			90
0	97.43	1.75	0.82	0.47	28
1	87.59	6.74	5.67	0.84	19
5	87.31	6.88	5.81	0.84	18
15	91.40	4.75	3.85	0.81	18
20	88.51	5.96	5.53	0.92	18

Note: 1. The PDMA polymer theoretically contains 71.4% carbon, 14.3% oxygen and 14.3% nitrogen without counting the hydrogen atoms.

This may suggest that the degree of physisorption of PVP onto unmodified PP is much smaller than onto other substrates.

In the XPS analysis, the surface nitrogen concentration for the PDMA-g-PP prepared by the plasma/gamma method is significantly higher than that by the gamma method. For example, the surface nitrogen concentration for the gamma treated and one minute plasma/gamma treated is 0.82% and 5.67%, respectively. This indicates that the plasma/gamma method is much more effective than the gamma method alone.

As the plasma treatment time increased, the surface nitrogen concentration remains the same except for a small decline at 15 minutes plasma treatment. This suggests that it is not necessary to spend a lengthy plasma treatment time for PP substrates. The result has followed the same trend as the PVP/NVP-g-PP present in Table 4-11. The physisorption of PVP molecules on PP seems to have minor effects on the PVP/NVP grafting. The grafting of PVP/NVP and the grafting of DMA onto PP is therefore believed to be controlled by the diffusion of monomer to the PP surface.

Figure 4-48 gives a typical XPS spectrum for PDMA-g-PP prepared by the plasma/gamma method and its expanded C1s peak. A very intense N1s peak is presented in the spectrum. This suggests that PP surface is covered with a thin layer of PDMA. Also, the presence of a small hump on the left shoulder of the expanded C1s peak is due to the chemical shift of the amide carbonyl group of PDMA.

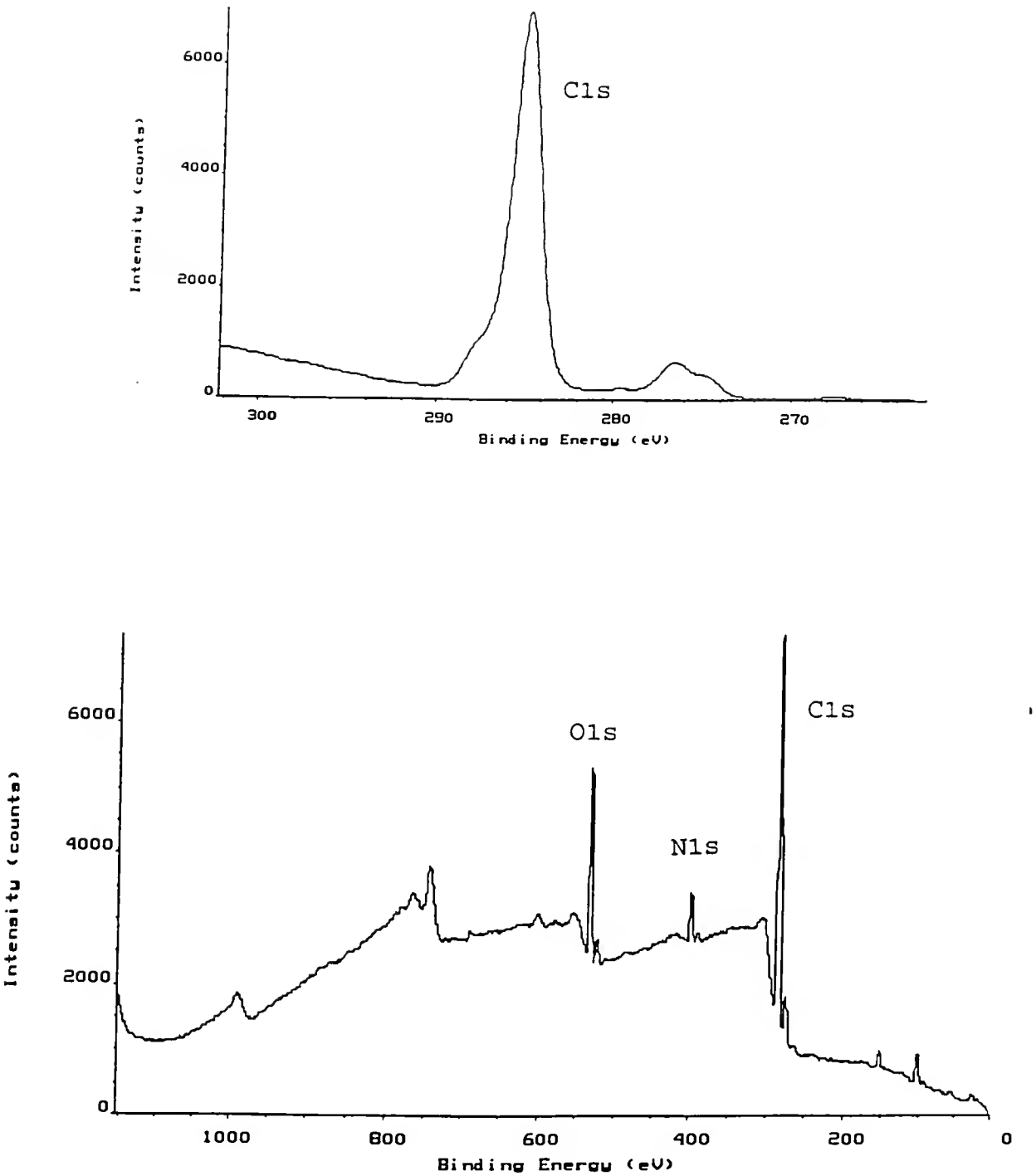

Figure 4-48. Typical XPS spectrum for PDMA-g-PP prepared by plasma/gamma method and an expanded C1s peak. (5 minutes water RFGD, 3 wt% DMA, 0.064 Mrad)

4.4.3.2 FT-IR/ATR

A typical FT-IR/ATR spectrum of PDMA-g-PP is given in Figure 4-49. The spectrum of PDMA-g-PP displays a very distinct peak at 1640 cm^{-1}. Therefore, FT-IR/ATR analysis has further confirmed the presence of PDMA graft which must be in the range of 0.6-3 μm thick for FT-IR/ATR detection using KRS-5 crystal. The FT-IR/ATR result for the PVP/NVP-g-PP in Figure 4-32 is also very identifiable as the FT-IR/ATR for PDMA-g-PP in Figure 4-49. In addition to contact angle results, both XPS and FT-IR/ATR also indicate that the grafting of DMA onto PP exhibits a similar trend as the grafting of PVP/NVP onto PP in terms of the surface nitrogen concentration and the plasma treatment time. This suggests that the grafting of PVP/NVP onto PP is not dominated by the physisorption of PVP molecules onto PP surface.

4.4.4 Surface Graft Polymerization of DMA onto PC Using "Plasma/Gamma" Method

4.4.4.1 XPS analysis and contact angle measurements

The results of XPS analysis and contact angle measurements for the PDMA-g-PC samples are listed in Table 4-21. The PC surface becomes very hydrophilic after grafting with PDMA. The contact angles are 24° for the gamma method and less than 20° for the plasma/gamma method. In the XPS analysis, the surface nitrogen concentration is gradually increasing as the plasma treatment time increases. The surface nitrogen concentration reaches a value of

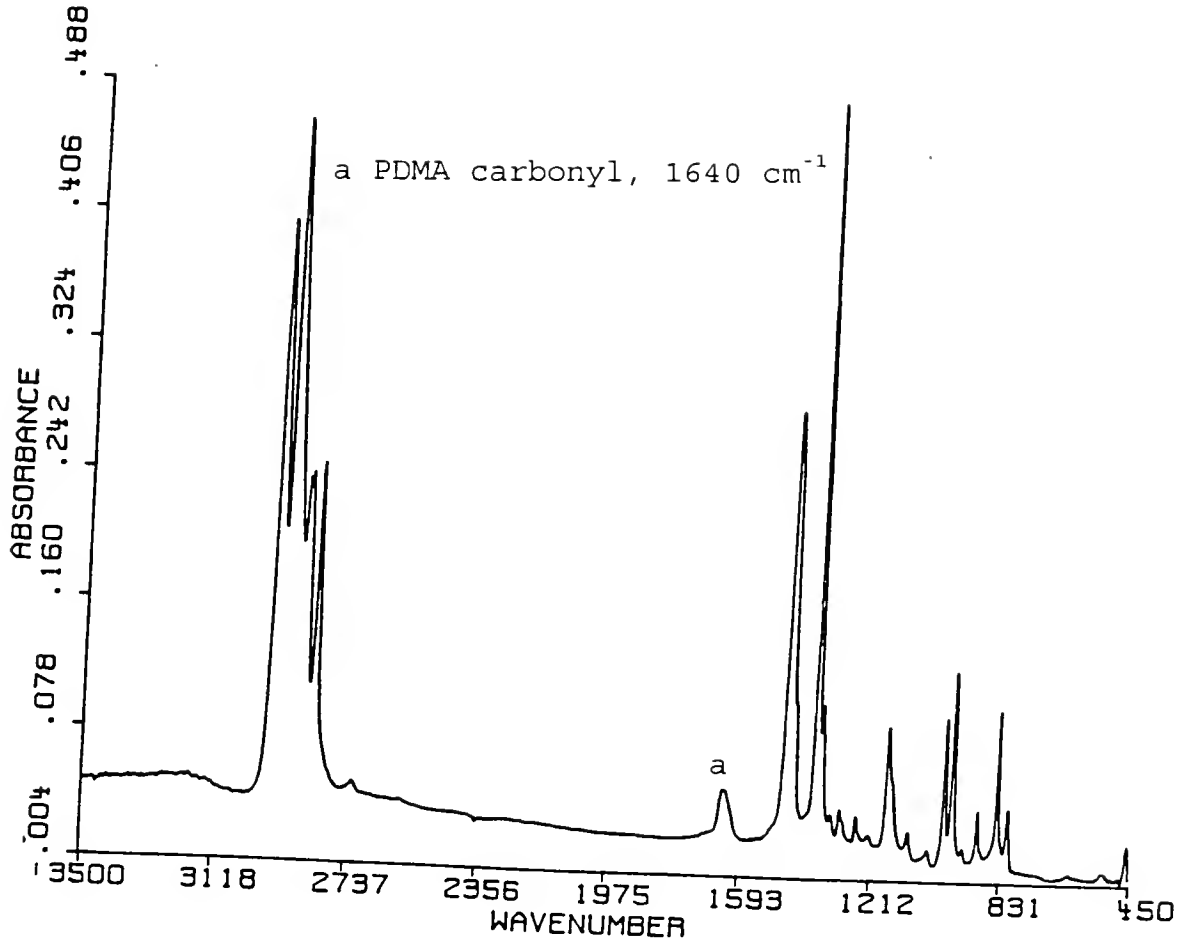

Figure 4-49. Typical FT-IR/ATR spectrum for the PDMA-g-PP prepared by the plasma/gamma method. (5 minutes water RFGD, 3 wt% DMA, 0.064 Mrad)

Table 4-21. XPS analysis and contact angle measurements for PDMA grafting onto PC using plasma/gamma method. (50 watts, 100 mTorr, 3 wt% DMA, 0.064 Mrad)

Plasma Treatment Time (minutes)	Atomic Concentration (%)				Contact Angle (±5°)
	C1s	O1s	N1s	N1s/O1s	
unmodified PC	86.11	13.89	-	-	83
0	82.96	45.09	1.95	0.13	24
1	80.66	16.92	2.42	0.14	19
5	77.81	14.99	7.20	0.48	18
15	75.10	13.34	11.56	0.87	18
20	74.90	12.43	12.67	1.02	17

Note: 1. The PDMA polymer theoretically contains 71.4% carbon, 14.3% oxygen and 14.3% nitrogen without counting the hydrogen atoms.

12.7 % at 20 minutes, which is close to the theoretical value of PDMA (14.3 %). The results suggest that the reactive sites produced on PC surface using RF-plasma pre-treatment are increasing with the plasma treatment time. On the other hand, the result for the PVP/NVP system in section 4.3.4 did not reveal such a trend. The surface nitrogen concentration for the PVP/NVP-g-PC present in Table 4-13 does not change much with increasing plasma treatment time. This may indicate that the grafting of PVP/NVP onto PC is mainly through the physisorption of PVP molecules onto PC surface and then by radical recombinations.

A typical XPS spectrum for PDMA-g-PC prepared by the plasma/gamma method and its expanded C1s peak is given in Figure 4-50. A very sharp and distinct N1s peak is present in the spectrum. Also, no minor peak for ester group can be found in the expanded C1s peak except a minor peak for amide carbonyl group. Therefore, these results suggest that the modified PC surface was covered with a uniform layer of PDMA graft.

4.4.4.2 FT-IR/ATR

A typical FT-IR/ATR spectrum of PDMA-g-PC prepared by plasma/gamma method is presented in Figure 4-51. The amide carbonyl absorption peak at 1640 cm^{-1} is too weak to be observed. In the PVP/NVP system, the PVP graft onto PC is also not detectable by FT-IR/ATR. This may be due to a very thin graft.

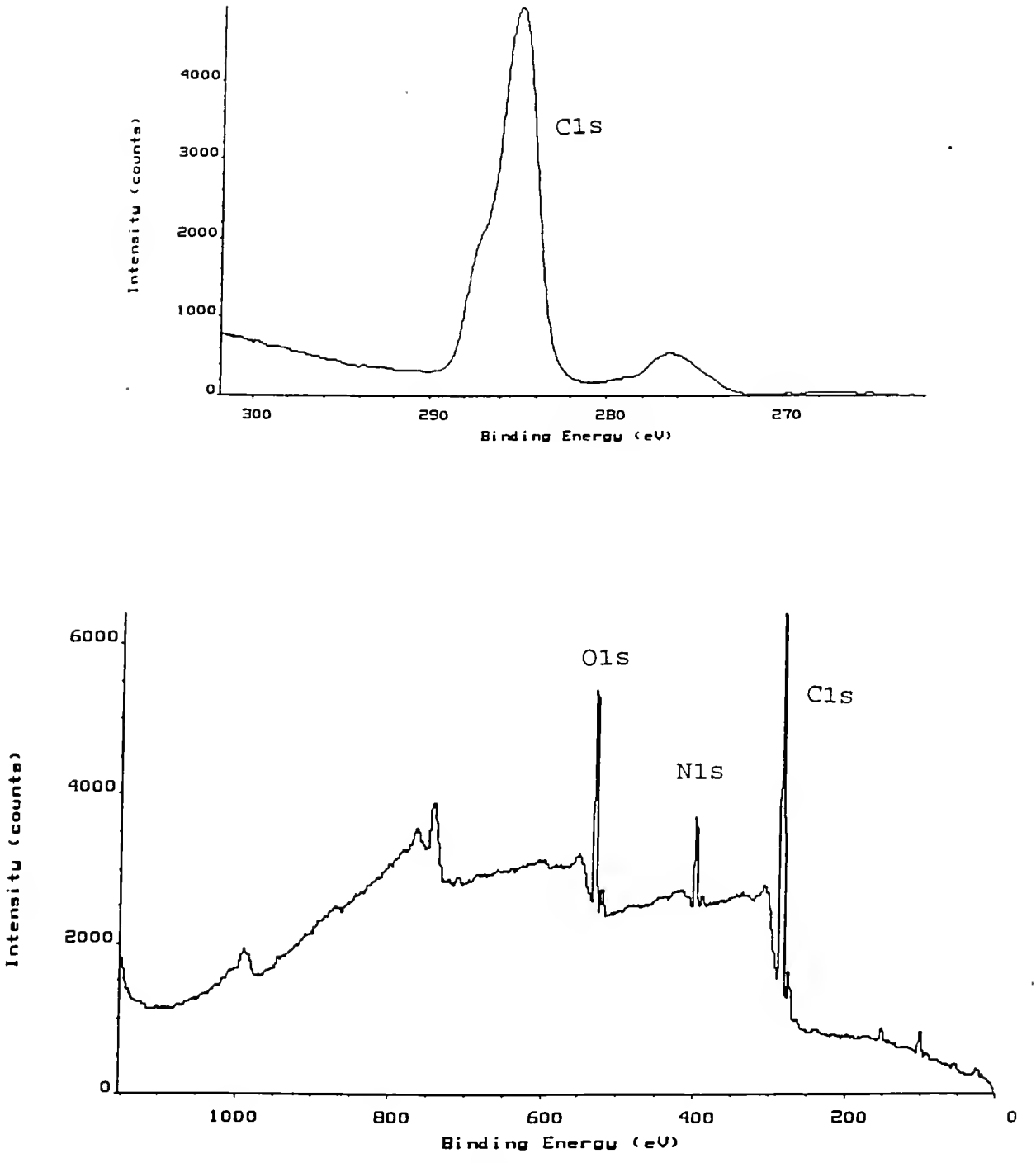

Figure 4-50. Typical XPS spectrum for PDMA-g-PC prepared by plasma/gamma method and an expanded C1s peak. (20 minutes water RFGD, 3 wt% DMA, 0.064 Mrad)

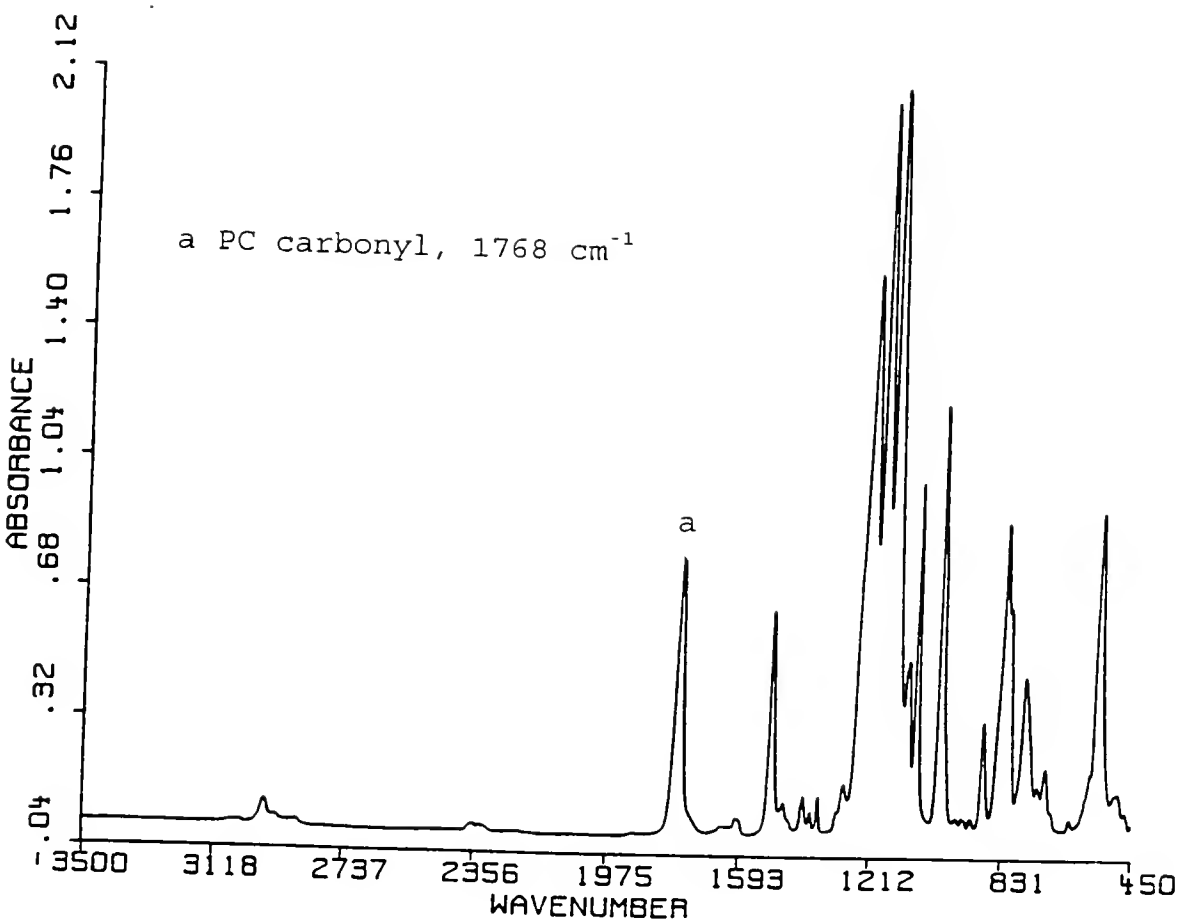

Figure 4-51. Typical FT-IR/ATR spectrum for the PDMA-g-PC prepared by the plasma/gamma method. (20 minutes water RFGD, 3 wt% DMA, 0.064 Mrad)

4.4.5 Surface Graft Polymerization of DMA onto FEP Using "Plasma/Gamma" Method

4.4.5.1 XPS analysis and contact angle measurements

Table 4-22 summarizes the XPS analysis and contact angle results for the PDMA-g-FEP samples. Contact angle data indicate that the gamma method alone treated sample remains very hydrophobic (contact angle = 78°), but the plasma/gamma method treated becomes very hydrophilic (contact angle ≤ 20°). In the XPS analysis, the surface nitrogen concentration increases from 0.46 % to 7.92 % with one minute plasma pre-treatment. This suggests that the improvement of PDMA graft on FEP surface is very significant by the plasma/gamma method. Also, the surface nitrogen concentration for the 5, 15, and 20 minute plasma pre-treated is 6.81%, 10.57%, and 9.89%, respectively. The prolonged plasma treatment time did not significantly enhance or reduce the grafting of DMA onto FEP. This may suggest that the prolonged plasma treatment does not increase the number of reactive sites on FEP surface. The XPS results for the PDMA-g-FEP are similar to the PVP/NVP-g-FEP present in the Table 4-15. Since the long chain PVP molecules does not affect the trend of PVP/NVP grafting, this may indicate that the grafting of PVP/NVP and DMA onto FEP is mainly contributed by the number of reactive sites on FEP surface and the diffusion of monomer to the FEP surface.

Figure 4-52 gives a typical XPS spectrum for PDMA-g-FEP prepared by the plasma/gamma method and its expanded C1s

Table 4-22. XPS analysis and contact angle measurements for PDMA grafting onto FEP using plasma/gamma method. (50 watts, 100 mTorr, 3 wt% DMA, 0.064 Mrad)

Plasma Treatment Time (minutes)	Atomic Concentration (%)					Contact Angle (±5°)
	C1s	O1s	F1s	N1s	N1s/F1s	
unmodified FEP	41.58	0.50	57.92	-	-	110
0	37.99	0.47	61.08	0.46	0.007	78
1	59.25	7.83	25.00	7.92	0.316	20
5	57.94	7.24	28.02	6.81	0.243	18
15	66.08	10.93	12.42	10.57	0.851	18
20	67.88	10.56	11.67	9.89	0.847	17

Note: 1. The PDMA polymer theoretically contains 71.4% carbon, 14.3% oxygen, and 14.3% nitrogen without counting the hydrogen atoms.

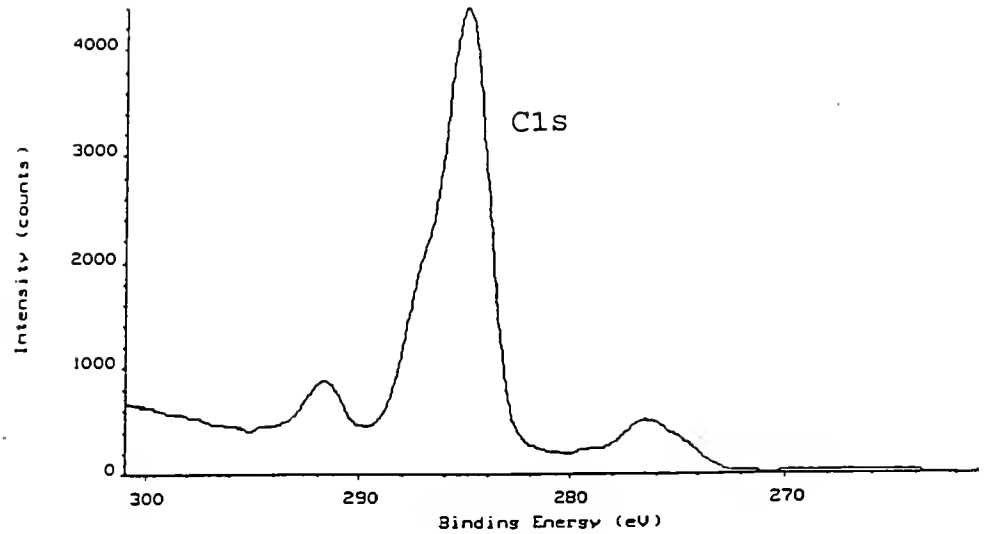

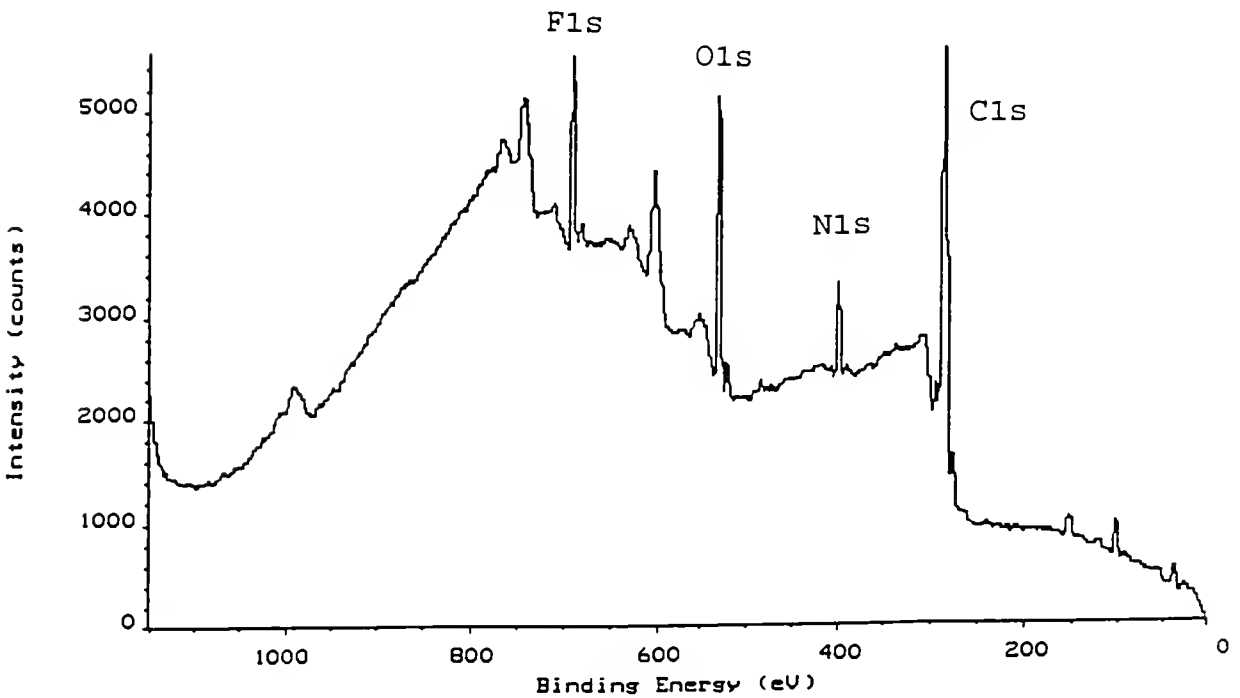

Figure 4-52. Typical XPS spectrum for PDMA-g-FEP prepared by plasma/gamma method and an expanded C1s peak. (15 minutes water RFGD, 3 wt% DMA, 0.064 Mrad)

peak. The nitrogen peak is very sharp and distinguishable. In addition, the CF_x peak for the plasma/gamma treated FEP is much smaller than that for the unmodified FEP. The minor peak for amide carbonyl group also appears on the left shoulder of C1s peak. Therefore, the evidence of PDMA graft onto FEP surface is further supported by XPS analysis.

4.4.5.2 FT-IR/ATR

A typical FT-IR/ATR spectrum for the PDMA-g-FEP prepared by the plasma/gamma method is shown in Figure 4-53. The amide carbonyl absorption peak at 1640 cm^{-1} is small but significant. This indicates the presence of the PDMA graft.

4.4.6 Surface Graft Polymerization of DMA onto PVDF Using "Plasma/Gamma" Method

4.4.6.1 XPS analysis and contact angle measurements

Table 4-23 presents the XPS and contact angle results for the PDMA-g-PVDF samples. The contact angles for all of surface modified PVDF samples are around 20° regardless of the method of treatment. This suggests that PDMA graft readily transforms the PVDF surface from a hydrophobic surface into a hydrophilic surface. In the XPS analysis, the surface nitrogen concentration increases from 4.26 % to 10.85 % using one minute plasma pre-treatment. However, the surface nitrogen concentration did not change significantly as the plasma treatment time was increased. This suggests that the number of reactive sites on PVDF surface produced

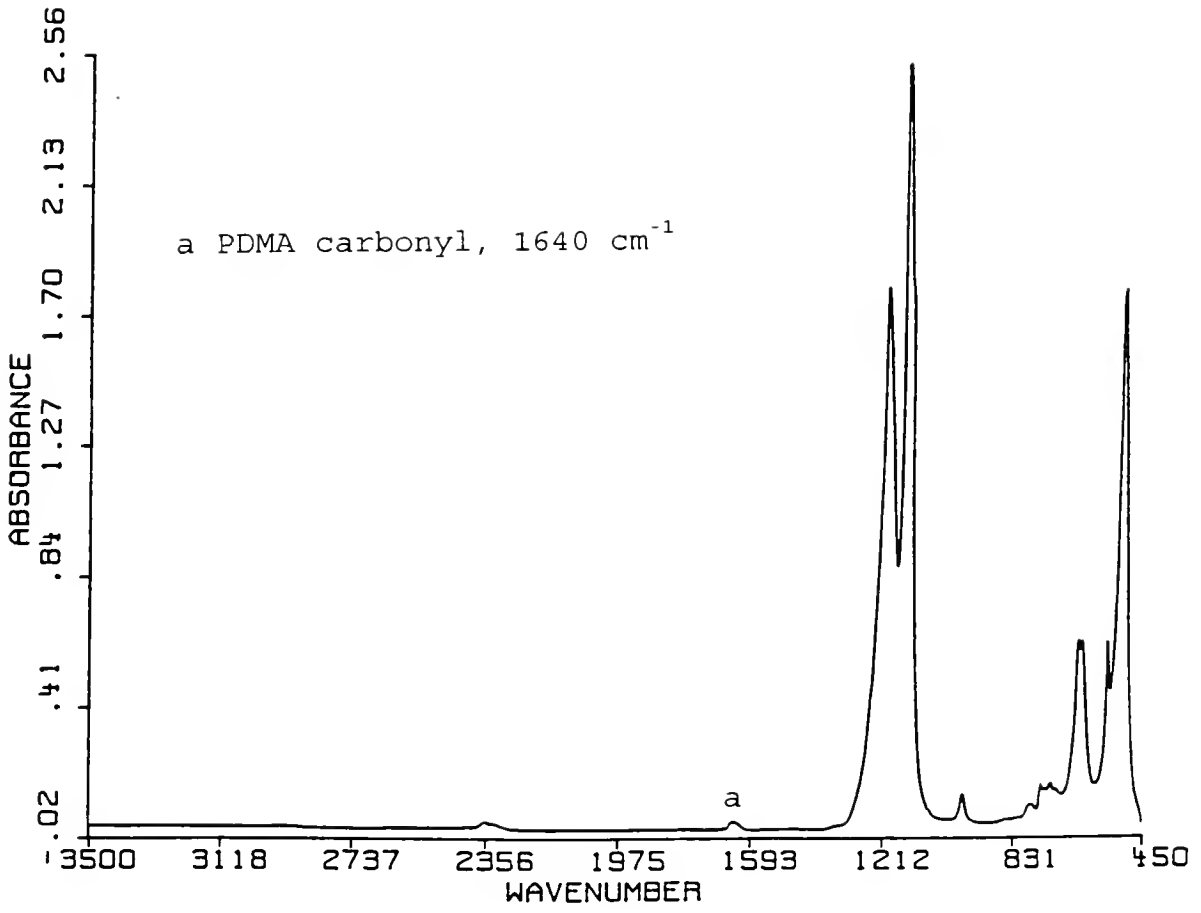

Figure 4-53. Typical FT-IR/ATR spectrum for the PDMA-g-FEP prepared by the plasma/gamma method. (20 minutes water RFGD, 3 wt% DMA, 0.064 Mrad)

Table 4-23. XPS analysis and contact angle measurements for PDMA grafting onto PVDF using plasma/gamma method. (50 watts, 100 mTorr, 3 wt% DMA, 0.064 Mrad)

Plasma Treatment Time (minutes)	Atomic Concentration (%)					Contact Angle (±5°)
	C1s	O1s	F1s	N1s	N1s/F1s	
unmodified PVDF	55.67	1.29	43.05	-	-	90
0	58.18	4.70	32.87	4.26	0.129	20
1	72.66	11.65	4.84	10.85	2.241	19
5	72.08	11.95	5.17	10.80	2.088	20
15	71.61	11.70	6.76	9.93	1.468	20
20	71.97	11.40	6.67	9.96	1.493	19

Note: 1. The PDMA polymer theoretically contains 71.4% carbon, 14.3% oxygen, and 14.3% nitrogen without counting the hydrogen atoms.

by the plasma pre-treatment does not decrease with increasing the treatment time which happens to some polymeric substrates. PVDF surface is one of the most treatable substrate in this study. PVDF can be easily grafted with NVP only solution without presoak [6]. Previous XPS data for PVP/NVP-g-PVDF samples present in Table 4-17 also shows that the surface nitrogen concentration does not change significantly as the plasma treatment time increases. This may suggest that the plasma pre-treated PVDF surface is very reactive and can be easily grafted with DMA or PVP/NVP monomer solutions using a short plasma treatment time.

A typical XPS spectrum for PDMA-g-PVDF prepared by the plasma/gamma method and its expanded C1s is shown in Figure 4-54. In the spectrum, a strong and distinct nitrogen peak correlating to the presence of PDMA graft can be observed. Also, the left shoulder of the first major C1s peak displays a small hump which is contributed by the amide carbonyl group of PDMA.

4.4.6.2 FT-IR/ATR

A typical FT-IR/ATR spectrum for PDMA-g-PVDF prepared by the plasma/gamma method is given in Figure 4-55. The amide carbonyl peak at 1640 cm^{-1} is small but distinguishable. This indicates the presence of a very thin PDMA graft.

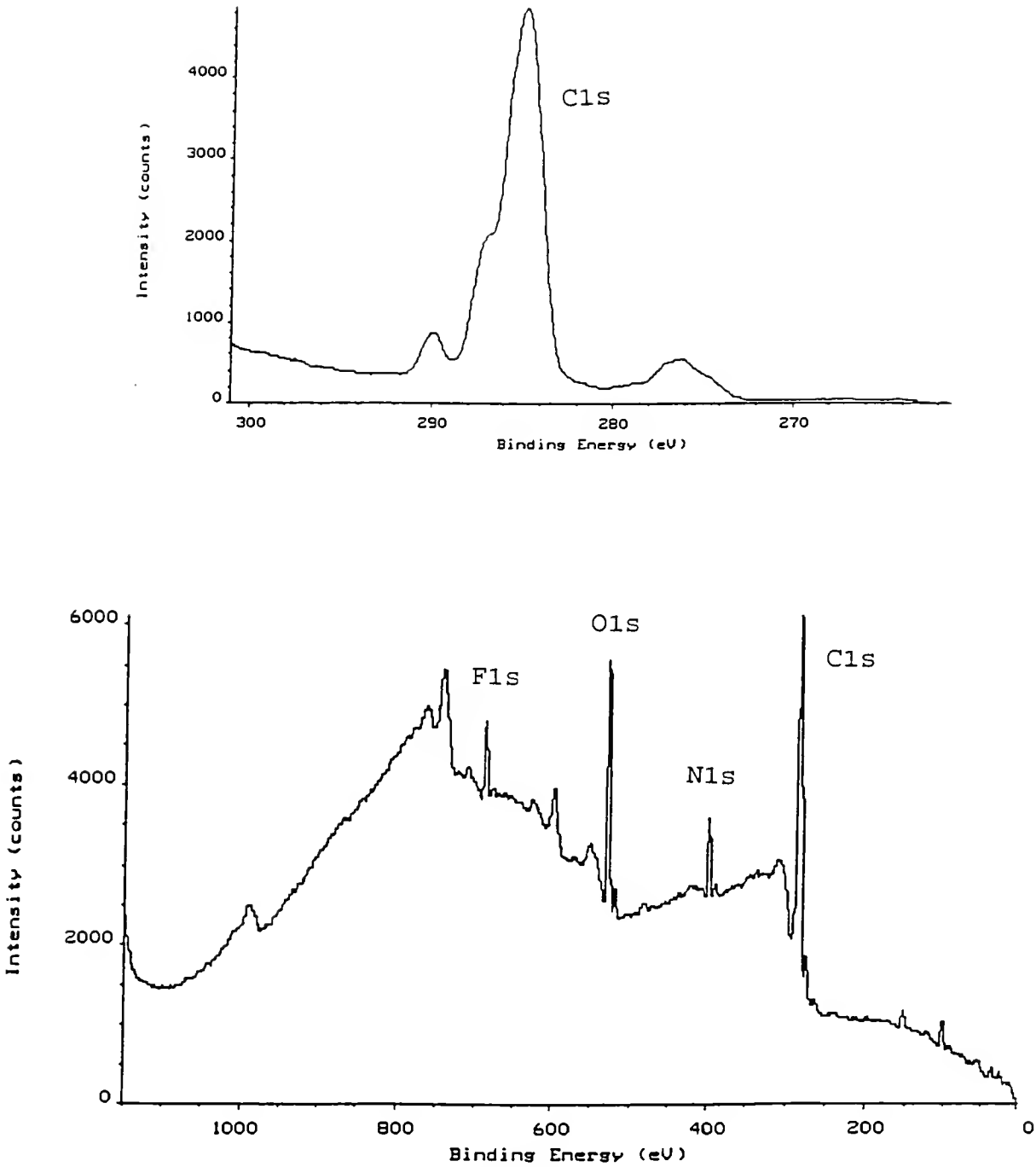

Figure 4-54. Typical XPS spectrum for PDMA-g-PVDF prepared by plasma/gamma method and an expanded C1s peak. (15 minutes water RFGD, 3 wt% DMA, 0.064 Mrad)

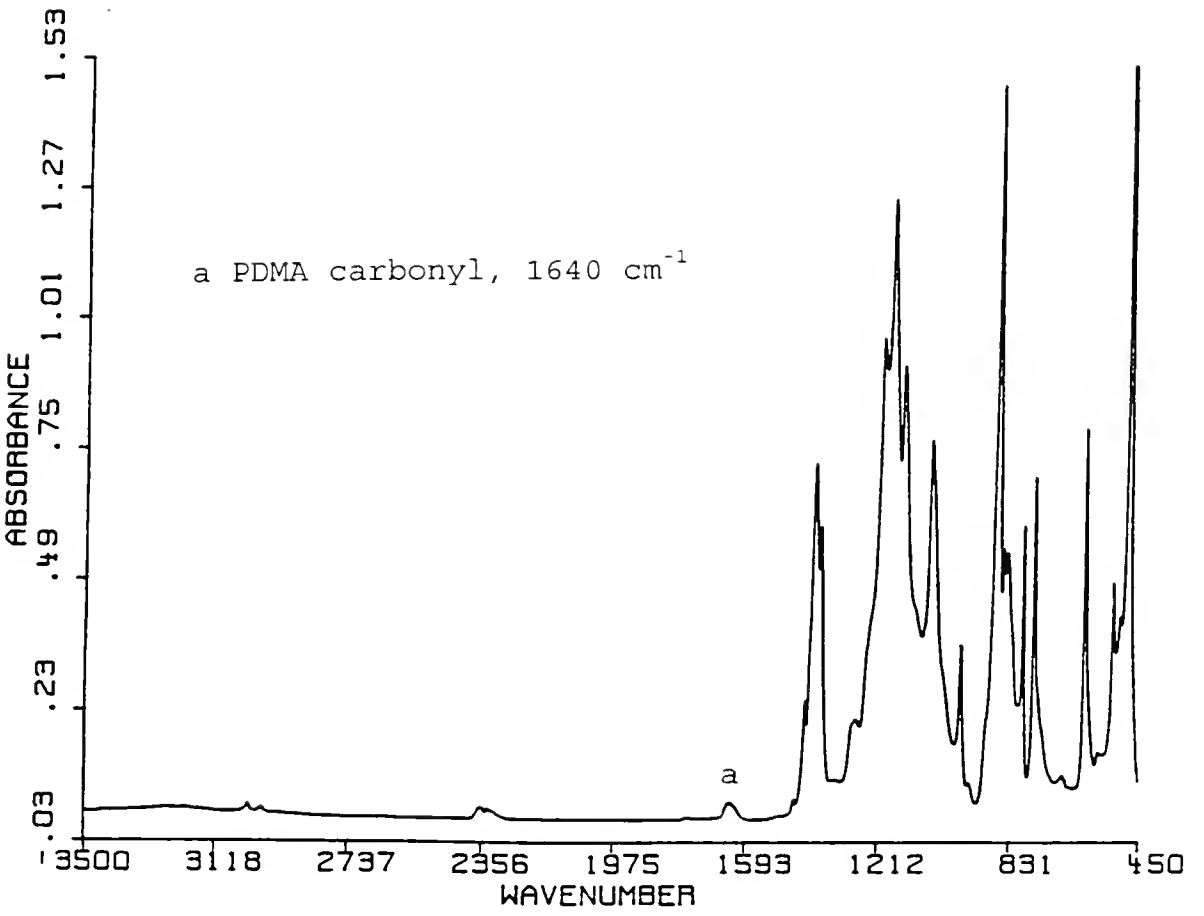

Figure 4-55. Typical FT-IR/ATR spectrum for the PDMA-g-PVDF prepared by the plasma/gamma method. (15 minutes water RFGD, 3 wt% DMA, 0.064 Mrad)

4.4.7 Summary of Grafting of DMA onto PMMA, PDMS, PP, PC, FEP, and PVDF Using "Plasma/Gamma" Method

The grafting of PDMA onto polymeric substrates was significantly improved by the plasma pretreatment. The surface nitrogen concentration for the PDMA grafts prepared by the plasma/gamma method were significantly increased from the lowest of 0.46% for the PDMA-g-FEP without plasma treatment to the highest of 12.67% for the PDMA-g-PC with plasma pre-treatment. The hydrated PDMA surfaces exhibited extremely low contact angle (ca. 18°).

The effects of plasma pre-treatment time on the DMA grafting are different from substrate to substrate. The number of reactive sites produced may decrease for PMMA and PDMS, and may remain unchange for PP, FEP, PVDF with increasing the plasma treatment time. Therefore, the plasma treatment time for PMMA and PDMS is very critical during plasma treatment.

The formation of PDMA grafts was mainly through the addition polymerization of DMA monomer initiated by the activated polymeric surface radicals. The grafting was believed to be dominated by 1) the number of reactive sites produced by plasma pre-treatment and gamma irradiation (the G value); 2) the number of monomer molecules available to the substrate surface; and 3) the monomer diffusion rate. As compared to NVP alone solution, the grafting NVP may follow the mechanisms except DMA has a higher gelation rate than NVP alone solution. This is quite different from the

PVP/NVP system for certain substrates, such as PMMA and PC. In the PVP/NVP system, the physical adsorption of PVP onto substrate surface may be more important than other factors for these polymeric substrates. The structure of PDMA grafts was expected to be a thin and dense graft with less penetration as compared to the "presoak method" [6].

4.5 Surface Graft Polymerization of PVP/NVP onto PMMA Using "Two-step" Method

The "two-step" method involved two consecutive steps of gamma-induced graft polymerization. The purpose of first gamma-induced graft polymerization is to increase the wettability of PMMA surface and function similarly to the RF plasma pre-treatment in the plasma/gamma method. Therefore, it was important to assess the minimum radiation dose in the first step required to produce enough PVP graft to enhance the second gamma-induced graft polymerization step.

In this study, the radiation dose in the first step was varied from 0.03 to 0.15 Mrad and the radiation dose in the second step was fixed at 0.15 Mrad. Monomers including 10 % NVP and 10% PVP/NVP at a weight ratio of 2/8 were evaluated. The results of XPS analysis, solution viscosity, contact angle measurements, and graft thickness are listed in Table 4-24.

The XPS results listed in the Table are for the PVP-g-PMMA samples after two-step modification. They indicated that as the radiation dose in the first step increased, the

Table 4-24. The results of XPS analysis, contact angle measurements, and graft thickness measurement for PVP-g-PMMA prepared by the two-step method

10 % NVP radiation dose in 1st step (Mrad)	Viscosity (cps)	Atomic Concentration (%)				Graft thickness (A°)	Contact angle (± 5°)
		C1s	O1s	N1s	N1s/O1s		
0.03	732	76.20	20.19	3.61	0.178	2293±2388xn	19
0.09	2660	76.33	18.61	4.75	0.255	2791±2387xn	18
0.15	5720	76.50	18.40	5.56	0.302	2288±2386xn	17
10 % PVP/NVP ratio of 2/8							
0.03	274	75.82	20.86	3.32	0.159	2415±2400xn	17
0.09	654	76.17	20.39	3.44	0.168	2228±2389xn	17
0.15	1570	76.95	16.33	6.72	0.411	2340±2390xn	18

Note: 1. The PVP polymer theoretically contains 75% carbon, 12.5% oxygen and 12.5% nitrogen without counting the hydrogen atoms.
2. Viscosity of polymer solution was measured at shear rate of 3.75 (1/sec) and temperature of 25 °C.
3. The radiation dose used in the second step was 0.15 Mrad.
4. The graft thickness is measured using the ellipsometry.

surface nitrogen concentration for both monomer groups increased. Obviously, the proper radiation dose in the first step should be 0.15 Mrad for both 10% NVP and 10% PVP/NVP (ratio of 2/8) monomer solutions, since the surface nitrogen concentration reaches the highest value of 5.56% and 6.72%, respectively at 0.15 Mrad. The results are comparable to the PVP-g-PMMA prepared by the plasma/gamma method in which the surface nitrogen concentration is about an average value of 8.5%. In the contact angle measurements, all the surface modified PMMA gave a low contact angle (below 20°). Thus the PVP graft has changed the PMMA surface into an extremely hydrophilic surface. The minimum graft thickness measured by ellipsometry for surface modified PMMA prepared by the two-step method is around 2,200 to 2,700 Å. Consequently, the results of the two-step method suggested that the minimum radiation dose for both monomer systems in the first step would be 0.15 Mrad, and the PVP/NVP ratio of 2/8 monomer solution gave a better PVP graft on PMMA surface.

In addition to the PVP/NVP monomer solution with ratio of 2/8, PVP/NVP ratios of 3/7 and 5/5 were also evaluated by the two-step method. The radiation dose used in the first and second steps was fixed at 0.15 Mrad in this case. The result of XPS analysis is given in Table 4-25. The nitrogen content for both PVP/NVP ratio of 3/7 and ratio of 5/5 was 6.59% and 7.25% respectively. Obviously, these results are close to the result of PVP/NVP at a ratio of 2/8.

Table 4-25. XPS analysis and contact angle measurements of PVP/NVP modified PMMA using two-step method

Monomer System	Atomic Concentration (%)				Contact Angle (±5°)
	C1s	O1s	N1s	N1s/O1s	
10 % PVP/NVP ratio of 3/7	78.52	14.89	6.59	0.442	18
10 % PVP/NVP ratio of 5/5	78.15	14.60	7.25	0.496	19

Note: 1. The conditions for both monomer solutions are 10% monomer/0.15 Mrad for two times.

Therefore, both solutions are also suitable for two-step surface modification.

4.6 In Vitro Studies on the Hydrophilic Surface Modified Substrates

Adhesion and spreading of lens epithelial cells on the IOL optics is a complication during cataract and IOL surgery which may lead to post-operative inflammation and lens opacification [6]. Therefore, the use of adhesion and spreading of rabbit lens epithelial cells as an *in vitro* model may be a useful technique for evaluating the biocompatibility of implants. The procedure used for rabbit lens epithelial cell adhesion and spreading was developed by F. Hofmeister [112] and the epithelial cell adhesion tests were performed by P. Martin in this laboratory.

The modified and unmodified substrates including PMMA, PDMS, PP, PC, PVDF, and FEP were evaluated with rabbit lens epithelial cells for adhesion and spreading. The test was conducted for all of the above materials except the PP and FEP substrates. These two substrates were not readily immersed into the cell culture solutions because of their low density.

The optical micrographs of PMMA substrates are exhibited in Figure 4-56. The unmodified PMMA surfaces displayed good cell adhesion and spreading as shown in Figure 4-56 (a). However, the cell adhesion and spreading on the plasma treated PMMA surface in Figure 4-56 (b) is

greater than for the unmodified PMMA surface. On the other hand, the PVP/NVP-g-PMMA surface in Figure 4-56 (c) exhibits essentially zero cell adhesion and the PDMA-g-PMMA surface in Figure 4-56 (d) displays only a few adherent cells. The contact angle for the unmodified, plasma treated, plasma/gamma PVP/NVP treated, and plasma/gamma DMA treated PMMA are 70°, 34°, 19°, and 20°, respectively. The surface nitrogen concentration for the plasma/gamma treated PMMA is around 8.5%. The results indicate that rabbit lens epithelial cell likes to grow on the hydrophobic and plasma treated PMMA surface, but does not like to grow on hydrated PVP hydrophilic surface. Cell behavior on biomaterial surface has been correlated to several substratum properties, for example chemical groups on the surface [129-131], surface charge [132,133], hydrophilicity/hydrophobicity [134-138], equilibrium water content [43], roughness [139], and substratum contractility [140]. Hydrophilic polymers such as poly(hydroxyethyl methacrylate) (PHEMA) or poly(vinyl pyrrolidone) (PVP) have a good biotolerability and usually exhibit very low cell adhesion [36,137,141]. The results from this investigation suggest that 1) hydrated PVP surface can significantly reduce the cell adhesion; 2) hydrophilicity is not the only factor in preventing cell adhesion and spreading; and 3) hydrated PDMA graft may be not as effective as the PVP graft in preventing the cell adhesion. Possible reasons for low cell adhesion on PVP and PDMA surfaces may be because of

their low interfacial free energy within aqueous environment and their soft, slippery, and non-sticking characters.

Figure 4-57 shows the optical micrograph of PDMS substrates. The features exhibited in these micrographs are similar to the PMMA substrates in Figure 4-56. The unmodified PDMS surface shows good cell adhesion and spreading, but the plasma modified PDMS surface again exhibits much greater cell adhesions. The contact angles for unmodified PDMS and plasma treated PDMS are 90° and 20°, respectively. On the other hand, the PVP/NVP-g-PDMS surface displays essentially zero cell adhesion, and the PDMA-g-PDMS surface shows only a few cells with no spreading. Both PVP/NVP-g-PDMS and PDMA-g-PDMS have a contact angle around 20°.

The optical micrographs of PC substrate and PVDF substrate are shown in Figures 4-58 and 4-59, respectively. Results for PC and PVDF substrates show a similar trend as compared to PMMA. Both unmodified PC and PVDF show good cell adhesion and spreading. The contact angles for unmodified PC and PVDF are 83° and 90° , respectively. Conversely, the PVP/NVP-g-PC and PVP/NVP-g-PVDF surfaces display virtually no cell adhesion, and the PDMA-g-PC and PDMA-g-PVDF surfaces show only a few cells with no spreading.

Therefore, one can confirm that the hydrated PVP and PDMA surfaces significantly reduce the incidence of cell adhesion. Moreover, low interfacial surface tension is not

the only factor in inhibiting cell adhesion since the plasma treated surfaces have contact angle of 20° and exhibit extensive cell adhesion.

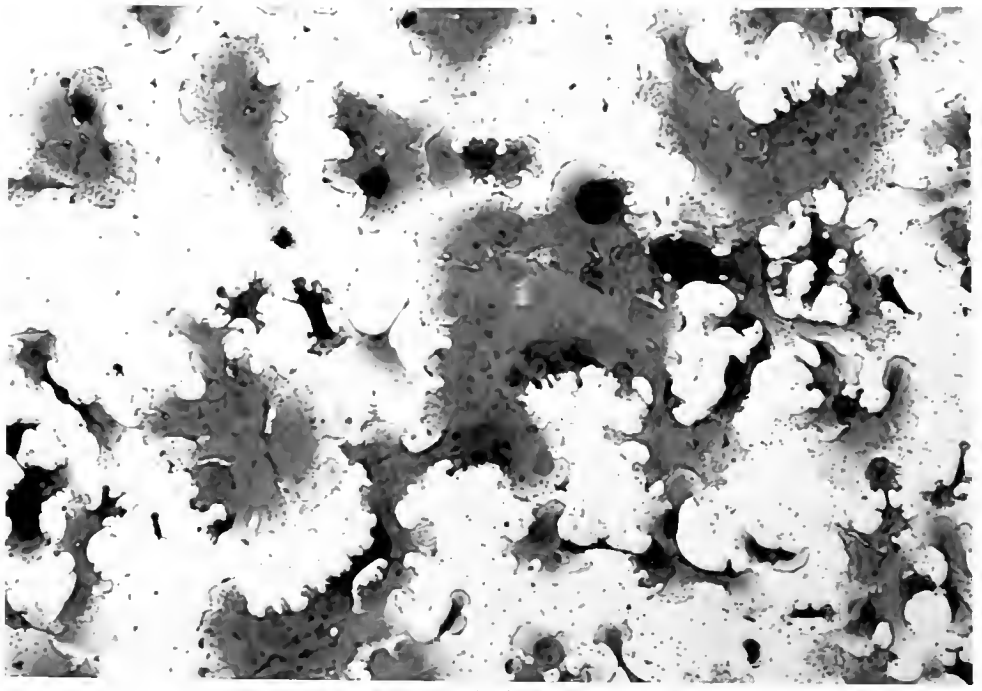

(a)

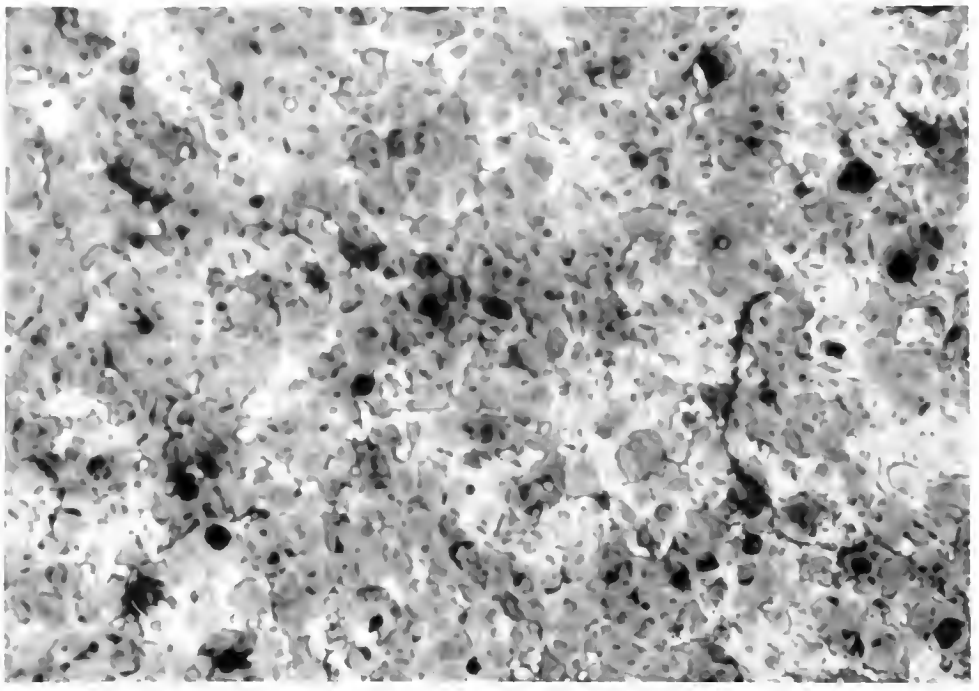

(b)

Figure 4-56. The optical micrograph of PMMA substrates (70X)
(a) unmodified PMMA
(b) plasma treated PMMA (15 minutes, 50 watts, 100 mTorr)

(c)

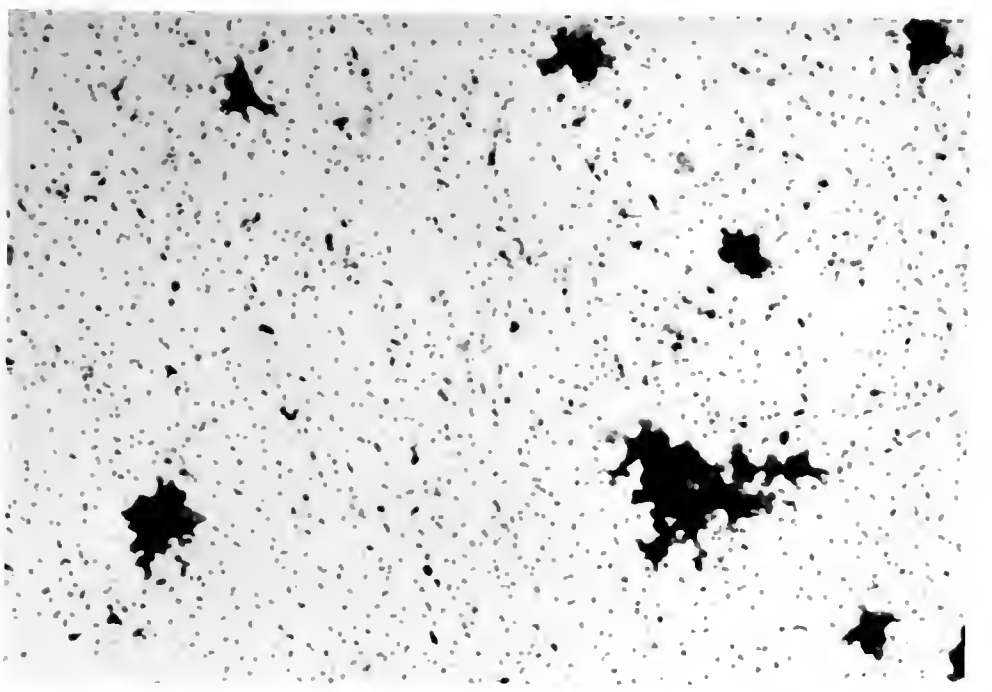

(d)

Figure 4-56 --- continued
(c) PVP/NVP-g-PMMA (15 minutes, 50 watts, 100 mTorr, 10% PVP/NVP ratio of 2/8, 0.15 Mrad)
(d) PDMA-g-PMMA (15 minutes, 50 watts, 100 mTorr, 3% DMA, 0.064 Mrad)

(a)

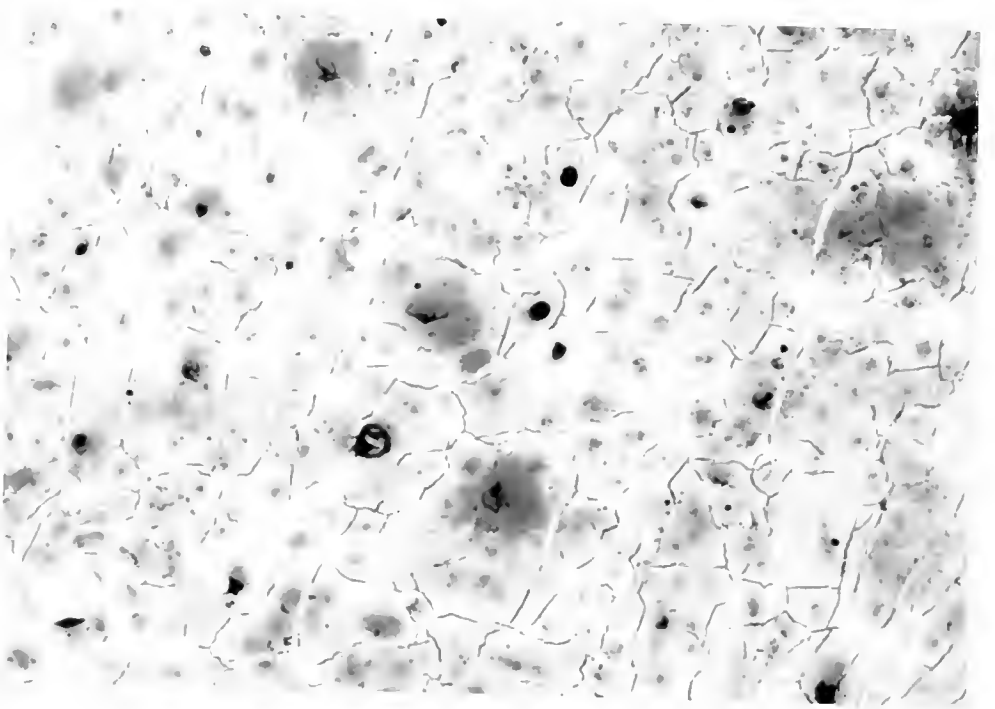

(b)

Figure 4-57. The optical micrograph of PDMS substrates (70x)
(a) unmodified PDMS
(b) plasma treated PDMS (15 minutes, 50 watts, 100 mTorr)

(c)

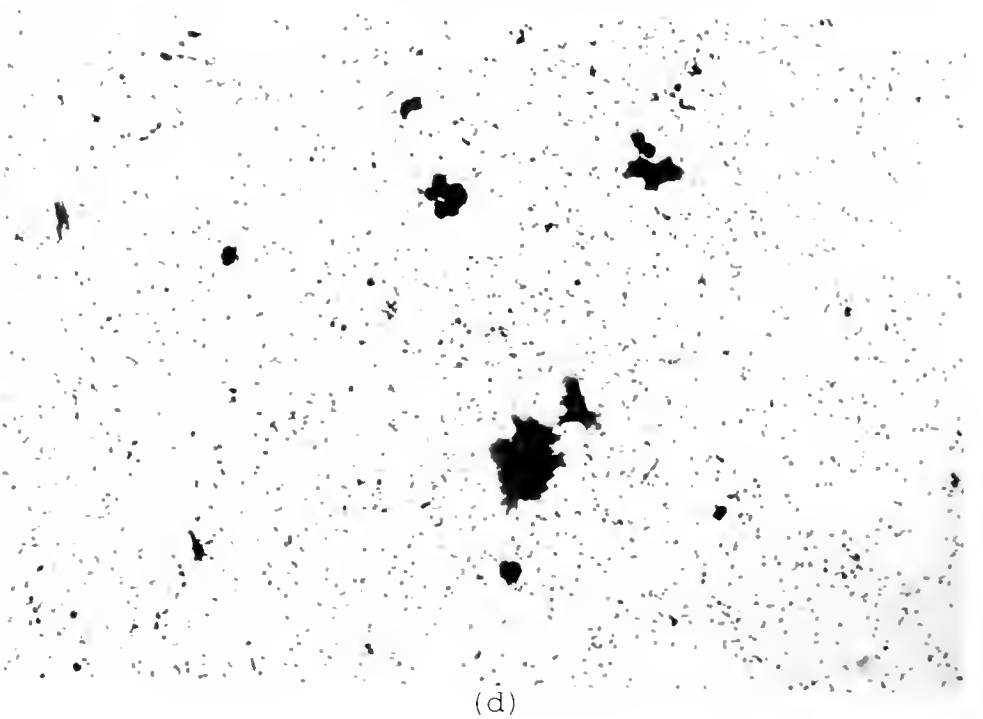

(d)

Figure 4-57 --- continued
(c) PVP/NVP-g-PDMS (15 minutes, 50 watts, 100 mTorr, 10% PVP/NVP ratio of 2/8, 0.15 Mrad)
(d) PDMA-g-PDMS (15 minutes, 50 watts, 100 mTorr, 3% DMA, 0.064 Mrad)

(a)

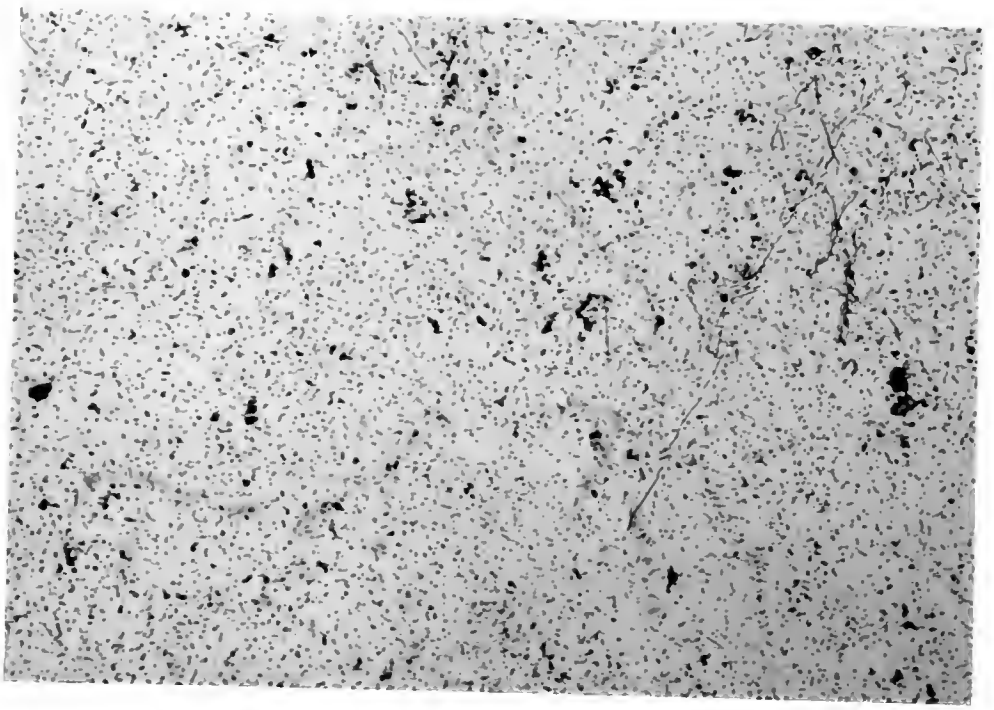

(b)

Figure 4-58. The optical micrograph of PC substrates (70x)
(a) unmodified PC
(b) PVP/NVP-g-PC (15 minutes, 50 watts, 100 mTorr, 10% PVP/NVP ratio of 2/8, 0.15 Mrad)

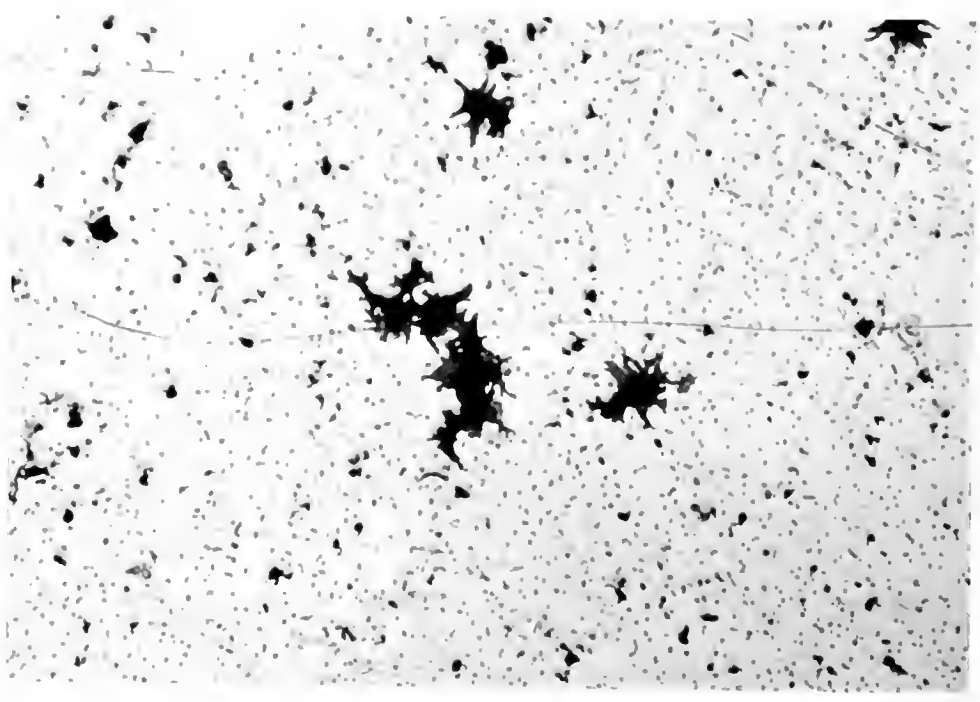

(c)

Figure 4-58 --- continued
(c) PDMA-g-PC (15 minutes, 50 watts, 100 mTorr, 3% DMA, 0.064 Mrad)

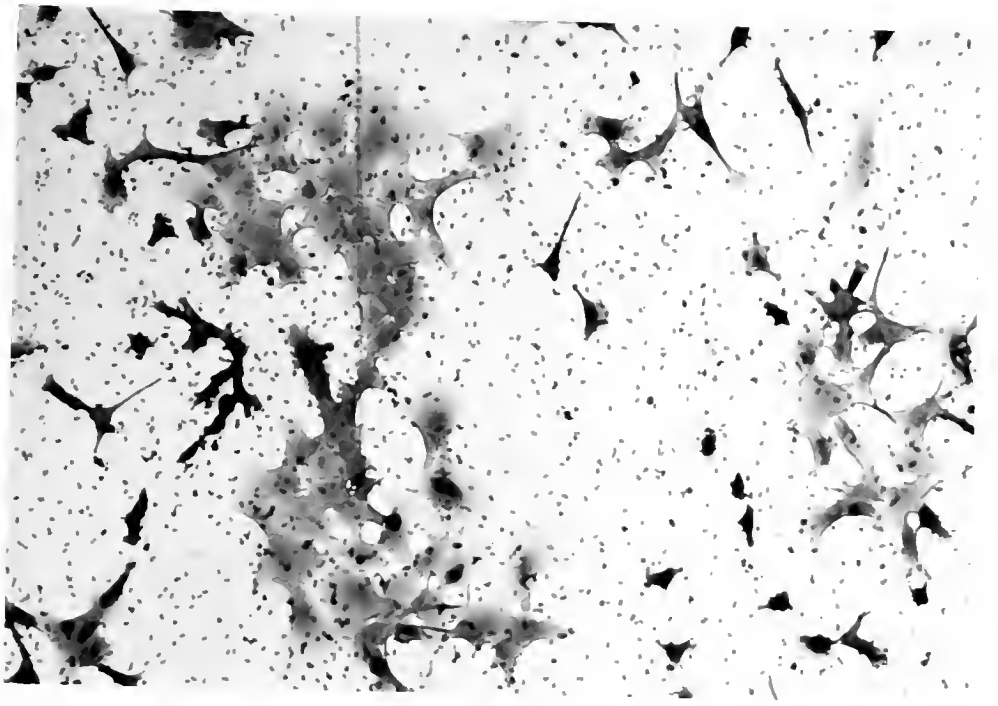

(a)

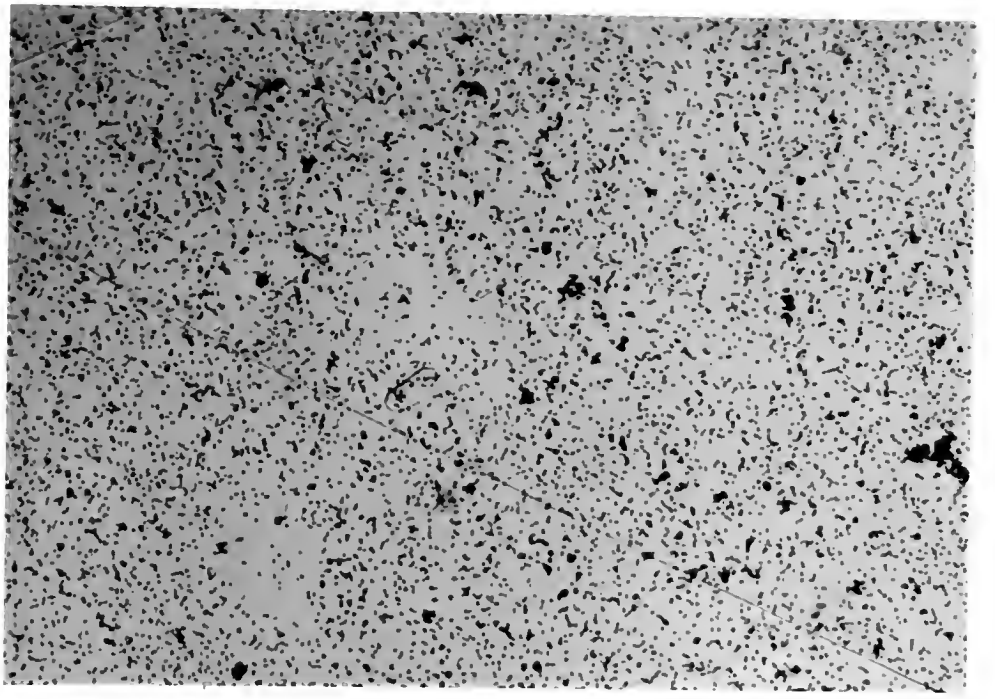

(b)

Figure 4-59. The optical micrograph of PVDF substrates (70x)
(a) unmodified PVDF
(b) PVP/NVP-g-PVDF (15 minutes, 50 watts, 100 mTorr, 10% PVP/NVP ratio of 2/8, 0.15 Mrad)

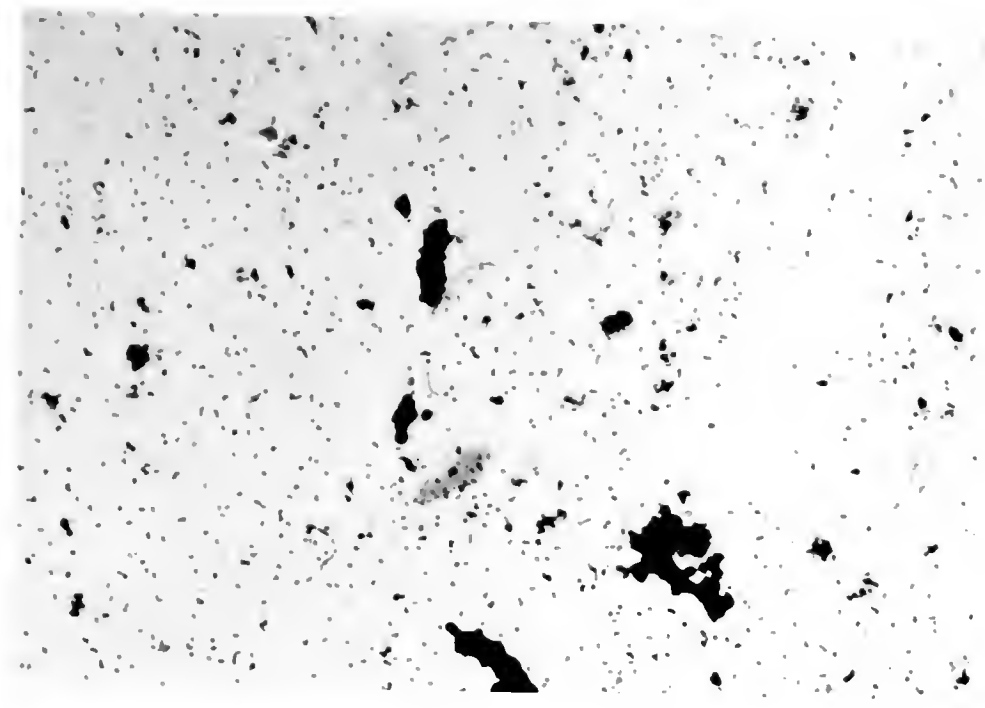

(c)

Figure 4-59 --- continued
(c) PDMA-g-PVDF (15 minutes, 50 watts, 100 mTorr, 3% DMA, 0.064 Mrad)

CHAPTER 5
SUMMARY AND SUGGESTED FUTURE WORK

5.1 Summary and Conclusions

The studies presented in this dissertation are part of the ongoing research in this laboratory, Center of Biomedical Engineering at the University of Florida, one of the major goals of which is to develop high efficiency surface modification techniques using low radiation dose (< 0.2 Mrad). Hydrophilic surface modification using the plasma/gamma method is a promising approach to meet these requirements. The major conclusions from this study are summarized as follows:

1. The PVP/NVP system produced much lower solution viscosities than NVP monomer alone under the same radiation conditions (10% total concentration, 0.15 Mrad).

2. Gelation did not readily occur in the PVP/NVP system at 0.15 Mrad radiation dose. However, gelation did occur in the PVP alone solutions when the PVP concentration was below 4% and higher than 0.3%.

3. The use of 10% PVP/NVP at a weight ratio of 2/8 as a monomer solution not only yields PVP grafts on PMMA comparable to NVP alone but also exhibits a fairly low solution viscosity after gamma irradiation. Sample's post-

washing and handling are easier when the solution viscosity is lower. The structure of PVP/NVP graft is expected to be a thin and dense graft with less penetration due to the diffusion limit of PVP molecules as compared to the PVP graft using NVP alone monomer.

4. Physisorption of PVP molecules onto PMMA surface was observed in this study. XPS data indicated that certain amounts of physically adsorbed PVP molecules were chemically grafted onto PMMA surface.

5. Water RFGD plasma is a very effective technique for reducing the contact angles of PMMA PDMS, PP, PC, FEP, and PVDF surfaces with short RF plasma exposure time ($\leq$ 5 minutes). The surface oxygen concentrations on PMMA, PDMS, PP, PC, and PVDF were significantly increased after exposing these substrates to RF water plasma for 15 minutes at 50 Watts and 100 mTorr.

6. The plasma/gamma method significantly enhanced the extent and quality of PVP/NVP gamma grafting onto PMMA, PDMS, PP, PC, FEP, and PVDF surfaces. The surfaces of PMMA, PDMS, PP, PC, FEP, and PVDF became very hydrophilic (contact angle $\leq 20^{\circ}$) after grafting with PVP/NVP.

7. The effects of plasma treatment time on the grafting of PVP/NVP depends on the characteristics of polymeric substrate such as the glass transition temperature, the chain flexibility and mobility. The PVP migration can be observed especially on the PDMS substrate if the plasma treatment time is varied from a short time to a long time.

For most substrates mentioned in this research, a short plasma treatment time (ca. one to five minutes) is enough to enhance the PVP/NVP grafting. The prolonged plasma treatment may degrade or ablate the surface region of substrate.

8. The structure of PVP/NVP graft prepared by the plasma/gamma method was a thin and dense graft with less penetration as compared to the PVP graft using the "presoak method". The PVP/NVP grafting may rely on the physisorption of PVP molecules onto substratre surface and the cross-reaction between PVP molecules and surface reactive sites.

9. The results for the DMA grafting were also significantly improved by the plasma pre-treatment but the grafting mechanisms were quite different from the PVP/NVP system. The surfaces of PMMA, PDMS, PP, PC, FEP, and PVDF became extremely hydrophilic after grafting with DMA using the plasma/gamma method. The extent and quality of PDMA graft on these polymeric substrates was remarkably improved by the plasma pretreatment. However, the PDMA grafting was highly dependent upon the number of active sites produced on the substrate surface and the number of monomer molecules available to the surface.

10. The effects of plasma treatment time on the grafting of PDMA also are not very significant. The effects are still dependent on the properties of substrates. A short plasma time is enough for most substrates mentioned in this research.

11. The rabbit lens epithelial cells adhesion and spreading test indicate: 1) the control PMMA, PDMS, PC, and PVDF surfaces adhere and spread cells very well; 2) the hydrated PVP surfaces do not adhere cells at all in most cases; 3) the hydrated PDMA surfaces adhere few cells without spreading in most cases; 4) the hydrated plasma treated surfaces adhere cells in a very significant manner. Therefore, hydrophilicity or low interfacial free energy is not the only control factor in the prevention of cell adhesion and spreading.

5.2 Future Work

1. Investigate the stability of PVP/NVP graft on various substrates and compare this study with the NVP graft prepared by the presoak method.

2. Investigate the molecular weight and molecular weight distribution of PVP/NVP solutions using GPC.

3. Investigate the incorporation of biomolecules (e.g. heparin, albumin, etc.) and drugs (e.g. anti-inflammation, anti-infection drugs) into PVP/NVP graft using the plasma/gamma method.

4. Conduct *in vivo* evaluations on these hydrophilic surface modified substrates to confirm the biocompatibility results of *in vitro* tests.

5. Conduct the study on the PDMA/DMA system and compare the results with the DMA only solution.

APPENDIX A
HYDROPHILIC SURFACE MODIFICATION OF SILICONE COPOLYMER CONTACT LENSES

A.1 Introduction

Silicone copolymers exhibiting high oxygen permeability are considered to be candidate materials for long-wear contact lenses. The objective of this study was to modify several silicone copolymer contact lens compositions. These lenses include SII disc shape lenses having a C.A. 44° and good mechanical strength, SI disc shape lenses having a C.A. 36° and good mechanical strength, AII disc shape having a C.A. 31° and low mechanical strength, SIMAC-I lenses, and Alabama-20 lenses. The silicone copolymer contact lenses supplied by a contact lens manufacturer were modified with PVP using the "presoak method" developed by Yahiaoui [6] in this laboratory. Changes in the procedure were made depending upon the hydrophilicity and swearing of the components in monomer solutions. The surface modified contact lenses then were characterized by contact angle measurement, gravimetric analysis, and graft thickness measurement and provided to the contact lens company who supplied them.

A.2 Materials and Methods

A.2.1 Materials

Silicone copolymer contact lenses were supplied by a contact lens company. These contact lenses, including three categories, were listed as follows:

group one: 25 SII disc shape lenses;

group two: 25 SI disc shape lenses and 20 SIMAC-I lenses;

group three: 25 AII disc shape lenses and 20 Alabama-20 lenses.

Previous studies, in this research group, show that the hydrated PVP graft can significantly reduce the incidence of epithelial cell adhesion to the IOL optics. Therefore, N-vinylpyrrolidone (NVP) was selected as a monomer in this study. Ultrapure® water was used as a solvent for preparing monomer solutions and for sample rinsing after gamma irradiation. Biological stains, including crystal violet, eosin Y, and hemotoxylin, were used in the graft thickness measurement.

A.2.2 Methods

The "presoak method" was used to prepare these PVP modified contact lenses. After gamma irradiation, samples were placed into test tubes individually and rinsed with Ultrapure® water two times per day for one week. After washing, samples were air-dried for 24 hours and

characterized by graft thickness measurement and contact angle measurement. Sample's weight was monitored before and after surface modification.

A.3 Results and Discussion

Table A-1 shows the results for the SII group modified with various conditions. The SII disc shape lens is a transparent silicone copolymer lens and exhibits good properties in mechanical strength. The contact angle for the untreated SII is 44°. After surface modification by the D condition, the contact angle for the SII is 19° and the SII maintains well both in its optical and mechanical properties. The D condition is then chosen as the final condition for the SII group.

Table A-1. The results for the SII group

Sample #	Group	Condition	C.A. (±5°)	Graft Thickness (μm)	Yield (wt%)	Properties
CV001	SII	A	20	30±15	9	OK
CV002	SII	B	20	35±15	8.4	OK
CV009	SII	D	19	15±5	5.2	OK

Table A-2 shows the results for the SI group treated with various conditions. Before surface modifications, most SI lenses are transparent except several lenses are partially opaque and their contact angle is 36°. The SI lenses are easy to swells up in monomer solution and the

SIMAC I lenses are too thin to handle without breakage. Several lenses have been broken before surface modification. Since most biological dyes, such as crystal violet, eosin Y, and hemotoxylin, stain SI lens, graft thickness for SI lens remains indeterminable. A mild condition, the H condition, is chosen as the final because of the swelling problem. Under the H condition, the contact angle for modified SI lens is 20^{o} and the yield is 4.8 wt%.

Table A-2. The results for the SI group

Sample #	Group	Condition	C.A. (±5)	Graft Thickness (μm)	Yield (wt%)	Properties
CV003	SI	A	19	N/A	33	swelling
CV004	SI	B	20	N/A	28	swelling
CV007	SI	C	18	N/A	13	swelling
CV010	SI	E	19	N/A	4 (?)	swelling
CV012	SI	F	30	N/A	0.4	OK
CV014	SI	G	21	N/A	2	OK
CV036	SI	H	20	N/A	5.3	OK

The results for the AII group are summarized in Table A-3. Before surface modification, AII lenses exhibit yellowish color and low tear strength. The contact angle for the control AII is 31^{o}. The mechanical properties is not as good as SI or SII lens. Occasionally, samples are very fragile after treatment. In the same category, the Alabama-20 lenses exhibit a better mechanical strength than

the AII lenses. Since the biological dyes also stain the AII lens very well, the thickness of graft remains indeterminable. A mild condition, the H condition, is selected as the final to prevent the low strength problem. The contact angle and yield for AII lens under the H condition are 20° and 1.7 wt% respectively.

Table 3. The results for AII group

Sample #	Group	Condition	C.A. (±5°)	Graft Thickness (μm)	Yield (wt%)	Properties
CV005	AII	A	20	N/A	N/A	low me. st.
CV006	AII	B	19	N/A	N/A	low me. st.
CV008	AII	C	19	N/A	N/A	low me. st.
CV011	AII	E	19	N/A	N/A	low me. st.
CV013	AII	F	25	N/A	0	OK
CV015	AII	G	21	N/A	0	OK
CV037	AII	I	22	N/A	0.9	OK
CV038	AII	H	20	N/A	1.7	OK

The condition codes used in Tables A-1, A-2 and A-3 are listed as follows:

Condition Code	Presoak	Gamma Irradiation
A	40%NVP/60°/4hrs	15%NVP/0.10 Mrad
B	40%NVP/60°/4hrs	10%NVP/0.15 Mrad
C	20%NVP/50°/2hrs	10%NVP/0.15 Mrad
D	30%NVP/60°/4hrs	10%NVP/0.15 Mrad
E		10%NVP/0.15 Mrad
F		5%NVP/0.10 Mrad
G		8%NVP/0.10 Mrad
H		8%NVP/0.15 Mrad
I		5%NVP/0.15 Mrad

A-E:@ 4" position in gamma source

F-I:@ 2" position in gamma source

A.4 SUMMARY

The final conditions for each group and results are summarized as follows:

Group	Condition	Yield (wt%)	C.A.(o)	Thickness (μm)	Properties
SII	D	5.2	19	15±5	OK
SI	H	4.8	20	N/A	OK
AII	H	1.7	20	N/A	OK
S_{imac} I	H	N/A	N/A	N/A	OK
$A_{lsbs.}$20	H	N/A	N/A	N/A	OK

APPENDIX B
QUANTITATIVE ANALYSIS OF MIGRATORY SILICONE IN THE TISSUE OF IMPLANT SURROUNDING BY FT-IR/ATR LIQUID CELL

B.1 Introduction

A FT-IR/ATR liquid cell technique was developed to quantify the migratory silicone oil in the tissue surrounding in a rabbit implant model. In the FT-IR spectra, silicone can show a very intense peak at 1096 cm^{-1} which indicates -Si-O-Si- siloxane stretching vibration. A calibration curve was built and based on the IR absorbance at 1096 cm^{-1} and the concentration of silicone in the control samples.

B.2 Materials and Methods

B.2.1 Animals

Eleven female New Zealand White rabbits weighing 3-3.5 kg were used. Rabbits were raised at the University of Florida's Animal Resources facility, an AAALAC-approved facility.

B.2.2 Implants

Three different types of miniature silicone implants were evaluated: A-Smooth, a very soft 2g prosthesis (n=6); B-Smooth, a more rigid 4g prosthesis; and B-Texture, a rough surfaced 4g prosthesis similar to B-Smooth (n=11).

B.2.3 FT-IR/ATR liquid cell

A Nicolet 20SXB FT-IR spectrometer and a ZnSe ATR liquid cell (The Circle®) attachment were used for the quantitative analysis. ATR liquid cell was filled with 5 ml solution for each run. FT-IR/ATR spectra were usually measured with a resolution of 2 cm^{-1} and 30 scans. Data processing was done with standard Nicolet software.

B.2.4 Data Collection

Implants were retrieved by a surgery team in this laboratory at 2 weeks, 2 months, and 6 months. Different size of tissues (average weight = 4g) were cut from implant surrounding. The tissues were extracted in methylene chloride (Optima grade; Fisher Scientific, Fair Lawn, NJ) for 48 hours at room temperature. Extracted solution was filtered through 8μ Whatman filter paper. Solvent in the extracted solution was evaporated at room temperature. Then 15 grams of methylene chloride were added and mixed with each tissue extract before FT-IR/ATR measurement. A standard control spectrum was obtained using extracted

tissue from a rabbit which had not received an implant. Low molecular weight PDMS (Shin-Etsu Co., Japan) was added to the control tissue samples at 0, 5, 10, and 20 mg silicone/g tissue concentrations to construct an calibration curve using the same analytic procedure.

B.3 Results and Discussion

The calibration curve obtained from the control tissue samples is shown in Figure B-1. The results of silicone concentration in tissue are listed in Table B-1. At 6 months post-operatively, mean tissue silicone concentration were 4.6 and 11.6 mg per gram tissue for B-Textured and A-Smooth implants, respectively. The methylene chloride tissue extraction and FT-IR/ATR analysis in a liquid cell developed in this laboratory is a simple and low cost technique to determine silicone concentration in tissue. However, the silicone concentration in tissue must be greater than 1 mg/g tissue to be detectable, because lower concentration is beyond the sensitivity limit of FT-IR.

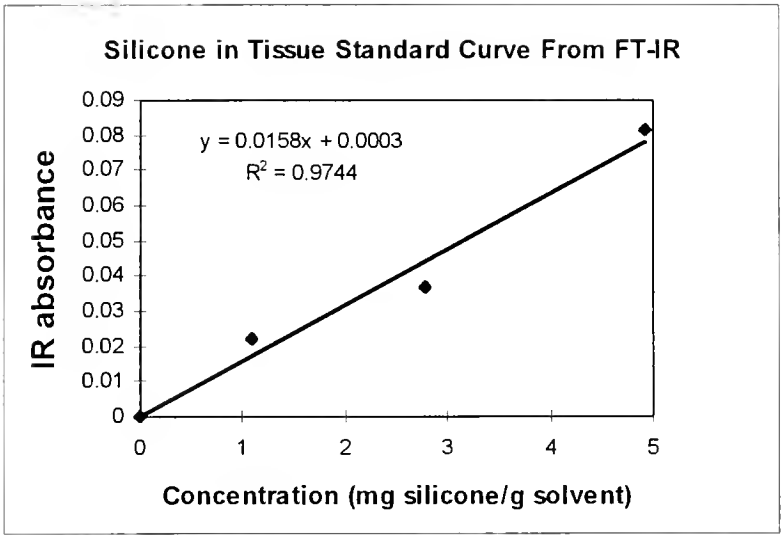

Figure B-1. The standard curve for tissue silicone concentration

Table B-1. Tissue silicone concentration

	Implant time	n	Silicone (mg/g tissue)
A-Smooth	6 months	5	9.7±3.9*
B-Textured	6 months	4	4.6±3.7
B-Smooth	6 months	1	11.6

* n=4: data excluded from one animal due to insufficient tissue harvested for silicone analysis.

LIST OF REFERENCES

1. S.A. Barenberg, MRS Bulletin, 16, 27(1991).

2. O. Wichterle and D. Lim, Nature (London), 185, 117(1960).

3. O. Wichterle, Encyclopedia of Polymer Science and Technology, Vol. 15, p. 273, M.H. Mark and N.G. Gaylord, Eds., Wiley Interscience, New York, 1971.

4. N.A. Peppas, Hydrogels in Medicine and Pharmacy, Vol. 1, N.A. Peppas, Ed., CRC Press, Boca Raton, Florida, 1987.

5. J.W. Sheets, Hydrophilic Polymer Coatings to Prevent Tissue Adhesion, Ph.D. Dissertation, University of Florida, 1983.

6. A. Yahiaoui, Surface Modification of Intraocular Lens Polymers by Hydrophilic Graft Polymerization for Improved Ocular Implant Biocompatibility, Ph.D. Dissertation, University of Florida, 1990.

7. M. Yalon, J.W. Sheets, S. Reich, and E.P. Goldberg, ACTA XXIV: International Congress of Ophthalmology, p. 273, P. Henkind, Ed., JB Lippincott Company, Philadephia, Pennsylvania, 1982.

8. F.M. Hofmeister, M. Yalon, S. Iida, and E.P. Goldberg, J. Cataract Refract. Surg., 14, 514(1988).

9. A. Chapiro, Radiation Chemistry of Polymeric Systems, Interscience Publishers, New York, 1962.

10. A.S. Hoffman, Advances in Polymer Science, p. 142, K. Dusek, Ed., Springer Verlag, New York, 1983.

11. H. Yasuda, Plasma Polymerization, Academic Press, Orlando, Florida, 1985.

12. A. Heinglein, W. Schnabel, and K. Heine, Angew. Chem., 15, 461(1958).

13. G. Burillo and A. Chapiro, Eur. Polym. J., 22, 653 (1986).

14. H. Ridley, Trans. Opthalmol. Soc., UK, 71, 617(1951).

15. M.F. Refojo, Surv. Ophthalmol., 26, 257(1982).

16. A.C. Neumann, G.R. McCarty, and R.H. Osher, J. Cataract Refract. Surg., 13, 653(1987).

17. R. Champion, P.J. McDonnell, and W.R. Green, Surv. Ophthalmol., 30, 1(1985).

18. R.H. Keates and D.R. Ehrlich, Ophthalmol, 85, 408(1978).

19. E.P. Goldberg, M. Yalon, M. Kaneda, H. Ariki, J. Stacholy, F. Hofmeister, C.W. Luo, F.M. Li, J. Burns, A. Yahiaoui, and J. Sheets, The Third World Biomaterials Congress, Kyoto, Japan, 1988.

20. H.A. Stein, B.J. Slatt, and R.M. Stein, Ophthalmic Terminolog, 3rd Ed., Mosby-Year Book, St. Louis, Missouri, 1992.

21. L. Allakharia, R. Knoll, and R.L. Lindstrom, J. Cataract Refract. Surg., 13, 607(1987).

22. J.C. Tsai, V.E. Castaneda, D.J. Apple, D. Wasserman, J.P. Hoggatt, and U.F.C. Legler, J. Cataract Refract. Surg., 18, 232(1992).

23. D.W. Meltzer, Arch. Ophthalmol., 98, 100(1980).

24. M.B. Habal, Arch. Surg., 119, 843(1984).

25. Shanghi Hospital, Department of Ophthalmology: Clinical Report of Transparent Silicone Intraocular Lens Implantation, Chung-Hua Yen Ko Chih, 17, 17(1981).

26. K.Y. Zhou, Chin. Med. J., 96(3), 175(1983).

27. H.J. Mondino, G.H. Rajacich, and H. Summer, Arch. Ophthalmol., 105, 989(1987).

28. A.T. Milauskas, J. Cataract Refract. Surg., 13, 644(1987).

29. A.D. Ruedemann, Jr., Trans Am. Ophthalmol. Soc., 75, 436(1977).

30. R.B.S. Packard, A. Garner, and E.J. Arnott, Br. J. Ophthalmol., 65, 585(1981).

31. K.R. Mehta, S.N. Sathe, and S.D. Karyekar, Am. Intra-Ocular Implant Soc. J., 4(4), 200(1978).

32. C.M. Cunanan, N.M. Tarbaux, and P.M. Knight, J. Cataract Refract. Surg., 17, 767(1991).

33. R. Menapace, C. Skorpik, M. Juchem, W. Scheidel, and R. Schranz, J. Cataract Refract. Surg., 15, 257(1989).

34. H. Hattori, P. Martin, D. Osborn, and E.P. Goldberg, Fourth World Biomaterials Congress, Berlin, Germany, 1992.

35. H. Hattori, P. Martin, and E.P. Goldberg, Ninth Annual Scientific Session, Academy of Surgical Research, Brecknridge, Colorado, 1992.

36. T.A. Horbett, M.B. Schway, and B.D. Ratner, J. Colloid Interf. Sci., 104, 28(1985).

37. D.R. Absolom, W. Zingg, and A.W. Neumann, J. Biomed. Mater. Res., 21, 161(1987).

38. E. Ruckenstein and S.V. Gourisankar, J. Colloid Interf. Sci., 101, 436(1984).

39. J.D. Andrade, Med. Instrum., 7, 110(1973).

40. W.R. Gombotz, W. Guanghui, T.A. Horbett, and A.S. Hoffman, J. Biomed. Mater. Res., 25, 1547(1991).

41. N.P. Desai and J.A. Hubbell, J. Biomed. Mater. Res., 25, 829(1991).

42. R.E. Baier, Adhesion in Biological Systems, R.S. Manly, Ed., Academic Press, New York, 1970.

43. M.J. Lydon, T.W. Minett and B.J. Tighe, Biomaterials, 6, 396(1985).

44. J.D. Andrade, Surface and Interfacial Aspects of Biomedical Polymers, Vol. 2, p. 1, J.D. Andrade, Ed., Plenum Press, New York, 1985.

45. S. Wu, Polymer Interphase and Adhesion, Marcel Dekker, New York, 1982.

46. M. Hudis, Techniques and Applications of Plasma Chemistry, p.113, J.R. Hollahan and A.T. Bell, Eds., Wiley-Interscience, New York, 1974.

47. H. Yasuda, J. Macromol. Sci.-Chem., A10(3), 383(1976).

48. K.G. Muller, Chem. Ing. Tech., 3, 122(1973).

49. F.K. McTaggart, Plasma Chemistry in Electrical Discharges, Elsevier, Amsterdam, 1967.

50. H. Hudis and L.E. Prescott, J. Polym. Sci., B10, 179(1972).

51. H. Hudis, J. Appl. Polym. Sci., 16, 2397(1972).

52. C.H. Bamford and J.C. Ward, Polymer, 2, 277(1961).

53. J.R. Hall, C.A.L. Westerdahc, A.T. Devine, and M.J. Bodnar, J. Appl. Polym. Sci., 13, 2085(1969).

54. P. Blais, D.J. Carlsson, and D.M. Wiles, J. Appl. Polym. Sci., 15, 129(1971).

55. J.R. Hollahan and B.B. Stafford, J. Appl. Polym. Sci., 13, 807(1969).

56. T.G. Vargo, J.A. Gardella, and L. Salvati, Jr., J. Polym. Sci., Part A, 27, 1267(1989).

57. J.R. Hollahan and G.L. Carlson, J. Appl. Polym. Sci., 14, 2499(1970).

58. P.M. Triolo and J.D. Andrade, J. Biomed. Mater. Res., 17, 129(1983).

59. R.R. Sowell, N.J. DeLollis, H.J. Gregory, and O. Montoya, J. Adhesion, 4, 15(1972).

60. R.H. Hansen, J.V. Pascale, T. DeBenedicts, and P.M. Rentzepis, J. Polym. Sci., Part A, 3, 2205(1965).

61. D.T. Clark and R. Wilson, J. Polym. Sci., Polymer Chemistry Ed., 21, 837(1983).

62. H. Schonhorn and F.W. Ryan, J. Polym. Sci., Part A-2, 7, 105(1972).

63. J.R. Hall, C.A.L. Westerdahl, M.J. Bodnar, and D.W. Levi, J. Appl. Polym. Sci., 16, 1465(1972).

64. C.A.L. Westerdahl, J.R. Hall, E.C. Schramm, and D.W. Levi, J. Colloid and Interface Sci., 47, No.3(1974).

65. J.E. Wilson, Radiation Chemistry of Monomers, Polymers, and Plastics, Marcel Dekker, New York, 1974.

66. A.J. Swallow, Radiation Chemistry of Organic Compounds, Pergamon Press, New York, 1960.

67. M. Dole, The Radiation Chemistry of Macromolecules, Vol. III, Academic Press, New York, 1973.

68. J.F. Kircher, F.A. Sliemers, R.A. Markle, W.B. Gager, and R.I. Leininger, J. Phys. Chem., 69, 189 (1965).

69. A. Todd, J. Polym. Sci., XLII, 223(1960).

70. P. Kourim and K. Vacek, Trans. Faraday Soc., 61, 415(1964).

71. M.C.R. Symons, J. Chem. Soc., 5, 1186(1963).

72. J.L. Williams and T.S. Dunn, Radiat. Phys. Chem., 15, 59(1980).

73. H. Fischer and K.-H. Hellwege, J. Polym. Sci., 56, 33(1962).

74. B.R. Loy, J. Polym. Sci., A1, 2251(1963).

75. L.J. Forrestal and W.G. Hodgson, J. Polym. Sci., A2, 1275(1964).

76. M. Iwasaki, T. Ichikawa, and K. Tariyama, J. Polym. Sci., B5, 423(1967).

77. A.M. Bueche, J. Polym. Sci., 19, 297(1956).

78. E.L. Warrick, Ind. Eng. Chem., 47, 2388(1955).

79. M.G. Omerod and A. Charlesby, Polymer, 4, 459(1963).

80. H. Menhoffer and H. Hensinger, Radiat. Phys. Chem., 29, 243(1981).

81. W.E. Skiens, Radiat. Phys. Chem., 15, 47(1980).

82. D. Acierno, F.P. LaMantia, G. Titomanlio, E. Calderaro, and F. Castiglia, Radiat. Phys. Chem., 16, 95(1980).

83. J.H. Golden and E.A. Hazell, J. Polym. Sci., Part A, 1, 1671(1963).

84. E.E. Schneider, J. Chem. Phys., 23, 978(1955).

85. H.N. Rexroad and W. Gordy, J. Chem. Phys., 30, 399(1959).

86. J.W. Ryan, Modern Plastics, 31, No.2, 152(1953).

87. A. Chapiro, Radiat. Phys. Chem., 14, 101(1979).

88. A. Charlesby, Atomic Radiation of Polymers, Pergamon Press, Oxford, 1960.

89. J. Danon, A. Chapiro, and M. Magat, French Pat. 1,157,006 (1957) to Centre National de la Recherche Scientifique.

90. G. Burillo and A. Chapiro, Eur. Polym. J., 22, 653(1986).

91. A. Heinglein, W. Schnabel, and K. Heine, Angew. Chem., 15, 461(1958).

92. K. Mentak, Tissue-Protective Hydrophilic Polymer Solutions and Surface Modification, Ph.D. Dissertation, University of Florida, 1993.

93. J.D. Fales, A. Bradley, and R.E. Howe, Vac. Technol, 53, (1976).

94. M.R. Wertheimer and H.P. Schreiber, J. Appl. Polym. Sci., 26, 2087(1981).

95. M. Suzuki, A. Kishida, H. Iwata, and Y. Ikada, Macromolecules, 19, 1804(1986).

96. C.I. Simionescu, F. Denes, M.M. Macoveanu, and J. Negulescu, Makromol. Chem. Suppl., 8, 17(1984).

97. Modern Plastics Encyclopedia, Ed. R. Juran, McGraw Hill, New York, 1989.

98. H. Fricke and S. Morse, Phil. Mag., 7, 129(1929).

99. N. Miller, J. Chem. Phys., 18, 79(1950).

100. J.R. Van Wazer, J.W. Lyons, K.Y. Kim, and R.E. Colwell, Viscosity and Flow Measurement, p15, Interscience Publishers, New York, 1963.

101. T.C. Patton, Paint Flow and Pigment Dispersion, p55, John Wiley & Sons, New York, 1979.

102. N.P. Cheremisinoff, An Introduction to Polymer Rheology and Processing, p7, CRC Press, Boca Raton, Florida, 1993.

103. J.D. Andrade, R.N. King, D.E. Gregonis, and D.L. Coleman, J. Polym. Sci., Symp., 66, 313(1979).

104. T. Young, Phil. Trans. Roy. Soc., London, 65, 65(1805).

105. A.W. Adamson, Physical Chemistry of Surfaces, p750, Interscience, New York, 1967.

106. W.A. Zisman, Ind. Eng. Chem., 55, 19(1963).

107. W.A. Zisman, Advan. Chem. Ser., 57, 26(1964).

108. R.M.A. Azzam and N.M. Bashara, Ellipsometry and Polarized Light, p. 283, North-Holland Publishing Company, New York, 1977.

109. R.R. Stromberg, E. Passaglia, and D.J. Tutas, Ellipsometry in the Measurement of Surfaces and Thin Film, Symposium Proceedings, p. 281, E. Passaglia, R.R. Stromberg, and J. Kruger, Eds., National Bureau of Standards Miscellaneous Publication 256, Washington, DC, 1964.

110. Din-Guo Chen, Synthesis and Characterization of GeO_2-SiO_2 Waveguides, Ph.D. Dissertation, University of Florida, 1991.

111. H.G. Tompkins, A User's Guide to Ellipsometry, p. 10, Academic Press, New York, 1993.

112. F.M. Hofmeister, Biosurface Properties of Ocular Implant Polymers, M.S. Thesis, University of Florida, 1988.

113. Catalog of Plasdone® K-90, #5M-1089, GAF Chemicals Corporation, Wayne, NJ, 1989.

114. A. Charlesby and P. Alexander, J. Chim. Phys., 52, 694(1955).

115. P. Alexander and A. Charlesby, J. Polym. Sci., 23, 355(1957).

116. A. Henglein, J. Phys. Chem., 63, 1852(1959).

117. G. Odian, Principles of Polymer Science, 2nd ed., Wiley-Interscience Publ., New York, 1981.

118. H. Iwata, A. Kishida, M. Suzuki, Y. Hata, and Y. Ikada, J. Polym. Sci., Part A, 26, 3309(1988).

119. F.P. Del Greco and F. Kaufman, Disc. Faraday Soc., 33, 128(1962).

120. R.H. Jones and C.A. Winkler, Trans. Faraday Soc., 29, 1010(1951).

121. P.A. Giguere, E.A. Secco and R.S. Eaton, Disc. Faraday Soc., 14, 104(1952).

122. G.J. Minkoff, Frozen Free Radicals, p20, Interscience Publishers Inc., New York, 1960.

123. J.W. Edwards, Formation and Trapping of Free Radicals, Chap. 8, A.M. Bass and H.P. Broida, Eds., Academic Press, New York, 1960.

124. D.T. Clark and A. Dilks, J. Polym. Sci., Polym. Chem. Ed., 15, 2321(1977).

125. J.D. Andrade, Surface and Interfacial Aspects of Biomedical Polymers, Vol. 1, P. 1, J.D. Andrade, Ed., Plenum Press, New York, 1985.

126. B.D. Ratner, P.K. Weathersby, A.S. Hoffman, M.A. Kelly, and L.H. Scharpen, J. Appl. Polym. Sci., 22, 643(1978).

127. H. von Brecht, F. Mayer and H. Binder, Makromol. Chem., 33, 89(1973).

128. D.W. Dwight and W.M. Riggs, J. Coll. Interface Sci., 47, 650(1974).

129. N.G. Maroudas, J. Cell. Physiol., 90, 511(1977).

130. H.G. Klemperer and P. Knox, Lab. Pract., 26, 179(1977).

131. F. Grinnel and M. Feld, J. Biol. Chem., 257, 4888(1982).

132. A. Kishida, H. Iwata, Y. Tamada, and Y. Ikada, Biomaterials, 12, 786(1991).

133. M.N. Helmus, D.F. Gibbons, and R.D. Jones, J. Biomed. Mater. Res., 18, 165(1984).

134. J.J. Rosen and M.B. Schway, Polym. Sci. Technol., 12B, 667(1980).

135. R.J. Klebe, K.L. Bentley, and R.C. Schoen, J. Cell. Physiol., 109, 481(1981).

136. P.B. van Wachem, T. Beugeling, J. Feijen, A. Bantjes, J.P. Defmers, and W.G. van Aken, Biomaterials, 6, 403(1985).

137. T.A. Horbett, J.J. Waldburger, B.D. Ratner, and A.S. Hoffman, J. Biomed. Mater. Res., 22, 383(1988).

138. W. Zingg, A.W. Neumann, A.B. Strong, O.S. Hum, and D.R. Absolom, Biomaterials, 2, 156(1981).

139. L. Weiss, Fed. Proc., 30, 1649(1971).

140. N.G. Maroudas, Nature, 244, 353(1973).

141. J.J. Rosen and M.B. Schway, Polym. Sci. Technol, 12B, 667(1980).

BIOGRAPHICAL SKETCH

Tung-Liang Lin was born at Pin-tung, Taiwan, R.O.C., on February 17, 1959. He received his B.S. degree in chemical engineering from the National Central University in 1982. After two years service in the Army, he worked for the Tai-tung Enterpise as a assistant engineer and then for the National Sun Yat-Sen University as a research assistant.

He attended the graduate school at the Auburn University, Alabama, in September, 1986. He earned an M.S. degree in materials engineering in March, 1989. He began his graduate studies at the University of Florida in January, 1990.

While working toward the degree of Doctor of Philosophy in materials science, he served as a research assistant in the Department of Materials Science and Engineering. The author is a member of the Society for Biomaterials and the Society for the Advancement of Material and Process Engineering.

I certify that I have read this study and that in my opinion it conforms to acceptable standards of scholarly presentation and is fully adequate, in scope and quality, as a dissertation for the degree of Doctor of Philosophy.

Eugene P. Goldberg, Chairman
Professor of Materials Science
and Engineering

I certify that I have read this study and that in my opinion it conforms to acceptable standards of scholarly presentation and is fully adequate, in scope and quality, as a dissertation for the degree of Doctor of Philosophy.

Christopher D. Batich
Professor of Materials Science
and Engineering

I certify that I have read this study and that in my opinion it conforms to acceptable standards of scholarly presentation and is fully adequate, in scope and quality, as a dissertation for the degree of Doctor of Philosophy.

E. Dow Whitney
Professor of Materials Science
and Engineering

I certify that I have read this study and that in my opinion it conforms to acceptable standards of scholarly presentation and is fully adequate, in scope and quality, as a dissertation for the degree of Doctor of Philosophy.

James H. Adair
Associate Professor of
Materials Science and
Engineering

I certify that I have read this study and that in my opinion it conforms to acceptable standards of scholarly presentation and is fully adequate, in scope and quality, as a dissertation for the degree of Doctor of Philosophy.

Randolph S. Duran
Associate Professor of
Chemistry

This dissertation was sumitted to the Graduate Faculty of the College of Engineering and to the Graduate School and was accepted as partial fulfillment of the requirements for the degree of Doctor of Philosophy.

May, 1995

Winfred M. Phillips
Dean, College of Engineering

Karen A. Holbrook
Dean, Graduate School

LD
1739
1985
.L7351

UNIVERSITY OF FLORIDA
3 1262 08556 8201